

KINETIC STUDIES for DIMETHYL ETHER and DIETHYL ETHER
PRODUCTION

A THESIS SUBMITTED TO
THE GRADUATE SCHOOL OF NATURAL AND APPLIED SCIENCES
OF
MIDDLE EAST TECHNICAL UNIVERSITY

BY

DİLEK VARIŞLI

IN PARTIAL FULFILLMENT OF THE REQUIREMENTS
FOR
THE DEGREE OF DOCTOR OF PHILOSOPHY
IN
CHEMICAL ENGINEERING

SEPTEMBER 2007

Approval of the thesis:

**“KINETIC STUDIES for DIMETHYL ETHER and DIETHYL ETHER
PRODUCTION”**

submitted by **DİLEK VARIŞLI** in partial fulfillment of the requirements for the
degree of Master of Science in **Chemical Engineering Department, Middle East
Technical University** by,

Prof. Dr. Canan Özgen _____
Dean, Graduate School of **Natural and Applied Sciences**

Prof. Dr. Nurcan Baç _____
Head of Department, **Chemical Engineering**

Prof. Dr. Timur Doğu _____
Supervisor, **Chemical Engineering, METU**

Prof.Dr. Gülşen Doğu _____
Co-Supervisor, **Chemical Engineering, Gazi Univ.**

Examining Committee Members:

Prof. Dr. H. Önder Özbelge _____
Chemical Engineering Dept., METU

Prof.Dr. Timur Doğu _____
Chemical Engineering Dept., METU

Prof. Dr. H.Tunçer Özdamar _____
Chemical Engineering Dept., Ankara Univ.

Prof Dr. İnci Eroğlu _____
Chemical Engineering Dept., METU.

Prof. Dr. Gürkan Karakaş _____
Chemical Engineering Dept., METU

Date: 05.09.2007

I hereby declare that all information in this document has been obtained and presented in accordance with academic rules and ethical conduct. I also declare that, as required by these rules and conduct, I have fully cited and referenced all material and results that are not original to this work.

Name, Last name: Dilek Varışlı

Signature :

ABSTRACT

KINETIC STUDIES FOR DIMETHYL ETHER AND DIETHYL ETHER PRODUCTION

Varışlı, Dilek

Ph.D., Department of Chemical Engineering

Supervisor: Prof. Dr. Timur Doğu

Co-Supervisor: Prof. Dr. Gülşen Doğu

September 2007, 206 pages

Fast depletion of oil reserves necessitates the development of novel alternative motor vehicle fuels. Global warming problems also initiated new research to develop new fuels creating less CO₂ emission. Nowadays, dimethyl ether (DME) and diethyl ether (DEE) are considered as important alternative clean energy sources. These valuable ethers are produced by the dehydration reaction of methanol and ethanol, respectively, in the presence of acidic catalysts. Besides DEE, ethylene which is very important in petrochemical industry, can also be produced by ethanol dehydration reaction.

In the first part of this study, the catalytic activity of tungstophosphoric acid (TPA), silicotungstic acid (STA) and molybdophosphoric acid (MPA), which are well-known heteropolyacids were tested in ethanol dehydration reaction. The activities of other solid acid catalysts, such as Nafion and mesoporous aluminosilicate, were also tested in the dehydration reaction of ethanol. In the case of DME production by dehydration of methanol, activities of STA, TPA and aluminosilicate catalysts were tested. Among the heteropolyacid catalysts, STA showed the highest activity in both ethanol and methanol dehydration reactions.

With an increase of temperature from 180°C to 250°C, Ethylene selectivities increased while DEE selectivities decreased. Ethylene yield values over 0.70 were obtained at 250°C. The presence of water in the feed stream caused some reduction in the activity of TPA catalyst. Very high DME yields were obtained using mesoporous aluminosilicate catalyst at about 450°C.

The surface area of heteropolyacids are very low and they are soluble in polar solvents such as water and alcohols. Considering these drawbacks of heteropolyacid catalysts, novel mesoporous STA based high surface area catalysts were synthesized following a hydrothermal synthesis route. These novel catalysts were highly stable and they did not dissolve in polar solvents. The catalysts containing W/Si ratios of 0.19 (STA62(550)) and 0.34 (STA82(550)) have BJH surface area values of 481 m²/g and 210 m²/g, respectively, with pore size distributions ranging in between 2-15 nm. These catalysts were characterized by XRD, EDS, SEM, TGA, DTA, DSC, FTIR and Nitrogen Adsorption techniques and their activities were tested in ethanol dehydration reaction. Calcination temperature of the catalysts was shown to be a very important parameter for the activities of these catalysts. Considering the partial decomposition and proton lost of the catalysts over 375°C, they are calcined at 350°C and 550°C before testing them in ethanol dehydration reaction. The catalysts calcined at 350°C showed much higher activity at temperature as low as 180°C. However, the catalysts calcined at 550°C showed activity over 280°C. Ethylene yield values approaching to 0.90 were obtained at about 350°C with catalysts calcined at 350°C. DEE yield past through a maximum with an increase in temperature indicating its decomposition to Ethylene at higher temperatures. However, at lower temperatures (<300°C) Ethylene and DEE were concluded to be formed through parallel routes. Formation of some acetaldehyde at lower temperatures indicated a possible reaction path through acetaldehyde in the formation of DEE. DRIFTS results also proved the presence of ethoxy, acetate and ethyl like species in addition to adsorbed ethanol molecules on the catalyst surface and gave additional information related to the mechanism.

Keywords: Heteropoly acid, silicotungstic acid, Diethyl Ether, Dimethyl Ether, Ethylene, MCM-41

ÖZ

DİMETİL ETER VE DİETİL ETER ÜRETİMİ İÇİN KİNETİK ÇALIŞMALAR

Varışlı, Dilek

Doktora, Kimya Mühendisliği Bölümü

Tez Yöneticisi: Prof. Dr. Timur Doğu

Ortak Tez Yöneticisi: Prof. Dr. Gülşen Doğu

Eylül 2007, 206 sayfa

Petrol kaynaklarının hızlıca azalması araştırmaların yeni motor yakıt alternatiflerine yönelmesine neden olmuştur. Küresel ısınma problemi daha az karbondioksit emisyonu yapan yakıtların araştırılmasını özendirmektedir. Son yıllarda dimetil eter (DME) ve dietil eter (DEE) alternatif temiz enerji kaynaklarının önemlilerindendir. Bu değerli eterler, sırasıyla metil alkol ve etil alkolün, asitik katalizörlerle dehidrasyon reaksiyonu ile üretilmektedir. DEE'in yanısıra petrokimya endüstrisinde önemli bir ürün ve girdi olan etilen de etil alkolün dehidrasyon reaksiyonu sonucu oluşmaktadır.

Çalışmanın ilk aşamasında Tungstofosforik asit (TPA), Silikotungstik asit (STA) ve Molibdofosforik asitin etil alkolün dehidrasyon reaksiyonunda katalitik aktiviteleri test edilmiştir. Ayrıca diğer katı asit katalizörlerden Nafyon ve Aluminosilikat da aynı reaksiyonda çalışılmıştır. Heteropoli asitlerden STA ve TPA ve aluminosilikat metil alkol dehidrasyon reaksiyonu ile DME üretiminde kullanılmıştır. Bu çalışmayla silikotungstik asitin alkollerin dehidrasyon reaksiyonlarında en yüksek aktiviteyi gösterdiği tespit edilmiştir. Yüzey alanının

düşük olması ve su, alkol gibi sıvılarda çözünüyor olması nedeniyle bu heteropoliasitin MCM-41 yapısındaki mezogözenekli nanoyapıda bir malzemeyle desteklenmesi amaçlanmıştır. Bu hazırlanan katalizörler yeni silikotunstik asit katalizörler diye adlandırılmıştır.

Sıcaklığın 180°C den 250°Cye çıkarılması ile etilen seçimliliğinde yükselme, buna karşın DEE seçimliliğinde düşüş görülmektedir. Ortamda suyun bulunması TPA katalizörünün aktivitesinde azalmaya neden olmaktadır. Mezogözenekli yapıdaki aluminasilikat kullanıldığında ise 450°C’de yüksek DME verimi elde edilmektedir.

Heteropoliasitlerin yüzey alanlarının düşük olması ve alkol, su gibi polar çözücülerde çözünmesi göz önüne alınarak hidrothermal yöntem ile yeni mezogözenekli silikotungstik asit tabanlı yüksek yüzey alanına sahip katalizörler sentezlenmiştir. Bu katalizörler XRD, EDS, SEM, TGA, DTA, DSC, FTIR ve azot adsorplanma teknikleri kullanılarak karakterize edildi ve katalitik aktiviteleri etil alkol dehidrasyon reaksiyonu ile test edilmiştir. Katalizörlerin aktivitelerinde kalsinasyon sıcaklığının önemli bir etkisi olduğu görülmüştür. 375°C üzerinde meydana gelen kısmi parçalanma ve proton kaybı düşünülerek katalizörler 350°C ve 550°’ de kalsine edilmiştir. Hazırlanan katalizörlerden W/Si oranı 0.19 olan katalizörün 481m²/g (STA62(550)), bu oranın 0.34 olduğu diğer katalizörün ise 210m²/ yüzey alanına sahip olduğu belirlenmiştir.

Katalizörlerden 350°C’de kalsine edilenlerin 180°C gibi düşük sıcaklıklarda da yüksek aktivite gösterdiği; buna rağmen 550°C de kalsine edilenlerin 280°C üzerinde aktif oldukları görülmüştür. 350°C de kalsine edilen katalizör ile 0.90’a varan etilen verimi 350°C civarında kaydedilmiştir. Reaksiyonlarda DEE veriminin bir tepe noktasından geçiyor olması yüksek sıcaklıklarda DEE’nin etilene dönüştüğünü buna karşın düşük sıcaklıklarda etilen ve DEE’nin paralel reaksiyonla oluştuğunu ortaya koymuştur. DRIFTS çalışması reaksiyon mekanizması ile ilgili birçok önemli bulgulara ulaşılmasını sağlamıştır.

Anahtar Kelimeler: Heteropoli asit, silikotungstik asit, Dietil eter, Dimetil Eter, Etilen, MCM-41

To my beloved family,

ACKNOWLEDGEMENTS

First of all, I would like to express my deepest appreciation to my supervisor Prof. Dr. Timur Doğu for his guidance, his suggestions, his encouragement, his motivation and for his help in every aspect in my graduate study. Also, I would like to express greatest thanks especially his kindly attitude, like a father, related with not only my thesis but also in every subject throughout this time interval.

Also, I would like to express my greatest appreciation to my co-supervisor Prof Dr. Gülşen Doğu for her continuous encouragement, her guidance, her discussions and her kindly attitude to me related with every subject. It is great pleasure for me to work with Mr. and Ms. Doğu, to learn lots of things related to Chemical Engineering.

I would like to express my thanks to Prof. Dr. H. Tunçer Özdamar for his valuable discussions, suggestions, comments and his great encouragement during this study. I would like to thank to Assoc. Prof. Dr. Naime Aslı Sezgi for her support, her encouragement, for sharing her knowledge with me, for her kindly attitude to me at ever time and for help.

I would like to express special thanks to Özge Oğuzer for her friendship, for her support every time and to Zeynep Obalı helping me every time I need and for her friendship; to Canan Şener especially for sharing with me her knowledge in catalysis study, to Almıla Bahar, İsmail Doğan, Işıl Severcan, Mustafa Dokucu, Ekin Özdoğan, Ceren Oktar Doğanay, Eda Çelik, Işıl Işık, Burcu Mirkelamoğlu and to my friends that I could not write them all down here, for their good friendships for sharing me your knowledge experience for sparing good time during the thesis study.

I would like to express my sincere thanks to Dr. Yeřim Glbilmez, Dr. Nezahat Boz and Dr. Glsn Karamullaoęlu for their support, for the knowledge and experience they have shared with me and their greatfull friendship

I would like to thank Glten Orakęı for BET analysis, Mhrican Aęıkęz for TGA and DSC analysis.

I would like to thank METU Central Laboratories for Supercritical Fluid Extraction, FTIR, NMR and Nitrogen Adsorption Analysis.

Special thanks to Assoc.Prof.Dr. Nuray Oktan, Assoc.Prof. Sena Yaşyerli from Gazi University for their supports.

I am also very grateful to my family for their endless love, support, encouragement.

Finally, Governmental Planning Organization was also gratefully acknowledged for the research fund BAP-03-04-DPT2003(06K12092017) and TUBITAK for the research fund 106M073 for their financial supports.

TABLE OF CONTENTS

ABSTRACT	iv
ÖZ	vi
DEDICATION	viii
ACKNOWLEDGEMENTS	ix
TABLE OF CONTENTS	xi
LIST OF TABLES.....	xvi
LIST OF FIGURES.....	xvii
LIST OF SYMBOLS.....	xxv
CHAPTER	
1 INTRODUCTION	1
2 ALTERNATIVE FUELS	3
2.1 Two Important Problems of the World	3
2.2 Alternative Clean Sources for Fuels and Petrochemicals	4
3 CATALYTIC DEHYDRATION OF ETHANOL	9
3.1 Synthesis of Ethanol	9
3.2 Ethanol Selective Oxidation and Dehydration Reactions	10
4 CATALYTIC DEHYDRATION OF METHANOL.....	12
4.1 Synthesis of Methanol	12
4.2 Physical Properties of DME	13
4.3 Direct Synthesis of DME from Syngas.....	15
4.4 Methanol Dehydration Reaction to Produce DME	17
5 HETEROPOLYACID CATALYSTS	19
5.1 Properties of Heteropolyacids	19
5.2 Supported Heteropolyacids	23
5.3 Heteropolyacids in Dehydration of Alcohols	28
6 MESOPOROUS MATERIALS	30

6.1 Formation of MCM-41	30
6.2 Characterization of MCM-41	32
6.3 MCM-41 Incorporated Heteropolyacid Catalysts	37
7 EXPERIMENTAL STUDIES for ALCOHOL DEHYDRATION REACTIONS.....	39
7.1 Experimental Setup.....	40
7.2 Chemicals and Experimental Conditions.....	41
7.3 Analytical Method	44
8 EXPERIMENTAL STUDIES FOR NOVEL MESOPOROUS CATALYST SYNTHESIS FOR ALCOHOL DEHYDATION	45
8.1 Synthesis of MCM-41.....	46
8.1.1 Chemicals	46
8.1.2 Procedure	46
8.2 Novel Silicotungsticacid Catalysts by Direct Hydrothermal Synthesis	47
8.2.1 Chemicals	48
8.2.2 Procedure	49
8.3 Novel Silicotungstic Acid Catalysts by Impregnation Method	51
8.3.1 Chemicals	52
8.3.2 Procedure (1)	53
8.3.3 Procedure (2)	53
8.3.4 Procedure (3)	54
8.4 Characterization of Novel Catalysts.....	55
8.4.1 X-Ray Diffraction (XRD)	55
8.4.2 Nitrogen Adsorption	55
8.4.3 Energy Dispersive Spectrum (EDS)	55
8.4.4 Scanning Electron Microscopy (SEM)	56
8.4.5 Thermal Analysis (TGA, DTA, DSC).....	56
8.4.6 Fourier Transform Infrared Spectroscopy (FT-IR)	56
8.4.7 Diffuse Reflectance FT-IR (DRIFTS)	56
9 RESULTS of ALCOHOL DEHYDRATION REACTIONS WITH COMMERCIAL CATALYSTS	57
9.1 Ethanol Dehydration Reaction over Tungstphosphoric Acid	58
9.1.1 Effects of Reaction Temperature	60
9.1.2 Effects of Feed Composition	61
9.1.3 Effects of Water Present in the Feed Stream.....	65
9.1.4 Effects of Space Time	67
9.2 Ethanol Dehydration Reaction over Different HPA Catalysts	69
9.3 Ethanol Dehydration Reaction over Nafion	71

9.4 Ethanol Dehydration Reaction over Mesoporous Aluminosilicate	74
9.5 Methanol Dehydration Reaction over STA.....	76
9.5.1 Effects of Reaction Temperature	76
9.6 Methanol Dehydration Reaction over TPA.....	78
9.7 Methanol Dehydration Reaction over Aluminosilicate	81
10 RESULTS of CHARACTERIZATION of NOVEL MESOPOROUS SILICOTUNGSTIC ACID CATALYSTS	84
10.1 Characterization of MCM-41 Catalyst	84
10.1.1 XRD Patterns	84
10.1.2 Nitrogen Physisorption	85
10.2 Characterization of STA52.....	86
10.2.1 XRD.....	87
10.2.2 EDS.....	87
10.2.3 Nitrogen Adsorption.....	88
10.3 Characterization of STA62.....	89
10.3.1 XRD Patterns	90
10.3.2 EDS Results.....	94
10.3.3 SEM.....	94
10.3.4 Nitrogen Physisorption	95
10.3.5 FTIR	97
10.4 Characterization of STA72.....	98
10.4.1 XRD Patterns	99
10.4.2 EDS.....	101
10.4.3 SEM.....	102
10.4.4 Nitrogen Physisorption	102
10.5 Characterization of STA8 Catalysts.....	103
10.5.1 XRD.....	106
10.5.2 EDS.....	107
10.5.3 SEM.....	107
10.5.4 Nitrogen Physisorption	107
10.5.5 FTIR	111
10.6 Characterization of STA92.....	112
10.6.1 XRD.....	113
10.6.2 EDS.....	114
10.6.3 SEM.....	114
10.6.4 Nitrogen Physisorption	117
10.6.5 FTIR	118

10.7 Comparison of Catalysts Prepared with Direct Hydrothermal Synthesis	119
10.7.1 Thermal Analysis of the Synthesized Catalysts	120
10.8 Characterization of STA impregnated on MCM41 Catalysts ...	124
10.8.1 XRD.....	124
10.8.2 EDS.....	125
10.8.3 Nitrogen Physisorption	125
10.9 Characterization of STA impregnated on Aluminosilicate	127
10.9.1 XRD.....	127
10.9.2 Nitrogen Adsorption.....	128
11 RESULTS OF ETHANOL DEHYDRATION OVER NOVEL SILICOTUNGSTIC ACID CATALYSTS SYNTHESIZED IN THIS WORK	131
11.1 Results obtained with STA52	131
11.2 Results obtained with STA62	133
11.2.1 Effect of Reaction Temperature	134
11.2.2 Effect of Space Time.....	136
11.2.3 The Effect of Calcination Temperature.....	139
11.3 Results obtained with STA72	144
11.4 Results obtained with STA82	146
11.4.1 The effect of Reaction Temperature	146
11.4.2 The effect of Calcination Temperature.....	148
11.4.3 The effect of Washing Step of Catalyst Synthesis using Different Solvents	153
11.5 Results obtained with STA92	158
11.5.1 The effect of Reaction Temperature	158
11.5.2 The effect of Space Time.....	160
11.5.3 The effect of Calcination Temperature.....	164
11.6 Comparison of these catalysts	168
11.7 Results obtained with STA impregnated MCM41	176
11.8 Results obtained with STA impregnated on Aluminosilicate...	180
12 RESULTS OF REACTION MECHANISM	183
13 CONCLUSION.....	188
REFERENCES.....	191
APPENDICES	
A CALIBRATION of GAS CHROMATOGRAPH	
A.1 Calibration Factor for DEE.....	199
A.2 Calibration Factor for Ethylene	200

A.3 Calibration Factor for Water	201
B SAMPLE CALCULATION.....	202
C SAMPLE of EDS CHARACTERIZATION RESULT	204
C.1 Sample of EDS Result of STA92(550)	204
VITA	205

LIST OF TABLES

Table 7.1 Summary of experimental conditions for ethanol dehydration reactions with commercial catalyts.....	43
Table 7.2 Summary of experimental conditions for methanol dehydration reactions with commercial catalysts	43
Table 7.3 Summary of experimental conditions for ethanol dehydration reactions over novel mesoporous silicotungstic acid catalysts	44
Table 8.1 Experimental Conditions in Direct hydrothermal Synthesis of Novel Silicotungstic acid Catalysts	51
Table 8.2 Catalysts synthesized by impregnation method.....	52
Table 10.1 EDS analysis results of STA5 catalyst.....	88
Table 10.2 The difference in synthesis procedure for STA6 samples.....	90
Table 10.3 EDS analysis results of STA6 catalyst.....	94
Table 10.4 EDS analysis results of STA7 catalysts	101
Table 10.5 The difference in synthesis procedure for STA8 samples.....	105
Table 10.6 EDS analysis results of STA8	108
Table 10.7 EDS analysis results of STA9 catalysts	115
Table 10.8 Characterization results of catalysts prepared with direct hydrothermal synthesis method.....	119
Table 10.9 EDS analysis results of samples prepared with impregnation	125
Table A.1 Calibration Results	201

LIST OF FIGURES

Figure 5.1. Heteropoly anion with Keggin Structure, $PW_{12}O_{40}^{3-}$ Primary and Secondary Structure (Adapted from Corma, 1995)	20
Figure 6.1. Liquid-crystal templating mechanism (LCT) for the formation of MCM-41 (Adapted from Ciesla and Schüth, 1999)	31
Figure 6.2 XRD pattern corresponding to MCM41 (Adapted from Ciesla and Schüth, 1999)	33
Figure 6.3 Nitrogen Adsorption Isotherm for MCM-41 (Adapted from Ciesla and Schüth, 1999)	34
Figure 7.1. Experimental Set-Up	41
Figure 8.1 Synthesis Procedure of MCM-41	47
Figure 8.2 Direct Hydrothermal Synthesis Procedure	48
Figure 8.3 Common steps in Impregnation Method	52
Figure 9.1 The variation in conversion of ethanol and selectivities of products, using 0.2 g of TPA, EtOH/(EtOH&He):0.05	60
Figure 9.2 The variation in yields of products using 0.2 g of TPA, EtOH/(EtOH&He):0.05	61
Figure 9.3 The variation in conversion of ethanol with reaction temperature at different feed compositions, using 0.2 g of TPA	62
Figure 9.4 The variation in conversion of ethanol with feed composition, using 0.2 g of TPA	63
Figure 9.5 The variation in selectivity of Ethylene with feed composition, using 0.2 g of TPA	64
Figure 9.6 The variation in selectivity of DEE with feed composition, using 0.2 g of TPA	64
Figure 9.7 The variation in conversion of ethanol with the presence of water in the feed stream using 0.2 g of TPA	65
Figure 9.8 The variation in selectivities of products with the presence of water in the feed stream using 0.2 g TPA	66
Figure 9.9 The variation in yields of products with the presence of water in the feed stream using 0.2 g of TPA	66

Figure 9.10 The variation in conversion of ethanol with the amount of catalyst, EtOH/(EtOH&He):0.48.....	68
Figure 9.11 The variation in selectivity of ethylene with the amount of catalyst, EtOH/(EtOH&He):0.48.....	68
Figure 9.12 The variation in selectivity of DEE with the amount of catalyst, EtOH/(EtOH&He):0.48.....	69
Figure 9.13 The variation in ethanol conversion using different heteropolyacids, EtOH/(EtOH&He):0.48, 0.2 g of catalyst.....	70
Figure 9.14 The variation in selectivities of products using different heteropolyacids, EtOH/(EtOH&He):0.48, 0.2 g of catalyst.....	71
Figure 9.15 The variation in ethanol conversion using Nafion, EtOH/(EtOH&He):0.48, 0.2 g catalyst.....	73
Figure 9.16 The variation in selectivities of products using Nafion, EtOH/(EtOH&He):0.48, 0.2 g catalyst.....	73
Figure 9.17 The variation in selectivities of products using Nafion, EtOH/(EtOH&He):0.48, 0.2 g catalyst.....	74
Figure 9.18 The variation in conversion of ethanol, using 0.1 g of Aluminosilicate, EtOH/(EtOH&He):0.48.....	75
Figure 9.19 The variation in selectivities of products, using 0.1 g of Aluminosilicate, EtOH/(EtOH&He):0.48.....	75
Figure 9.20 The variation in yield of products using 0.1 g of Aluminosilicate, EtOH/(EtOH&He):0.48.....	76
Figure 9.21 The variation in conversion of methanol, using 0.2 g of STA, MeOH/(MeOH&He):0.48	77
Figure 9.22 The variation in product selectivities with temperature, using 0.2 g of STA, MeOH/(MeOH&He):0.48	78
Figure 9.23 The variation in conversion of methanol using 0.2 g of different heteropolyacids, MeOH/(MeOH&He):0.48	79
Figure 9.24 The variation in selectivity of DME using 0.2 g of different heteropolyacids, MeOH/(MeOH&He):0.48	79
Figure 9.25 The variation in selectivity of formaldehyde using 0.2 g of different heteropolyacids, MeOH/(MeOH&He):0.48.....	80
Figure 9.26 The variation in selectivity of ethylene using 0.2 g of different heteropolyacids, MeOH/(MeOH&He):0.48	80
Figure 9.27 The variation in conversion of methanol using 0.1 g of Aluminosilicate in comparison with STA, MeOH/(MeOH&He):0.48 .	81
Figure 9.28 The variation in selectivity of DME using 0.1 g of Aluminosilicate in comparison with STA, MeOH/(MeOH&He):0.48	82

Figure 9.29 The variation in selectivity of Formaldehyde using 0.1 g of Aluminosilicate in comparison with STA, MeOH/(MeOH&He):0.48 .	82
Figure 9.30 The variation in yield of DME using 0.1 g of Aluminosilicate in comparison with STA, MeOH/(MeOH&He):0.48	83
Figure 10.1 XRD patterns of calcined MCM-41	85
Figure 10.2 Nitrogen isotherms of calcined MCM-41	86
Figure 10.3 Pore size distribution of calcined MCM-41	86
Figure 10.4 XRD patterns of STA52(550)	87
Figure 10.5 Isotherm plot of STA52(550)	88
Figure 10.6 Pore size distribution of STA52(550).....	89
Figure 10.7 XRD patterns of STA62(550) at 2 θ values upto 50	91
Figure 10.8 Low-angle XRD patterns of STA62(550)	91
Figure 10.9 XRD patterns of pure Silicotungstic acid	92
Figure 10.10 XRD patterns of STA61 and STA62	92
Figure 10.11 XRD patterns of STA62 before calcination and after calcined at different temperatures	93
Figure 10.12 SEM images of STA62(550)	95
Figure 10.13 Nitrogen isotherms of STA62(550)	96
Figure 10.14 Pore size distribution of STA62(550)	96
Figure 10.15 Nitrogen isotherms of STA62(350)	97
Figure 10.16 BJH adsorption pore size distribution of STA62(350)	97
Figure 10.17 FTIR result of uncalcined STA62	98
Figure 10.18 FTIR result of STA62(550)	98
Figure 10.19 XRD patterns of STA72(550)	99
Figure 10.20 Low-angle XRD patterns of STA72(550)	100
Figure 10.21 XRD patterns of uncalcined STA72.....	100
Figure 10.22 SEM photographs of STA72(550).....	102
Figure 10.23 Isotherm linear plot for STA72(550)	103
Figure 10.24 Pore size distribution of STA72(550)	103
Figure 10.25 XRD patterns of STA82 before and after the calcination at different temperatures	106
Figure 10.26 XRD patterns of STA8 washed with different methods	107
Figure 10.27 SEM images of STA82(550) (1)	109
Figure 10.28 SEM images of STA82(550) (2)	109
Figure 10.29 Isotherm linear plot for STA82(550)	110
Figure 10.30 Isotherm linear plot for STA82(350)	110
Figure 10.31 The Pore size distribution of STA82(550)	111
Figure 10.32 The Pore size distribution of STA82(350)	111

Figure 10.33 The FTIR of uncalcined STA82.....	112
Figure 10.34 The FTIR of STA82(550).....	112
Figure 10.35 XRD patterns of STA91(550) and STA92(550).....	113
Figure 10.36 XRD patterns of STA92 before and after calcined at different temperatures	114
Figure 10.37 SEM images of STA92(550), (Magnification X5,000)	115
Figure 10.38 SEM images of STA92(550) (Magnification X1,000)	116
Figure 10.39 SEM images of STA92(475)	116
Figure 10.40 Isotherm Linear Plot of STA92(550).....	117
Figure 10.41 The Pore Size Distribution of STA92(550).....	117
Figure 10.42 FTIR plot of uncalcined STA92.....	118
Figure 10.43 FTIR plot of STA92(475)	118
Figure 10.44 FTIR plot of STA92(550)	119
Figure 10.45 TGA Result of uncalcined STA62.....	121
Figure 10.46 TGA of uncalcined STA82	122
Figure 10.47 TGA of uncalcined STA92	122
Figure 10.48 DSC of uncalcined STA82	123
Figure 10.49 DSC of uncalcined STA92	123
Figure 10.50 XRD patterns of STA imp MCM41 catalysts	124
Figure 10.51 The isotherm for STAMCM41U.....	126
Figure 10.52 The isotherm for STAMCM41C.....	126
Figure 10.53 The pore size distribution of different STA impregnated on MCM41.....	127
Figure 10.54 XRD patterns of Pure aluminosilicate	128
Figure 10.55 XRD patterns of STA impregnated aluminosilicate.....	128
Figure 10.56 Isotherm of pure aluminosilicate	129
Figure 10.57 Isotherm of STA impregnated aluminosilicate	129
Figure 10.58 Pore size distribution for STA impregnated aluminosilicate.....	130
Figure 11.1 The variation in ethanol conversion with 0.1 g of STA52, EtOH/(EtOH&He):0.48.....	132
Figure 11.2 The variation of selectivities of products with 0.1 g of STA52, EtOH/(EtOH&He):0.48.....	133
Figure 11.3 The variation in ethanol conversion with 0.2 g STA62(550), EtOH/(EtOH&He):0.48.....	134
Figure 11.4 The variation in product selectivities with 0.2 g of STA62(550) EtOH/(EtOH&He):0.48.....	135
Figure 11.5 The variation in product yields with 0.2 g of STA62(550) EtOH/(EtOH&He):0.48.....	136

Figure 11.6 The variation in ethanol conversion with the amount of STA62(550), EtOH/(EtOH&He):0.48.....	137
Figure 11.7 The selectivity profiles with 0.1 g of STA62(550), EtOH/(EtOH&He):0.48.....	138
Figure 11.8 The variation in DEE selectivity with amount of STA62(550), EtOH/(EtOH&He):0.48.....	138
Figure 11.9 The variation in DEE selectivity with amount of STA62(550), EtOH/(EtOH&He):0.48.....	139
Figure 11.10 The effect of calcination temperature on activity of STA62 catalysts, EtOH/(EtOH&He):0.48, catalyst amount:0.2 g	140
Figure 11.11 The variation in selectivities of products with 0.2 g of STA62(350) EtOH/(EtOH&He):0.48.....	141
Figure 11.12 The effect of calcination temperature of STA62 on selectivity of DEE, EtOH/(EtOH&He):0.48, catalyst amount: 0.2 g	141
Figure 11.13 The effect of calcination temperature of STA62 on yield of DEE, EtOH/(EtOH&He):0.48, catalyst amount: 0.2 g.....	142
Figure 11.14 The effect of calcination temperature of STA62 on selectivity of Ethylene, EtOH/(EtOH&He):0.48, catalyst amount: 0.2 g.....	142
Figure 11.15 The effect of calcination temperature of STA62 on yield of Ethylene, EtOH/(EtOH&He):0.48, catalyst amount 0.2 g.....	143
Figure 11.16 The effect of calcinations temperature of STA62 on selectivity of Acetaldehyde, EtOH/(EtOH&He):0.48	143
Figure 11.17 The effect of calcinations temperature of STA62 on yield of Acetaldehyde, EtOH/(EtOH&He):0.48	144
Figure 11.18 The conversion profile of ethanol over 0.1 g of STA72(550) EtOH/(EtOH&He):0.48.....	145
Figure 11.19 The selectivity profile of productsI over 0.1 g of STA72(550) EtOH/(EtOH&He):0.48.....	145
Figure 11.20 The variation of conversion over 0.2 g STA82(550) EtOH/(EtOH&He):0.48.....	147
Figure 11.21 The variation in selectivities of products over 0.2 g STA82(550) EtOH/(EtOH&He):0.48.....	147
Figure 11.22 The variation in yields of products over 0.2 g STA82(550) EtOH/(EtOH&He):0.48.....	148
Figure 11.23 The effect of calcination temperature on ethanol conversion, 0.2g of STA82 calcined at 350 & 550°C.....	149
Figure 11.24 The effect of calcinations temperature on DEE selectivity, 0.2g of STA82, calcined at 350 & 550°C.....	149

Figure 11.25 The effect of calcination temperature on Ethylene selectivity, 0.2g of STA82, calcined at 350 & 550°C	150
Figure 11.26 The effect of calcination temperature on acetaldehyde selectivity, 0.2g of STA82, calcined at 350 & 550°C.....	151
Figure 11.27 The effect of calcination temperature on DEE yield, 0.2g of STA82, calcined at 350 & 550°C	151
Figure 11.28 The effect of calcination temperature on Ethylene yield, 0.2g of STA82, calcined at 350 & 550°C	152
Figure 11.29 The effect of calcination temperature on Ethylene yield, 0.2g of STA82, calcined at 350 & 550°C	152
Figure 11.30 The effect of washing step on ethanol conversion with 0.2g of STA81 treated	153
Figure 11.31 The effect of washing step on DEE selectivity with 0.2g of STA81 treated	154
Figure 11.32 The effect of washing step on Ethylene selectivity with 0.2g of STA81 treated	154
Figure 11.33 The effect of washing step on Acetaldehyde selectivity with 0.2g of STA81 treated	155
Figure 11.34 The effect of washing step on DEE yield with 0.2g of STA81 treated	155
Figure 11.35 The effect of washing step on Ethylene yield with 0.2g of STA81 treated	156
Figure 11.36 The effect of washing step on Acetaldehyde yield with 0.2g of STA81 treated	156
Figure 11.37 The conversion profile for catalyst both washed and extracted with CO ₂ , 0.1 g of catalyst	157
Figure 11.38 The yield of proucts for catalyst both washed and extracted with CO ₂ , 0.1 g of catalyst	157
Figure 11.39 The variation in ethanol conversion with 0.2 g of STA92(550), EtOH/(EtOH&He):0.48.....	159
Figure 11.40 The variation in product selectivities with 0.2 g of STA92(550), EtOH/(EtOH&He):0.48.....	159
Figure 11.41 The variation in product yield with 0.2 g of STA92(550), EtOH/(EtOH&He):0.48.....	160
Figure 11.42 The variation in ethanol conversion with amount of STA92(550), EtOH/(EtOH&He):0.48.....	161
Figure 11.43 The variation in DEE selectivity with amount of STA92(550), EtOH/(EtOH&He):0.48.....	162

Figure 11.44 The variation in Ethylene selectivity with amount of STA92(550), EtOH/(EtOH&He):0.48.....	162
Figure 11.45 The variation in Acetaldehyde selectivity with amount of STA92(550), EtOH/(EtOH&He):0.48.....	163
Figure 11.46 The variation in DEE yield with amount of STA92, EtOH/(EtOH&He):0.48.....	163
Figure 11.47 The variation in Ethylene yield with amount of STA92, EtOH/(EtOH&He):0.48.....	164
Figure 11.48 The variation in ethanol conversion with 0.2g of STA92, calcined at different temperatures	165
Figure 11.49 The effect of calcination temperature on DEE selectivity with 0.2g of STA92, calcined at different temperatures	165
Figure 11.50 The effect of calcination temperature on Ethylene selectivity with 0.2g of STA92, calcined at different temperatures.....	166
Figure 11.51 The effect of calcination temperature on acetaldehyde selectivity with 0.2g of STA92, calcined at different temperatures.....	166
Figure 11.52 The effect of calcination temperature on DEE yield with 0.2g of STA92, calcined at different temperatures	167
Figure 11.53 The effect of calcination temperature on Ethylene yield with 0.2g of STA92, calcined at different temperatures	167
Figure 11.54 The effect of calcination temperature on Ethylene yield with 0.2g of STA92, calcined at different temperatures	168
Figure 11.55 Comparison of ethanol conversion by using 0.2g of different novel catalysts calcined at 550°C, EtOH/(EtOH&He): 0.48.....	169
Figure 11.56 Comparison of ethanol conversion by using 0.2g of different novel catalysts calcined at 350°C, EtOH/(EtOH&He): 0.48.....	170
Figure 11.57 Comparison of DEE selectivity by using 0.2g of different novel catalysts calcined at 550°C, EtOH/(EtOH&He): 0.48	170
Figure 11.58 Comparison of DEE selectivity by using 0.2g of different novel catalysts calcined at 350°C, EtOH/(EtOH&He): 0.48	171
Figure 11.59 Comparison of Ethylene selectivity by using 0.2g of different novel catalysts calcined at 550°C, EtOH/(EtOH&He): 0.48.....	171
Figure 11.60 Comparison of Ethylene selectivity by using 0.2g of different novel catalysts calcined at 350°C, EtOH/(EtOH&He): 0.48.....	172
Figure 11.61 Comparison of Acetaldehyhde selectivity by using 0.2g of different novel catalysts calcined at 550°C, EtOH/(EtOH&He): 0.48.....	172

Figure 11.62 Comparison of Acetaldehyde selectivity by using 0.2g of different novel catalysts calcined at 350°C, EtOH/(EtOH&He): 0.48.....	173
Figure 11.63 Comparison of DEE yield by using 0.2g of different novel catalysts calcined at 550°C, EtOH/(EtOH&He): 0.48	173
Figure 11.64 Comparison of DEE yield by using 0.2g of different novel catalysts calcined at 350°C, EtOH/(EtOH&He): 0.48	174
Figure 11.65 Comparison of Ethylene yield by using 0.2g of different novel catalysts calcined at 550°C, EtOH/(EtOH&He): 0.48	174
Figure 11.66 Comparison of Ethylene yield by using 0.2g of different novel catalysts calcined at 350°C, EtOH/(EtOH&He): 0.48	175
Figure 11.67 Comparison of Acetaldehyde yield by using 0.2g of different novel catalysts calcined at 550°C, EtOH/(EtOH&He): 0.48.....	175
Figure 11.68 Comparison of Acetaldehyde yield by using 0.2g of different novel catalysts calcined at 350°C, EtOH/(EtOH&He): 0.48.....	176
Figure 11.69 The variation in ethanol conversion at different temperatures using 0.2 g of STA impregnated on MCM-41.....	177
Figure 11.70 The selectivity of DEE at different temperatures using 0.2 g of STA impregnated on MCM41	178
Figure 11.71 The selectivity of ethylene at different temperatures using 0.2 g of STA impregnated on MCM41.....	178
Figure 11.72 The yield of DEE at different temperatures using 0.2 g of STA impregnated on MCM41.....	179
Figure 11.73 The yield of ethylene at different temperatures using 0.2 g of STA impregnated on MCM41	179
Figure 11.74 The ethanol conversion at different temperatures using 0.2 g of STA impregnated on Aluminosilicate	180
Figure 11.75 The selectivities of products at different temperatures using 0.2 g of STA impregnated on Aluminosilicate	181
Figure 11.76 The yield of products at different temperatures using 0.2 g of STA impregnated on Aluminosilicate	181
Figure 12.1 DRIFT spectra obtained at 180 and 350°C	184

LIST OF SYMBOLS

a	Lattice parameter
C_i	Concentration of component i (mol/l)
K	Equilibrium constant
k	Forward reaction rate constant
n	mole number
P	Pressure (Pa)
r	Reaction rate
S	Selectivity
T	Temperature ($^{\circ}\text{C}$)
t	Time (min)
X	Conversion
x	Liquid mole fraction
y	Vapor mole fraction
Y	Yield

Greek Letters

β	Correction factor in the gas chromatography calibration
ε	Stoichiometric coefficient of the components
ρ	Liquid density (kg/m^3)
Θ	Diffraction angle

Subscripts

i	i^{th} component
-----	---------------------------

Superscripts

0	initial
-----	---------

Abbreviations:

BET	Brunauer-Emmet-Teller
BJH	Barret-Joyner-Halenda
DEE	Diethyl Ether
DME	Dimethyl Ether

DRIFT	Diffuse Reflectance FT-IR
DSC	Differential Scanning Calorimetry
DTA	Differential Thermal Analysis
EDS	Energy Dispersive Spectroscopy
FT-IR	Fourier Transform Infrared
HPA	Heteropoly acids
GC	Gas Chromatography
MCM	Mobil Composition of Matter
MPA	Molibdophosphoric Acid
NMR	Nuclear Magnetic Resonance
STA	Silicotungstic Acid
SEM	Scanning Electron Microscopy
TEM	Transmission Electron Microscopy
TPA	Tungstophosphoric Acid
TGA	Thermogravimetric Analysis
XRD	X-Ray Diffraction

CHAPTER 1

INTRODUCTION

Oil reserves on earth are being depleted due to their excessive consumption. Major transportation fuel and petrochemical feedstock shortages are expected in the coming century. Due to these factors, significant researchers are devoted to the development of alternative transportation fuels and petrochemical feedstocks. Alcohols and their derivatives are among the most attractive alternates of petroleum which can serve for both purposes. In this thesis work, ethanol dehydration reaction to produce DEE and Ethylene and methanol dehydration reaction to produce dimethyl ether (DME) were investigated using commercial and novel mesoporous solid acid catalysts synthesized in this work.

Ethanol and methanol are considered as alternative clean energy sources as well as feedstock for petrochemical industry. The properties that make these alcohols and their derivatives (diethyl ether and ethylene from ethanol, dimethyl ether from methanol) so important in this field are summarized in Chapter 2.

The most commonly used process to make ethanol is fermentation of sugars, starch and the wastes of crop and sugar. The direct synthesis of ethanol from CO₂ has attracted the researchers. Studies on this issue as well as catalytic reactions of ethanol, namely selective oxidation and dehydration reactions are given in Chapter 3.

Besides DEE, dimethyl ether (DME) has been considered as an attractive transportation fuel alternate. It is produced either directly from syngas or methanol dehydration reaction. The synthesis of methanol and the properties of

DME is summarized in Chapter 4. In the same chapter, literature survey on direct synthesis of DME from syngas and methanol dehydration reaction are presented.

Due to their high activity than conventional solid acid catalyst, heteropolyacid catalysts are considered in dehydration of alcohols. The properties of heteropolyacids and the studies on their supported form and their usage in alcohol dehydration reactions are summarized in Chapter 5.

Mesoporous materials have become important in the catalyst studies due to their high surface area. MCM-41 is the most important member of mesoporous material. In Chapter 6, the characteristic properties of MCM-41 and their usage as a support for heteropolyacid are summarized.

In this work, dehydration reaction of ethanol to produce DEE and ethylene and dehydration of methanol to produce DME were carried over different catalysts. In Chapters 7, the experimental procedure used for dehydration of alcohol reactions were given.

As indicated in Chapter 5, heteropolyacids have very low surface area and high solubility in polar solvents. It was aimed to synthesize new catalysts having higher surface area and higher stability. The synthesis procedures of novel mesoporous catalysts were given in Chapter 8.

Ethanol and methanol dehydration reactions were carried out using different solid acid catalyst. Results obtained with these experiments and related discussions are given in Chapter 9.

Results of characterization tests applied to novel mesoporous silicotungstic acid catalysts are presented in Chapter 10 and the catalytic activity of these catalysts on ethanol dehydration reaction are given in Chapter 11.

The DRIFTS study on ethanol dehydration reaction mechanism is presented in Chapter 12.

CHAPTER 2

ALTERNATIVE FUELS

2.1 Two Important Problems of the World

Fast depletion of the oil reserves due to their excessive use for energy needs and the global warming are the two of the most important problems of the next century.

Excessive use of fossil fuels as our major energy sources is the main reason of both of these problems. Among the fossil fuels, petroleum is the most convenient fuel to be used in transportation. Therefore, its very high consumption rate took us to the point that the ratio of proven oil reserves to its depletion rate reached to a value of about 40 years (Doğu and Varışlı, 2007). This ratio is reported as about 70 years for natural gas. Although the discovery of new oil and natural gas reserves may increase the duration for complete depletion of these fossil fuels, significant fuel shortage problems are expected in the coming century.

It is presented that, the yearly consumption rates of petroleum and natural gas increased more than 200 times during the last century. Although the shares of petroleum and natural gas were only about 2 % and 1 % of total energy consumption 100 years ago, today these shares increased to about 38 % and 23 %, respectively (Song, 2006).

The increase of carbon dioxide concentration in the atmosphere is considered as the most important reason for global warming. There is an increasing trend in the world energy use and also in the yearly CO₂ emission

rates to the atmosphere. Increase of CO₂ emission rates caused an increase in the atmospheric CO₂ concentration from about 295 ppm to 380 ppm during the last century. Also, an increase of about 0.6 °C was reported on the earth's surface temperature during the same period (Song, 2006).

The major consumption of petroleum is due to its excessive use in transportation. About 57 % of oil was consumed for transportation purposes (Olah et al., 2006). Its fast depletion rate will also cause a major problem in the synthesis of many of the petrochemical products we use in everyday life. Actually, petroleum and natural gas are too valuable raw materials to be burned wastefully for mobile and stationary energy needs.

2.2 Alternative Clean Sources for Fuels and Petrochemicals

The volumetric heating value and octane number are very important parameters for an alternative fuel for gasoline. The volumetric heating values of gasoline and diesel fuel, which are the two major transportation fuels, are about 32 and 36 MJ/l, respectively (Olah et al., 2006). Instead of octane number, cetane number is the key parameter for a diesel fuel. Cetane number which is an empirical measure of fuel ignitability is one of the important fuel properties. Fuels with a cetane number of 50 or higher are suitable for compression ignition in diesel engines. Fuels having low cetane number do not perform very well in a diesel cycle engines. For a conventional diesel fuel, cetane number is around 40-55. Fuels with high cetane numbers cause smoother engine operation and less emission of NO_x, particulate matter, hydrocarbons and carbon monoxide.

Ethanol, methanol and number of ethers have very high octane numbers, over 100 (Doğu and Varışlı, 2007). Ethanol with an octane number of 113 and low Reid vapor pressure is considered as an excellent alternate for gasoline. The volumetric heating value of ethanol (about 21 MJ/l) is higher than methanol (which is about 15 MJ/l). Although the low vapor pressure of ethanol is an advantage from the point of view of its loss during fueling the cars, it also causes some problems in cold-start of the engine. Fuel regulations mandate that motor vehicle fuels should have sufficient vapor pressure to cold start even at a temperature of -30 °C. Diethyl ether (DEE), which can be produced by dehydration of ethanol over acidic catalysts, has high vapor pressure and also very high octane number. Consequently, ethanol-DEE mixtures are considered as

excellent gasoline alternates. The latent heat of ethanol is about 3.7 times higher than gasoline, which causes lower temperatures during combustion in the engine. Decrease of engine temperature also causes formation of less amount of NO_x . The engine compression ratio of ethanol using cars is also higher than the compression ratio of gasoline using conventional gasoline. Combustion of alcohols and ethers produce much less unburned hydrocarbons and CO and CO_2 than conventional gasoline. (Doğu and Varışlı, 2007).

Diesel engines are an important source of particulate emissions and smoke. About 0.2 -0.5 % of the fuel mass is emitted as small particulate which is approximately 0.1 μm diameter. This small particulate consists of mainly soot with some additional absorbed hydrocarbon material. The particulate emissions from diesel engines are 15 % of the total emissions whereas that of gasoline derived engines are 5 % of the total emissions (Miller Jothi et al., 2007). Therefore, it is important to reduce oxides of nitrogen, smoke and particulate coming from diesel engine in an environmental standpoint.

In a conventional diesel engine, fuels like vegetable oils having high cetane number can be used directly in neat form. LPG has a high octane rating and is therefore well suited for gasoline derived engine. It has good burning characteristics and it is easy to store. But in conventional diesel engine, burning LPG has a difficulty in self-ignition because the cetane number of LPG is very low (<3) and so it will not ignite within the time available in an engine cylinder. Therefore, if LPG is to be used as an alternate to diesel, the cetane rating needs to be improved. Adding a cetane number improver to LPG is one of the solution for this problem. Ethers and oxygenates are known to be effective cetane improvers. Oxygenates based ignition improvers like DME, DEE which has a self ignition temperature of 160°C are effectively used to enhance the cetane number and ignition quality (Miller Jothi et al., 2007). Alcohols such as ethanol also can be used with DEE as an ignition improver in conventional diesel engine.

Cetane numbers of dimethyl-ether (DME) and especially DEE are impressively higher than premium diesel fuel (Doğu and Varışlı, 2007), while ethanol, methanol, methane and propane have very low cetane numbers. Besides the cetane number, flash point and pour point temperatures are also some of the important parameters for a diesel fuel. DME and DEE can be considered as excellent alternates for compression-ignition engine fuels. They can also be used as fuel blending oxygenates. DEE was also reported to have

good cloud point depression properties of diesel fuel (Suppes et al., 1998). DME is reported as a non-toxic and environmentally benign diesel fuel alternate, resulting low NO_x emissions in premixed combustion (Song et al., 204).

Tests with fuel blends of DME added to propane (LPG), natural gas, and n-butane have been conducted and it is founded that DME shows a zero level in NO_x emissions and a good ignition quality as an ignition additive in HCCL (homogeneous charge compression ignition) LPG engine. The performance, combustion and emission characteristic were investigated also by using LPG as a primary fuel with DEE as an ignition enhancer in a direct diesel engine. At full load, NO emission is reduced 65 % as compared to that of diesel operation due to temperature drop of cylinder charge. Since LPG has a lower carbon/hydrogen ratio and it contains low molecular weight as well as lesser number of carbon-carbon bonds as compared to diesel, there is a reduction in smoke and particulate emissios, reaching to maximum values of 85 % and 89 %, respectively. Whereas it is observed that CO and HC emissions are higher than that of diesel at part loads due to lower cylinder charge temperature. This incomplete combustion of LPG air mixture can be decreased with increase in load. Also, due to lower carbon to hydrogen ratio, CO₂ levels for LPG operation is lower than diesel operation (Miller Jothi et al., 2007).

The highly adventegous properties of DME, DEE and DME/methanol, DEE/ethanol blends as alternative transportation fuels were discussed above. On board conversion of methanol to DME or ethanol to DEE using catalysts with acidic character is a proposed technology for future motor vehicles.

Acidic catalysts such as Nafion, Al₂O₃ and heteropolyacids may be used for the dehydration of ethanol and methanol to DEE and DME, respectively. It was also reported that H-ZSM5 showed good activity for vapor phase dehydration of methanol to DME in the presence of water vapor (Vishwanathan et al., 2004). Activities of Cs salt and titania supported molybdophosphoric and molybdovanadophosphoric acid catalysts in dehydration of alcohols were also illustrated in the literature (Damyanova et al., 1999; Yang et al., 2000). Generally, acid catalysts show high activity in dehydration of ethanol to DEE and ethylene, while basic catalysts act to dehydrogenate ethanol to produce acetaldehyde. In the dehydration reaction, alcohols are considered to adsorb on an acid site forming ethoxy or methoxy species in DEE or DME synthesis, respectively. The work of Damyanova et al. (1999) indicated that incorporation

of Ni into the heteropolyacid structure improved the dehydrogenation selectivity by decreasing the dehydration selectivity of methanol.

For heavy-duty transport industry, the diesel cycle engine is the chosen one due to its fuel efficiency, durability and reliability. Researchs and developments have been supported in diesel engine technologies to enable heavy-duty trucks to continue operating efficiently with meeting EPA emissions standarts proposed. According to researches, diesel engines can run on alternative fuels such as natural gas, methanol, ethanol, DME, DEE and biodiesel, with lower efficiency as compared to petroleum derived-diesel fuel. To use alternative fuels for heavy duty trucks, the important points that needs to be considered are being a cost-competitive fuel, having a reliable supply and having a distribution infrastructure. Also, the cost and expected service life of engines are also important in commercial applications. Therefore, to produce fuel which has the properties suitable for the heavy duty diesel cycle engine from plentiful feedstocks, is the main subject for future fuels. Nonpetroleum resources such as natural gas, coal and biomass can be converted into fuels which are appropriate for diesel engine. Cetane number, energy density, emission characteristics and being cost competitive are the common diesel specifications. It is known that coal can be converted to diesel fuels by Fischer-Tropsch (FT) synthesis. The same process also can be used to convert natural gas (methane) to FT diesel fuel. Synthesis gas which is a mixture of carbon monoxide and hydrogen can be produced by gasification of biomass, and from this syngas a number of high quality fuels appropriate for compression ignition engines can be made, such as DME and FT diesel. If the alternative fuel which have the required diesel specifcation, uses the existing fuel infrastructure and can be used by a one energy conversion system, like diesel engine, this alternative fuel could a significant place in heavy duty transport market (Eberhardt, 1997).

Methanol and ethanol are considered as alternative energy sources, as well as starting feedstock for the production of number of petrochemicals. Ethylene is a key feedstock for the petrochemical industry. It is produced by the steam cracking of hydrocarbons such as naphtha and gas oil which occurs at high temperatures and in the presence of steam. There are numerous applications of ethylene and its derivatives. The primary use of polyethylene is in film applications for packaging, carrier bags and trash liners. Over the past 25 years, global demand for ethylene has grown by almost 5% each year. It is reported that this level of growth is over three times higher than the increase in

demand for crude oil (www.shellchemicals.com). In recent studies (Gayubo et al., 2005; Gayubo et al., 2007) it was shown that ethanol and methanol can also be used as feedstock to produce ethylene. Selective oxidation of ethanol over V-MCM-41 type catalysts (Gucbilmez et al., 2006) or dehydration of alcohols over acidic catalysts (Gayubo et al., 2005; Gayubo et al., 2007) are some alternative methods proposed for the production of ethylene.

As a summary, it is important for chemical and petroleum industries to produce desirable, higher value chemicals and fuels from clean, cheap, abundantly available feeds to contribute to the solution of the two major problems of the next century, namely global warming and depletion of oil reserve.

CHAPTER 3

CATALYTIC DEHYDRATION OF ETHANOL

Ethanol which can be produced from plants is called as a renewable source and especially for countries having very efficient farms for sugar beet or corn cultivation is an important and cheap feedstock. Also, it is produced directly from CO₂ which may open new pathways to reduce CO₂ emissions to the atmosphere. As well as it can be used directly as an alternative clean fuel or fuel additive, the products obtained from its dehydration and selective oxidation reactions are also valuable mainly in petrochemical industry and transportation.

In this chapter a literature survey on the synthesis of ethanol and its dehydration and selective oxidation reactions are presented.

3.1 Synthesis of Ethanol

Ethanol is a clear, colorless alcohol which can be obtained from any organic source that contains sugar or starch, using current technology. This includes crops such as corn, rice, wheat, barley, potatoes, sugar beets, and sugar cane. Since ethanol is produced from plants, it is called as a renewable fuel. There are several ways to make ethanol from biomass. The most commonly used process today is fermentation of sugars and starch and the wastes of crop and sugar. This process involves the capture and conversion steps of CO₂ by the green plants through a photosynthesis route (Doğu and Varışlı, 2007).

All over the world, there is a capacity to produce more than 2 billion tonnage of bioethanol. This value is approximately equivalent to 1.3 billion tonnage of petroleum energy. USA and Brazil are the countries having the largest

bioethanol production capacity. China, EC and India follows these countries (Ar, 2006). Turkey has very efficient farms for sugar beet cultivation. In 2005-2006 term, 2.07 million tons of sugar was produced from sugar beets. This amount was 1.4 % of the world production and 9.5 % of EU production. According to these results, there is capacity of our country to produce 2-2.5 million tons of bioethanol from sugar which is equivalent to 70-90 % of our gasoline consumption (Ar, 2006).

Direct synthesis of ethanol from CO_2 through a catalytic route also attracted the attention of researchers (Izumi et al., 1998, Inui et al., 1999). Results obtained with Rh-Se based catalysts supported on TiO_2 , SiO_2 , Al_2O_3 and MgO showed that ethanol synthesis from $\text{CO}_2 + \text{H}_2$ mixtures was observed only when TiO_2 was used as the support, through a path involving acetate species on the catalyst surface (Izumi et al., 1998). Fe/Cu/Zn/Al/K based FT-type catalysts modified by Pd-Ga were shown to give high yields of ethanol due to the hydrogen spillover enhancement of the catalyst by Pd (Inui et al., 1999). In this catalyst, the functions of Fe and Cu were reported as C-C bond formation and OH group insertion.

3.2 Ethanol Selective Oxidation and Dehydration Reactions

Catalytic transformation of ethanol over vanadium/silicate molecular sieves indicated the formation of acetaldehyde, ethylene and DEE (Gucbilmez et al., 2006). Formation of acetaldehyde was mainly due to the involvement of vanadyl species ($\text{V}=\text{O}$), while DEE formation was due to the simultaneous involvement of vanadyl and V-O-Si species on the surface (Kannan et al., 1997). Similar conclusions were reached in our recent work in selective oxidation of ethanol (Gucbilmez et al., 2006). The mechanism of ethanol dehydration and dehydrogenation reactions were also discussed by Golay et al. (1999) and Marin et al. (1998).

In this thesis work, ethanol dehydration reaction was worked and the main products obtained by this reaction are diethyl ether and ethylene. Conventionally, alcohol dehydration reactions can be achieved, by heating the alcohol with strongly acidic compound like H_2SO_4 or H_3PO_4 . Researchers are interested in replacing these hazard liquid acids by environmentally friendly solid acids. Different transition metal catalysts such as titanium oxides (Gao and

Wachs, 1999); magnesium oxides (Di Cosimo et al., 1998; Golay et al., 1999); $\text{Fe}_2\text{O}_3/\text{Al}_2\text{O}_3$ (El-Sharkawy et al 2000); cobalt oxides (Doheim et al., 2002); silver salts of tungstophosphoric acid (Haber et al., 2002), $\text{Fe}_2\text{O}_3, \text{Mn}_2\text{O}_3$ and calcined physical mixture of both ferric and manganese oxides with alumina and /or silica gel (Zaki, 2005) were used for catalytic dehydration reaction of ethanol.

Different heteropolyacid catalysts and their salts such as barium salt of 12-tungstophosphoric acid (Saito and Niiyama, 1987); potassium and silver salts of tungstophosphoric acid and their supported form which were prepared by incipient wetness method using silica as a support (Haber et al., 2002); different types of zeolites such as H-Mordenites, H-ZSM5 zeolites, H-beta-zeolite, H-Y zeolite and silica-alumina (Takahara et al., 2005); as well as gamma-alumina, silica-alumina, aluminophosphate-alumina, phosphoric acid on γ -alumina and on silica (Kito-Borsa and Cowley, 2004) were used in ethanol dehydration reaction.

Different reaction models were proposed for ethanol dehydration reaction (Kito-Borsa and Cowley, 2004; Saito and Niiyama, 1987). Saito and Niiyama, 1987, suggested two kinds of adsorbed ethanol molecules, namely physisorbed and chemisorbed. In their model, physisorbed ethanol behaves like a reservoir of chemisorbed ethanol which was later converted to products. They suggested that ethylene was formed by the decomposition of ethanol while ether was formed with both chemically activated ethanol and the physically sorbed one.

CHAPTER 4

CATALYTIC DEHYDRATION OF METHANOL

In this chapter, a brief information on the properties and the synthesis of methanol is given. After giving the properties of dimethyl ether (DME), the literature survey on the direct synthesis and methanol dehydration reaction to produce DME is presented.

4.1 Synthesis of Methanol

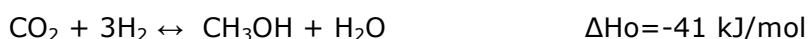
Methanol is the simplest alcohol which is a light, colourless, volatile, flammable, poisonous liquid with a distinctive odor.

It is conventionally produced from synthesis gas over Cu-ZnO based catalysts.



Thermodynamic limitations enforce the use of high pressures over 50 bar in methanol synthesis. For this reaction, copper is considered as the active metal, while ZnO enhances stability, prevents agglomeration of copper and neutralizes the acidity of the alumina support (Doğu and Varışlı, 2007).

Synthesis of methanol directly from CO₂ has attracted significant attention of researchers in recent decade.



Recent studies proved that the activity and the stability of Cu-Zn oxide based catalyst was significantly improved by doping the catalyst with ZrO_2 (Yang et al., 2006; Zhang et al., 2006). ZrO_2 was reported to cause higher copper dispersion in the catalyst structure. ZrO_2 doped catalyst was found to have higher activity and selectivity in the synthesis of methanol from CO_2 , rather than from CO (Yang et al., 2006). Results reported by Sloczynski et al. (2006) proved the significant effect of crystal size of copper on the methanol yield. These studies showed that, the addition of Ga_2O_3 improved the stability of the catalyst and copper dispersion. Their results indicated that, additions of oxides of Ga, B etc. on Cu/ZnO/ ZrO_2 catalyst caused alterations in both the activation energy and also in the number of active centers (Sloczynski et al., 2006). These studies also showed that Cu containing catalysts had much higher activity than Ag and Au containing catalysts (Sloczynski et al., 2004). Different challenging catalytic routes for the synthesis of methanol starting from CO_2 and methane are discussed in the excellent book of Olah and coworkers (2006).

4.2 Physical Properties of DME

DME is a simple oxygenate compound which has been commonly used as an environmentally benign propellant for spray cans. It is a colorless gas at ambient temperature and chemically stable, its flame is visible blue like natural gas and its liquid form is also colorless.

Its boiling point is -25°C and its vapor pressure is 0.6 MPa at 25°C so it can be easily liquefied. It has a liquid viscosity of 0.12-0.15 kg/ms which is in the same range with that of propane or butane. The physical and chemical properties of DME are very close to LPG which consists of mainly propane and butane so it can be stored by using LPG handling technology (Ogawa et al., 2003). Also, the LPG infrastructure can be utilized by changing the sealing materials for DME (Song et al., 2004).

Toxicity study of dimethyl ether in the use of propellant shows that its toxicity is extremely low, which is very similar to that of LPG. Also, this value is lower than that of methanol (Ogawa et al., 2003). Therefore its use is very safe in terms of human health. Besides this advantageous property it is also an environmentally friendly alternative fuel, it does not have any greenhouse effect

and does not cause any ozone layer depletion since it is decomposed in troposphere in several ten hours (Ohno and Omiya, 2003).

DME does not contain sulfur so there is no SO_x emission from its combustion of DME. Also there is no particulate matter or soot formation during the combustion of this alternative fuel. Since DME does not contain carbon-carbon bond in its structure and oxygen content of the molecule is 35% this avoid the formation of particulate matter. Due to this high oxygen content NO_x formation is also low (www.greencarcongress.com). Emissions of hydrocarbons can be oxidized using conventional oxidizing agents.

DME explosion limit is 3.4-17 % while that of butane is 1.9-8.4 % and that of propane is 2.1-9.4 %. This large explosion limit interval makes DME potentially safer than LPG when there is a leakage (www.jfe-holdings.co.jp).

It has a calorific value of 28.90×10^6 J/kg which is 1.37 times higher than that of methanol or 59.44×10^6 J/Nm³ as a gas which is 1.65 times greater than that of methane (Ogawa et al., 2003). On net calorific value basis, 1.6 kg of DME is 1 kg of LPG or in terms of volumetric scale 1.25 m³ of DME is equivalent to 1 m³ of LPG and when it is compared with diesel 1.2 m³ of DME is equivalent to 1 m³ of diesel (Bollon, 2007).

DME is not only a substitute for LPG but also for diesel fuel. DME has a cetane number in the range of 55-60 which is higher than that of diesel having a cetane number of 40-55. So this high cetane number makes it appropriate for diesel engines, some technical difficulties are recognized while using DME in conventional diesel engines due to its low boiling temperature, high vapor pressure, low viscosity and relatively high compressibility. Low viscosity can cause fuel leakage in conventional diesel plunger pump supply system and low efficiency of fuel pressurization. Due to its lower lubricity, wear of moving parts in the fuel injection system are observed and addition of lubricating agent is required (www.greencarcongress.com). Vapor choke in the fuel line also occur (Song et al., 2004). It is non-corrosive but its compatibility with polymers is very low indeed it is not compatible with most of the elastomers only fluorine based polymers can be used (Song et al., 2004; www.greencarcongress.com). For this reason, researchers are interested in new engine and combustions systems such as controllable premixed combustion (CPC) for an internal combustion system (Song et al., 2004), to overcome these difficulties because DME is both an

environmentally clean fuel and it can be used in diesel engines with high efficiency.

In the work of Wang and Zhou (2003), 10 % DME was added to diesel fuel, and the performance of a direct injection diesel engine with this blend fuel was investigated. Results showed that smoke was reduced significantly, the NO_x and HC emissions were clearly reduced as compared to diesel operation whereas CO emission stayed at the same level (Wang and Zhou, 2003).

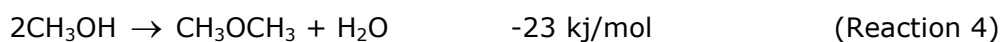
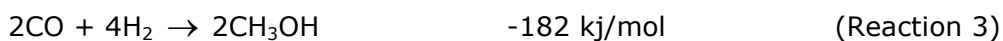
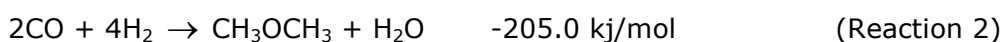
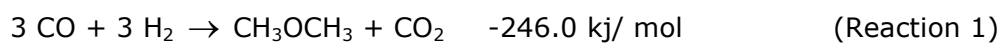
DME can be used in different fields such as residential, power generation besides transportation. It has a Wobe index (the ratio of calorific value and flow resistance of gaseous fuel) of 52 to 54 which is similar to that of natural gas. Therefore it can be used in cooking stove without or with very small modification (Ohno and Omiya, 2003).

DME is produced in two ways, either direct synthesis or indirect synthesis which is also named as methanol dehydration reaction. In direct synthesis of DME, syngas which is made up of hydrogen and carbonmonoxide is used. This syngas is produced from natural gas, coal etc. Gasified waste and waste plastics, the methane given off by animal manure and sewage sludge also can be used in the production of DME besides natural gas and coal (www.jfe-holdings.co.jp).

4.3 Direct Synthesis of DME from Syngas

In recent years, direct DME synthesis from syngas has increased the attention of researchers and companies in order to produce DME at low cost and in high quantities.

In direct DME synthesis, either Reaction 1 or Reaction 2 takes place (Ogawa et al., 2003). The Reaction 1 occurs in three steps which are methanol synthesis reaction from syn-gas (Reaction 3), dehydration reaction of this synthesized methanol (Reaction 4) and water gas shift reaction (Reaction 5). The difference of the Reaction 2 from the Reaction 1 is the absence of water-gas shift reaction in reaction steps. According to equilibrium conversion calculations of DME synthesis, the Reaction 1 is found to be superior to the Reaction 2 and the nature of the catalyst has an effect on determining which route is more dominant (www.jfe-holdings.co.jp).



The overall reaction is exothermic and there is an increase in reaction temperature during the methanol synthesis stage. For both Reaction 1 and Reaction 2, increasing pressure of the system favors the conversion.

Since the DME synthesis reaction is highly exothermic, it is important to remove heat produced during the reaction and to control the reaction temperature in order to obtain higher conversion and to prevent catalyst deactivation. A bubble column slurry reactor has been developed for this purpose (Ogawa et al., 2003). This slurry bed reactor contains catalyst in the form of fine powder suspended in inert high-boiling point oil solvent. The reaction takes place while gas bubbles are rising through the surface and the heat evolved during the reaction is absorbed by the oil solvent. The catalyst appropriate for the slurry bed reaction which enabled the synthesis of DME from syngas having a H_2/CO ratio of 1 was also studied (www.jfe-holdings.co.jp).

For the direct synthesis of DME by hydrogenation of CO and CO_2 requires a catalyst or a mixture of catalysts capable of producing methanol and ether from syngas in the same reactor. A series of bifunctional catalysts $\text{CuO}/\text{ZnO}/\text{ZrO}_2/\text{HZSM-5}$ prepared with different ZrO_2 contents (Sun et al., 2003) were tested for this reaction. A physical mixture of commercial methanol synthesis catalyst with porous and non porous alumina, sulfated-zirconia, tungsten-zirconia and HZSM-5 (Ramos et al., 2005) were the other catalysts used in direct synthesis of DME. Studies carried out with sulfate modified γ -alumina catalysts (Mao et al., 2006) indicated an increase in CO conversion from 0.85 to about 0.95 and an increase in DME selectivity from about 0.50 to 0.60, with an increase of sulfate content from 0 % to 15 %. The enhanced activity of the catalyst by sulfate addition was related to the increase of acid strength of the

catalyst. One of the important results derived from these studies is that the rate of DME direct synthesis is determined by the acid properties (acid strength and number of acid sites) of dehydrating catalysts (Ramos et al., 2005).

4.4 Methanol Dehydration Reaction to Produce DME

The conventional route for producing DME is methanol dehydration reaction. Several solid acid catalysts were used in methanol dehydration reaction to produce DME such as γ -alumina and modified γ - Al_2O_3 with silica prepared by coprecipitation (sol-gel) method (Yaripour et al., 2005), Na-modified H-ZSM-5 prepared by impregnation method (Vishwanathan et al., 2004), A novel catalyst bed packed with two layers of gamma- Al_2O_3 and Na-H-ZSM-5 were used for methanol dehydration reaction. Reducing the strong acid sites of H-ZSM-5 by Na-impregnation in an appropriate amount, 100% of DME selectivity value was obtained (Roh et al., 2004).

γ - Al_2O_3 catalyst gave good catalytic activity for methanol dehydration reaction but it was deactivated by rapidly and irreversibly (Yaripour et al., 2005). It was reported that water which was the by-product of dehydration reaction competed with methanol for the same sites on alumina. The surface of alumina had the tendency to adsorb water molecules more strongly on the Lewis acid sites. The increase in activation energy for DME synthesis due to presence of water in feed stream was considered as another indication of adsorption of water preferentially on the surface rather than methanol. This situation decreased the catalytic activity of methanol and selectivity for DME (Vishwanathan et al., 2004).

Silica modified γ -alumina catalyst gave better catalytic performance than pure γ - Al_2O_3 . For this aluminasilicate catalyst, it was observed that by increasing the silica loading, the surface area and the surface acidity of catalyst was increased. It is important to find out the optimum silica loading for aluminasilicate to get high catalytic activity and total selectivity for DME (Yaripour et al., 2004).

In an industrial plant for DME synthesis, the tolerance level of water in methanol feed is below the few hundred ppm level. However, methanol produced directly from syngas contains water 10-20 mol % (Vishwanathan et al., 2004).

Therefore, the crude methanol needs to be processed before entering the reactor. Researchs are concentrated on finding catalysts having higher selectivity for ether formation and less tendency to coke formation.

During the methanol dehydration reactions, hydrocarbons are formed as secondary products. It is well known that hydrocabons are formed on the strong acid sites on the surface of the catalyst. Therefore to increase DME selectivity and prevent the formation of hydrocarbons, the stength of the acid sites of the catalyst needs to be reduced.

It was reported that H-ZSM-5 had a strong resistance towards water, which was being adsorbed during the reaction due to its hydrophobic properties. Higher activity and stability of H-ZSM-5 than V-alumina, in the presence of water was explained with this behavior. On the other hand, unlike H-ZSM-5, hydrocarbon formation was not recognized with V-alumina so total selectivity for DME was obtained with V-alumina (Vishwanathan et al., 2004).

It is known that strong acid sites on the catalyst surface facilitate the polymerization of olefins and than increase the rate of coke formation. For zeolites coke formation is a shape-selective process and coke deposits much more slowly on medium-pore zeolites. For this reason, in spite of having strong acid sites, H-ZSM-5 inhibited coke formation due to absence of large pores. By Na loading in H-ZSM-5, decreased the total acidity of the surface and the strength of the stronger acid sites was observed and with this catalyst total DME selectvitiy and prevention of hydrocarbon and/or coke formation was observed (Vishwanathan et al., 2004; Roh et al., 2004).

CHAPTER 5

HETEROPOLYACID CATALYSTS

In this work, due to their higher catalytic activity than conventional solid acid catalysts, heteropolyacid catalysts were selected for alcohol dehydration reactions. In this chapter, properties of pure and supported form of heteropolyacids, and the literature survey on the usage of these catalysts for alcohol dehydration reactions are given.

5.1 Properties of Heteropolyacids

Keggin type heteropolyacid is represented by the formula $\text{XM}_{12}\text{O}_{40}^{x-8}$ where X represents the central atom, which is typically Si^{4+} or P^{5+} ; x is the oxidation state and M is used for the metal ion, which can be Mo^{6+} , W^{6+} , V^{5+} , Co^{2+} , Zn^{2+} , etc. Other heteropolyanions which are also used as catalysts are the Dawson structure $\text{X}_2\text{M}_{18}\text{O}_{62}^{2x-16}$; Keggin and Dawson lacunary anions $\text{XM}_{11}\text{O}_{39}^{x-12}$ and $\text{X}_2\text{M}_{17}\text{O}_{61}^{2x-20}$ (Corma, 1995; Kozhevnikov, 1998). Among a wide variety of HPAs, the Keggin heteropolyacids, which are the first characterized of heteropolyanions, are the most important for catalysis since they are the most stable and more easily available.

For heteropolyacids, the fundamental unit structure is called the primary structure and the secondary structures are formed when the primary units are connected forming a solid (Figure 5.1). For a Keggin structure, the primary structure is formed by a central tetrahedron XO_4 surrounding by 12 MO_6 octahedra that are arranged in four groups of M_3O_{13} . Each M_3O_{13} group is formed by three octahedra sharing edges and shares an oxygen atom with the central

tetrahedron. The secondary structure is formed by packing the polyanions into a bcc structure (Corma, 1995; Kozhevnikov, 1998).

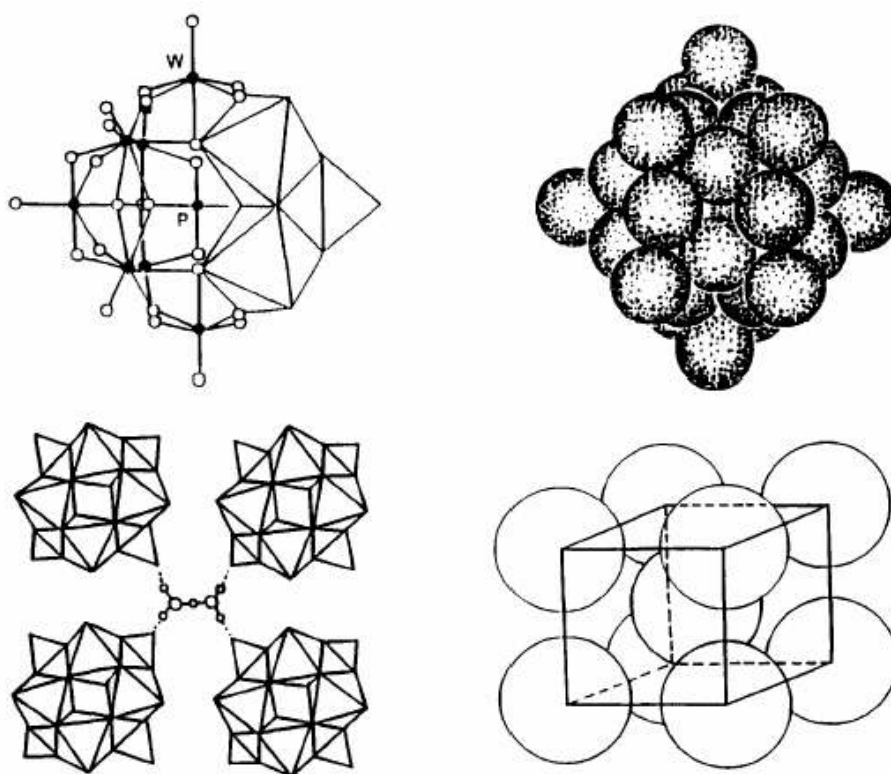


Figure 5.1. Heteropoly anion with Keggin Structure, $PW_{12}O_{40}^{3-}$ Primary and Secondary Structure (Adapted from Corma, 1995)

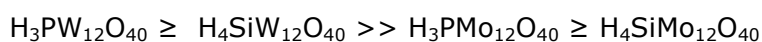
Solid heteropolyacids form ionic crystals comprising heteropolyanions, counteranions, i.e. H^+ , H_3O^+ , $H_5O_2^+$, etc., and hydration water. In this secondary structure, crystallographic arrangements depend on the amount of hydration water, which can be easily removed by heating, and on the counteranion. In solid HPAs, the protons take part in the formation of crystal structure by linking the neighboring heteropolyanions. For example, the crystal structure of PW hexahydrate is formed by packing heteropolyanions into a body centered cubic structure. In this structure, the protonated water dimer $H_5O_2^+$ is connected to four neighboring heteropolyanions by forming hydrogen bonds at the terminal oxygen atoms (Kozhevnikov, 1998; Corma, 1995).

The primary and secondary structure of heteropoly anions in the form of solids or in solutions, are characterized by using different techniques such as IR

spectroscopy, Laser Raman Spectroscopy, Surface Raman scattering, NMR spectroscopy, Visible and UV Absorption (Corma, 1995).

Heteropolyacids are very soluble in polar solvents, such as alcohols, water, ethers, esters; whereas they are insoluble in nonpolar solvents like hydrocarbons. In solutions, the acid properties of heteropolyacids are best defined by using their dissociation constants and Hammett acidity function. The hardness of the acid or the softness of the corresponding base can also be used for this aim (Kozhevnikov, 1998). The dissociation constants of heteropolyacids were determined in solvents such as H₂O, Me₂CO, EtOH etc.; the Hammett acidity function was measured in H₂O and H₂O-AcOH, H₂O-EtOH, H₂O-dioxane and H₂O-Me₂CO mixtures (Kozhevnikov, 1998). In both methods, the acidity of heteropolyacids solutions depends weakly on their compositions. H₃PW₁₂O₄₀, H₄SiW₁₂O₄₀ and H₃PMo₁₂O₄₀ are strong fully dissociated acids in aqueous solutions and their pK₁ values measured in acetone at 25°C were reported as 1.6, 2.0 and 2.0, respectively. In comparison, the dissociation constant values of H₂SO₄, HCl and HNO₃ are 6.6, 4.3 and 9.4, respectively, at the same condition. These data show that heteropolyacids in solution are stronger than the usual mineral acids such as H₂SO₄, HCl, HNO₃, etc. and among the heteropolyacids, the tungsten acids are stronger than molybdenum ones (Kozhevnikov, 1998).

Solid heteropolyacids have very strong Brönsted acidity exceeding that of conventional solid acids such as SiO₂-Al₂O₃, H₃PO₄/SiO₂ and HX and HY zeolites. The acid strengths of heteropolyacids can be determined by either microcalorimetry or temperature-programmed desorption (TPD) methods. According to microcalorimetry data which was obtained by the sorption of NH₃ at a temperature of 50°C after pretreatment of solids at 150°C, the order of acid strengths some of the important heteropolyacids were reported as (Kozhevnikov, 1998);



Superacids are defined as acids which are stronger than 100% H₂SO₄ having the Hammett acidity function less than -12. Solid heteropolyacids are approaching to the superacidity region. The Hammett acidity function of concentrated heteropolyacid solutions is stronger than that of inorganic acids (Kozhevnikov, 1998). As in the case of strong solid acids, heteropolyacids can generate carbocations from adsorbed olefins and so on (Kozhevnikov, 1998).

Heteropolyacids have high thermal stability. When they are thermally decomposed, they lose their acidity. The decomposition temperature of silicotungstic acid is 445°C. In contrast to tungsten heteropolyacids, molybdenum ones become reconstructed under exposure to water vapor allowing their usage at high temperatures under wet conditions (Kozhevnikov, 1998).

Heteropolyacids have discrete and mobile ionic structures and not only water but also different polar organic molecules can enter and leave crystal. Therefore, they absorb a large amount of polar molecules such as alcohols, in the catalyst bulk. Due to this property, polar molecules give reactions not only on the surface but also in the bulk of the crystalline heteropolyacid. This situation was termed 'pseudoliquid phase'. Nearly all proton sites present in the structure of the heteropolyacid participate in the reaction of polar substances. In the case of nonpolar molecules, they are not absorbed in the bulk of heteropolyacid; interaction occurs only with the surface of the heteropolyacid. By the virtue of pseudoliquid phase behavior which is unusual for heterogeneous acid catalysis, high catalytic activities were obtained for the reaction of polar molecules at relatively low temperatures (Corma, 1995; Kozhevnikov, 1998).

Solid heteropolyacids have an extremely high proton mobility. Generally, the proton conductivities of solids are correlated with their acid-base catalytic activities (Kozhevnikov, 1998).

The partial neutralization of the acid, the dispersion on different supports and selecting suitable HPA building components are important factors to control the acidity of the heteropolyacid (Haber et al., 2003).

The usage of heteropolyacids in liquid phase acid catalyzed reactions, such as ether cleavage, hydration of olefin and acetylene, transesterification, methanol addition to isobutene at moderate temperatures, were reported and their efficiencies were found to be higher than the ordinary protonic acids such as sulfuric acid (Izumi et al., 1983). Moreover, supported heteropolyacids have been used in vapor phase reactions such as olefin hydration, alcohol dehydration, methanol conversion (Izumi et al., 1983).

5.2 Supported Heteropolyacids

Heteropolyacids are widely used in acid catalyzed reactions due to their strong acidity but pure heteropolyacids in solid form are nonporous materials. Also, they have very low surface area changing in the range of 1-10 m²/g. When reactants are polar molecules, heteropolyacids shows high catalytic activity due to pseudoliquid phase behaviour. However, for nonpolar molecules it is important to increase the surface area. Acid salts containing large cations such as K⁺, Rb⁺, Cs⁺ and NH₄⁺, having surface areas around 150 m²/g, can be prepared to overcome this problem (Liu et al., 2004). Also improvement in the surface area can be achieved by supporting heteropolyacid on solids having high surface area.

Since heteropolacids are very soluble in several organics and water, it is important to develop supported heteropolyacid catalysts which can not be leached either in liquid or vapor phase.

The type of heteropolyacid and the distribution of protons of the heteropolyacid; the surface area, the particle size, the pore structure and the nature of the support; conditions of pretreatment; conditions of catalyst preparation such as the HPA loading, pH and the concentration of impregnating solution, the interaction of the heteropolyacid with support are important criterias for the acidity, stability and catalytic activity of supported heteropolyacids (Kozhevnikov, 1998, Tarlani 2006).

A soluble compound can be immobilized in organic or inorganic material by physisorption, chemical attachment or entrapment. The physisorption process may not be resulted with a stable final product. A leaching or desorption can be observed. By chemical attachment or entrapment, more stable materials are prepared (Staiti et al., 1999).

Acidic or neutral substances such as silica (Molnar et al., 1999; Vazquez et al., 2000, Zhang et al., 2004), activated carbon (Izumi et al., 1983), aluminosilicate, mesoporous molecular sieves MCM-41 (Blasco et al., 1998; Verhoef et al., 1999; Jalil et al., 2004), SBA-3 (Nowinska et al., 2003), SBA-15 (Liu et al., 2004) which are members of mesoporous silicate materials, γ -alumina (Caliman et al., 2005), Al-MCM-41 (Nandhini et al., 2006) and zeolites (Haber et al., 2003) such as HZSM-5 (Wang et al., 2000) are suitable as

supports for heteropolyacids. Basic solids like MgO can decompose HPA (Kozhevnikov, 1998).

Silica has been considered most frequently as a support due to its low cost of production, ease of availability and modification of physiochemical properties. There are various types of silica and the interaction of heteropolyacids depends on the type and surface characteristics of the silica (Tarlani et al., 2006).

It seems that the thermal stability of silica supported heteropolyacids is comparable to or slightly lower than that of the heteropolyacid. A thermally decomposed Keggin structure on the silica surface may be reconstructed when it is exposed to water vapor (Kozhevnikov, 1998; Wang et al., 2000). Also reported that, in contrast to tungstophosphoric acid molybdophosphoric acid and molybdosilicic acids are thermally stable when they are supported on silica (Pizzio et al., 1998). When carbon and TiO_2 was used, the supported tungstophosphoric acid was thermally stable up to 425°C , on the other hand the SiO_2 supported HPA some partial degradation was occurred starting from the temperature of 365°C (Pizzio et al., 1998).

It was reported that at low loadings, $\text{H}_3\text{PW}_{12}\text{O}_{40}$ and $\text{H}_4\text{SiW}_{12}\text{O}_{40}$ formed finely dispersed species on the SiO_2 surface; heteropolyacid crystal phase on silica was developed at loading of HPA above 20 wt %. Various HPA forms of discrete molecules, i.e. clusters 50 \AA in size and large crystallites of 500 \AA were observed on the silica surface by transmission electron microscopy (TEM). The HPA loading determined their relative amounts (Kozhevnikov, 1998).

The study carried out with 12-molybdophosphoric acid showed that the tendency of heteropolyacid adsorption on silica was very low in high loading and very weak interactions occurred between the support silica and the heteropoly acid which remained in crystalline form. On the contrary, a chemical interaction occurred between the species in low loading. Higher solubility of heteropolyacids caused the physically adsorbed HPA to be leached out on the surface of the support which prevented the recovery of the catalyst (Tarlani et al., 2006). As indicated previously by Nowinska et al. (2003), leaching of heteropolyacids from modified sample limits their usage in liquid phase reactions. Amine groups were introduced on MCM-41 surface by aminosilation in order to built strong link with the protons of hetropolyacids (Nowinska et al., 2003). Tarlani et al., 2006, also

concentrated on functionalized silica materials, modified with the method of aminosililation, to immobilize $\text{H}_3\text{PW}_{12}\text{O}_{40}$ and $\text{H}_{15}\text{P}_5\text{W}_{30}\text{O}_{110}$ which are the Keggin and Preyssler tungsten heteropolyacids respectively, by means of chemical bonding. They reported that among MCM-41, silica-gel and fume silica, the functionalized MCM-41 showed the least tendency for anchoring with heteropolyacids (Tarlani et al., 2006). If the catalyst is leached with the solvents having low polarity such as chloroform or toluene, in which HPA is insoluble, instead of ethanol or water, the synthesized catalyst preserves the adsorbed heteroployacids (Vazquez et al., 2000).

In the work of Molnar et al., (1999), heteropolymolybdc acids, which are $\text{H}_4\text{SiMo}_{12}\text{O}_{40}$ and $\text{H}_3\text{PMo}_{12}\text{O}_{40}$, and heteropolytungstic acids which are $\text{H}_4\text{SiW}_{12}\text{O}_{40}$ and $\text{H}_3\text{PW}_{12}\text{O}_{40}$ were immobilized into silica by sol-gel technique. The weight ratio of the silica to acid was an important parameter in preparing these silica included samples, so that, by increasing this value from 5 to 8 they reduced the leakage of heteropolyacids. It was observed that heteropolyacids were dispersed and strong bounds were formed in the porous silica network. In this study, heteropolyacids were also supported on silica by impregnation techqnique. The silica included heteropolyacids showed higher catalytic activity in the hydrolysis of ethyl acetate than heteropolyacids supported on silica.

Silica supported tungstophosphoric acid prepared by incipient impregnation method was used in liquid phase alkylation of benzene with ethylene and transalkylation of benzene with diethylbenzene (Zhang et al., 2004). Conventionally, aluminum chloride has been used but their corrosive property and large amount of waste produced, solid acid catalysts, such as zeolites, have become important for these reactions. Zeolites are non-corrosive, environmentally benign and consume less raw material and energy but require high reaction temperature and pressure. Silica supported tungstophosphoric acid are found to be more active and selective than bulky solid form in liquid phase alkylation and transalkylation reactions; also, the temperature and pressure could be much lower comparing to zeolites (Zhang et al., 2004). It was reported that this new catalyst have both Bronsted and Lewis acidity while bulky tungstophosphoric acid has only stong Bronsted acid sites. The Bronsted acid sites were increased by increasing HPA loading.

Heteropolyacids can be used as solid electrolytes or as aqueous solutions in fuel cells due to their suitable characteristics such as strong Bronsted acidity.

Staiti et al., (1999) worked on phosphotungstic acid and silicotungstic acid on silica to be used as solid electrolytes by sol gel process. The interaction between the heteropolyacid and the support was stronger for samples prepared with silicotungstic acid with respect to sample prepared with phosphotungstic acid. Silicotungstic acid molecule has four protons and at the same HPA loadings, which was 15 and 30wt % HPA, samples prepared with STA showed higher proton conductivity. Increase in the relative humidity allowing an easier movement of protons and heteropoly acid loading indicating higher numbers of mobile protons, resulted in increase of proton conductivity.

Molybdophosphoric acid and tungstophosphoric acid supported on silica were used in the aromatic alkylation reactions and it was reported that quantitative conversions were obtained with these catalyst in shorter time (Pizzio et al., 2005).

Studies which were carried out SiO_2 , $\text{SiO}_2\text{-Al}_2\text{O}_3$ and $\gamma\text{-Al}_2\text{O}_3$ impregnated with tungstophoric acid showed that primary Keggin structure is preserved, but heating above 200°C might result in some degradation in the case of $\gamma\text{-Al}_2\text{O}_3$ support (Pizzio et al., 1998).

In the work of Caliman et al. (2005), impregnation of tungstophosphoric acid was done on γ -alumina by evaporation technique using different solvents such as ethanol, acetonitrile, water acidified with HCl. It was reported that, the tungstophosphoric acid supported on γ -alumina, which was best prepared in aqueous solution of HCl, was a weaker acid than pure heteropolyacid but stronger than pure alumina.

Among the heteropolyacids, tungstophosphoric acid and silicotungstic acid are supported on the activated carbon by using their concentrated aqueous solutions. Their Keggin structures are retained and highly dispersion of acids the support was observed. On the contrary, in the case of low heteropoly acid contents partial decomposition of the tungstophosphoric acid was occurred (Pizzio et al., 1998).

Mesoporous siliceous material MCM-41 have attracted researchers since it has a very high surface area as well as regular hexagonal array of uniform pore sizes within the mesoporous region (Liu et al., 2004). The property of having larger pore size makes novel mesoporous pure silica molecular sieve MCM-41

superior comparing to zeolites (Kozhevnikov, 1998). As in the case of silica, supporting tungstophosphoric acid on siliceous MCM-41 decreases the stability of the heteropolyacid and the crystallinity was destroyed (Jalil et al., 2004). The study related with the impregnation of tungstophosphoric acid on MCM-41 showed that the activity of the catalyst was decreased by heating even at 200°C due to surface structural damage of the acid molecules. Also, some tungsten oxides formation were reported due to decomposition of tungstophosphoric acid at 400°C (Jalil et al., 2004).

Another mesoporous material, SBA-3 was used for the incorporation of $\text{H}_3\text{PW}_{12}\text{O}_{40}$ and $\text{H}_5\text{PMo}_{10}\text{V}_2\text{O}_{40}$ under acidic pH (Nowinska et al., 2003). Heteropoly acid was added while preparing the synthesis solution of SBA-3. It was reported that a new mesostructure that contained Keggin units in mesoporous materials walls was formed by this method. The calcination stage in order to remove template did not decay the mesoporous structure whereas washing of calcined sample with solvent such as methanol resulted in the destruction of mesostructure. Because, the Keggin units present in the initial gel entered the mesoporous structure taking part in the construction and removing of HPA by solvent treatment caused to collapse. When the washing with solvent was applied on the sample prepared by the impregnation method, it was observed that the structure of the SBA-3 was not decayed only heteropoly acid was removed (Nowinska et al., 2003).

In order to immobilize heteropolyacids on supports easily preventing the leaching of HPA and without losing acidity of HPA so that improve the catalyst performance, different techniques can be applied on support material. In the work of Damyanova et al. (2003) metals such as Ti, Zr, Al containing hexagonal mesoporous silicate (HMS) were prepared and heteropolyacids such as tungstophosphoric acid, molybdophosphoric acid were supported on them by the wetness impregnation method. Rao and coworkers (2005) studied on alumina grafting of silica gel and ordered mesostructured SBA-15 to be used for the immobilization of $\text{H}_3\text{PW}_{12}\text{O}_{40}$. Surface modified mesostructured cellular foam (SM-MCF) silica by grafting 3-aminopropyl-triethoxysilane were prepared to provide sites for the chemically immobilization of $\text{H}_3\text{PMo}_{12}\text{O}_{40}$ by Kim et al. (2006).

A deactivation of catalyst can be occurred during the organic reactions due to formation of coke, which is a carbonaceous deposits on the catalyst surface. For zeolites and aluminosilicates, the regeneration of material can be

done by burning coke at 500-550°C but the thermal stability of heteropolyacids is not sufficient to carry out this conventional process (Devassy and Halligudi, 2005).

5.3 Heteropolyacids in Dehydration of Alcohols

Conventionally, dehydration reactions of alcohols take place by heating the alcohol with strongly acidic compounds such as H_2SO_4 , H_4PO_3 , KHSO_4 , etc. For dehydration reactions of primary alcohol, concentrated H_2SO_4 used as the catalyst and the reaction temperature was adjusted around 170-180°C. For higher alcohols, milder conditions, i.e., dilute acid and lower reaction temperature, were sufficient to carry out the dehydration reaction (Vazquez et al., 2000).

Heteropoly acids are considered as a superior alternative catalysts for dehydration catalysts due to their strong acidity and structural properties. By using heteropolyacids, the proportion of side reactions are lowered and toxic waste would not be produced which is very important issue in an environmental point of view (Vazquez et al., 2000).

Dehydration of ethanol and 1-butanol were carried out with heteropolyacids and it was reported that HPAs showed higher activity than the conventional solid acid catalysts such as silica-alumina (Vazquez et al., 2000).

Since bulk HPAs have low specific surface area (1-10 m^2/g), supported heteropolyacids are important for many applications. In the case of unsupported ones, for polar reactants the catalytic reactions occur not only at the surface but also in the bulk of the solid heteropolyacids. For this reason, they show quite high catalytic activity despite their low surface area. In the case of nonpolar reactants, it is important to increase the surface area or to increase the number of accessible acid sites of heteropolyacid (Haber et al., 2003) and this can be done by dispersing the heteropolyacids on solid supports with high surface areas. Acidic or neutral substances like SiO_2 , active carbons or aluminosilicates are suitable as supports, but silica is the most often used.

The liquid phase dehydration of alcohols specifically, 1,2-diphenylethanol, 1-(3,4-dimethoxyphenyl)-2-phenylethanol and cholesterol were studied over

silica supported molybdophosphoric acid and tungstophosphoric acid prepared by equilibrium impregnation method (Vazquez et al., 2000).

Tungstophosphoric acid was supported on zeolite HY and silica by using incipient wetness method and their catalytic activities were tested in a conventional flow-type reactor by the vapor phase dehydration of ethanol (Haber et al., 2003). The structure of zeolite did not collapse after supporting HPA. An increase in the micropores area was observed after deposition of heteropolyacid on the silica in contrast to decrease in both surface area and volume of mesopores. This situation was indicated that micropores were formed in heteropolyacids after their adsorption on silica. The reaction temperature was changing in the range of 398 to 773 K, under atmospheric pressure and both diethyl ether and ethylene formation were observed. The catalyst loading of HPA supported on zeolite was changed from 46.8 wt % to smaller amounts but their activities were found to be similar indicating these catalysts had a very active sites at the surface in small concentration. It was reported a decrease in catalytic activity in tungstophosphoric acid supported on silica due to decrease in HPA concentration, indicating pseudo liquid phase reaction.

Besides pure heteropolyacids, their salts also can be supported on different materials. For example, the Potassium and silver salts of tungstophosphoric acid supported on silica by incipient wetness method and their activities were tested by vapor phase dehydration reaction of ethanol in a conventional flow-type reactor under atmospheric pressure at a temperature range of 398-773 K (Haber et al., 2002). The cesium acid salts and ammonium acid salts of tungstophosphoric acid supported on silica with different techniques (Soled et al., 1997).

The vapor phase ethanol conversion reaction was carried out over $\text{H}_3\text{PMo}_{12}\text{O}_{40}$ chemically immobilized on surface modified mesostructured cellular foam (SM-MCF) silica (Kim et al., 2006). Mesostuctured cellular foam silica was modified by grafting 3-aminopropyl-triethoxysilane to provide positive charge that enables anchoring sites for the immobilization of PMo_{12} . Due to finely and molecularly dispersion of PMo_{12} species on the support, higher ethanol conversion values were obtained over PMo_{12} /SM-MCF catalyst than that of obtained with unsupported HPA. It was also reported that PMo_{12} /SM-MCF especially enhanced the formation of acetaldehyde while suppressed the formation of ethylene and diethyl ether.

CHAPTER 6

MESOPOROUS MATERIALS

Porous solids have great importance in the field of catalysts and catalyst supports due to their high surface areas. In this chapter the formation mechanism and the characteristic properties of MCM-41 which is the well-known member of mesoporous materials are given in detail. After that, the literature survey on the heteropolyacid incorporated into the mesoporous materials is presented.

6.1 Formation of MCM-41

Porous solids are divided into 3 classes according to the pore diameter;

- Microporous materials: Their pore diameters are less than 2 nm. Zeolites are the well-known member of this class. The relatively small pore openings limit their applications (Ciesla and Schüth, 1999).
- Mesoporous materials: Their pore diameters are in the range of 2-50 nm. M41S family which was discovered by Mobil researchers at the beginning of 1990's, is the best known example for this class. They have large channels in the range of 1.5-10 nm and the pores are ordered in hexagonal, cubic and laminar array. They have high surface areas above 700 m²/g (Corma, 1997).
- Macroporous materials: Their pore diameters are greater than 50 nm (Ciesla and Schüth, 1999).

MCM (Mobil Composition of Matter) 41 is the most important member of M41S family having a regularly ordered pore arrangement with a very narrow pore size distribution in contrast to porous glasses and porous gels which have disordered pore arrangement with a broad size distribution (Ciesla and Schüth, 1999).

MCM-41 is synthesized by liquid crystal templating mechanism (Corma 1997). Liquid-crystalline self assembled surfactant molecules are used as templates to form ordered organic-inorganic composite material by electrostatic interaction between the positively charged surfactants and the negatively charged silicate species. The porous silicate network is obtained after removing the surfactants by calcination (Ciesla and Schüth, 1999).

M41S materials can be synthesized by using different silica sources, at different surfactant to silica ratio, within a broad time and temperature interval (Corma, 1997).

Beck et al. (1992) proposed a Liquid-crystal templating mechanism to explain the formation of MCM-41. He suggested, two different possible reaction pathways (Figure 6.1). The first pathway was liquid crystal initiated and the second one was silicate initiated. The surfactant molecules were organized to form liquid crystals which were used as templates. Firstly micellar rod around the surfactant micelle was formed then hexagonal array of rods were produced. After that silica was incorporated around the rodlike structure (Corma, 1997).

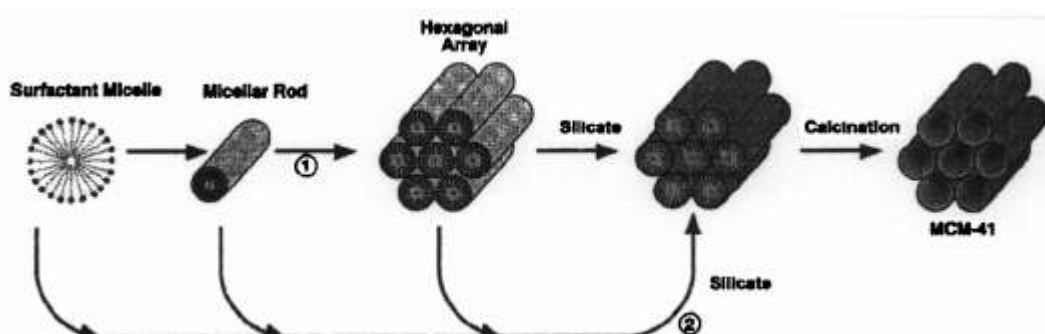


Figure 6.1. Liquid-crystal templating mechanism (LCT) for the formation of MCM-41 (Adapted from Ciesla and Schüth, 1999)

As in the pathway 2, the randomly ordered rod like organic micelles interacted with silica forming the composite sperices having two or thee monolayers of silica around the external surface of the micelles, resulted in long range order of characteristics of MCM41 (Corma, 1997).

The surfactant concentration in water and the presence of other ions strongly effect the reaction pathways (Ciesla and Schüth, 1999). In order to synthesize MCM-41, the surfactant concentration should be as low as the critical micelle concentration (CMC) up to concentrations in which liquid crystals are formed. When the surfactant concentration is $\approx 10^{-3}$ to 10^{-2} ml/l, which is very dilute aqueous solutions, species are spherical micelles. The self-assembly of surfactant rods are formed as the surfactant concentration is increased. The randomly ordered rod-like micelles interacted with the silicate forming tubular silica. The long-range order is formed from these composite species. Further increase in surfactant concentration resulted in the formation of mesospheres. These mesophases show hexagonal, cubic or lamellar structure depending on the nature of the surfactant, the concentration and the temperature. MCM-41 in monoliths can be formed in this way (Ciesla and Schüth, 1999).

Another material whose preparation is very similar to MCM-41, was prepared by using a layered silicate, kanemite, and was called as FSM-16 (Folded Sheet Mesoporous Materials). The formation mechanism can be explained by the "folded sheet" mechanism (Ciesla and Schüth, 1999).

MCM-48 which is the cubic member of the M41S family can be synthesized by adjusting the silica to cetyltrimethylammoniumbromide (CTAB) ratio and changing the synthesis conditions. Another way to form MCM-48 is using Gemini surfactants (Ciesla and Schüth, 1999).

MCM-50 is the lamellar mesosructure of the M41S family. The lamellar phase is represented by sheets or bilayers of surfactant molecules whose hydrophilic heads looks the silicate at the interface (Ciesla and Schüth, 1999).

6.2 Characterization of MCM-41

The structure of MCM-41 resembles like a honeycomb having a hexagonal packing of unidimensional cylindrical pores.

Typical X-Ray Diffraction (XRD) pattern of MCM41 has three to five reflections at 2θ values in the range of $2-5^\circ$ (Figure 6.2). Reflections may not be observed at higher angles because material is not crystalline at atomic level. The mesoporous MCM-41 is said to be amorphous at high angles. The ordered hexagonal array of parallel silica tubes are resulted in the formation of these reflections which can be indexed as (100), (110), (200), (210) and (300) (Ciesla and Schüth, 1999).

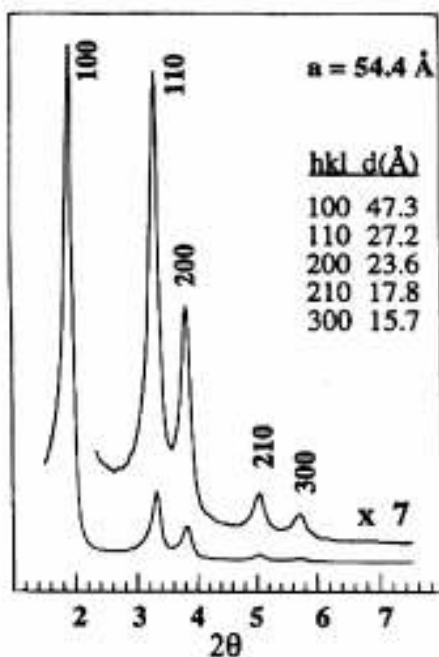


Figure 6.2 XRD pattern corresponding to MCM41 (Adapted from Ciesla and Schüth, 1999)

The hexagonal arrangement of MCM-41 was clearly seen by Transmission Electron Microscopy (TEM).

The surface area and the pore size distribution of the M41S samples are determined by the adsorption of different gases such as O_2 , N_2 and Ar (Corma, 1997). The nitrogen adsorption isotherm corresponding to MCM-41 having a pore diameter of 4 nm is presented in Figure 6.3 (Ciesla and Schüth, 1999). This isotherm is type IV in the IUPAC classification (Corma, 1997). A sharp capillary condensation step occurs at a relative pressure of 0.4 and there is no hysteresis between the adsorption and desorption at the boiling point of N_2 . This indicates the monolayer adsorption of nitrogen on the walls of mesopores.

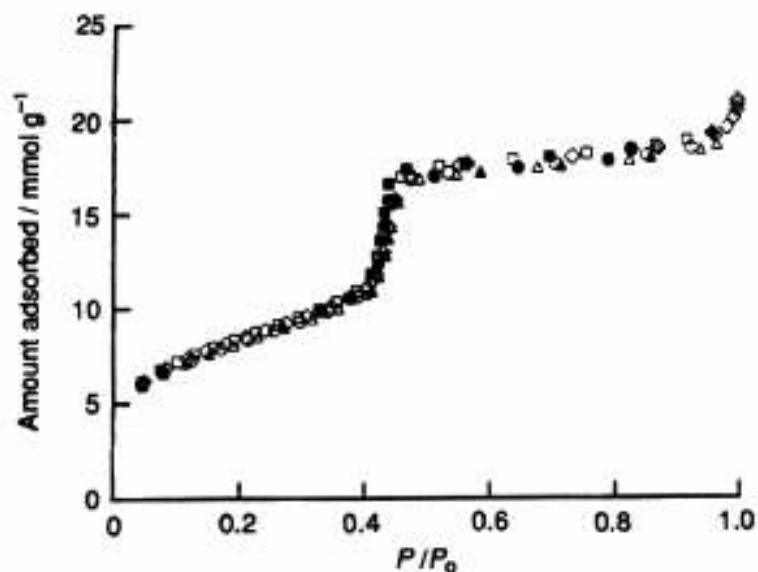


Figure 6.3 Nitrogen Adsorption Isotherm for MCM-41 (Adapted from Ciesla and Schüth, 1999)

The formation of hysteresis depends on the adsorbate, pore size and the temperature. For example, for pores having diameter larger than 4 nm, or using O₂ or Ar as the physisorption gases, an isotherm which is type IV with a hysteresis loop of the HI type was observed (Corma, 1997; Ciesla and Schüth, 1999).

The pore size distribution is calculated by Barrett-Joyner-Halenda (BJH) method. The difference between the lattice parameter, a , which is calculated from XRD data by the following equation,

$$a = 2d_{(100)} / \sqrt{3}$$

and the pore size found from the nitrogen adsorption analysis, gives the wall thickness. This value is reported as 1.0 nm for MCM-41 having pore sizes in the range of 2.5-10 nm (Ciesla and Schüth, 1999).

The Solid-state Nuclear Magnetic Resonance (NMR) spectroscopy is another characterization technique to determine the pore size, formation mechanism of M41S mesoporous materials. Also it is a useful tool for the

studies related with the diffusion of molecules in the pores and the conditions before and after the calcinations treatments (Corma, 1997).

The hydrophilic and hydrophobic properties of the surface were measured by adsorbing polar and unpolar molecules and than analysed by Fourier Transform Infrared (FT-IR). MCM-41 shows a hydrophobic character according to the study carried out the adsorption of cyclohexane, benzene and water. On the other hand, MCM-41 has high sorption capacity for hydrocarbons. In another study which was carried out by pyridine adsorption, small amount of OH sites and at least three different silanol groups, i.e. single, hydrogen bonded and geminal silanol groups, were detected (Ciesla and Schüth, 1999).

Firstly, MCM-41 was synthesized in water under alkaline conditions (Ciesla and Schüth, 1999). MCM-41 mesostructures with different chemical composition, d spacing and pore diameters would be expected by the procedure containing highly acidic synthesis conditions (Corma, 1997). It was observed that the characteristic reflections of MCM-41 prepared in acidic media which was prepared by HNO_3 , were shifted to lower 2θ values and there were a decrease in unit cell parameter from 4.4 nm to 4.1 nm. The template could be removed easily by simple washing with water at room temperature indicating a weak interaction, such as van der Waals interaction, between the silica layer and the surfactant to be occurred (Corma, 1997)

Studies have focused on synthesizing mesoporous materials at different conditions, such as lower temperature, lower synthesis time, as well as by controlling the crystal size and pore dimensions. The synthesis temperature was decreased to 25°C in alkaline media but the resultant product had a very low thermal stability compared to the one synthesized at high temperatures. Microwave heating was used in the synthesis of MCM-41, and high-quality hexagonal mesoporous material having good thermal stability and small crystal sizes was produced. The fast and homogeneous condensation reactions during the microwave synthesis is most likely the reason of formation of smaller crystal size. The pore diameter of MCM-41 is in the range of 1.5-10 nm, and the pore size can be changed either by changing the chain length of the surfactant or by the addition of organic molecules, such as n-alkanes, into the synthesis medium. It is more desirable to increase and control the pore sizes without adding organic swelling agents since it also requires larger reaction volume and additional separation processes. For this reason studies have been carried out by altering

the composition of gel and the crystallization variables such as crystallization time (Corma, 1997).

By controlling the synthesis conditions, mesoporous materials having different morphology such as ordered fibrous, spherical or thin film can be prepared (Mokaya, 2001). The preparation of well ordered MCM-41 ropes, fibres or rods have attracted the researchers interests since they can be used in the preparation of silica based nanotubes which are used as conducting wires. One of the method to prepare ropes, fibres or rods of MCM-41 is providing a highly acidic conditions in which the silica condensation rate is slow down and the uncontrollable precipitation of silica can be avoided. Another method to convert the sphere shaped particle observed for the standart MCM-41 sample to elongated or rope like particles is synthesizing MCM-41 under basic conditions by increasing the hydrothermal crystallization time applied during the high temperature (150°C) synthesis (Mokaya, 2001). As a result of this study, a shift in 2θ values of (100) peak was reported to lower angles indicating an expansion in lattice parameter, decrease in surface area and pore volume while increase in the pore size and in the wall thickness which is calculated from the difference between the lattice parameter and pore size.

To form the acid sites and to make MCM-41 catalytically active, isomorphic substitution of different cations were applied (Corma, 1997). First of all aluminium was incorporated into the silica framework. The Temperature-Programmed Desorption (TPD) and FT-IR studies showed that aluminum containing MCM-41 had an acidity at the same level with amorphous aluminosilicate (Ciela and Schüth, 1999). It was reported that both Lewis and Bronsted acid sites present in Al-MCM-41 (Zholobenko et al., 2001). SiOH groups in Al-MCM-41 materials were said to be acidic and similar to SiOH groups in amorphous aluminosilicate. The reason of the mild acidity of Al-MCM-41 was coming from these SiOH groups not the bridging Al(OH)Si groups. On the contrary, SiOH groups in Si-MCM-41 was not acidic (Zholobenko et al., 2001). However, the acidity of aluminium modified material was found to be lower than zeolites and their structure stabilities in modified form were decreased, so in order to make acidic mesoporous materials, heteropoly compounds and transition metal complexes have been tested (Nowinska et al., 2003).

Current procedure applied to synthesize MCM-41 includes the use of liquid surfactant as the liquid crystal templates. Conventionally, the templates are

removed by calcination yielding the porous materials. However, this procedure may destroy the templates which constitute 50 mass % of the as-synthesized material. The supercritical fluid extraction is considered as a new method for recovering the surfactant molecules (Kawi and Lai, 1998). Since the extraction is carried out at lower temperature than required for calcination, the destruction of mesopores may be prevented. It was reported that more uniform pore size distribution was obtained by using supercritical CO₂ extraction instead of calcination.

6.3 MCM-41 Incorporated Heteropolyacid Catalysts

Using homogeneous catalysts in the reactions may cause some problems such as recovery of the catalyst, disposal of the used catalyst, toxicity, corrosion. In order to overcome these problems, preparing catalysts which is separated easily, reused with high activity (Udayakumar et al., 2007).

The studies carried out on heteropolyacids show that they are efficient and environmentally friendly catalysts having superior activities than conventional ones such as H₂SO₄ or zeolites (Udayakumar et al., 2007). MCM-41 has been considered to be an excellent support for heteropoly acids due to its very high surface area and regular pore size distribution (Corma, 1997).

Generally impregnation technique has been used for the immobilization of heteropolyacids on these mesoporous material. By impregnating heteropolyacids into Si-MCM-41, the acidity and catalytic activity of silanol groups are increased. Also, these new catalysts have lower solubility than heteropolyacids which can be considered an advantageous property in separation, recovery and disposal of the catalyst which is a big problem of homogeneous catalysts (Udayakumar et al., 2007).

Blasco et al. (1998), supported 12-Tungstophosphoric acid on different carriers, one of them is pure silica MCM-41 having diameter of 30 and 65 Å and tested in the alkylation of 2-butene with isobutene at 33°C and 2.5 MPa. They reported that high acid dispersion was achieved. Increasing the acid content caused a decrease in the catalytic activity of the catalyst which could be due to the partial blockage of the monodisperse pores of MCM-41.

The study carried out by Verhoef et al. (1999) tungstphosphoric acid and silicotunstic acid were impregnated on MCM-41 .

In the work of Udayakumar et al. (2007) HPA was impregnated into Si-MCM-41 and its activity was tested in the liquid phase bisphenol synthesis. The activity of HPA was found to be higher than its supported form. It was reported that HPA was finely dispersed on the support, which was derived especially from TEM analysis. Also, increasing the amount of heteropolyacid loading resulted in lower BET surface area, pore volume and pore size in the new catalyst while increasing its acidity.

Besides MCM-41, mesoporous Al-MCM-41 which contains aluminium in the ratio of Si/Al=20, was used as a support for tungstophosphoric acid (Nandhini et al., 2006). The high aluminium content gives hydrophilic property to Al-MCM-41. Due to entrap more Keggin unit with this property, the acidity of the synthesized solid acid catalyst increases (Nandhini et al., 2006). It was reported that, the Keggin structure of the heteropolyacids was retained on Al-MCM-41 surface for samples prepared with high tungstophosphoric acid content (20 and 40wt%) whereas partial decomposition of Keggin structure occurred at low loading value (10wt % TPA), according to ^{31}P MAS-NMR analysis. Increasing the heteropolyacid loading resulted in decrease of pore volume, confirming the formation of bulk Keggin phase within the pores of the catalyst loaded with 20 and 40wt % HPA.

CHAPTER 7

EXPERIMENTAL STUDIES for ALCOHOL DEHYDRATION REACTIONS

In this chapter experimental studies carried out for alcohol dehydration reactions over different solid catalysts are presented. At the beginning, the experimental set-up will be introduced in detail.

Vapor phase ethanol dehydration reaction was studied over different solid catalysts namely heteropolyacids, (silicotungstic acid, tungstophosphoric acid, molybdophosphoric acid), Nafion (a perfluorinated ionomer) and aluminosilicate which is a mesoporous MCM41 type catalyst. And studies on vapor phase methanol dehydration reaction was carried out over silicotungstic acid, tungstophosphoric acid and aluminosilicate.

These experiments were planned to provide us the information about the catalytic activity of different solid catalysts on vapor phase ethanol and/or methanol dehydration reactions. Moreover, the effects of different reaction parameters such as reaction zone temperature, feed composition, water content of the feed, the space time on the overall alcohol conversion and on the selectivities of products were investigated.

Basing on the results obtained from this chapter, the most active heteropolyacid was selected and used for the synthesis of novel catalysts which was supposed to give high ethanol conversion and high product yield. It was aimed to bring together the activity of heteropolyacids and the high surface area of mesoporous materials in order to synthesize superior catalysts. The catalytic

activity tests of these synthesized catalysts were done by ethanol dehydration reaction.

7.1 Experimental Setup

A tubular flow reactor system is used for the vapor phase alcohol dehydration reaction. The schematic of experimental set up is given in Figure 7.1.

The stainless steel tubular reactor having an internal diameter of $\frac{1}{4}$ in was used. Before each experiment, fresh catalyst was placed in the middle of the reactor to prevent the effects of temperature gradients and it was fixated by using quartz wool from both ends.

Then the reactor was inserted into a temperature programmed tubular furnace in order to adjust the reaction temperature. The reaction temperature was changed from 180°C to 450°C.

Liquid alcohol (ethanol or methanol or in some experiments, ethanol-water mixture) was pumped by a syringe pump with a required flow rate to an evaporator which was placed in a constant temperature oven. Here, the gaseous feed was mixed with helium in different ratios. The evaporation chamber is kept at a temperature of 150°C.

The gaseous mixture of alcohol and helium leaving the evaporator went through the reactor to give reaction. The products and the unreacted alcohol leaving the reactor passed through the gas chromatograph, Varian CP 3800 GC equipped with Poropak T, for the online analysis of the product distributions. All the connection lines were kept at 150°C by using heating tape and isolated in order to prevent the condensation of feed and products.

For the gas chromatograph, Helium was used as the carrier gas with a constant flow rate of 30 cc /min. The TCD detector and the gas sampling valve were kept at 225 and 200°C, respectively. A temperature-ramped program was prepared for the separation of all products. Each analysis started at 75°C and the column was kept at this temperature for 2 minutes. Then it was heated to 170°C with a ramp rate of 10 °C/min. Finally, the column was kept at this temperature

for 3 minutes. During this period peaks corresponding to products and unreacted feed were obtained very clearly. For each experiment, analysis of the product was started after the system reached steady state.

After finishing each experiment, the column was conditioned for 1 hour with He gas to prevent condensation of any component.

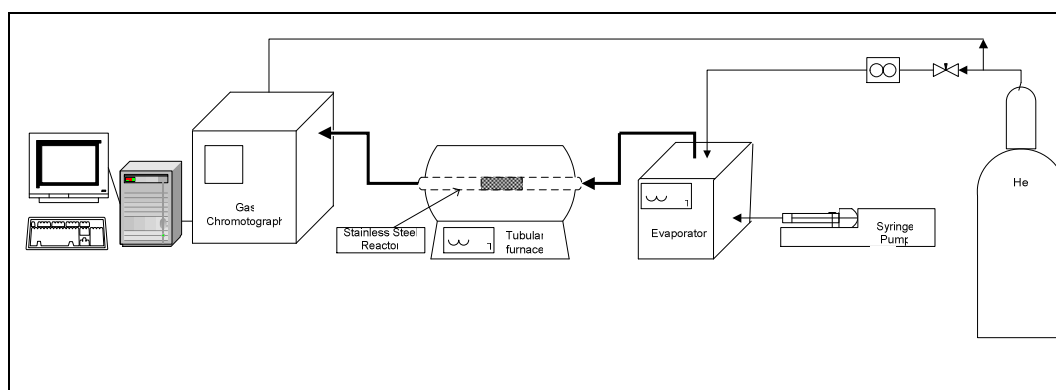


Figure 7.1. Experimental Set-Up

7.2 Chemicals and Experimental Conditions

In all experiments, high purity helium gas was used for feed stream and also as a carrier gas for GC. Pure ethanol (99.8% purity) from Sigma-Aldrich, and methanol (99.9%) from Merck were used.

In the content of this study, heteropolyacids were selected since it was known that they were highly acidic catalysts which were appropriate for dehydration of alcohols. Among the heteropolyacids, silicotungstic acid (Sigma-Aldrich), tungstophosphoric acid (Acros Organics) and molybdophosphoric acid (Acros Organics) were used for this study. Then other solid acid catalysts, namely, Nafion (H^+ form with 7-9 mesh, Fluka) and Aluminosilicate (mesostructured hexagonal framework MCM41 type, Acros Organics) were used. In the case of methanol dehydration reaction experiments silicotungstic acid, tungstophosphoric acid and aluminosilicate were used.

As it was indicated in the experimental chapter, the first parameter was the reaction zone temperature. Its range was changed between 125°C and 450°C. For commercial catalysts, experiments were carried out between 140-

250°C; for novel silicotungstic acid catalysts, ethanol dehydration reaction was tested in the range of 180 to 400°C.

The second parameter was mole fraction of alcohol in the feed stream. As indicated in Section 7.1, feed constituted alcohol and helium. The mole fraction of ethanol in the feed was increased from 0.05 to 0.61 keeping the total feed flow rate at 44.24 ml/min as constant. For methanol dehydration reaction the feed flow rate was the same, but the mole fraction of methanol in the feed was 0.48.

Another parameter was the amount of catalyst. Using tungstophosphoric acid as the catalyst, experiments were repeated with different amounts of catalysts (between 0.1g-0.8g) charged into the reactor. In methanol dehydration reactions the amount of catalyst was not changed. For some of the novel mesoporous silicotungstic acid catalysts, ethanol dehydration reaction experiment was repeated with 0.1 and 0.2 g of catalyst.

In industrial perspective, aqueous ethanol is more available and much cheaper than pure ethanol. For this reason, the water content of the feed became another parameter of the ethanol dehydration reaction experiments to see the effect of water on the DEE and ethylene production. In methanol dehydration experiments pure methanol was used.

Experimental conditions are presented as a summary in the following three tables. In these tables, the type and the amount of catalyst used for the given set; the composition of the feed stream and the reaction temperature interval for that set are given.

In Table 7.1, the experimental conditions for ethanol dehydration reaction experiments carried out over commercial solid acid catalysts are given.

In Table 7.2, the experimental conditions for methanol dehydration reaction experiments over commercial solid acid catalysts are summarized.

Finally, in Table 7.3, the experimental conditions for synthesized novel mesoporous silicotungstic acid catalysts whose properties and preparation steps are given in the next chapter, are presented.

Table 7.1 Summary of experimental conditions for ethanol dehydration reactions with commercial catalysts

# Set	Catalyst		Feed Composition (molar ratio in feed)		Reaction temperature (°C)
	Name	Amount(g)	Water	Ethanol	
1	TPA	0.2	-	0.05	180-250
2	TPA	0.2	-	0.10	180-250
3	TPA	0.2	-	0.13	180-250
4	TPA	0.2	-	0.25	180-250
5	TPA	0.2	-	0.48	140-250
6	TPA	0.2	-	0.61	180-250
7	TPA	0.1	-	0.48	180-250
8	TPA	0.5	-	0.48	180-250
9	TPA	0.8	-	0.48	180-250
10	TPA	0.2	0.15	0.43	180-250
11	STA	0.2	-	0.48	140-250
12	MPA	0.2	-	0.48	140-250
13	Nafion	0.2	-	0.48	140-250
14	Aluminosilicate	0.1	-	0.48	125-450

Table 7.2 Summary of experimental conditions for methanol dehydration reactions with commercial catalysts

# Set	Catalyst		Feed Composition (molar ratio in feed)		Reaction temperature (°C)
	Name	Amount(g)	Water	methanol	
1	TPA	0.2	-	0.48	125-300
2	STA	0.2		0.48	125-300
3	STA	0.1	-	0.48	125-450
4	Aluminosilicate	0.1	-	0.48	125-450

Table 7.3 Summary of experimental conditions for ethanol dehydration reactions over novel mesoporous silicotungstic acid catalysts

# Set	Catalyst		Molar ratio of EtOH in feed	Reaction temperature (°C)
	Name	Amount (g)		
1	STA52(550)	0.1	0.48	180-400
2	STA62(550)	0.2	0.48	180-400
3	STA62(550)	0.1	0.48	180-400
4	STA62(350)	0.2	0.48	180-400
5	STA72(550)	0.1	0.48	180-350
6	STA82(550)	0.2	0.48	180-375
7	STA82(350)	0.2	0.48	180-375
8	STA81(EtOH&HCl)	0.2	0.48	180-375
9	STA81(CO ₂)	0.2	0.48	180-375
10	STA82(UCCO ₂)	0.1	0.48	180-375
11	STA82(350)	0.2	0.48	180-375
12	STA81P	0.2	0.48	180-375
13	STA92(550)	0.2	0.48	180-400
14	STA92(550)	0.1	0.48	180-400
15	STA92(350)	0.2	0.48	180-375
16	STA92(400)	0.2	0.48	180-375
17	STA92(475)	0.2	0.48	180-400
18	STAMCM41C	0.2	0.48	180-350
19	STAMCM41U	0.2	0.48	180-350
20	STAMAS	0.2	0.48	180-350

7.3 Analytical Method

Calibration experiments were carried out by preparing related mixtures in order to determine the retention times and the calibration factors of the components. Calibration factors and their calculations are given in Appendix A.

CHAPTER 8

EXPERIMENTAL STUDIES FOR NOVEL MESOPOROUS CATALYST SYNTHESIS FOR ALCOHOL DEHYDRATION

In this chapter experimental studies on synthesis of the novel mesoporous silicotungstic acid catalysts are given.

One of the major aims of this study is to produce novel mesoporous high surface area catalysts by using heteropolyacid, which has high activity for ethanol dehydration reaction. The main objective is to synthesize water and alcohol insoluble high surface area mesoporous catalysts having acidic character. Following the results obtained with pure heteropolyacid catalysts, silicotungstic acid which showed the highest ethanol conversion and product yield for ethanol dehydration reaction, was selected.

Novel silicotungstic acid catalysts were synthesized via direct hydrothermal synthesis and impregnation methods and characterized by using XRD, EDS, Nitrogen Adsorption, FT-IR, TGA, DTA, DSC and SEM characterization techniques.

In the impregnation method, a mesoporous support was used for silicotungstic acid (STA) whereas in direct hydrothermal synthesis method, STA was added into the structure of mesoporous material during the synthesis.

8.1 Synthesis of MCM-41

In this study MCM-41 was synthesized according to the procedure described by Sener et al. (2006). The details of synthesis procedure are given in the following.

8.1.1 Chemicals

The main components in the synthesis of MCM-41 and chemicals used are given below;

- *Source of Silica:* Sodium silicate solution, $\text{SiO}_2 \cdot \text{Na}_2\text{OH}$, 27 wt% SiO_2 and 14 wt% NaOH, d 1.390
- *Source of surfactant:* Cetyltrimethylammonium bromide (CTMABr), $\text{C}_{16}\text{H}_{33}(\text{CH}_3)_3\text{NBr}$, (M 364.46 g/mol, powder, 99% pure, Merck)
- *Source of acid:* H_2SO_4 , 4 N (prepared in the laboratory)
- *Source of Solvent:* Deionized water, obtained from Millipore Ultra-Pure Water System (Milli-QPlus).

8.1.2 Procedure

Preparation of the synthesis solution, hydrothermal synthesis, filtering the solid product, washing, drying and calcination are the main steps of the synthesis procedure for MCM-41.

- To prepare synthesis solution 13.2 g hexadecyltrimethylammonium bromide ($\text{C}_{16}\text{H}_{33}(\text{CH}_3)_3\text{NBr}$) was dissolved in 87 ml deionized water by continuous stirring with a rate of 500 rpm at 30°C. A few minutes later a clear surfactant solution, having a pH value of 6.5 was obtained.
- Then, 11.3 ml of sodium silicate was added dropwise to this clear solution with continuous stirring. By this time, pH of the synthesis mixture increased up to 12. It was adjusted to 11.0 by adding sufficient amount of 4N H_2SO_4 . After that, the synthesis gel was stirred for 1 h.

- This synthesis gel was transferred into a Teflon-lined stainless-steel autoclave for hydrothermal synthesis. This autoclave was kept at 120 °C for 96 h. In this stage, the hydrothermal synthesis took place.
- The resultant solid was filtered and it was washed with deionized water to remove the excess template. During washing step, material was taken into a beaker, suspended in 300 ml of water and stirred for 15 minutes then by using vacuum pump filtered. This process was repeated until the pH of the residual water became constant.
- The washed solid product was dried in vacuum at 40 °C for 24 h.
- MCM-41 sample was placed in a quartz tube with a membrane filter and calcined by heating from ambient temperature to 550 °C at a rate of 1 °C/min and kept at 550 °C for 8 h in a flow of dry air in a tubular furnace. The flow rate of dry air was sufficiently high ($\geq 1\text{dm}^3/\text{min}$). Air was also flowing while the furnace was cooling.

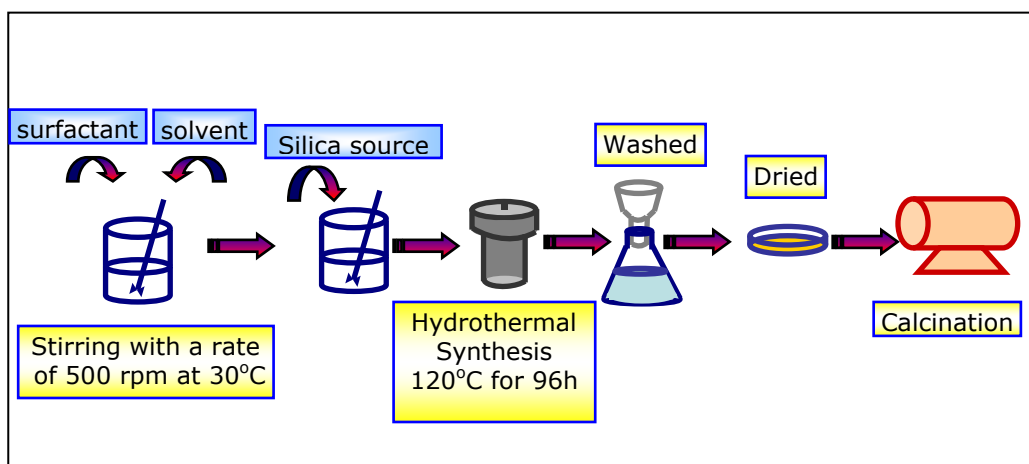


Figure 8.1 Synthesis Procedure of MCM-41

8.2 Novel Silicotungsticacid Catalysts by Direct Hydrothermal Synthesis

In this part silicotungstic acid was incorporated into mesoporous material by direct synthesis procedure. The procedure described for the preparation of MCM-41 which consisted of preparation of the synthesis solution, hydrothermal synthesis, washing, drying and calcination, was applied with some modifications.

The source of silica, the amount of silicotungstic acid, the solvent used in washing step and the calcination temperature are the parameters investigated in this part. Moreover in order to remove the template which is conventionally achieved by washing step, supercritical fluid extraction was applied in some experiments.

The steps applied in direct hydrothermal synthesis of STA incorporated mesoporous material are summarized schematically Figure 8.2.

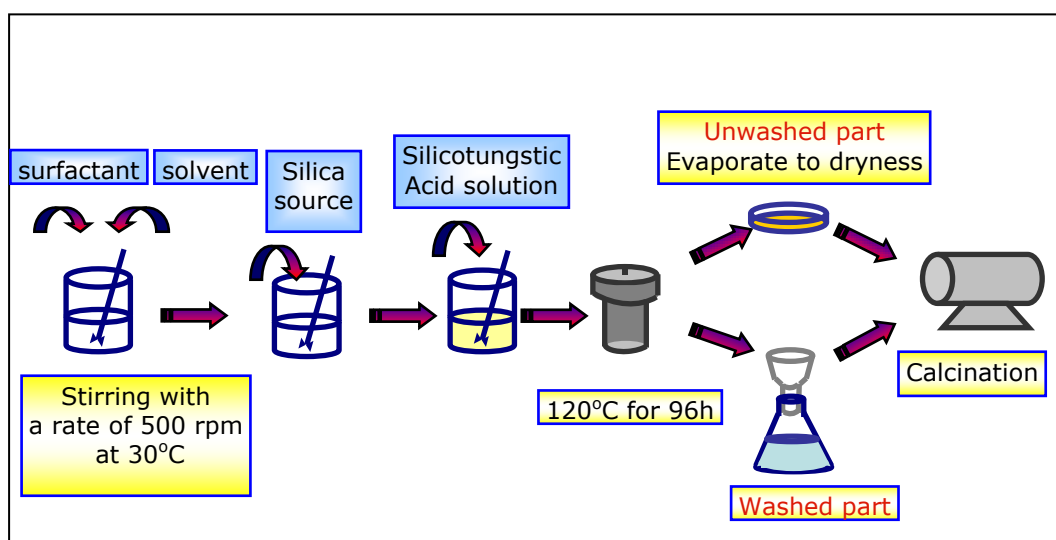


Figure 8.2 Direct Hydrothermal Synthesis Procedure

8.2.1 Chemicals

The chemical reagents used in direct hydrothermal synthesis of novel silicotungstic acid catalysts are given below;

- *Source of Silica:* Two different types of silica sources were used. Sodium silicate solution, $\text{SiO}_2 \cdot \text{Na}_2\text{OH}$, 27 wt% SiO_2 and 14 wt% NaOH , d 1.390, (Aldrich) and TEOS (Tetraethylorthosilicat) $\text{C}_8\text{H}_{20}\text{O}_4\text{Si}$ (Merck)
- *Source of surfactant:* Cetyltrimethylammonium bromide (CTMABr), $\text{C}_{16}\text{H}_{33}(\text{CH}_3)_3\text{NBr}$, (M 364.46 g/mol, powder, 99% pure, Merck)
- *Source of acid:* H_2SO_4 , 4 N (prepared in the laboratory)

- *Source of Solvent:* Deionized water, obtained from Millipore Ultra-Pure Water System (Milli-QPlus)
- Silicotungstic acid (Sigma-Aldrich)
- Ethanol (Sigma-Aldrich)
- HCl (Merck) and H₃PO₄ (Merck)

8.2.2 Procedure

The details of the procedure are given in the following;

- 13.2 g of cetyltrimethylammonium bromide (CTMABr) is dissolved in 87 ml of deionize water as being in MCM-41 synthesis. Temperature of the solution was kept at 30 °C. Clear solution was formed with continuous stirring at 500 rpm.
- The appropriate amount of Silicotungstic acid was dissolved in 5ml of deionize water. As indicated Table 8.1, the amount of STA was changed from 0.51 g to 16.93 g in order to adjust the the molar ratio of tungsten to silica in the range of 0.03 to 1.
- When sodium silicate was used as silica source; 11.3 ml of sodium silicate solution was added to surfactant solution dropwise and then STA solution was added. In spite of the added HPA, pH of this mixture is 12. In order to adjust pH of this synthesis solution at 11, sufficient amount of 4N H₂SO₄ was added and final solution is stirred for 30 minutes (Table 8.1).
- When TEOS was used as silica source; 15.64 ml of TEOS was added to surfactant solution dropwise and then STA solution was added. The pH of mixture was found to be in acidic range (Table 8.1).
- The resulting gel-solution was transferred to a Teflon-lined stainless-steel autoclave. The hydrothermal synthesis was carried out in this autoclave at 120 °C for 96 h.

- The resultant solid was divided into two parts. One part was kept without washing and evaporated to dryness and the other part was recovered by filtration, washed thoroughly with different solvents and dried at room temperature.

Washing with Deionize water: Deionize water is common solvent used in the washing step. The sample taken from the autoclave was filtered, taken into beaker, suspended in 300ml of deionize water and stirred for 15 minutes and then filtered. This procedure was repeated until the pH of residual water became constant.

Washing with H_3PO_4 Solution: Some samples were washed with H_3PO_4 solution for the removal of surfactant. 5 ml of H_3PO_4 (85% vol) was mixed with 145 ml of deionize water. Sample taken from the autoclave was put into 50 ml of acidic solution and stirred with a rate of 200 rpm at room temperature for 1 hour and then filtered. After repeating two more times with acidic solution, this procedure was applied with deionize water three times in order to remove H_3PO_4 that was adsorbed on the surface during the washing step. The final product was dried at 40°C in oven and calcined at 350°C with dry air flowing over it.

Washing with HCl & EtOH: Another washing procedure followed was by using HCl & EtOH mixture. 75 ml of 0.1 N HCl was mixed with 75 ml of ethanol. Sample taken from the autoclave was put into 50 ml of this solution and stirred with a rate of 200 rpm at 40°C and filtered. This procedure was repeated three times. After that, sample was allowed to dry at room temperature and calcined at 350°C.

Supercritical Fluid Extraction: Another method, supercritical CO_2 extraction was also applied in this study to remove the templates. This method was studied by Kawi and Lai (1998), for pure siliceous MCM-41 and found to be very efficient. ISCO-SFX 3560 which is present in the Central Laboratory was used. Sample was extracted with CO_2 having a flow rate of 1 ml/min for 3 hours. The extraction temperature was set at 100°C under the pressure of 350 bar considering the extraction efficiencies reported by Kawi and Lai (1998). Besides unwashed sample, this procedure was applied also to the sample washed with deionize water. The sample was washed with water as indicated previously, dried

and supercritical CO₂ extraction was applied. Sample was extracted with CO₂ having a flow rate of 3 ml/min for 30 minutes. The extraction temperature was set at 110°C under the pressure of 150 bar. For each case, the final product was calcined at 350°C.

- Finally, the dried sample was calcined in a quartz tube with a membrane filter by heating from ambient temperature to the desired temperature at a rate of 1°C/min and kept at this temperature for 8 hours in a flow of dry air. The temperature that should be set for calcination is decided according to TGA analysis of the synthesized catalysts. Moreover each sample was calcined at 550°C which was applied for the synthesis of MCM-41. However, calcination temperature is one of the major parameters of catalyst synthesis. Effect of calcination temperature was investigated in the range of 350°C-550°C.

Table 8.1 Experimental Conditions in Direct hydrothermal Synthesis of Novel Silicotungstic acid Catalysts

# Set	Silica Source	Amount of STA used (g)	Molar W/Si ratio in solution	pH of the solution
5	TEOS	0.51	0.03	2.3
6	TEOS	4.23	0.25	1.6
7	Sodium Silicate	4.23	0.25	11
8	TEOS	8.46	0.50	1.2
9	TEOS	16.93	1	1.2

8.3 Novel Silicotungstic Acid Catalysts by Impregnation Method

In this part, silicotungstic acid was supported on different mesoporous materials by impregnation method. MCM-41 and mesoporous aluminosilicate were used as supporting materials to synthesize STAMCM41U, STAMCM41C and STAMAS. These catalysts were prepared by different procedures, as indicated in

Table 8.2, but the basic points were the same and the general steps applied in the impregnation procedure were summarized schematically in Figure 8.3.

Table 8.2 Catalysts synthesized by impregnation method

Name	Support	Procedure
STAMCM41U	Uncalcined MCM-41	1
STAMCM41C	Calcined MCM-41	2
STAMAS	Aluminosilicate	3

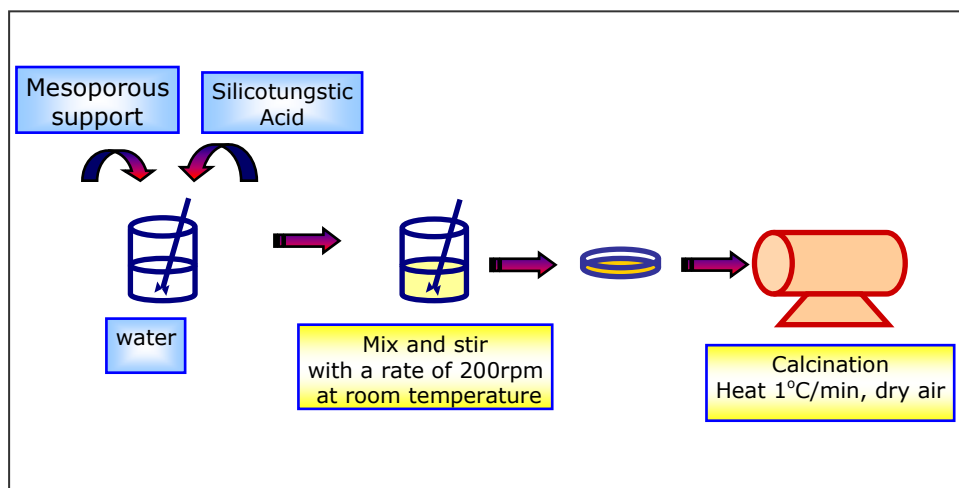


Figure 8.3 Common steps in Impregnation Method

8.3.1 Chemicals

The chemical reagents used in the impregnation procedure are given below;

- Uncalcined MCM-41, calcined MCM-41 synthesized by using the procedure given in the previous Section 8.1.2
- Aluminosilicate; mesostructured, hexagonal framework MCM-41 type

- Deionized water
- Silicotungstic acid (Sigma-Aldrich)

8.3.2 Procedure (1)

Silicotungstic acid supported on uncalcined MCM-41 was prepared in this part and this sample was called as STAMCM41U.

The procedure reported by Udayakumar and co-workers (2007) was modified and applied. Details of the procedure as follows;

- MCM-41 was synthesized by the procedure in Section 8.1.2 except the calcination stage.
- 1 gram of the uncalcined MCM-41 and 0.5 g of silicotungstic acid were dispersed in 12 ml of deionized water by stirring with a rate of 200 rpm at room temperature which was around 30°C.
- This solution was stirred at room temperature with a rate of 200 rpm at room temperature for 51 hours which was supposed to be long enough to attain equilibrium of adsorption-desorption processes as discussed in Vazquez et al. (2000).
- The resultant mixture was dried in oven at 70°C for 24 hours in order to evaporate the water. Then the sample was kept at 96°C for 21 hours and at 120°C for 2 hours.
- It was finally calcined by heating from ambient temperature to 350 °C at a rate of 1 °C/min and kept at 350 °C for 8 h in a flow of dry air in a tubular furnace.

8.3.3 Procedure (2)

Silicotungstic acid was supported on calcined MCM-41 and called as STAMCM41C. Procedure (1) was modified and applied in this section. Details of the procedure are;

- MCM-41 was prepared by the procedure described in Section 8.1.2.. As indicated in this section the final product was calcined by heating from room temperature to 550°C at a rate of 1 °C/min and kept at 550 °C for 8 h in a flow of dry air in a tubular furnace.
- 0.5 g of the calcined MCM-41 and 0.5 g of silicotungstic acid were mixed in 12 ml of deionized water by stirring with a rate of 200 rpm at room temperature.
- This solution was stirred at room temperature with a rate of 200 rpm which was around 30°C for 65 hours.
- The resultant mixture was dried at 70°C for 48 hours in order to evaporate the water and then the temperature of the oven was increased firstly to 96°C and kept at this temperature for 6 hours and then it was waited at 120°C for 2 hours.
- The dried sample was ready for reaction.

8.3.4 Procedure (3)

Silicotungstic acid was supported on mesoporous aluminosilicate and this catalyst was called as STAMAS The procedure reported by Nandhini and co-workers (2006) was modified and applied in this section. The details of the procedure are;

- 1 gram of the Aluminosilicate and 0.5 g of silicotungstic acid were dispersed in 10 ml of ethanol by stirring with a rate of 200 rpm at room temperature.
- This solution was stirred at room temperature with a rate of 200 rpm at room temperature which was around 30°C for 44 hours.
- The resultant mixture was dried at 80°C for 48 hours in order to evaporate the water.

- The sample was calcined at 200°C by heating from room temperature to 200°C at a rate of 1°C/min and kept at 200°C for 8 hours with a flow of dry air.

8.4 Characterization of Novel Catalysts

In the characterization of the synthesized catalysts, X-Ray Diffraction (XRD), Nitrogen Adsorption, Energy Dispersive Spectroscopy (EDS), Scanning Electron Microscopy (SEM), Fourier Transform Infrared Spectroscopy (FT-IR), Thermogravimetric Analysis (TGA), Differential Scanning Calorimetry (DSC), Differential Thermal Analysis (DTA) and Diffuse Reflectance FT-IR (DRIFTS) were employed.

8.4.1 X-Ray Diffraction (XRD)

X-ray diffraction provides information to identify the crystalline phases. The Rigaku D/MAX2200 diffractometer with a $\text{CuK}\alpha$ radiation source present in Metallurgical and Materials Engineering at METU was used for the analysis. The scanning range of 2θ was set between 1° and 50° with a step size of 0.01° .

8.4.2 Nitrogen Adsorption

Physical properties such as pore size, pore volume, specific surface area and the pore distributions were determined by Nitrogen Adsorption experiments results obtained at 77K. ASAP 2000 of Micromeritics Co.Inc. present at Department of Chemical Engineering at METU was used.

8.4.3 Energy Dispersive Spectrum (EDS)

Chemical compositions of materials are identified by Energy Dispersive Spectroscopy. JSM-6400 (JEOL) equipped with NORAN system Six in Department of Metallurgical and Materials Engineering at METU is used for analysis. Samples were coated with gold for the analyses.

8.4.4 Scanning Electron Microscopy (SEM)

JSM-6400 (JEOL) equipped with NORAN system Six in Department of Metallurgical and Materials Engineering at METU was used for SEM photographs of samples.

8.4.5 Thermal Analysis (TGA, DTA, DSC)

Thermal analysis of catalyst were carried out by using Dupont 951 Thermal Analyzer present in Department of Chemical Engineering at METU. The thermogravimetric experiments were performed under flowing nitrogen and with a heating rate of 10°C/min.

8.4.6 Fourier Transform Infrared Spectroscopy (FT-IR)

FT-IR measurement were done by Bruker IFS 66/S instrument, present the Central Laboratory at METU, using KBr pellet technique

8.4.7 Diffuse Reflectance FT-IR (DRIFTS)

In order to determine adsorbed species on the catalyst surface during the ethanol dehydration reaction diffuse reflectance FT-IR spectra (DRIFTS) were carried out in the flow reaction chamber of the FT-IR instrument. In this analysis a Perkin Elmer (Spectrum One) FTIR Spectrometer with a Graseby Specac DRIFT accessories present in the Department of Chemical Engineering is used. The reaction chamber is designed to be used with the optical system of the diffuse reflectance system. The chamber is connected to the reactant's gas line. About 100 mg of catalyst was placed in this sample pan which can be heated upto 500°C. The pan containing the catalyst directly faces to zinc-selenade window of the cell through which IR beam enters and the reflected beams leave. The distance between the pan and the zinc-selenade window is about 7mm. As it was shown in the earlier publications (Dogu et al., 2001; Karamullaoglu and Dogu, 2003) the contribution of gas phase to the absorption bands of the DRIFT spectra was negligibly small in this instrument.

CHAPTER 9

RESULTS of ALCOHOL DEHYDRATION REACTIONS WITH COMMERCIAL CATALYSTS

In this chapter, results corresponding to alcohol dehydration reactions on commercial solid acid catalysts and effect of operating parameters are reported.

Two important chemicals namely diethyl ether (DEE) and ethylene are produced by ethanol dehydration reaction. One of the major aim of this study is to increase the overall conversion of ethanol and to obtain high yield for the products. For this reason, different catalysts and operating parameters are tested to find out the most active and selective case.

Ethanol dehydration reaction was carried out over different catalysts. The catalytic activity of tungstophosphoric acid (TPA), silicotungstic acid (STA), molybdphosphoric acid (MPA), Nafion and mesoporous aluminosilicate in the ethanol dehydration reaction were tested individually. The product distribution and the total conversion of ethanol over these catalysts were compared.

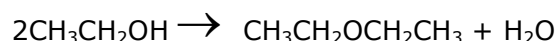
The temperature of the reaction zone, ethanol and water content of the feed and the space time are the important operating parameters that should be investigated in the content of the study. The effects of these parameters on the ethanol conversion and the selectivities of products were studied.

As well as ethanol, methanol dehydration reaction results in the formation of valuable products, namely dimethyl ether (DME) and formaldehyde. Experimental studies were planned to get high methanol conversion and product selectivities over different catalysts with different operating conditions.

The catalytic activity of silicotungstic acid, tungstophosphoric acid and aluminosilicate were tested in methanol dehydration reaction. The effect of reaction temperature and space time on the overall methanol conversion and the product distribution were investigated.

9.1 Ethanol Dehydration Reaction over Tungstophosphoric Acid

Ethanol which is considered as a clean, renewable feedstock give dehydration reaction over solid acid catalysts. As a result of catalytic dehydration reaction, it is converted into diethyl ether (DEE) and ethylene with the following reactions;



In this way, two valuable products can be derived from ethanol. As indicated previously, DEE can be used as an alternative fuel to gasoline and also as a fuel additive. On the other hand, ethylene is very important in petrochemical industry and obtaining ethylene from a renewable feedstock instead of petroleum makes ethanol dehydration reaction an attractive alternate.

Ethanol conversion and selectivity values of DEE and ethylene were evaluated basing on the chemical compositions of the reactor effluent stream which was online connected to Gas Chromotography. The mole fractions of products, i.e. ethylene, DEE and water, also unconverted ethanol, were calculated using the peak areas obtained from GC and multiplying by the corresponding calibration factors.

The total conversion of ethanol was calculated using Equation 9.1. In this expression, n_{EtOH}^0 is the total moles of ethanol. As indicated in Equation 9.2, it is calculated from carbon balance and n_{EtOH} is the uncovered ethanol.

$$X_{\text{EtOH}} = \frac{(n_{\text{EtOH}}^0 - n_{\text{EtOH}})}{n_{\text{EtOH}}^0} \quad (9.1)$$

$$\text{where } n_{EtOH}^0 = n_{Ethylene} + 2n_{DEE} + n_{EtOH} \quad (9.2)$$

The selectivity of DEE and ethylene were calculated using Equation (9.3) and (9.4) respectively, and, the yield of DEE and ethylene were calculated using Equation (9.5) and (9.6), respectively.

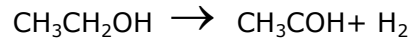
$$S_{DEE} = \frac{2 \times n_{DEE}}{(n_{EtOH}^0 - n_{EtOH})} \quad (9.3)$$

$$S_{Ethylene} = \frac{n_{Ethylene}}{(n_{EtOH}^0 - n_{EtOH})} \quad (9.4)$$

$$Y_{DEE} = X_{EtOH} \times S_{DEE} \quad (9.5)$$

$$Y_{Ethylene} = X_{EtOH} \times S_{Ethylene} \quad (9.6)$$

Depending on the characteristic of the used catalysts in some experiments acetaldehyde formation is also observed due to dehydrogenation reaction of ethanol given as follow,



In this case $n_{Acetaldehyde}$ was added to Equation 9.2 and the selectivity and yield were expressed as,

$$S_{Acetaldehyde} = \frac{n_{Acetaldehyde}}{(n_{EtOH}^0 - n_{EtOH})} \quad (9.7)$$

$$Y_{Acetaldehyde} = X_{EtOH} \times S_{Acetaldehyde} \quad (9.8)$$

For each experimental condition, conversion, selectivity and yield calculations were done. A sample calculation is presented in Appendix B. Each data point reported in all figures is actually an average of results obtained in at least four successive measurements. In some cases, steady state composition of the reactor effluent stream is determined from the average of up to seven

successive measurements. Fractional conversion of ethanol and selectivity values of products, evaluated in these repeated runs were all within 3 % error limits.

9.1.1 Effects of Reaction Temperature

One of the major parameter that can effect the conversion of ethanol is the temperature of reaction zone. For this reason, the fixed bed flow reactor was packed with 0.2 g of tungstophosphoric acid. A gaseous feed stream of 44.24 ml/min containing 5 % ethanol in the mixture of ethanol and helium, at room temperature were used. Reaction temperature was changed in the range of 180-250°C and results were evaluated.

Two main products obtained in ethanol dehydration reaction over tungstophosphoric acid were DEE and ethylene whereas acetaldehyde formation was not observed.

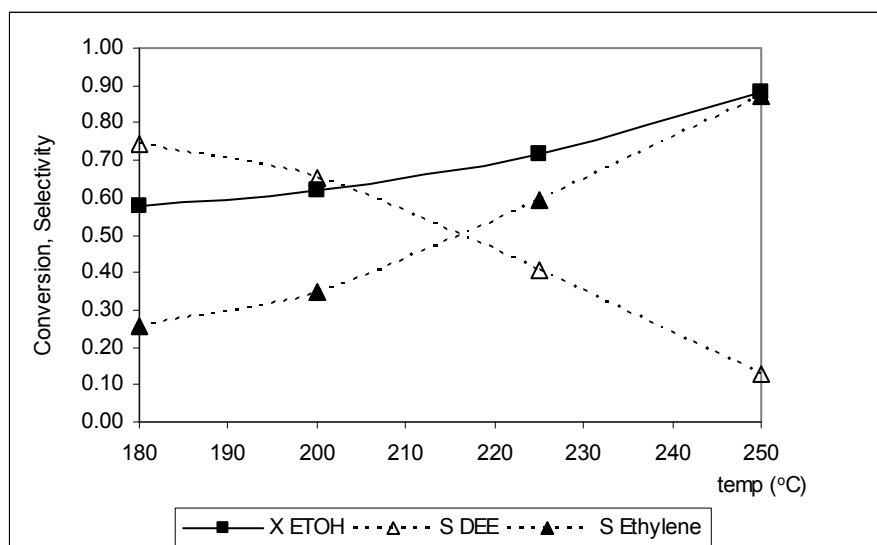


Figure 9.1 The variation in conversion of ethanol and selectivities of products, using 0.2 g of TPA, EtOH/(EtOH&He):0.05

Experimental results showed that higher reaction temperatures yield higher conversion of ethanol. By increasing reaction temperature from 180°C to 250°C, conversion of ethanol was increased from 0.58 to 0.88 (Figure 9.1).

In Figure 9.1, selectivity profiles of both products are also given. It was observed that as a result of increase in reaction temperature, selectivity of

ethylene increased while that of DEE decreased. Indeed, selectivity of ethylene was changed from 0.26 to 0.87 by increasing the temperature of the reaction medium from 180°C to 250°C, respectively.

Related with the conversion and selectivity profiles, a significant increase in ethylene yield, from 0.15 to 0.77, and a corresponding decrease in DEE yield, from 0.43 to 0.12, with an increase in reaction temperature from 180 to 250°C was occurred, respectively (Figure 9.2). An ethylene yield value of 0.77 obtained at 250°C indicated the possibility of a new avenue for ethylene production from a nonpetroleum feedstock, namely ethanol which might be produced by fermentation .

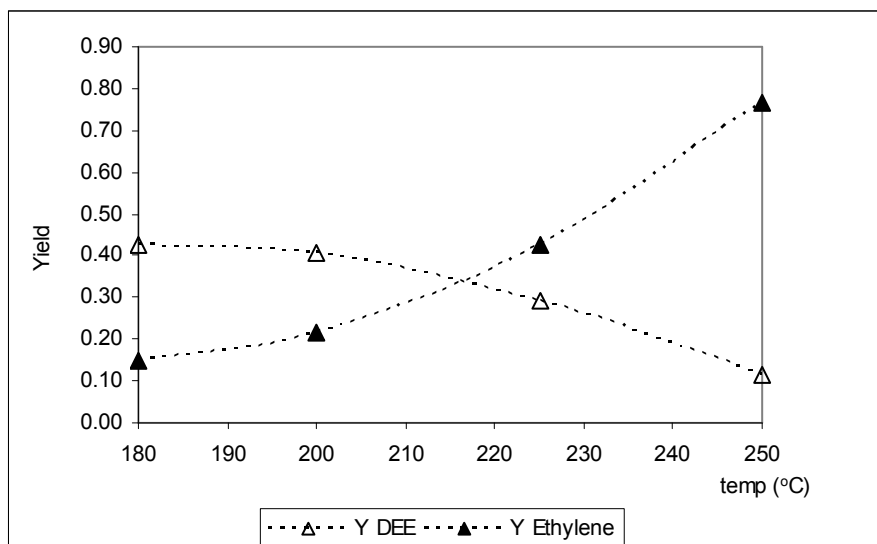


Figure 9.2 The variation in yields of products using 0.2 g of TPA, EtOH/(EtOH&He):0.05

9.1.2 Effects of Feed Composition

The next issue is to investigate the effects of ethanol content of the feed stream on ethanol dehydration reaction over heteropolyacid catalyst.

Six sets of experiment were prepared in which ethanol mole fraction in the feed stream was changed from 0.05 to 0.61 by keeping the total flow rate of feed at 44.24 ml/min. For each set, the reactor was packed with 0.2 g of tungstophosphoric acid, in order to prevent the error that may come due to deactivation of HPA, fresh catalyst was used. Moreover, for each set,

dehydration reaction of ethanol was carried out in the temperature range of 180 to 250°C.

An increase in the overall conversion of ethanol was observed with an increase in temperature for each feed condition (Figure 9.3). However, increasing the alcohol content of the feed stream caused a decrease in conversion values. For example, an increase in ethanol mole fraction in the feed stream from 0.05 to 0.48 caused a decrease in ethanol conversion from 0.88 to 0.53 at 250°C.

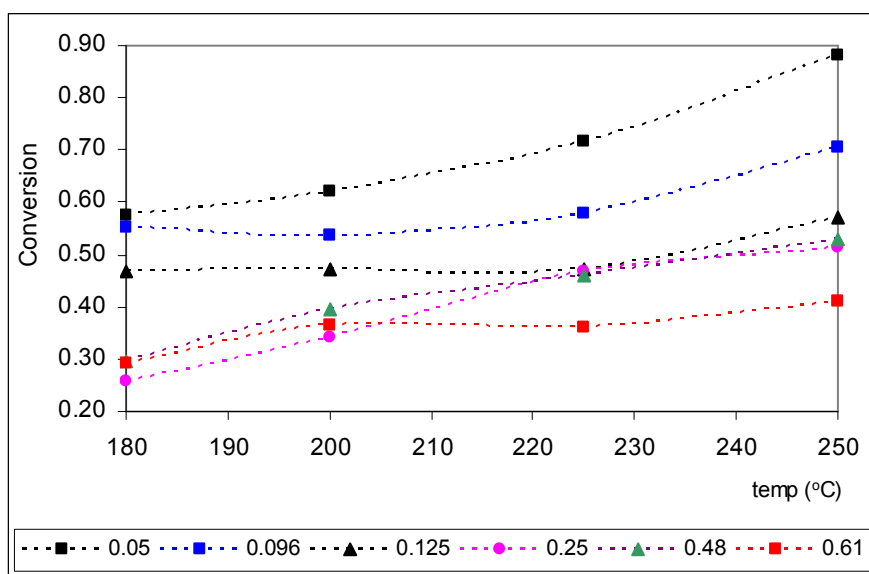


Figure 9.3 The variation in conversion of ethanol with reaction temperature at different feed compositions, using 0.2 g of TPA

The highest ethanol conversion could be obtained by using dilute feed stream containing ethanol mole fraction lower than 0.25, especially at high reaction temperature such as 250°C (Figure 9.4). At the same reaction temperature a sharp decrease in ethanol conversion was observed by increasing ethanol molar ratio from 0.05 to 0.15. Between 0.15 and 0.50, the change in conversion value was very small. For example conversion value is 0.47 for a feed stream containing ethanol with molar ratio of 0.25 and conversion value became 0.46 for a feed stream containing ethanol in molar ratio of 0.48, at 225°C.

This behavior indicated two parallel routes for the decomposition of ethanol. This is further discussed in Chapter 12.

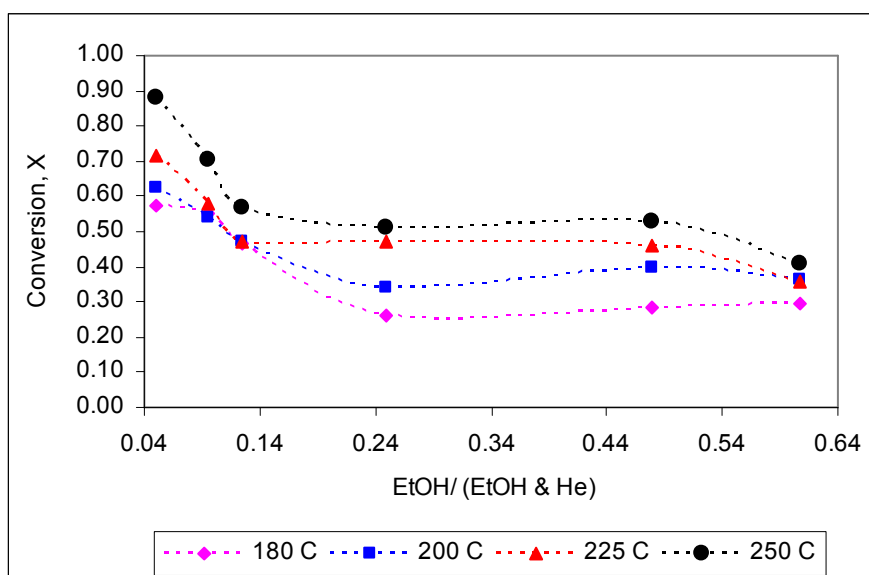


Figure 9.4 The variation in conversion of ethanol with feed composition, using 0.2 g of TPA

Increase of temperature from 180°C to 250°C caused a decrease in DEE selectivity and an increase in ethylene selectivity (Figure 9.5 and Figure 9.6).

Dependence of selectivity values of DEE and ethylene on ethanol mole fraction showed interesting symmetrical behavior (Figure 9.5 and Figure 9.6). For example at 200°C, ethylene selectivity was increased from 0.35 to 0.50 by increasing alcohol content from 0.05 to 0.096. This trend is also observed at the other temperatures in the same figure. Opposite behaviour was observed for DEE formation. At 200°C, its selectivity decreased from 0.65 to 0.50 when the ethanol content of the feed stream was increased from 0.05 to 0.096 (Figure 9.6).

According to these results which were obtained over 0.2 g of tungstoposphoric acid, maximum ethylene selectivity of 0.87 at 250°C was obtained for a feed stream containing ethanol in molar ratio of 0.05. In the case of DEE, maximum value of 0.92 was obtained when a feed stream containing ethanol in molar ratio of 0.61 was used at 180°C (Figure 9.5 and Figure 9.6).

Over an ethanol mole fraction of 0.1 ethylene selectivity first increased passing through a maximum, then decreased. The behavior of DEE selectivity is just opposite. Possible reasons of such concentration dependences of selectivity values were discussed in Chapter 12 while discussing the mechanism of the

dehydration reaction. Diffuse reflectance FT-IR (DRIFTS) results gave further information about the reaction mechanism (Chapter 12).

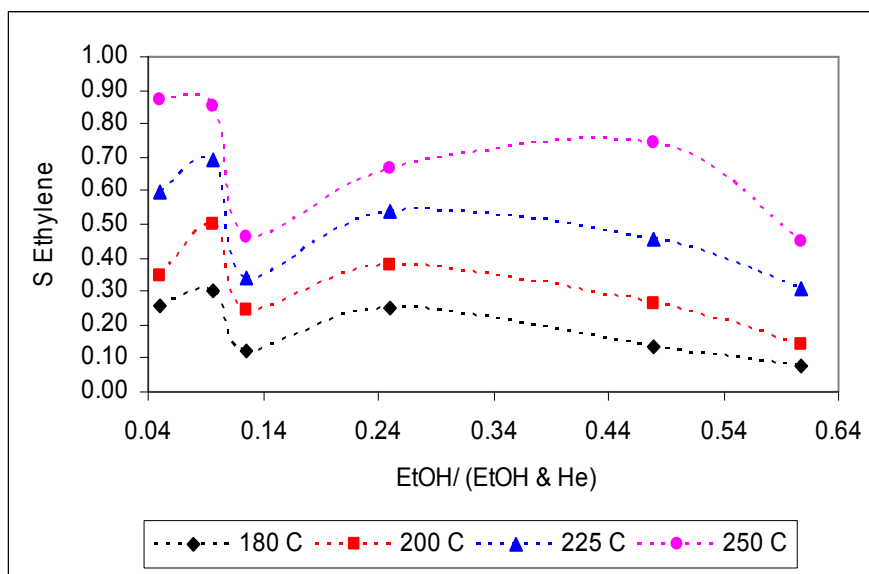


Figure 9.5 The variation in selectivity of Ethylene with feed composition, using 0.2 g of TPA

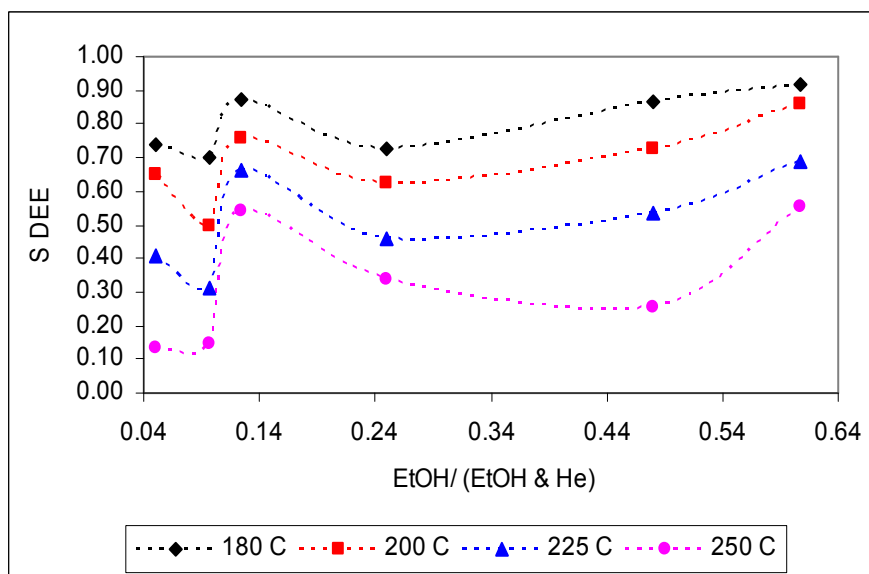


Figure 9.6 The variation in selectivity of DEE with feed composition, using 0.2 g of TPA

9.1.3 Effects of Water Present in the Feed Stream

Upto now, experiments were carried out with a feed stream containing pure ethanol. But it should be remembered that the economics of ethylene and DEE production by the dehydration reaction of ethanol strongly depend upon the possible use of bio-ethanol which contains some water in the feed stream. For this reason, possible effects that comes from the presence of water should be checked in the catalytic activity of HPA in ethanol dehydration reaction.

A feed stream containing water in a molar ratio of 0.15 in the mixture was prepared adjusting the flow rate of ethanol, water and helium at 19.1 ml/min, 6.8 ml/min and 18.3 ml/min, respectively, by keeping the total flow rate at 44.2 ml/min. The volume ratio of water to ethanol was 0.1 in liquid phase. 0.2 g of TPA was used and reaction temperature was changed from 180 to 250°C.

Obtained results showed that the presence of water ($\text{H}_2\text{O}/\text{Ethanol}=0.1$ v/v) in the feed stream caused some reduction in ethanol conversion. For example, a decrease was observed in ethanol conversion from 0.53 to 0.37 at a reaction temperature of 250°C due to water effect (Figure 9.7). Indeed, water is expected to adsorb more strongly than ethanol on such acidic catalyst surface, causing reduction in number of available active sites for the chemisorption of ethanol (Varisli et al., 2007).

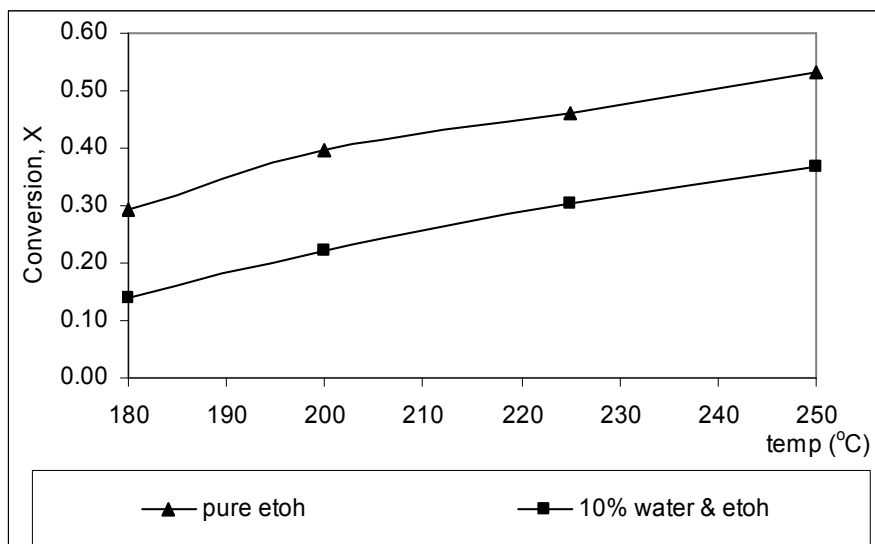


Figure 9.7 The variation in conversion of ethanol with the presence of water in the feed stream using 0.2 g of TPA

Lower DEE selectivity and higher ethylene selectivity were observed in the presence of water at temperatures lower than 230°C (Figure 9.8). This behavior was reversed at higher temperatures. Upto seven repeated experimental results proved that this observation was not due to any experimental errors.

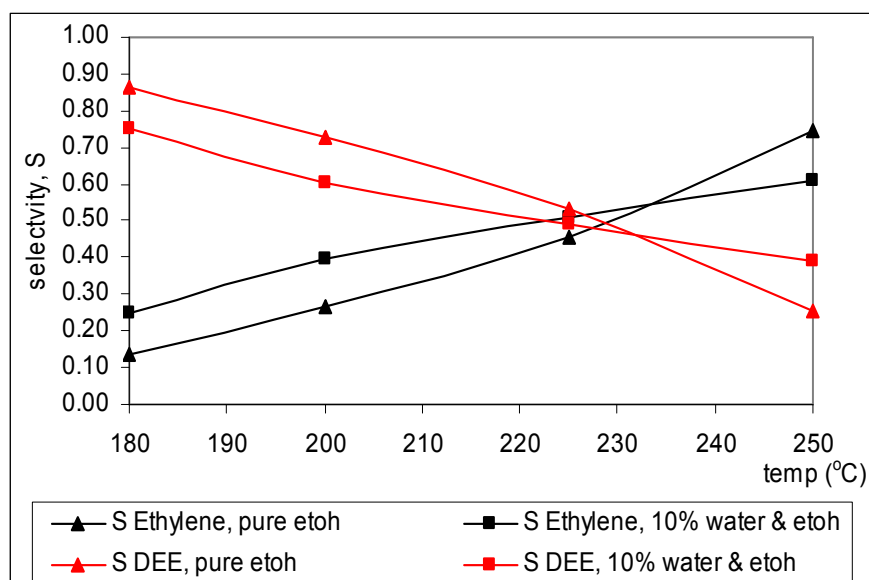


Figure 9.8 The variation in selectivities of products with the presence of water in the feed stream using 0.2 g TPA

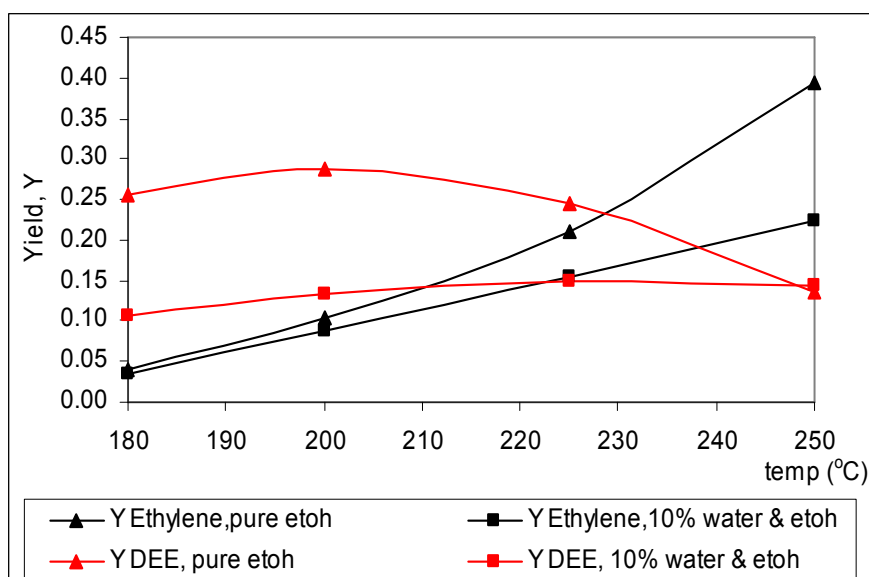


Figure 9.9 The variation in yields of products with the presence of water in the feed stream using 0.2 g of TPA

As seen in Figure 9.9, an ethylene yield value of 0.40 was obtained when pure ethanol was used whereas 10 vol % of water addition to the feed stream resulted approximately an ethylene yield value of 0.20, at 250°C. For DEE, the difference in yield was observable upto 250°C, at this temperature the same yield value was obtained in the presence and absence of water.

9.1.4 Effects of Space Time

The other parameter that should be investigated in ethanol dehydration reaction to get high conversion and selectivity values is the amount of catalyst used in the experiment.

For this aim, four experimental sets were planned in which the amount of tungstophosphoric acid catalyst charged to the reactor was changed from 0.1 and 0.8 g. For each case, feed stream containing ethanol in a molar ratio of 0.48 was used and the reaction temperature was changed in the range of 180°C to 250°C.

As expected, an increase in ethanol conversion was observed with an increase in the amount of used catalyst (Figure 9.10). Indeed, increase of catalyst amount caused an increase in the space time within the reactor. At 250°C, by using 0.1 g of TPA ethanol conversion was 0.29 and it was increased to 0.94 by using 0.8 g of the catalyst.

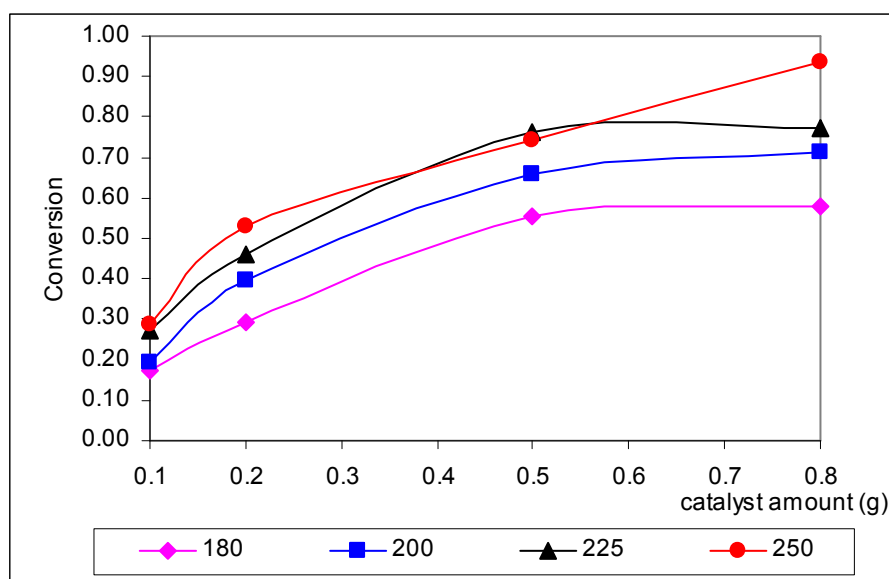


Figure 9.10 The variation in conversion of ethanol with the amount of catalyst, EtOH/(EtOH&He):0.48

Although higher conversion values were obtained, product selectivities did not differ much with the increase in space time such as ethylene selectivity was 0.47 when 0.1 g of TPA was used at 225°C and it was 0.51 when 0.5 g of TPA used at the same temperature (Figure 9.11 and 9.12).

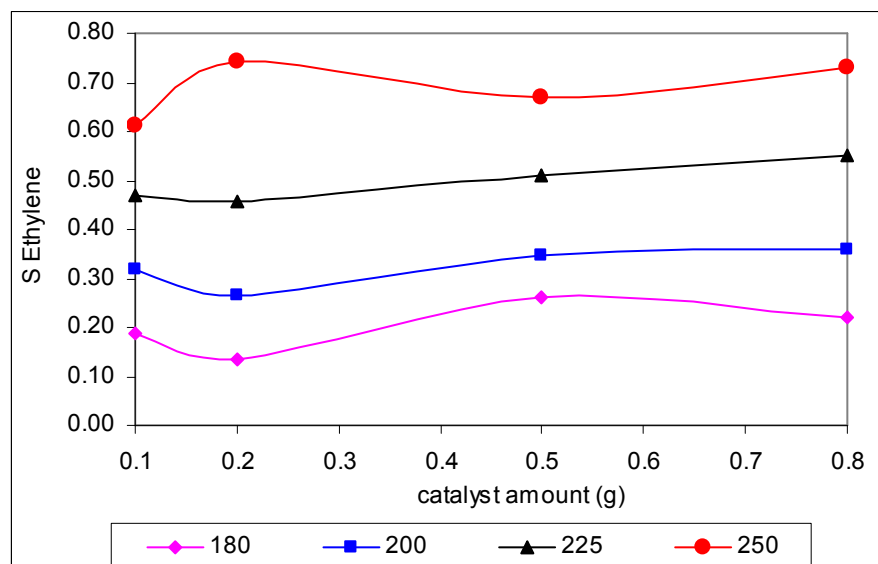


Figure 9.11 The variation in selectivity of ethylene with the amount of catalyst, EtOH/(EtOH&He):0.48

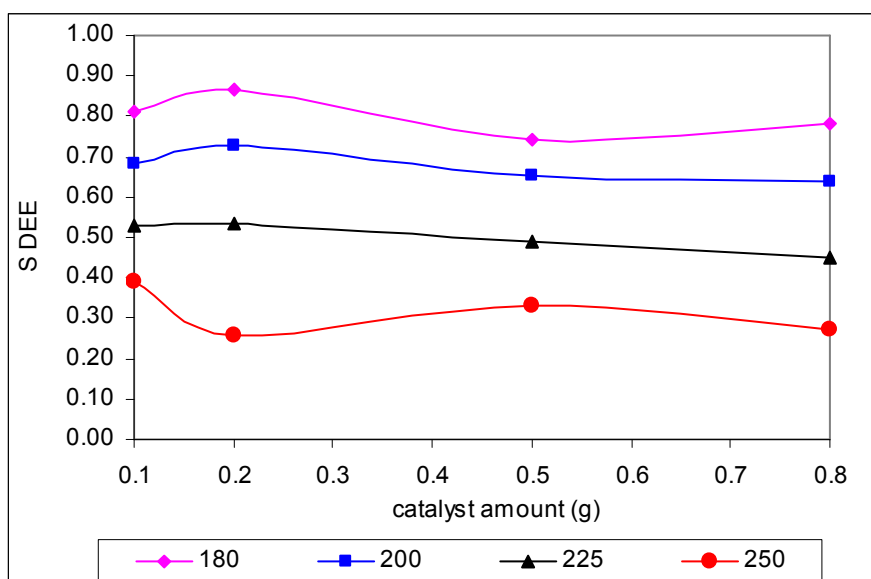


Figure 9.12 The variation in selectivity of DEE with the amount of catalyst, EtOH/(EtOH&He):0.48

These results indicated that DEE and ethylene are probably produced mostly through parallel routes rather than following a consecutive reaction scheme for this feed composition. These results supported the reaction mechanism proposed in the early work of Saito and Niiyama (1987), suggesting the formation of ethylene by the decomposition of chemisorbed ethanol molecules and formation of DEE by the reaction between chemisorbed and physisorbed ethanol molecules on the catalyst surface. Using a catalyst amount of 0.8 g, ethanol conversion and ethylene selectivity values of 0.94 and 0.73 were obtained, respectively at 250°C (Figure 9.11). An ethylene yield value approaching 0.7 is quite promising for possible use of bioethanol to produce petrochemicals.

9.2 Ethanol Dehydration Reaction over Different HPA Catalysts

In this part of the study, activities of other heteropolyacid catalysts, namely molybdophosphoric acid (MPA) and silicotungstic acid (STA) in the ethanol dehydration reaction were compared with tungstophosphoric acid (TPA).

Experiments were carried out over 0.2 g of each catalyst using feed stream of 44.24 ml/min in which ethanol molar ratio was 0.48. The temperature of the fixed bed flow reactor was changed from 140 to 250°C.

Among these three heteropolyacid catalysts, STA showed the highest activity (Figure 9.13. At a reaction temperature of 250°C, ethanol conversion value was 0.70 with STA, while it was 0.53 with TPA and only 0.10 with MPA.

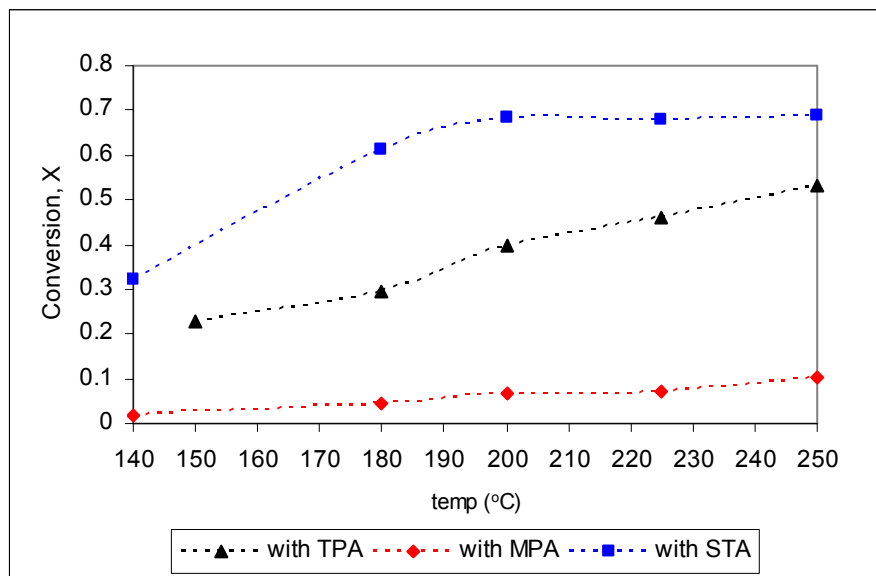


Figure 9.13 The variation in ethanol conversion using different heteropolyacids, EtOH/(EtOH&He):0.48, 0.2 g of catalyst

The ratio of ethylene yield to W/F (W being the catalyst mass and F being molar flow rate of ethanol) obtained with STA, TPA and MPA at 250°C were about 2.1, 1.8 and 0.14 mol/lg respectively. Corresponding values reported in the literature (Takahara, 2005) using other solid acid catalysts, such as different zeolites and silica-alumina, are about one to two orders of magnitude smaller than the results obtained in this study with STA and TPA.

Ethylene selectivity values obtained with STA and TPA are quite close to each other in the temperature range studied (Figure 9.14). The acid strengths of these three HPA catalysts are reported to follow the following trend TPA>STA>MPA (Wang et al., 2000). Considering this reported result, the higher ethanol dehydration activity of STA than TPA can not be explained by the differences of acid strengths only. Results reported by Verhoef et al. (1999) for the esterification reactions carried out using supported TPA and STA catalysts also showed higher activity of STA than TPA and this was explained by the presence of higher number of Keggin protons of STA (four) as compared to TPA (three).

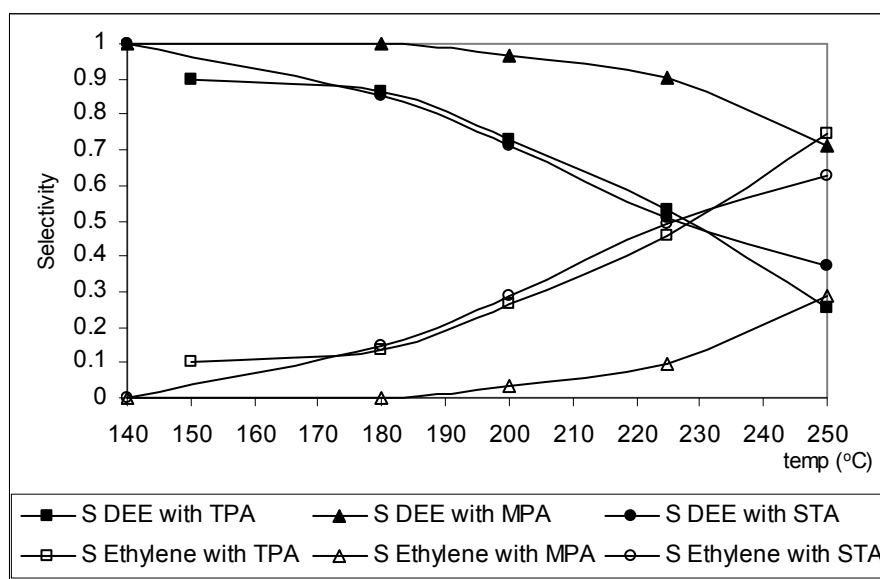


Figure 9.14 The variation in selectivities of products using different heteropolyacids, EtOH/(EtOH&He):0.48, 0.2 g of catalyst

Other differences of these two heteropoly acids are their dehydration behavior and their thermal stability. At room temperature TPA is expected to have hexahydrate structure ($\text{H}_3\text{PW}_{12}\text{O}_{40} \cdot 6 \text{H}_2\text{O}$). At higher temperatures anhydrous TPA is formed by the removal of water (Thomas, et al., 2005) and at temperatures over 180°C TPA starts to decompose. As reported by Obali (2004), thermal analysis (TGA and DSC) of TPA shows decomposition of this heteropoly acid catalyst within the temperature range between 180°C and 330°C. However, STA ($\text{H}_4\text{SiW}_{12}\text{O}_{40}$) is in completely dehydrated form, even at room temperature and as reported by Thomas et al., (2005) it is much more stable than TPA at temperatures higher than 200°C. These findings supported our results that STA was more active than TPA in the dehydration reaction of ethanol to produce ethylene and DEE.

9.3 Ethanol Dehydration Reaction over Nafion

Heteropolyacids have very strong acidity and they are preferred for the acid catalyzed reactions as in the case of ethanol dehydration reaction to produce DEE and ethylene. STA, TPA and MPA are commercially available and these are very well known examples of this class. They were examined in the vapor phase dehydration reaction and it was reported that especially STA was found to be very active in ethanol dehydration reaction. Since heteropolyacids

are very soluble in polar solvent such as ethanol, ethanol dehydration reaction is not tried in liquid phase heterogeneously. For liquid phase reaction, another type of catalyst, i.e. Nafion is supposed to be very suitable in terms of its nonsolubility in polar solvents.

Nafion is a perfluorinated ion-exchange polymer and can be effectively in acid catalyzed reactions. It is a copolymer of a tetrafluoroethene and perfluoro-2-(fluorosulfonylethoxy)propyl vinyl ether. Its Hammett acidity ($-H_0 \approx 12$) is similar to 100% H_2SO_4 (Harmer et al., 1996). In this experiment, Nafion NR50 was used. Nafion NR50 is in the form of millimeter size beads and it has a very low surface area which is around $0.02 \text{ m}^2/\text{g}$ or less. To investigate the catalytic activity of this catalyst in ethanol dehydration reaction, a new set of vapor phase dehydration experiment was planned.

A feed stream of 44.24 ml/min , containing ethanol in a molar ratio of 0.48 was supplied to fixed bed flow reactor in which 0.2 g of Nafion was packed. The reaction temperature was changed between 140 and 250°C .

The conversion values of ethanol obtained at different temperatures by using Nafion was compared with that of heteropolyacids in Figure 9.15. The catalytic activity of Nafion was higher than MPA whereas it was lower than STA and TPA at the same reaction conditions. The temperature of the reactor packed with Nafion should be higher than that is packed with STA or TPA to get the same conversion value, such as 140°C for STA, 180°C for TPA whereas 225°C for Nafion to obtain 30% conversion of ethanol.

DEE and Ethylene formation occurred during the reaction while acetaldehyde was not observed in the reactor effluent. Higher selectivity values for DEE and lower selectivity values of Ethylene were obtained by using Nafion comparing to TPA. For example, at 200°C selectivity values of DEE were 0.84 and 0.73 for Nafion and TPA, respectively (Figure 9.16). However, considering the conversion and selectivity together, the higher yield values for both DEE and Ethylene were obtained for heteropolyacid (Figure 9.17).

These experimental results showed that in spite of its superacidity, the catalytic activity of Nafion was limited by its lower surface area, as mentioned by Harmer et al. (1996).

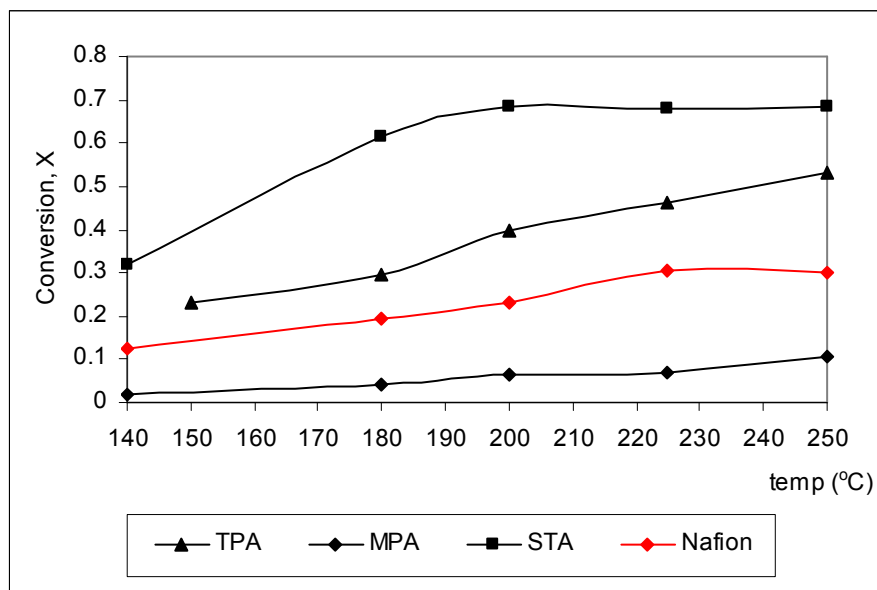


Figure 9.15 The variation in ethanol conversion using Nafion, EtOH/(EtOH&He):0.48, 0.2 g catalyst

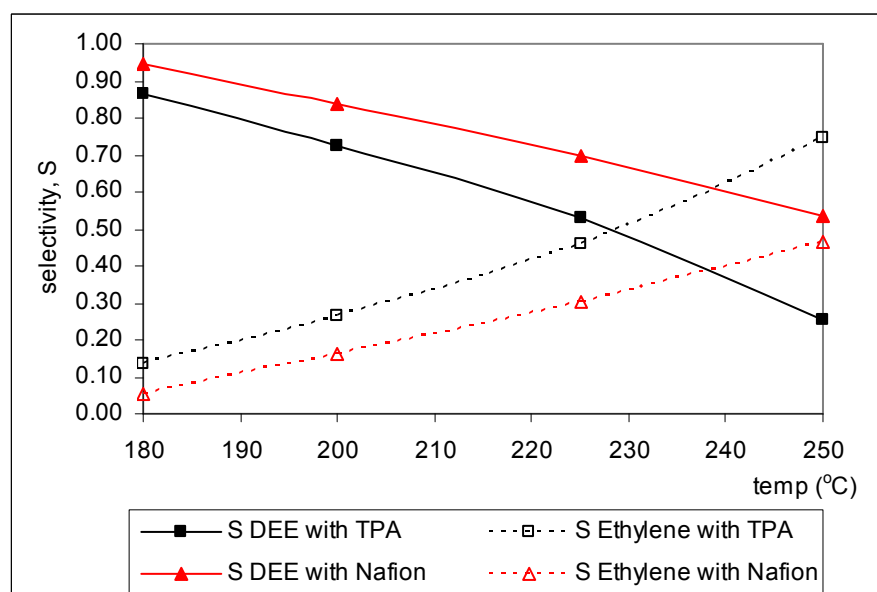


Figure 9.16 The variation in selectivities of products using Nafion, EtOH/(EtOH&He):0.48, 0.2 g catalyst

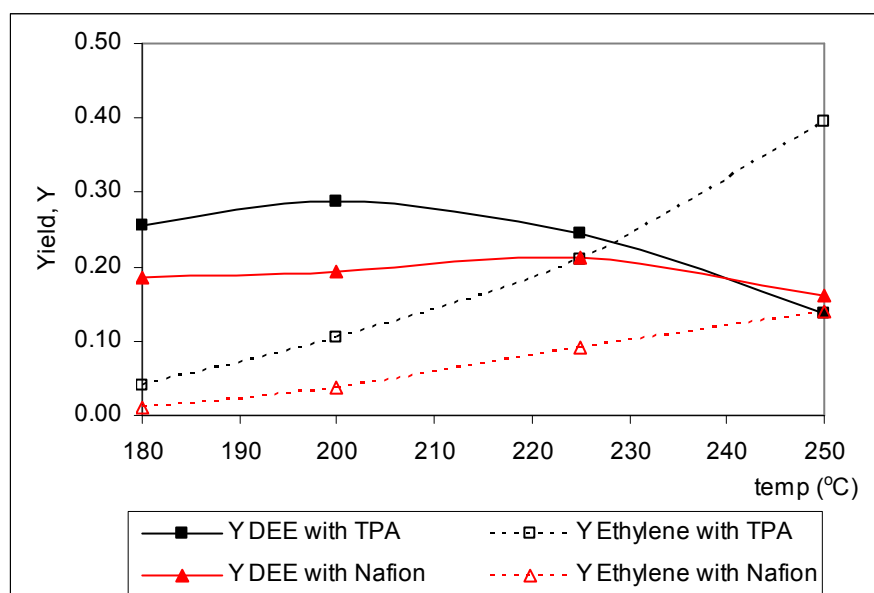


Figure 9.17 The variation in selectivities of products using Nafion, EtOH/(EtOH&He):0.48, 0.2 g catalyst

9.4 Ethanol Dehydration Reaction over Mesoporous Aluminosilicate

Upto now different heteropolyacids, namely STA, TPA, MPA and Nafion were used in ethanol dehydration reaction and high conversion values were reported with heteropolyacids especially for STA. However it should be noted that heteropolyacids have very low surface area and at the end of the reaction period coke formation is observed. Mesoporous aluminosilicate has a large surface area, 903 m²/g, with a pore volume of 0.96 cm³/g and an average pore diameter of 2.9 nm. It contained alumina in a molar ratio of 3 % in its mesoporous structure. A set of experiment was planned to analyze the catalytic activity of this catalyst in ethanol dehydration reaction.

A feed stream of 44.24 ml/min containing ethanol in a molar ratio of 0.48 was supplied to fixed bed flow reactor in which 0.1 g of aluminosilicate was packed. The range of reaction temperature was extended from 125 to 450°C.

A negligible conversion of ethanol was observed upto 300°C and maximum ethanol conversion value of 0.58 was obtained at 450°C without any deactivation in the catalyst (Figure 9.18). In comparison to heteropolyacids, higher reaction temperature was required to obtain considerable conversion of

ethanol on the other hand coke formation was hardly observed in the reactor even at 450°C.

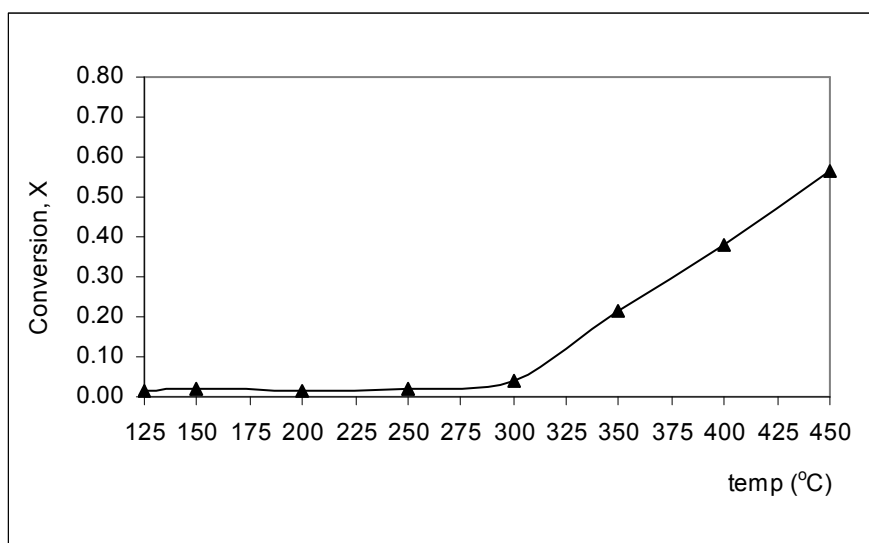


Figure 9.18 The variation in conversion of ethanol, using 0.1 g of Aluminosilicate, EtOH/(EtOH&He):0.48

When aluminosilicate was used as a catalyst, besides DEE and ethylene formation, some acetaldehyde was observed in the reactor effluent (Figure 9.19). Indeed, acetaldehyde was produced upto 350°C.

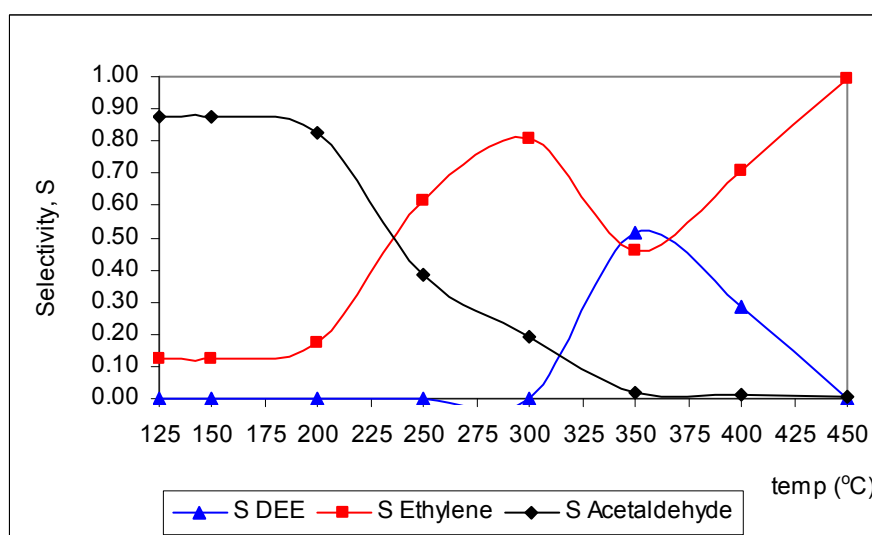


Figure 9.19 The variation in selectivities of products, using 0.1 g of Aluminosilicate, EtOH/(EtOH&He):0.48

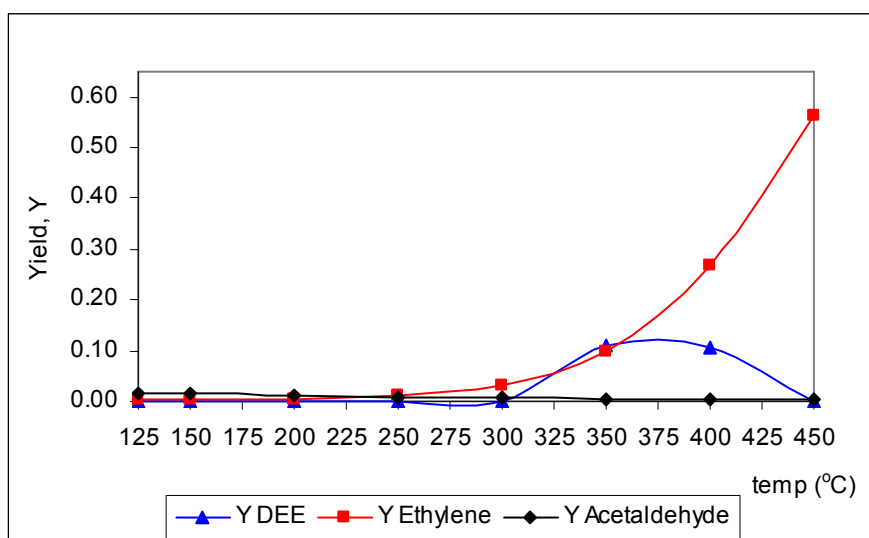


Figure 9.20 The variation in yield of products using 0.1 g of Aluminosilicate, EtOH/(EtOH&He):0.48

In terms of yield values, it can be said that main product is Ethylene for dehydration reaction of ethanol over aluminosilicate and under these experimental conditions a maximum Ethylene yield of 0.56 is obtained with Aluminosilicate (Figure 9.20). The maximum observed in DEE yield indicated further decomposition of DEE to ethylene after temperatures over 375°C.

9.5 Methanol Dehydration Reaction over STA

DME has been considered as a clean and effective gasoline alternative. It can be produced by methanol dehydration reaction which is written below,



In the content of this study, it is seen that among the heteropolyacids STA and TPA are very active in ethanol dehydration reaction. Aluminosilicate is found to be active as well. In this section, the catalytic activities of these catalysts are tested in the methanol dehydration reaction to produce DME.

9.5.1 Effects of Reaction Temperature

It was seen that reaction temperature enhanced the conversion of ethanol over STA. In order to investigate the effects of the reaction temperature

on the conversion of methanol over STA, feed flow stream containing methanol in helium with a molar ratio of 0.48 was sent continuously to the reactor. The liquid methanol flow rate was adjusted to 2.1 ml/hr and total flow rate of the vapor stream was set to 44.24 ml/min. The stainless steel tubular reactor was packed with 0.2 g of STA and the temperature was changed in the range of 125°C to 300°C.

Two important products were obtained in these experiments, namely DME and formaldehyde. Obtained results showed that the maximum conversion value was approximately 0.32, at a reaction temperature of 250°C (Figure 9.21). According to TGA and DSC results, which are discussed in Chapter 10, STA did not decompose at this temperature interval. The decrease in conversion of methanol may be explained by coke formation. Mainly dimethyl ether formation occurred and formaldehyde was produced as a by product especially at temperatures lower than 200°C (Figure 9.22).

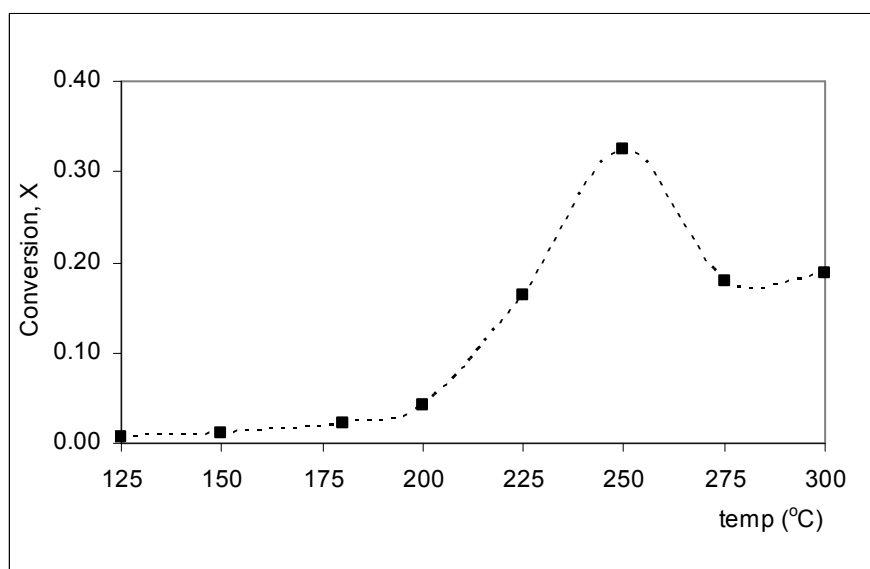
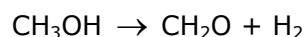


Figure 9.21 The variation in conversion of methanol, using 0.2 g of STA, MeOH/(MeOH&He):0.48

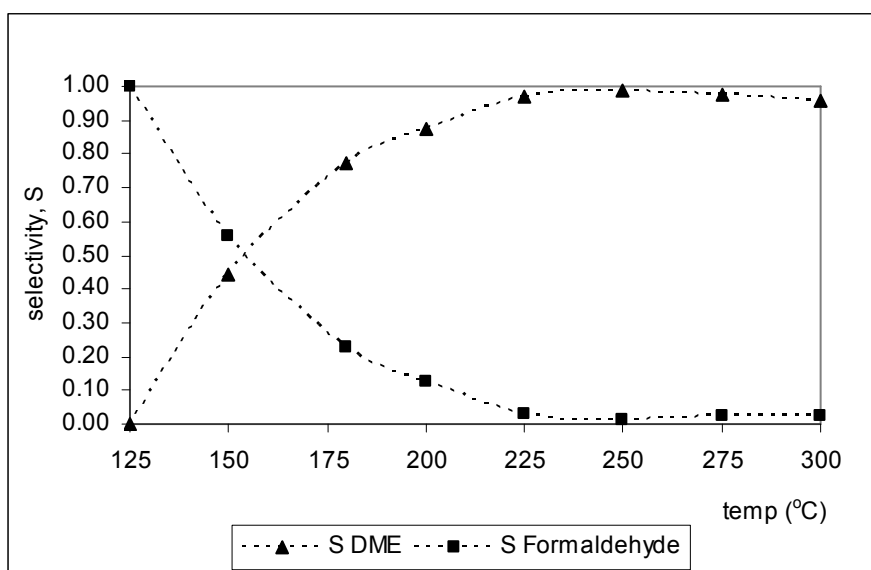


Figure 9.22 The variation in product selectivities with temperature, using 0.2 g of STA, MeOH/(MeOH&He):0.48

9.6 Methanol Dehydration Reaction over TPA

In order to compare the catalytic activity of STA and TPA in methanol dehydration reaction, a new set of experiment was planned.

In this experiment, a feed stream containing methanol in helium with a molar ratio of 0.48 was used as in the case of STA. The reactor was packed with 0.2 g of tungstophosphoric acid and reaction temperature was changed from 125 to 300°C.

Results indicated that silicotungstic acid showed higher catalytic activity than tungstophosphoric acid (Figure 9.23) in methanol dehydration reaction at temperatures higher than 225°C. The conversion of methanol was 0.32 whereas it was around 0.14 with TPA at 250°C. At temperatures lower than 225°C, TPA gave higher conversion values for methanol.

When the product distribution obtained with STA and TPA are compared; mainly DME formation was observed for both of them. The selectivity value of DME obtained with TPA was higher than that of obtained with STA upto 180°C and then situation occurred in the opposite direction. Selectivity of DME increased

upto 96% over STA whereas decreased to 47 % over TPA at 300°C (Figure 9.24).

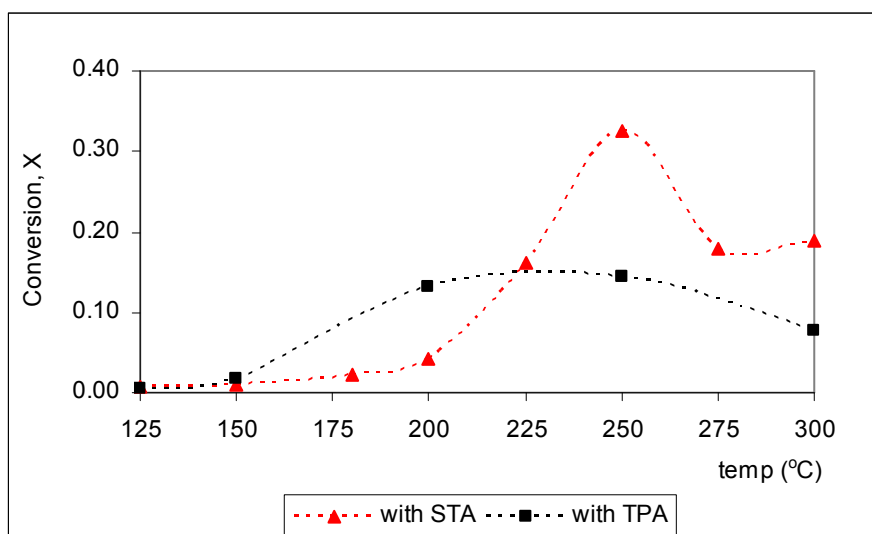


Figure 9.23 The variation in conversion of methanol using 0.2 g of different heteropolyacids, MeOH/(MeOH&He):0.48

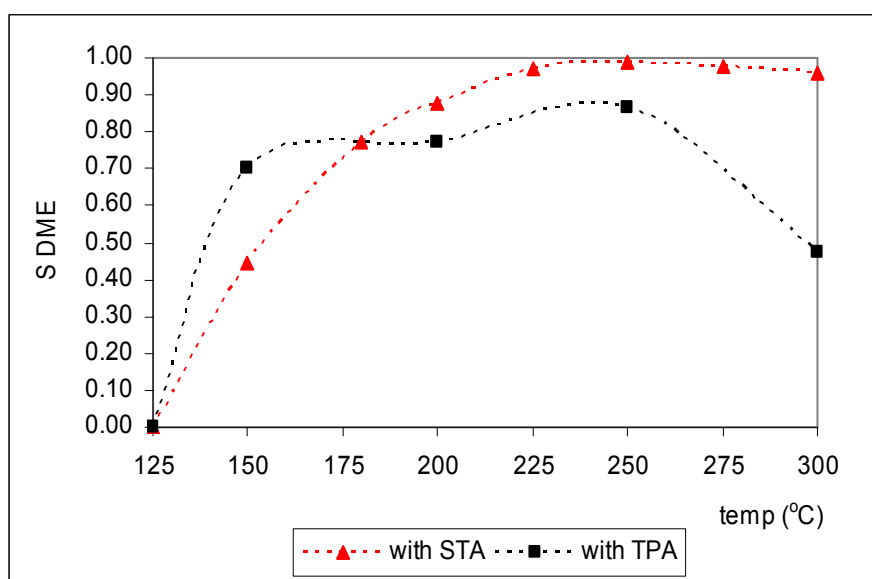


Figure 9.24 The variation in selectivity of DME using 0.2 g of different heteropolyacids, MeOH/(MeOH&He):0.48

Formaldehyde formation occurred at low temperatures for HPA catalysts (Figure 9.25) with a decreasing amount upto 225°C and after that temperature it is in negligible amount.

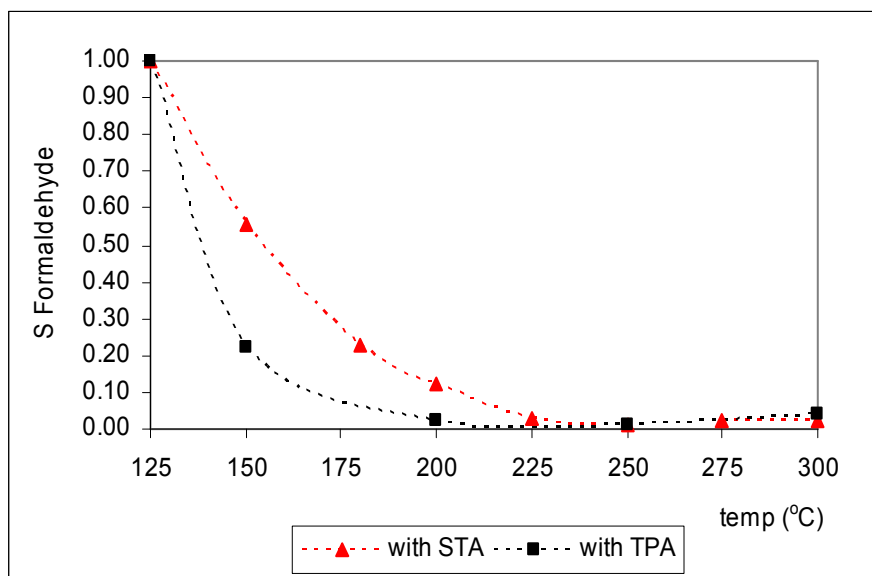


Figure 9.25 The variation in selectivity of formaldehyde using 0.2 g of different heteropolyacids, MeOH/(MeOH&He):0.48

These experimental results also indicated the formation of ethylene when the methol dehydration reaction was catalyzed with TPA (Figure 9.26). At 300°C the selectivity of ethylene reached to 0.50 indicating TPA can be considered as a potential catalyst for transformation of methanol to olefis (MTO) process (Gayubo et al., 2005).

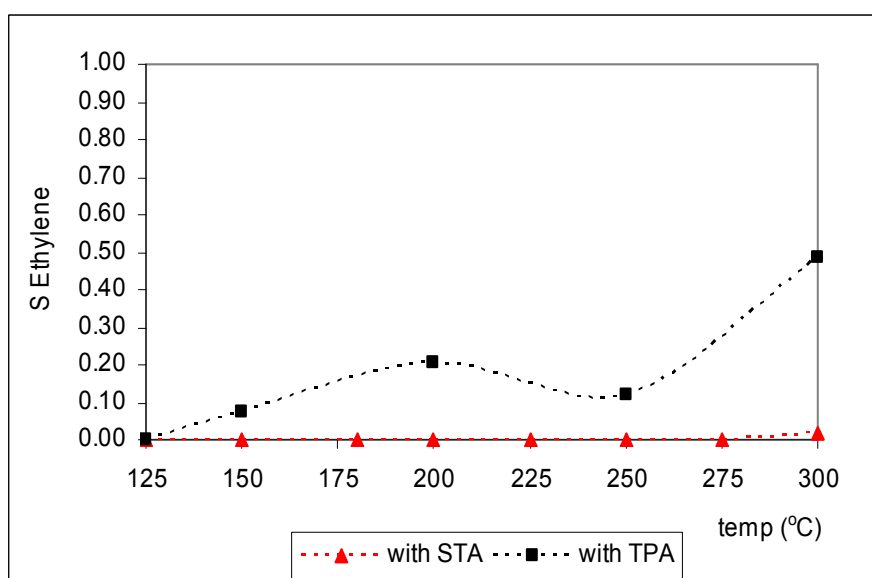


Figure 9.26 The variation in selectivity of ethylene using 0.2 g of different heteropolyacids, MeOH/(MeOH&He):0.48

9.7 Methanol Dehydration Reaction over Aluminosilicate

Apart from heteropolyacids, aluminosilicate which is a mesostructured MCM-41 type catalyst was used in methanol dehydration reaction and a conversion value reaching 0.70 was observed by using 0.1 g of this catalyst for a feed containing 48 % methanol (Figure 9.27).

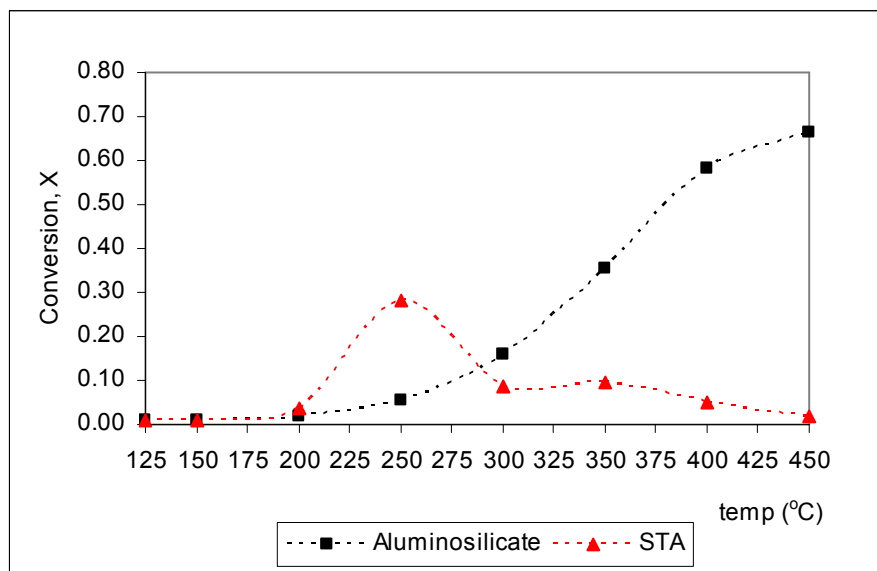


Figure 9.27 The variation in conversion of methanol using 0.1 g of Aluminosilicate in comparison with STA, MeOH/(MeOH&He):0.48

As it is seen in Figure 9.27, upto 300°C, higher conversion values were obtained with silicotungstic acid. However, as it was mentioned previously the maximum conversion was obtained with STA at around 250°C and after this temperature conversion value decreased with an increase in temperature. On the contrary, the catalytic activity of aluminosilicate continuously increased up to a temperature value of 450°C reaching to a value of 0.70 for methanol dehydration reaction for the given experimental conditions. The decrease of activity of STA over 250°C was due to coke formation. STA was quite active at low temperatures. However coke formation caused a sharp decrease in its activity at higher temperatures. For aluminosilicate coke formation was not observed even at temperatures as high as 450°C. Selectivity of aluminosilicate for DME was also very high reaching to 100% at around 300°C (Figure 9.28). These results showed that aluminosilicate was a very good catalyst for dehydration of methanol to produce DME.

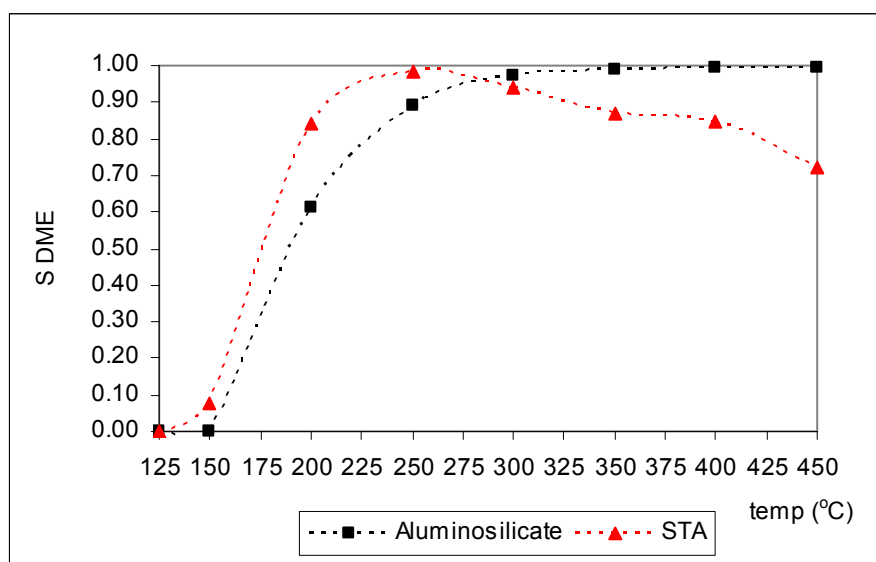


Figure 9.28 The variation in selectivity of DME using 0.1 g of Aluminosilicate in comparison with STA, MeOH/(MeOH&He):0.48

At low temperatures (<250°C) formaldehyde formation was observed with higher amount than that of obtained with STA. However, The amount of formaldehyde became negligible at higher temperatures (Figure 9.29).

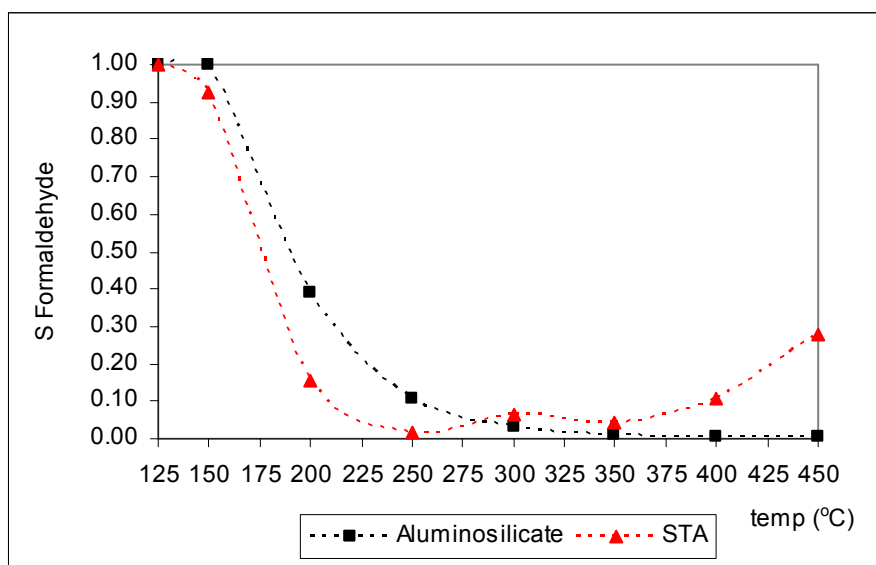


Figure 9.29 The variation in selectivity of Formaldehyde using 0.1 g of Aluminosilicate in comparison with STA, MeOH/(MeOH&He):0.48

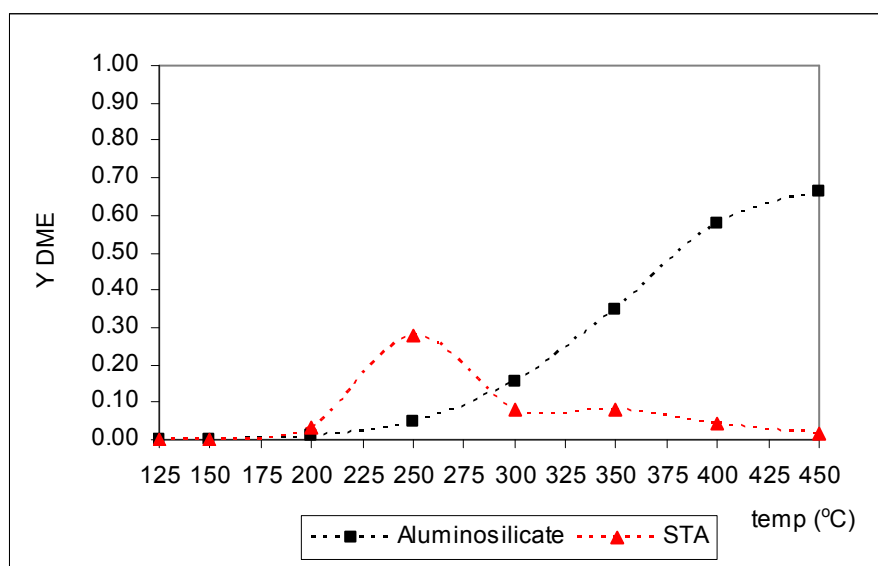


Figure 9.30 The variation in yield of DME using 0.1 g of Aluminosilicate in comparison with STA, MeOH/(MeOH&He):0.48

These experiments showed that for DME production mesoporous aluminosilicate gave the best result having a yield value of 0.7 with no coke formation (Figure 9.30).

CHAPTER 10

RESULTS of CHARACTERIZATION of NOVEL MESOPOROUS SILICOTUNGSTIC ACID CATALYSTS

The results presented in Chapter 9, showed that heteropolyacids are excellent catalysts for ethanol dehydration reactions. Considering their low surface area and their solubility in polar solvent, it was aimed to synthesize new catalysts having higher surface area and higher stability. The synthesis procedures of novel mesoporous catalysts were given in Chapter 8. In this chapter, characterization results of these catalysts are discussed.

10.1 Characterization of MCM-41 Catalyst

MCM-41 is synthesized by direct hydrothermal synthesis procedure which is given in Section 8. Two different routes were tried by changing the source of silica. These catalysts were characterized by XRD, EDS, BET Techniques. Later, it was used as a support for silicotungstic acid to synthesize silicotungstic acid incorporated MCM-41.

10.1.1 XRD Patterns

The XRD pattern corresponding to MCM-41 is presented in Figure 10.1. The characteristic peak corresponding to 2θ value of 2.3° is obtained with some secondary peaks. The secondary peaks are observed at the 2θ values of 3.90° , 4.47° and 5.85° . This pattern approximately matches with the one given in the study of Gucbilmez (2005). Gucbilmez (2005) presented four reflections corresponding to 2.5° , 3.89° , 4.85° and 5.93° for MCM-41 which was prepared by a basic hydrothermal procedure. In the literature, it is indicated that a typical

MCM-41 material should have reflections corresponding to 2.49° , 4.27° , 4.93° and 6.50° (Ciesla and Schüth, 1999). Small deviations in the 2Θ values were observed in the samples synthesized in our laboratory.

The 2Θ value of the most intense peak is used in the Bragg's law to calculate the d_{100} value. According to the Bragg's law, which is ;

$$n\lambda = 2d \sin(\Theta)$$

d_{100} value of 3.84 nm is calculated for $2\Theta \approx 2.3$ (Figure 10.1).

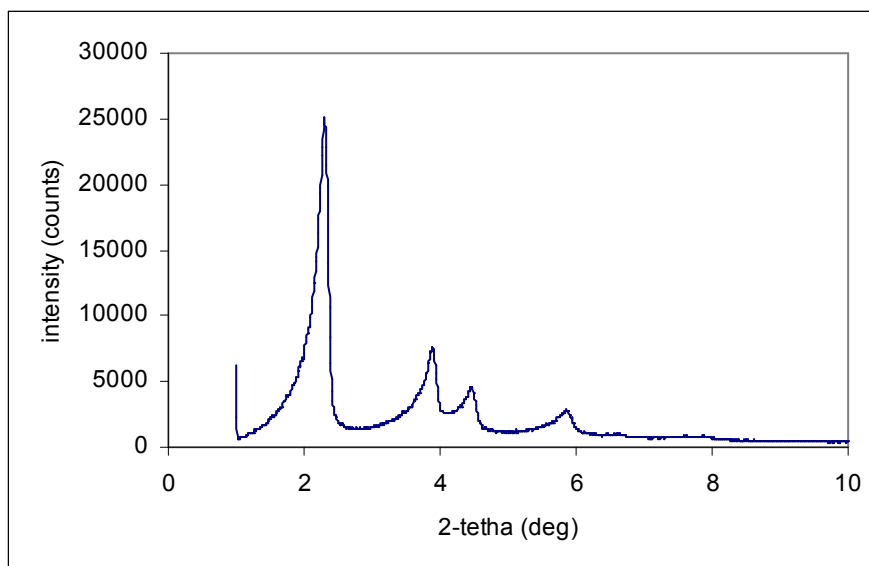


Figure 10.1 XRD patterns of calcined MCM-41

10.1.2 Nitrogen Physisorption

The synthesized MCM-41 had a surface area of $1038 \text{ m}^2/\text{g}$ with a narrow pore size distribution. As shown in Figure 10.2 and 10.3, the nitrogen adsorption isotherm corresponding to this synthesized sample, having an average pore diameter of 4 nm and pore volume of $1 \text{ cm}^3/\text{g}$, was Type IV and a capillary condensation occurred at a relative pressure of 0.4 as indicated in the literature (Ciesla and Schüth, 1999).

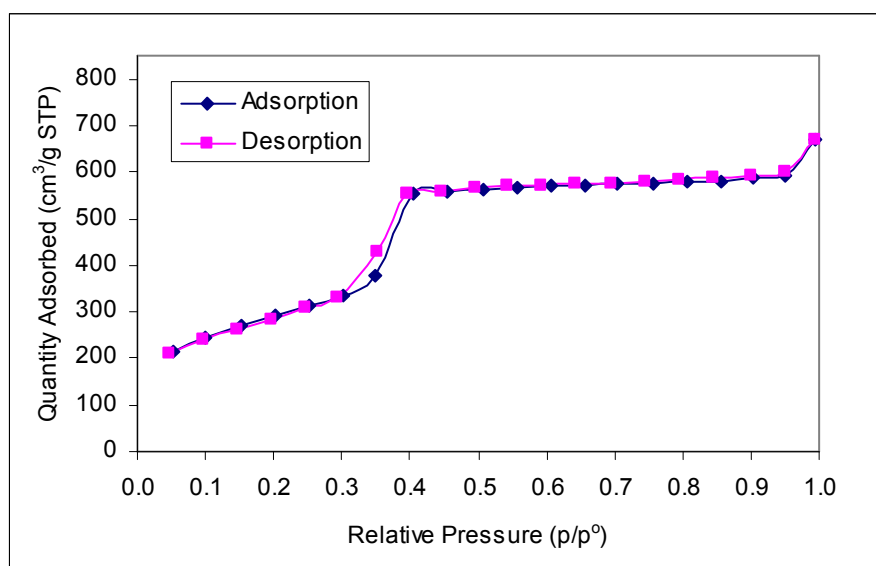


Figure 10.2 Nitrogen isotherms of calcined MCM-41

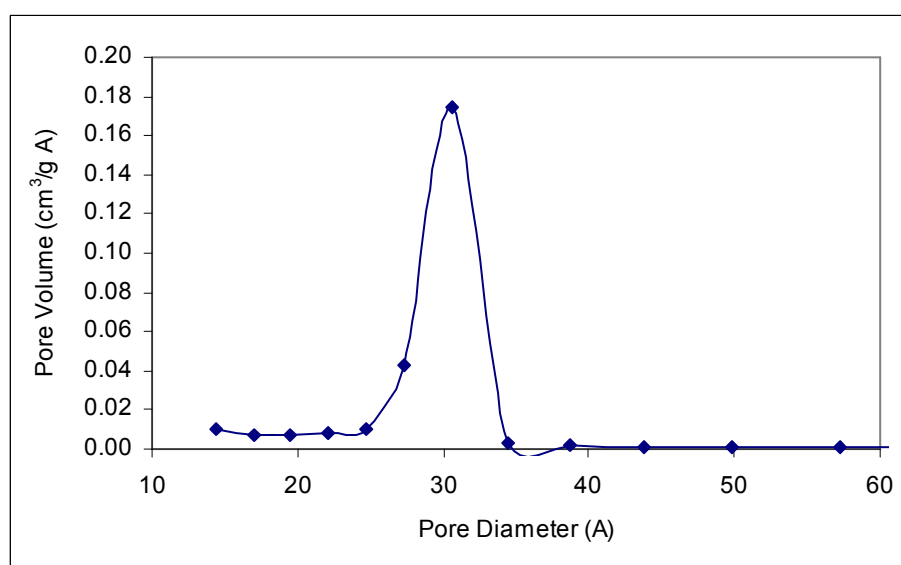


Figure 10.3 Pore size distribution of calcined MCM-41

10.2 Characterization of STA52

STA52 was synthesized by direct hydrothermal synthesis procedure by using TEOS as a silica source. In order to adjust the W/Si molar ratio at 0.03, 0.5 g of silicotungstic acid was added to the solution. Some part of the sample was not washed, after dried at room temperature it was calcined at 550°C. This part was called as STA51(550). The remaining part was washed with deionized

water, dried and calcined at 550°C as indicated in Chapter 8. This sample was called as STA52(550). XRD, EDS and Nitrogen Adsorption techniques were used for characterization of STA51(550) and STA52(550).

10.2.1 XRD

The XRD pattern corresponding to STA52(550) is presented in Figure 10.4. This result indicated that silicotungstic acid did not incorporated into the structure. However the mesoporous structure was not collapsed.

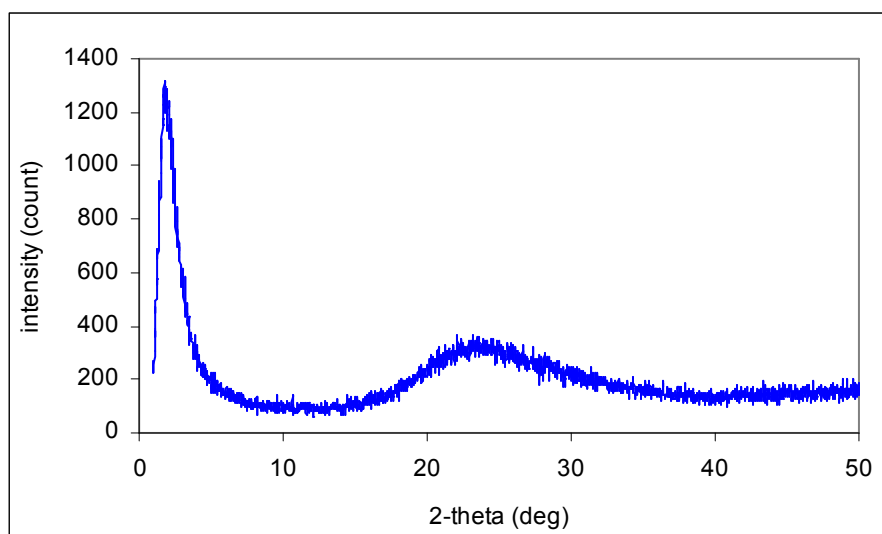


Figure 10.4 XRD patterns of STA52(550)

10.2.2 EDS

The molar W/Si ratio was found as 0.08 for STA51(550) but it decreased to trace amount for STA52(550) which was washed with water before the calcination (Table 10.1). This result indicated that silicotungstic acid used during the synthesis was not incorporated into the mesoporous structure and removed by washing with water.

Table **10.1** EDS analysis results of STA5 catalyst

Sample	Element	Weight Conc%	Atom Conc %	W/Si Ratio	
				weight	atomic
STA51(550)	Si	65.86	92.66	0.52	0.08
	W	34.14	7.34		
STA52(550)	Si	100	100	trace	trace
	W	trace	trace		

10.2.3 Nitrogen Adsorption

The single point surface area of STA51(550) and STA52(550) are 679.0 m²/g and 661.30m²/g, respectively. The BET surface area of STA52(550) is 687.14 m²/g; BJH Adsorption cumulative surface area of pores and BJH Adsorption cumulative volume of pores are 976.38 m²/g and 1.21cm³/g, respectively. BJH adsorption average pore diameter of the corresponding sample is 49.75 Å.

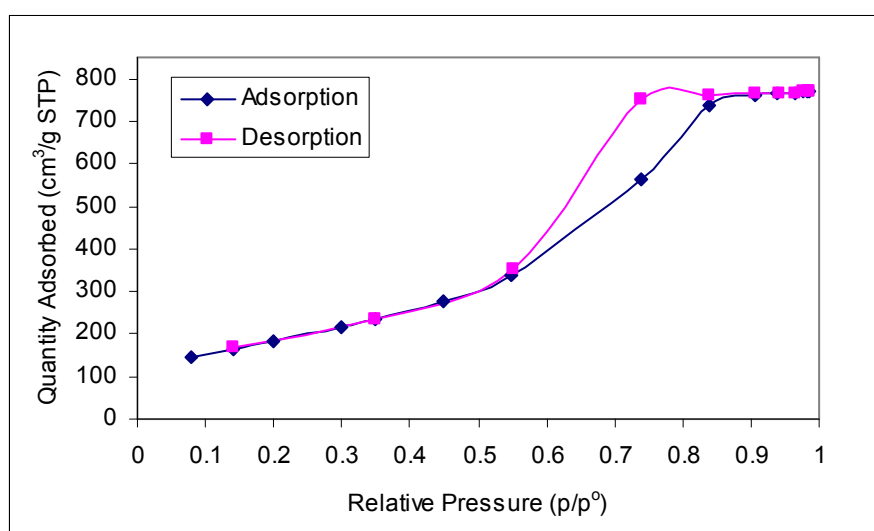


Figure 10.5 Isotherm plot of STA52(550)

A typical Type 4 adsorption isotherm was obtained for STA52(550) (Figure 10.5). As shown in Figure 10.6 this material has a relatively wider pore size distribution in the 2-15 nm range.

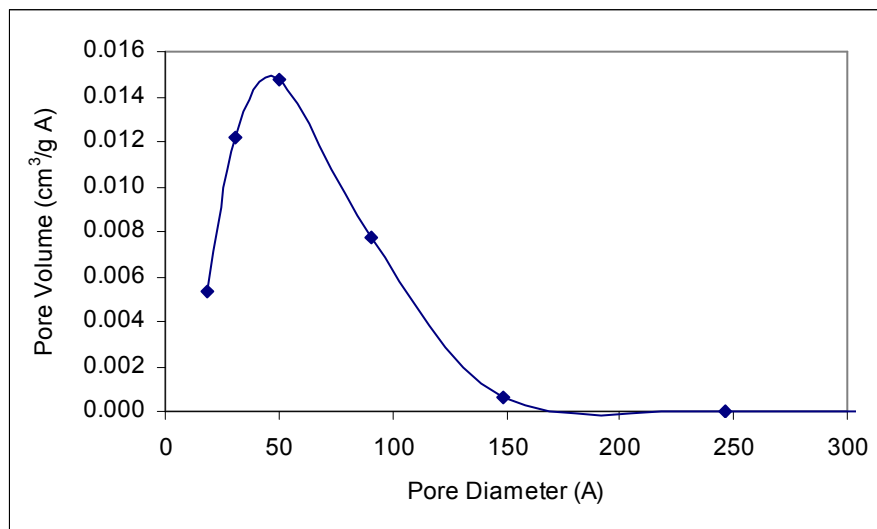


Figure 10.6 Pore size distribution of STA52(550)

10.3 Characterization of STA62

STA6 series catalysts are novel silicotungstic acid catalysts prepared with a direct hydrothermal synthesis procedure. Three samples, namely, STA61(550), STA62(350), STA62(550) are investigated in this section. The differences among these samples are related with washing step and calcination step during the synthesis procedure.

In the synthesis of these materials, a surfactant solution was mixed with TEOS which was used as the silica source, at the given amount as indicated in Chapter 8 and a homogeneous gel was obtained with no undissolved species. 4.23 g of silicotungstic acid which was dissolved in 5 ml of deionize water was added to this mixture by stirring at 35°C. The amount of silicotungstic acid to be added was determined according to the W/Si ratio of 0.25 in the synthesis solution. The pH of the final synthesis solution was stabilized at 1.6. After finishing the hydrothermal synthesis of the catalyst in autoclave, solid sample which had a yellow color was obtained.

Some part of this sample was crashed into smaller size, without applying washing stage allowed to dry at room temperature and then calcined at 550°C. This one is called as STA61(550) and characterization results of XRD, EDS are used in the comparison of washing step on the catalyst preparation.

Remaining part of the synthesized material was washed with deionized water until the pH of the filtrate became constant. After drying at room temperature, sample was ready for calcination. In order to see the effect of calcination temperature on the structure of the new catalyst, sample was divided into two parts. One part was calcined at 550°C, and called as STA62(550); the other part was calcined at 350°C and called as STA62(350). The differences in the synthesis procedure for these samples were summarized in Table 10.2.

Table 10.2 The difference in synthesis procedure for STA6 samples

Sample	Washing	CalcinationTemperature(°C)
STA61(550)	No	550
STA62(550)	Yes	550
STA62(350)	Yes	350

10.3.1 XRD Patterns

The XRD pattern corresponding to STA62(550) at a 2θ values range between 1-50° is given in Figure 10.7. A broad signal was observed at 2θ values of 1.63°-1.93°. When the low-angle XRD pattern of STA62(550) was investigated, the main characteristic peaks of hexagonal MCM-41 structure were not observed (Figure 10.8). This situation indicated that this novel silicotungstic acid catalyst had a different structural texture than MCM-41.

The XRD analysis of pure silicotungstic acid was also done. Pure silicotungstic acid was dried at 100°C overnight and XRD characterization was carried out at 2θ values of 0-50° (Figure 10.9). The diffraction peaks are

obtained at 2θ values of 10.39° , 25.5° , 29.51° , 34.74° , 37.86° mainly. Besides them, there are some lower intensity peaks at 2θ values of 14.68° , 17.98° , 20.78° , 23.25° , 31.34° , 33.08° , 40.80° , 44.88° , 46.17° , 48.69° .

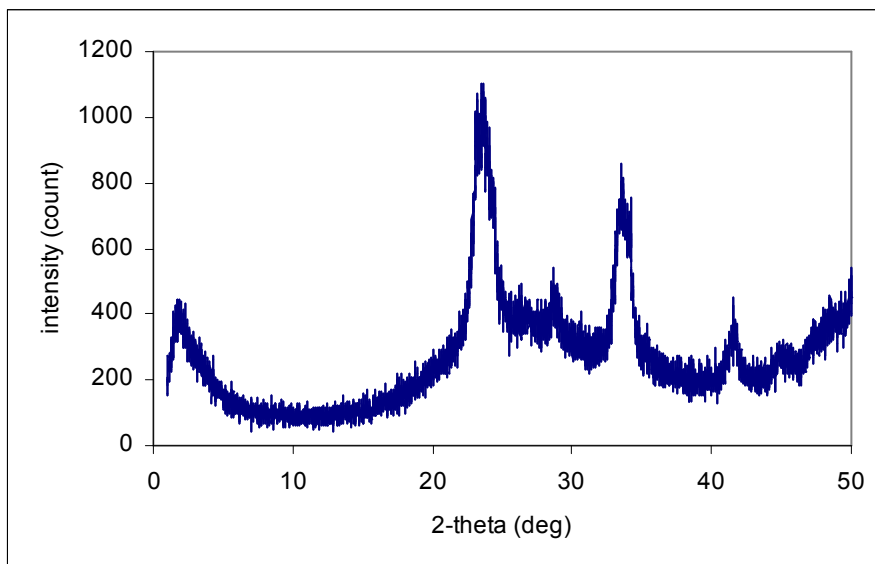


Figure 10.7 XRD patterns of STA62(550) at 2θ values upto 50

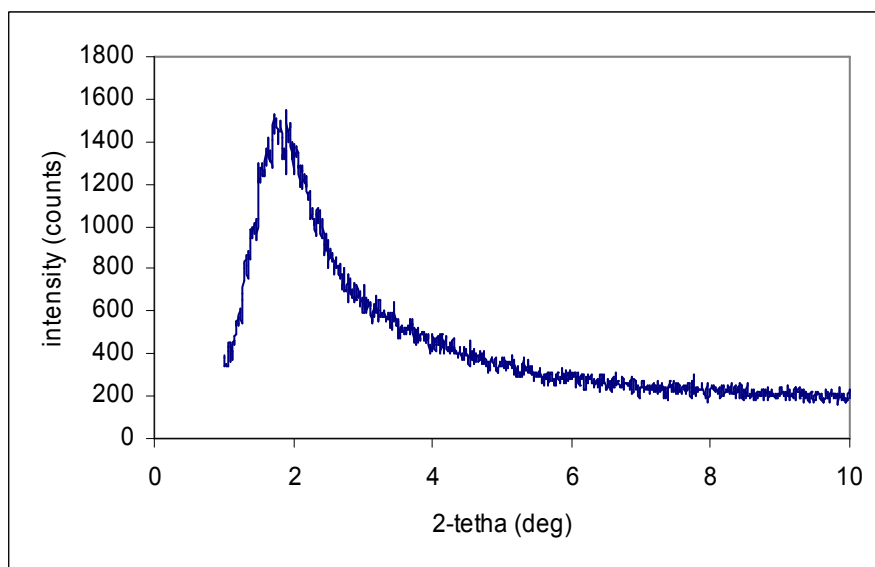


Figure 10.8 Low-angle XRD patterns of STA62(550)

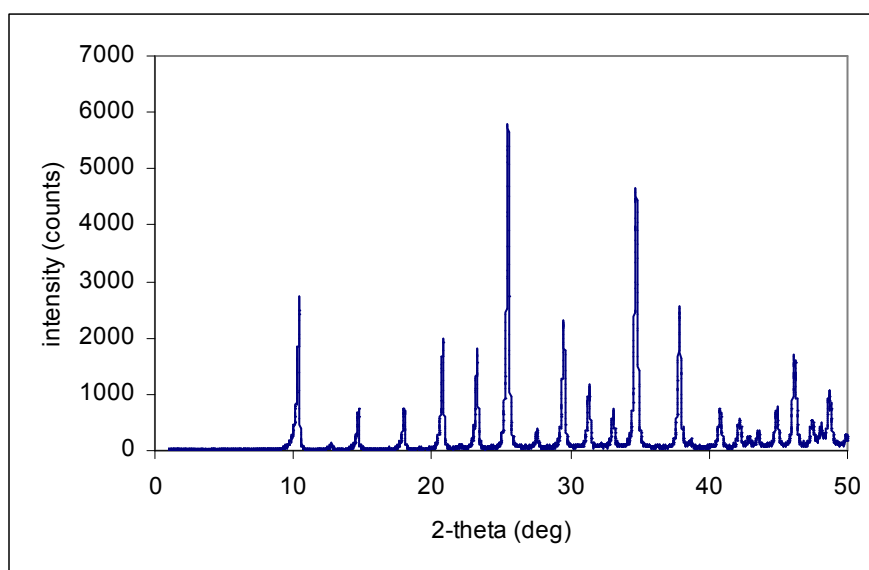


Figure 10.9 XRD patterns of pure Silicotungstic acid

In the XRD diagram of STA62(550) broad diffraction corresponding to 2θ values of 23.13° - 23.77° , 33.5° - 33.68° , 40.91° - 42.6° which are very close to the characteristic main peaks of pure silicotungstic acid (Figure 10.7). Only, the peak corresponding to 2θ value of 10.9 is not observed.

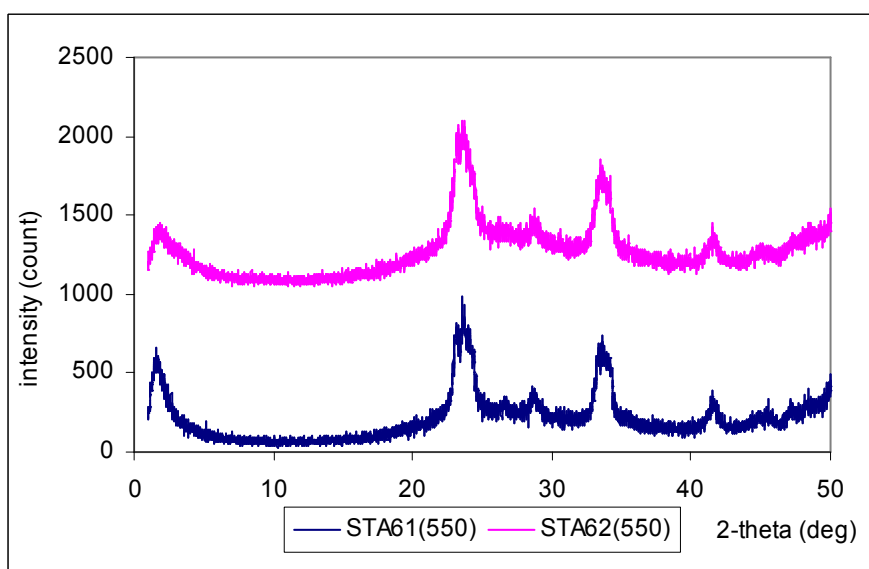


Figure 10.10 XRD patterns of STA61 and STA62

In Figure 10.10. the XRD pattern of STA61(550) and STA62(550) is given together in order to see the effect of washing stage. There is a decrease in the

intensity of the broad peaks observed at 2θ values less than 2° . Apart from this change, approximately the same patterns were obtained.

In order to see the effect of calcination temperature on the crystal structure of the STA62 sample, XRD analysis was applied to STA62 before the calcination stage (Figure 10.11). Then the result was compared with the diffractograms of STA62(550) and STA62(350). In the XRD pattern of uncalcined sample, peaks were observed at 2θ values of 1.98° , 2.04° , 4.02° , 5.88° , 8.08° , 8.23° , 8.98° , 9.50° , 20.6° , 2.44° , 24.54° , 30.06° .

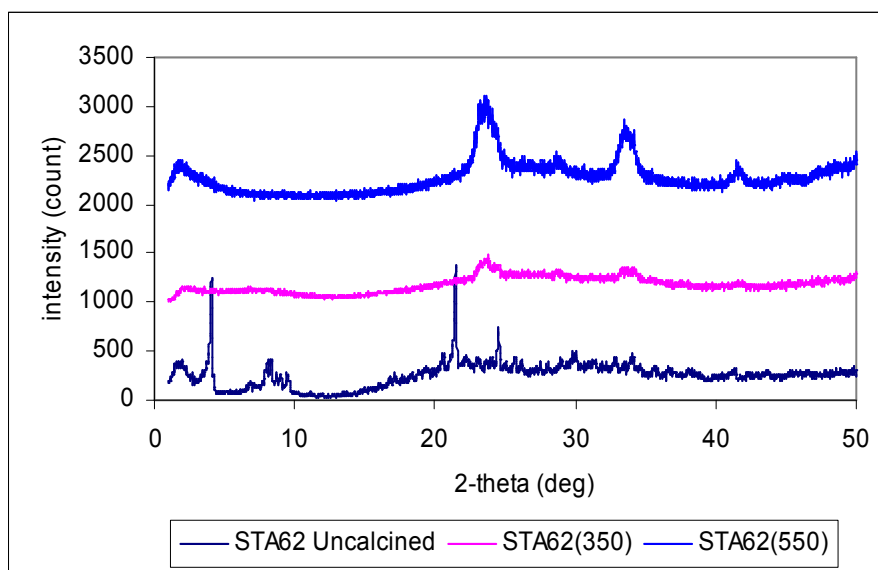


Figure 10.11 XRD patterns of STA62 before calcination and after calcined at different temperatures

The peaks which are located at 2θ values between 7.98° - 9.05° were not seen after the calcination of the sample. Peaks which are located at 4.02° , 5.88° observed for uncalcined sample were overlap with the characteristic peaks of MCM-41 presented in Figure 10.1. The disappearance of these peaks in STA62(350) and STA62(550), as seen in Figure 10.11. The XRD pattern of the sample calcined at 350°C is quite close to the XRD pattern of the sample calcined at 550°C (Figure 10.11).

10.3.2 EDS Results

During the direct hydrothermal synthesis procedure, 4.23 gram of silicotungstic acid was added to synthesis solution to get W/Si molar ratio of 0.25 in the solution. The atomic concentration of tungsten incorporated in the structure and the atomic concentration of Si was found from the EDS analysis; using these concentration values, the W/Si molar ratio in the bulk of the sample can be found. The results corresponding to STA61(550), STA62(550) and STA62(350) are summarized in Table 10.3.

Table 10.3 EDS analysis results of STA6 catalyst

Sample	Element	Weight Conc%	Atom Conc %	W/Si Ratio	
				weight	atomic
STA61(550)	Si	45.42	84.49	1.20	0.18
	W	54.58	15.51		
STA62(550)	Si	44.54	84.02	1.25	0.19
	W	55.46	15.98		
STA62(350)	Si	49.13	86.34	1.04	0.16
	W	50.87	13.66		

The W/Si molar ratio for STA61(550) and STA62(550) was nearly the same value. Leaching of heteropolyacid was not observed for STA6 catalysts with washing indicating very stable structure.

10.3.3 SEM

In Figure 10.12, the SEM photograph of STA62(550) is given.

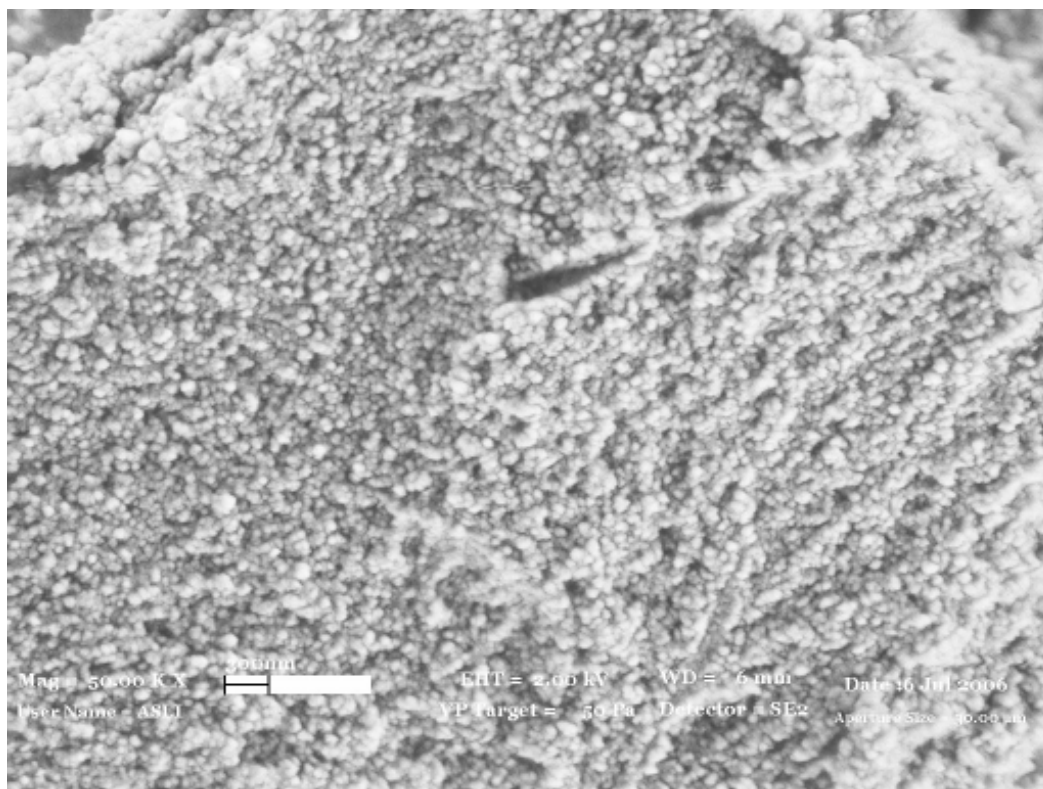


Figure **10.12** SEM images of STA62(550)

10.3.4 Nitrogen Physisorption

The single point and multi point BET Surface areas of STA62(550) are recorded as $313.60 \text{ m}^2/\text{g}$ and $326.52 \text{ m}^2/\text{g}$, respectively. BJH adsorption cumulative surface area of pores between 17.000 \AA and 3000.000 \AA width is $481.08 \text{ m}^2/\text{g}$; BJH adsorption cumulative volume of pores between 17.000 \AA and 3000.000 \AA width is $0.59 \text{ cm}^3/\text{g}$. BJH adsorption average pore width is 49.05 \AA . The nitrogen isotherm and the pore size distribution of STA62(550) is plotted in Figure **10.13** and Figure 10.14, respectively. STA62(550) had Type IV nitrogen adsorption isotherm with a pore size distribution in the range of 2-15 nm.

The multipoint BET surface area of STA62(350) is found as $393.80 \text{ m}^2/\text{g}$. Decreasing the calcination temperature from 550°C to 350°C is resulted in an increase in BET surface area from $326.52 \text{ m}^2/\text{g}$ to $393.80 \text{ m}^2/\text{g}$. The nitrogen isotherm plot of STA62(350) is given in Figure **10.15**, it is also Type IV, and the pore size distribution of STA62(350) calculated by the BJH method is displayed in Figure **10.16**. A wider pore size distribution in the range of 1-10 nm was observed and the average pore diameter and total pore volume were found as

5.5 nm and 0.55 cm³/g, for STA62(350). The pore size distribution is not as sharp as MCM-41, but still it is not a highly distributed pore-size distribution.

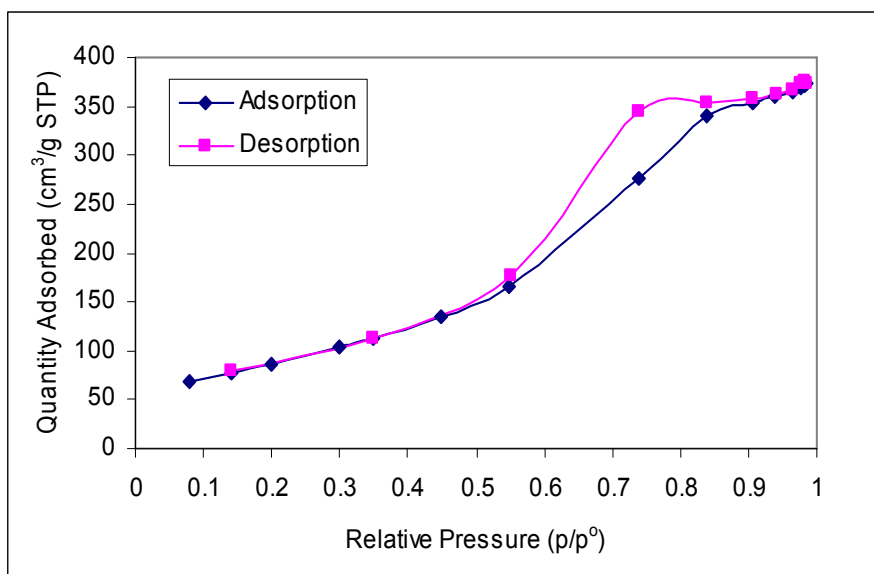


Figure 10.13 Nitrogen isotherms of STA62(550)

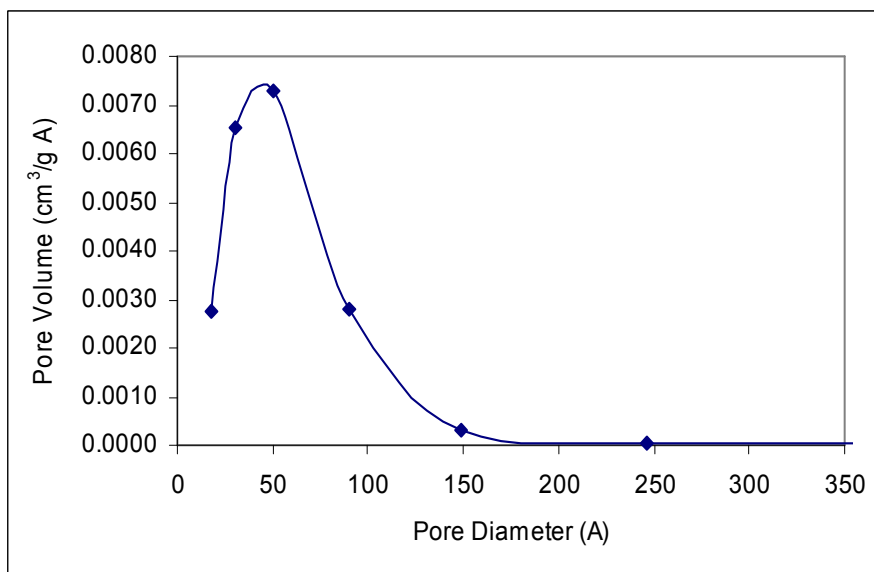


Figure 10.14 Pore size distribution of STA62(550)

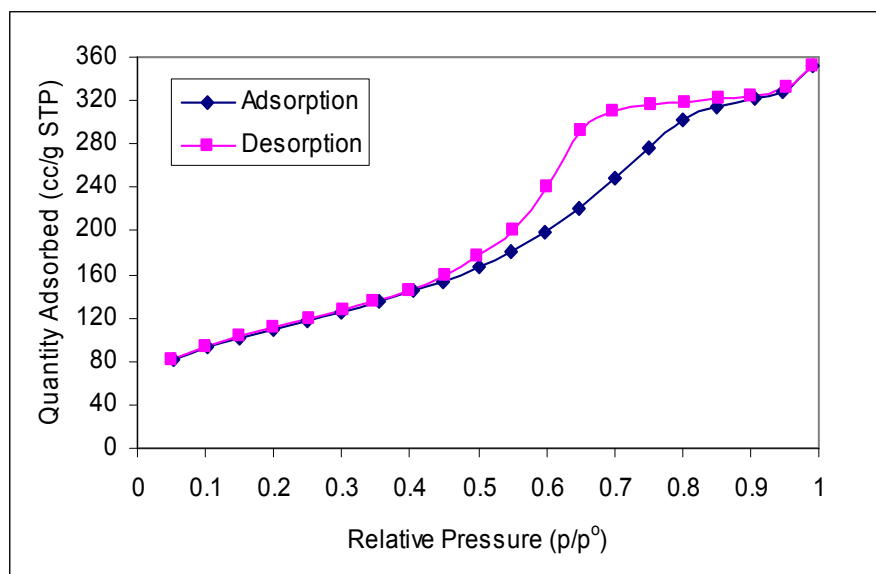


Figure 10.15 Nitrogen isotherms of STA62(350)

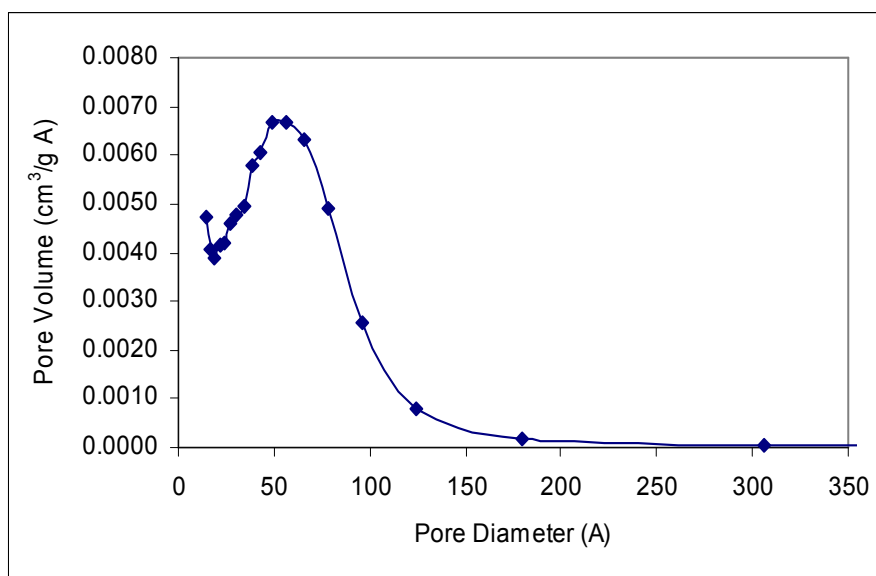


Figure 10.16 BJH adsorption pore size distribution of STA62(350)

10.3.5 FTIR

In Figure 10.17 and 10.18, the FTIR results of uncalcined STA62 and STA62(550) are given, respectively. These results indicate a deterioration of the structure of heteropolyacids after calcined at 550°C.

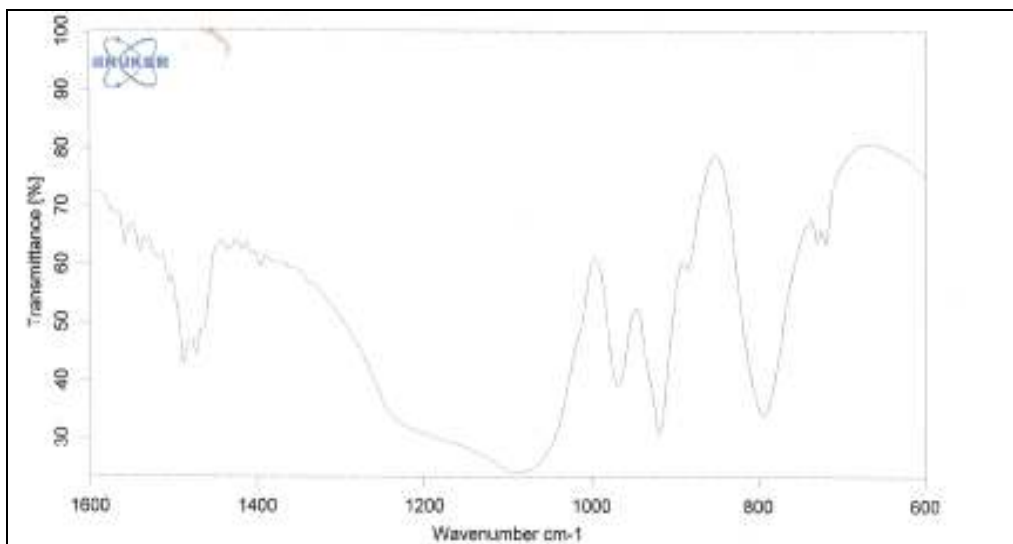


Figure 10.17 FTIR result of uncalcined STA62

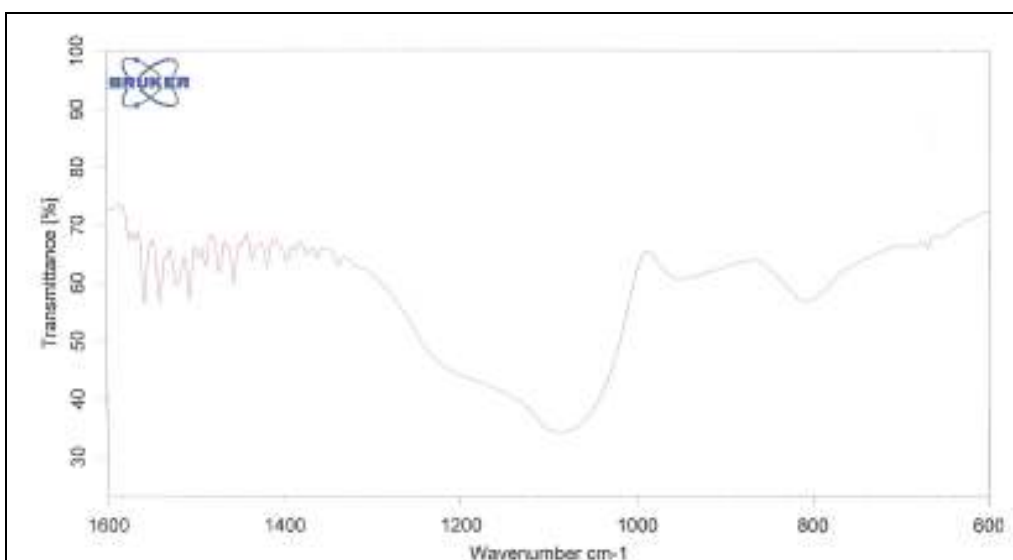


Figure 10.18 FTIR result of STA62(550)

10.4 Characterization of STA72

STA7 is prepared by direct hydrothermal synthesis procedure by using sodium silicate as the silica source instead of TEOS in order to investigate the effects of different silica sources on the final product. To compare the results with that of STA6 catalysts, again 4.23 g of silicotungstic acid which was dissolved in 5 ml deionize water, was used to adjust the W/Si ratio of 0.25 in the synthesis solution. This ratio was the same as STA6 type catalysts. The pH of

synthesis solution was in acidic range, i.e 1.6 when TEOS is used; on the contrary, the pH of the synthesis solution was 11 when sodium silicate was used.

In order to see the effect of washing stage, some part of the STA7 sample was not washed with deionize water. After calcined at 550°C, its bulk composition was determined with EDS analysis. This sample was called as STA71(550). The remaining part, which was called as STA72(550), was washed and then calcined at 550°C. XRD, Nitrogen physisorption, EDS and SEM characterizations were done for this sample.

10.4.1 XRD Patterns

The XRD pattern corresponding to STA72(550) at a 2θ values range 0-50 is given in Figure 10.19. A sharp peak at 2θ value of 2.28° which is the main peak of MCM-41 structure (Figure 10.1), was observed more clearly in the low-angle x-ray diffraction pattern, also (Figure 10.20).

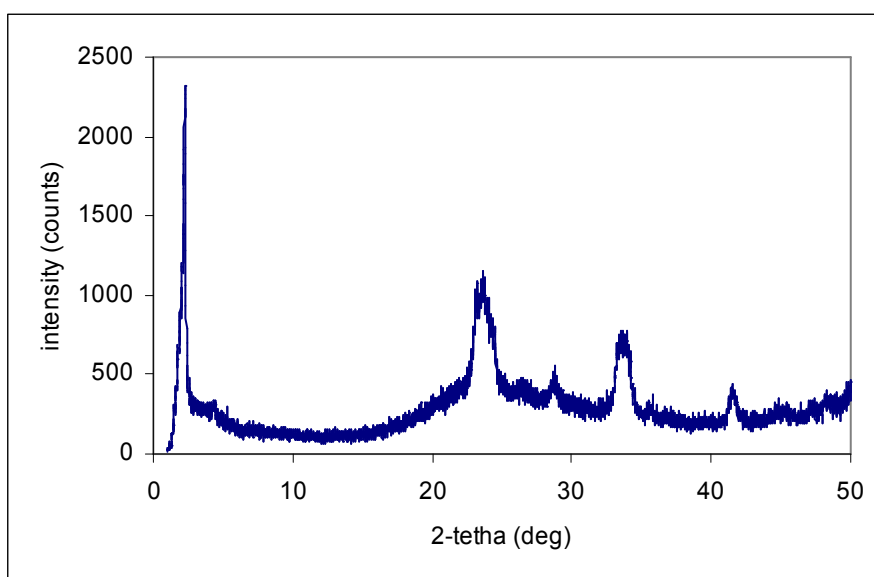


Figure 10.19 XRD patterns of STA72(550)

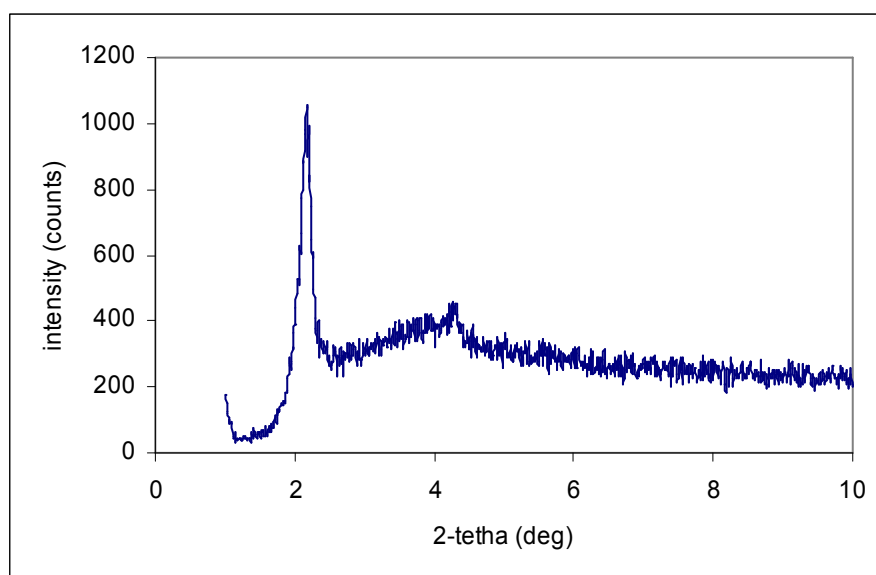


Figure 10.20 Low-angle XRD patterns of STA72(550)

The peaks observed at 2θ values between 23.12 - 23.69° , 33.27 - 33.99° and 41.5 - 41.58° are corresponding to crystal structure of silicotungstic acid (Figure 10.19). Before the calcination stage, more intense peaks are observed in 2θ values between 21.44 - 24.5° , however peaks observed at $2\theta > 30^\circ$ for calcined sample are not visible before its calcination (Figure 10.21).

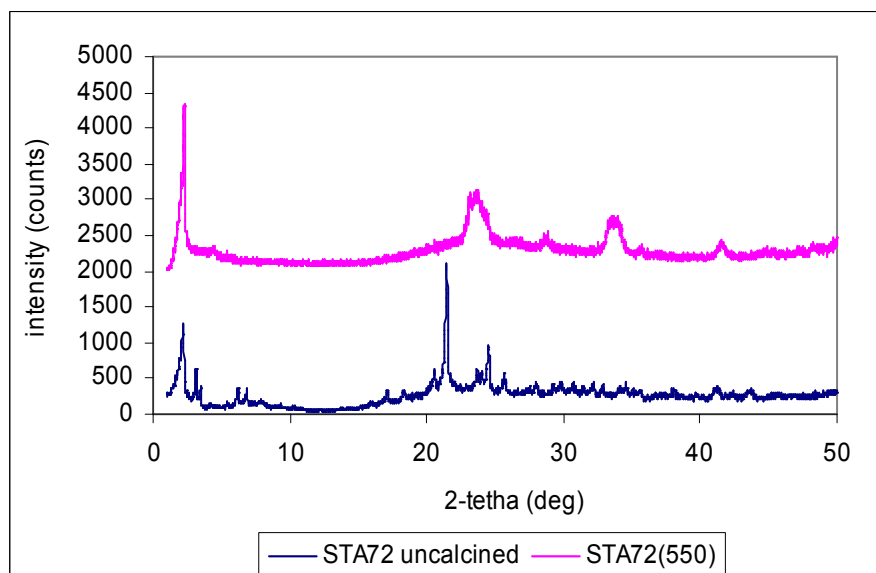


Figure 10.21 XRD patterns of uncalcined STA72

10.4.2 EDS

While preparing STA7, 4.23 gram of silicotungstic acid was added to synthesis solution to get a W/Si molar ratio of 0.25 in the solution. The atomic concentration of tungsten incorporated in the structure and the atomic concentration of Si for STA71(550) and STA72(550) corresponding to the EDS analysis is presented in Table **10.4**.

Table **10.4** EDS analysis results of STA7 catalysts

Sample	Element	Weight Conc%	Atom Conc %	W/Si Ratio	
				weight	atomic
STA71(550)	Si	52.88	88.02	0.89	0.14
	W	47.12	11.98		
STA72(550)	Si	75.00	95.16	0.33	0.05
	W	25.00	4.84		

The aim of washing stage is the removal of the surfactant. The fact that W/Si molar ratio for STA71(550) is higher than that of STA72(550), shows that the ratio of silicotungstic acid which entered into the structure is low. Due to high solubility of HPA in water, molecules which are only hold on the structure is removed easily. However, in the case of STA6 type catalyst STA was more tightly incorporated into the lattice and STA had not been removed during the washing step.

Although the same amount of silicotungstic acid was used and the same W/Si ratio of 0.25 is considered while synthesis procedure, the W/Si ratio of STA7 samples are found to be lower than that of STA6 samples. Especially, the difference becomes higher for the washing samples, i.e. for STA62(550) W/Si molar ratio is 0.19 (Table **10.3**) whereas for STA72(550) it is only 0.05. This may be explained by using different silica sources. When sodium silicate is used as the silica source a final synthesis solution having a basic pH was obtained. On the other hand, when TEOS is used as the silica source, the pH of final synthesis

solution is in the acidic range. These results showed that TEOS was a better silica source and pH should be acidic in the synthesis of novel mesoporous STA catalysts synthesized in this work.

10.4.3 SEM

In Figure 10.22 SEM photographs of STA72(550) is presented.

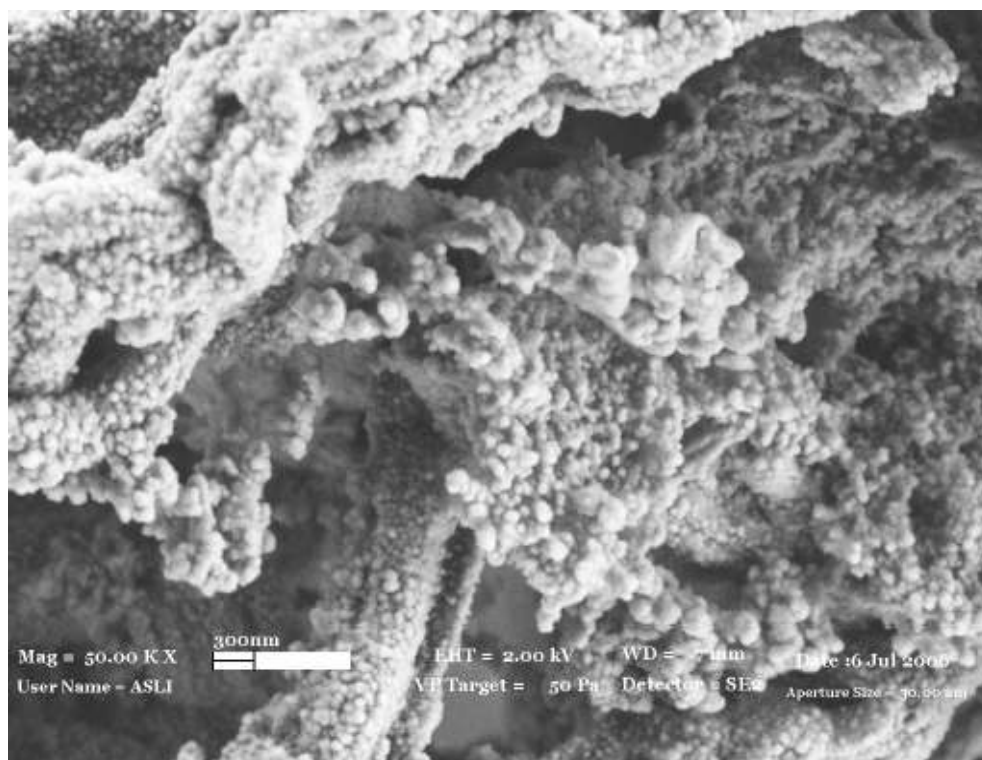


Figure 10.22 SEM photographs of STA72(550)

10.4.4 Nitrogen Physisorption

The single point and BET surface areas of STA72(550) are 334 and 361 m^2/g , respectively. According to BJH calculation, surface area of pores and volume of pores are found as 392 m^2/g and 0.65 cm^3/g , respectively. The average pore diameter is 6.7 nm. In Figure 10.23, isotherm plot of STA72(550) is presented. The pore size distribution is given in Figure 10.24.

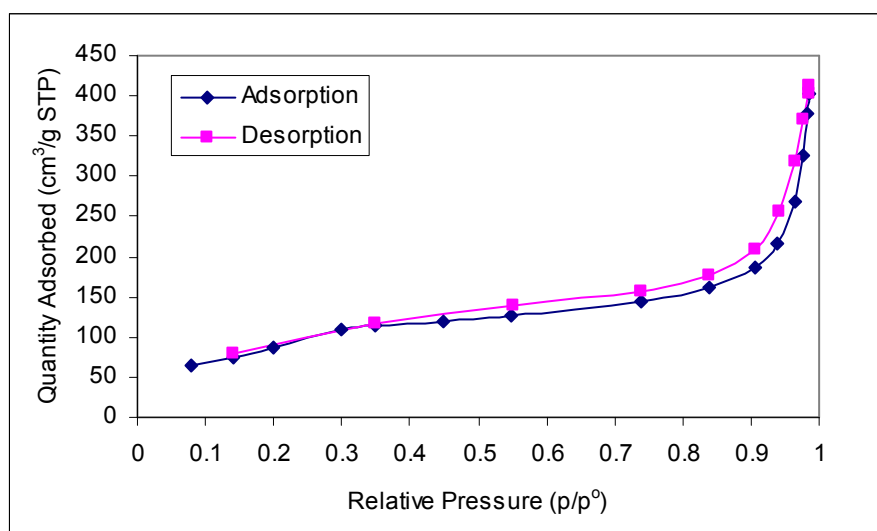


Figure 10.23 Isotherm linear plot for STA72(550)

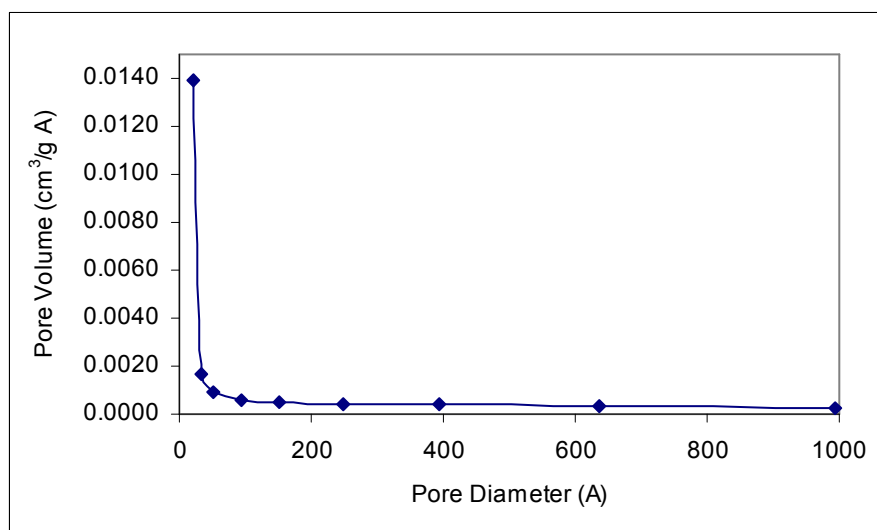


Figure 10.24 Pore size distribution of STA72(550)

The nitrogen isotherm plot for STA72(550) was Type 2 indicating macropores formation.

10.5 Characterization of STA8 Catalysts

STA8 series novel silicotungstic acid catalysts are prepared with direct hydrothermal synthesis procedure by using TEOS as the silica source. 8.46 g of silicotungstic acid is used to adjust the W/Si ratio of 0.50 in the synthesis

solution. The pH of the final synthesis solution is found as 1.2. After completing the hydrothermal synthesis of the catalyst in autoclave at 120°C for 96 hours, solid sample which has a yellow-orange color is obtained.

As indicated in Chapter 8, the next step in the synthesis procedure is the washing stage. Some modifications were done in this stage for STA8 catalysts. Apart from water, different washing solvents such as hydrochloric acid & ethanol mixture and dilute phosphoric acid was used. Also, in order to remove the excess template, supercritical carbondioxide extraction was carried out instead of washing with a solvent. After removal of excess template by different ways, sample is dried and than calcined. The temperature range at which the calcination should be carried out is also important parameter in the synthesis of novel silicotungstic acid catalysts.

Catalysts prepared in this part are called as STA81(550), STA82(550), STA82(350), STA81(HCl&EtOH), STA81(P), STA81(UCCO₂) and STA82(CO₂) according to difference in washing stage and calcination temperature applied after taken from autoclave. The catalysts and differences in their synthesis procedure are summarized in Table 10.5.

The one, which is not washed, is crashed into smaller size and calcined at 550°C. This sample is called as STA81(550) and XRD,EDS characterization tests are applied.

Some part of the sample is washed with deionized water, namely STA82. In order to see the effect of calcination temperature on the structure of STA82, it is divided into two part, one part is calcined at 550°C, and called as STA82(550); the other part is calcined at 350°C and called as STA82(350).

Another part is washed with a mixture of chloric acid (HCl) and ethanol which is prepared in 1:1 volume ratio from 0.1 N HCl and 99.8 % purity ethanol and than it was calcined at 350°C. This one is called as STA81(HCl&EtOH).

The other part is washed with firstly dilute phosphoric acid (H₃PO₄) and than with deionized water. After that, it was calcined at 350°C, and this sample is called as STA81(P).

In order to remove excess template, super critical carbon dioxide extraction is applied on some part of the sample instead of washing with a solvent. After the extraction of some of the organic solvent, the sample is calcined at 350°C. This one is called as STA81(UCCO₂).

Finally both washing with deionized water and extraction procedure are applied together to part of sample which is taken from autoclave in solid form. Firstly it was washed with deionized water and then in extraction unit it was treated with Supercritical CO₂ having a pressure of 350 bar and at 100°C during 180 min. Finally sample is calcined at 350°C and it is called as STA82(CO₂).

Table 10.5 The difference in synthesis procedure for STA8 samples

Sample	The way of excess template removal	Calcination Temp(°C)
STA81(550)	No treatment	550
STA82(550)	Washing with deionized water	550
STA82(450)	Washing with deionized water	450
STA82(350)	Washing with deionized water	350
STA81(P)	Washing with dilute H ₃ PO ₄ then with deionized water	350
STA81(HCl&EtOH)	Washing with a mixture of HCl & ethanol (vol ratio 1:1)	350
STA81(UCCO ₂)	Supercritical CO ₂ Extraction	350
STA82(CO ₂)	Firstly washing with deionized water then Supercritical CO ₂ Extraction	350

10.5.1 XRD

The XRD patterns corresponding to uncalcined STA82, STA82(350), STA82(450) and STA82(550) is plotted together in Figure 10.25. The intensity of peaks belongs to crystal structure of heteropolyacid is the highest for STA82(550) in all calcined samples. Some of the peaks which are observed in uncalcined STA82 disappear, especially at 2θ values less than 10° for the calcined samples.

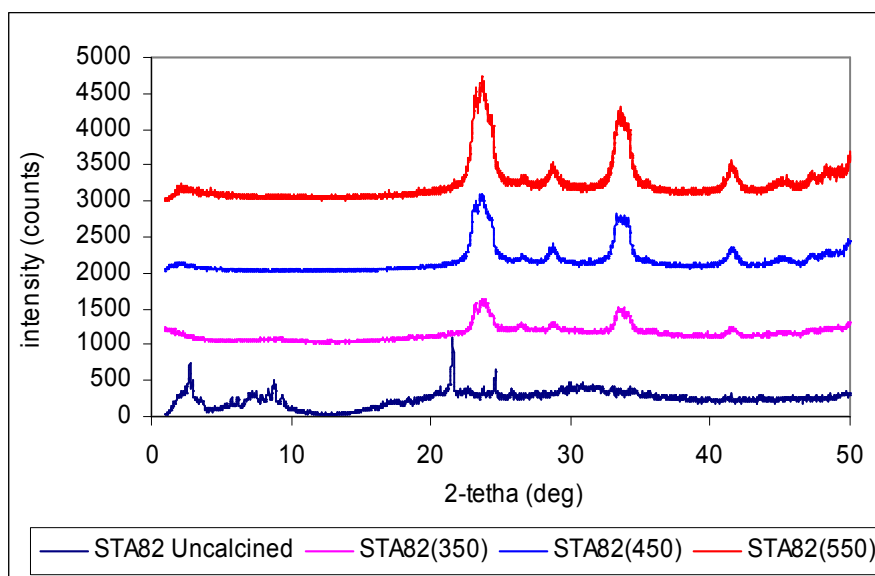


Figure 10.25 XRD patterns of STA82 before and after the calcination at different temperatures

In Figure 10.26, in order to investigate the effect of washing step on the crystal structure of the catalyst, XRD patterns corresponding to STA81(HCl&EtOH) and STA82(350) are given together. Also diffraction pattern of STA81(UUCO₂) is also added to this figure to compare with the washing ones. As indicated previously, all of these samples are calcined at 350°C . The diffractogram corresponding to STA81(UCCO₂) is very different from that of STA81(HCl&EtOH) and STA82(350). The structure of heteropolyacid can not be seen in xrd diagram of STA81(UCCO₂) unlike the other. This means that heteropolyacid is finely dispersed in mesoporous structure.

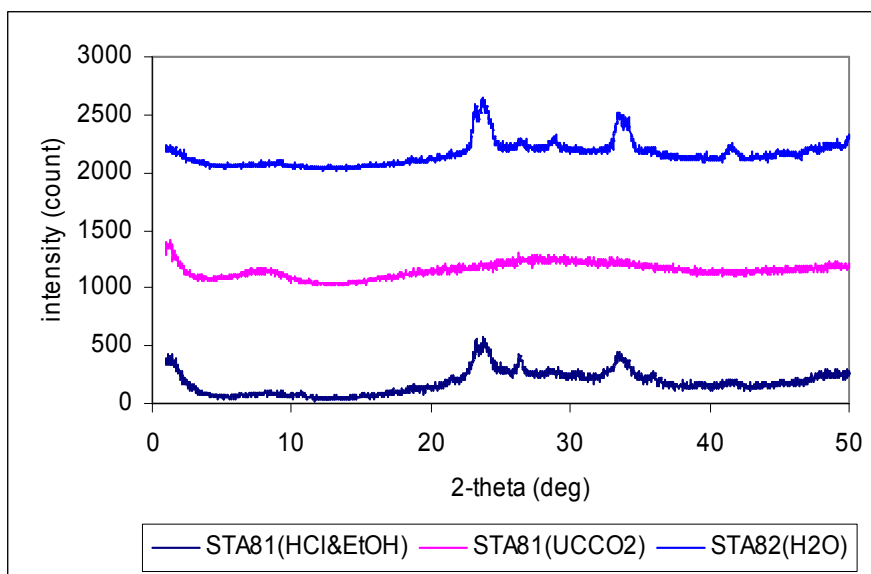


Figure 10.26 XRD patterns of STA8 washed with different methods

10.5.2 EDS

The molar W/Si ratio for these novel silicotungstic acid catalysts are given in Table **10.6**. Although, all of the catalysts investigated in this part are prepared with the same synthesis solution that contains a molar W/Si ratio of 0.50, the atomic ratio of tungsten to silicate is different for each of products. Except for STA81(HCl&EtOH) W/Si ratio within the solid product was obtained to be in the range of 0.34-0.47. Only for STA81(HCl&EtOH) washed catalyst this ratio was found as 0.77, which indicated loss of some Si during the washing step.

10.5.3 SEM

The SEM photographs of STA82(550) in Figure 10.27 and Figure 10.28. A needle like structure is observed in these photographs.

10.5.4 Nitrogen Physisorption

The Single Point and BET surface area values of STA82(550) are 150.2 m²/g and 155.7 m²/g, respectively. BJH adsorption cumulative surface area of pores is 209.66 m²/g and BJH adsorption cumulative volume of pores is 0.307 cm³/g, between 17.000Å and 3000.000Å diameter. BJH adsorption average pore diameter is 58.53 Å.

The isotherm plot and the pore size distribution corresponding to STA82(550) is shown in Figure 10.29 and Figure 10.31, respectively.

The multipoint BET surface area of STA82(350) is 178.7 m²/g. The isotherm plot and the pore size distribution corresponding to STA82(350) is shown in Figure 10.30 and Figure 10.32, respectively. It is seen that pores in the range of 2-20 nm having an average pore diameter of 10 nm were formed in this catalyst. The total pore volume was calculated as 0.5 cm³/g.

Table **10.6** EDS analysis results of STA8

Sample	Element	Weight Conc%	Atom Conc %	W/Si Ratio	
				weight	atomic
STA81UCCO2	Si	30.58	74.25	2.27	0.35
	W	69.42	25.75		
STA81(HCl&EtOH)	Si	16.55	56.49	5.04	0.77
	W	83.45	43.51		
STA82 Uncalcined	Si	27.41	71.19	2.65	0.40
	W	72.59	28.81		
STA82(350)	Si	24.47	67.96	3.09	0.47
	W	75.53	32.04		
STA82(450)	Si	26.44	70.18	2.78	0.42
	W	73.56	29.82		
STA82(550)	Si	31.10	74.72	2.22	0.34
	W	68.90	25.28		

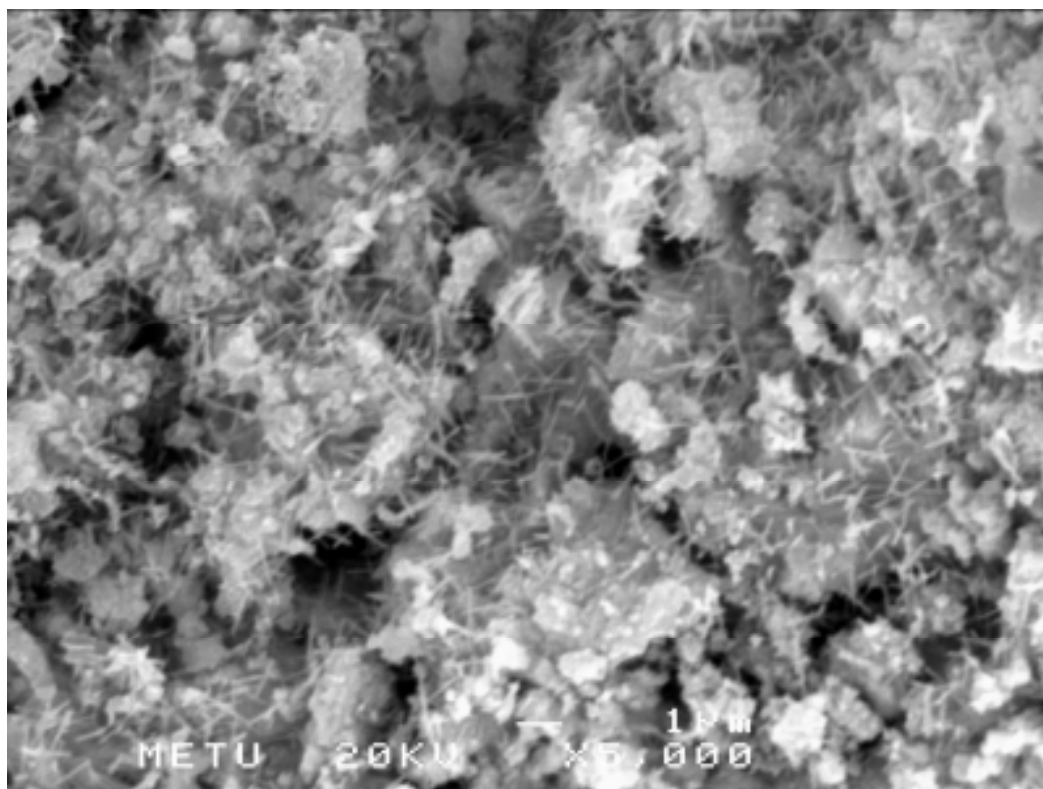


Figure 10.27 SEM images of STA82(550) (1)

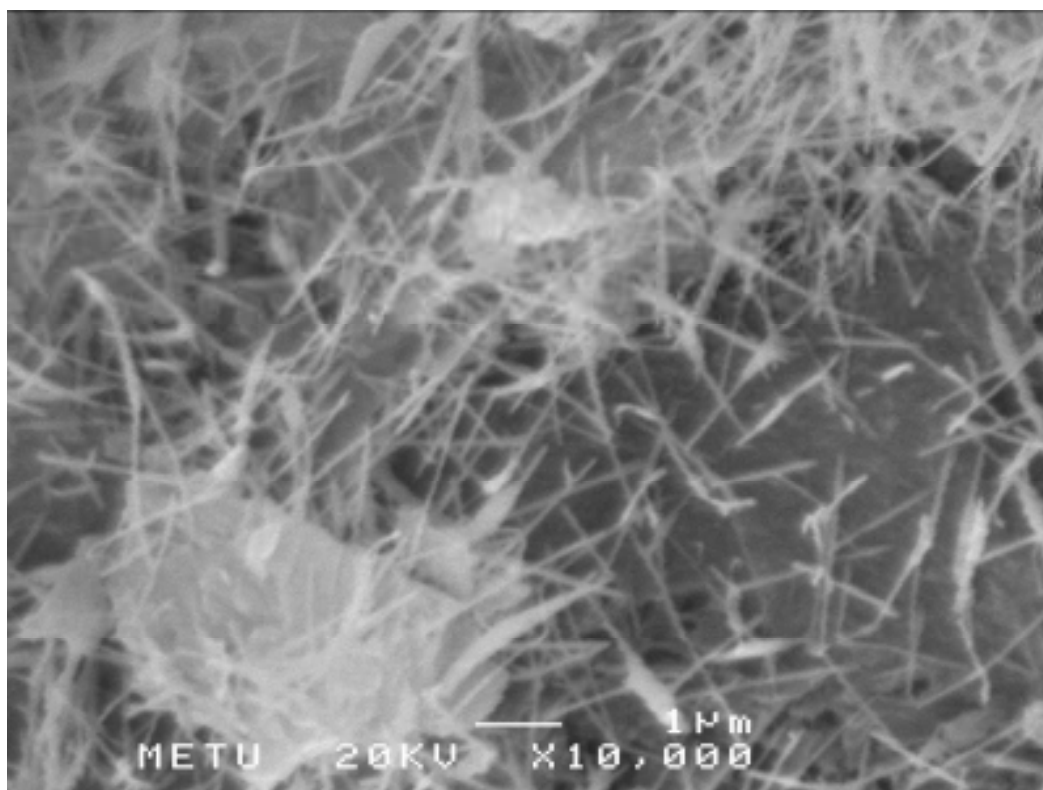


Figure 10.28 SEM images of STA82(550) (2)

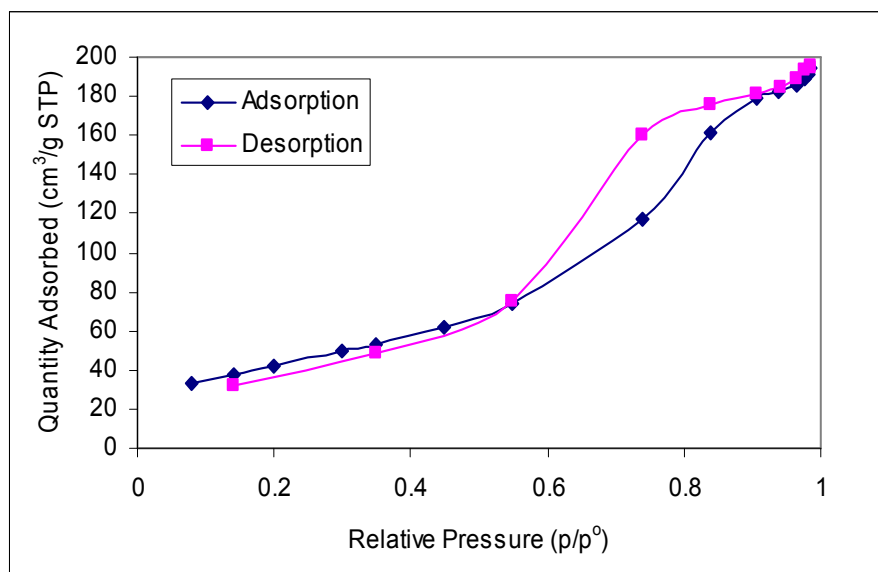


Figure 10.29 Isotherm linear plot for STA82(550)

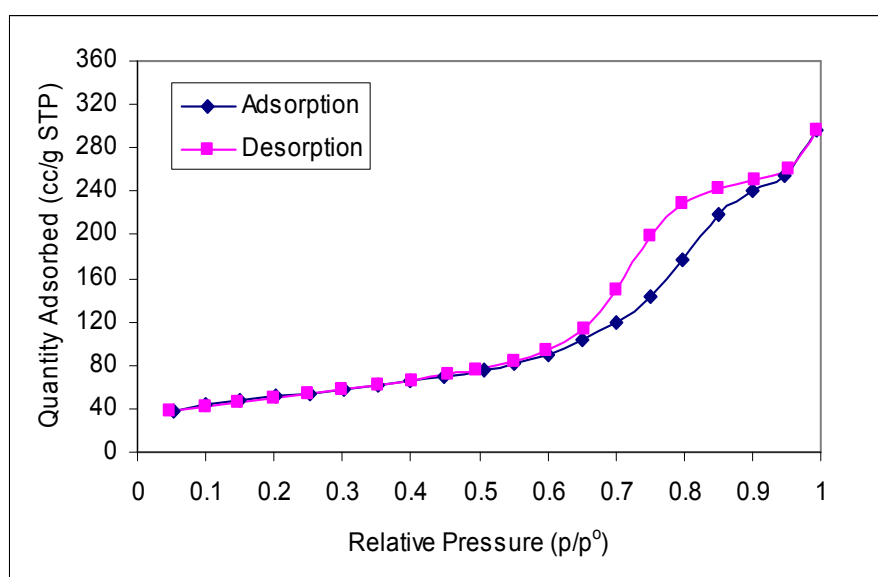


Figure 10.30 Isotherm linear plot for STA82(350)

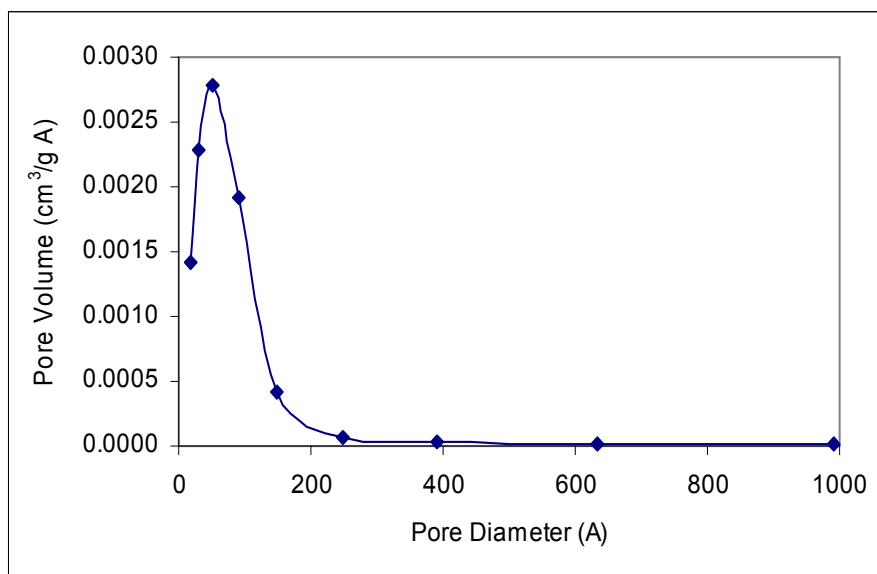


Figure 10.31 The Pore size distribution of STA82(550)

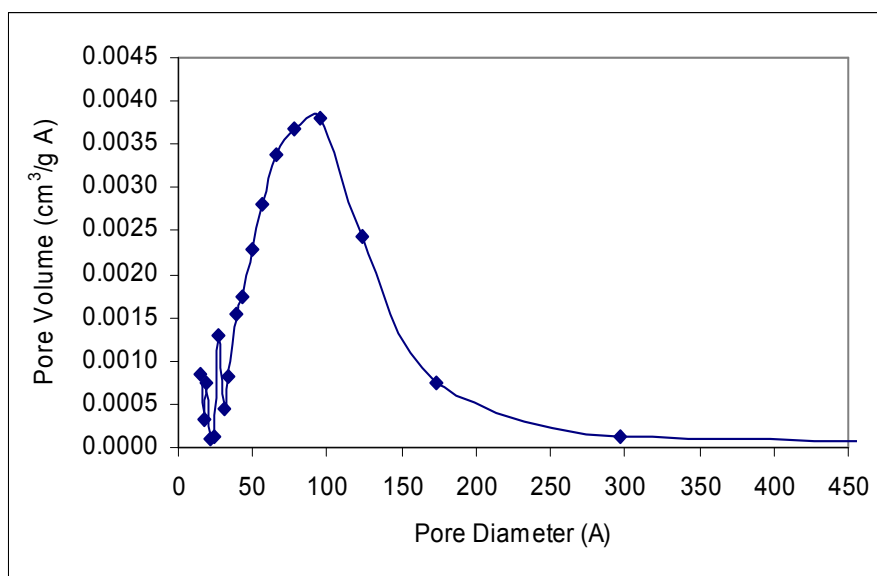


Figure 10.32 The Pore size distribution of STA82(350)

10.5.5 FTIR

The FTIR characterization of uncalcined STA82 and STA82(550) is given Figure 10.33 and 10.34, respectively. The deterioration of the STA structure was observed after calcination at 550°C.

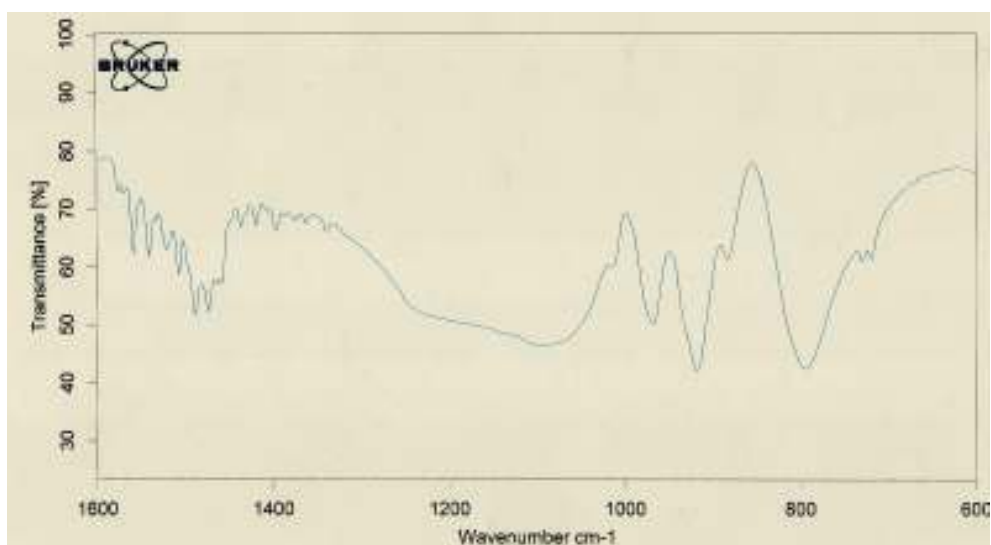


Figure 10.33 The FTIR of uncalcined STA82

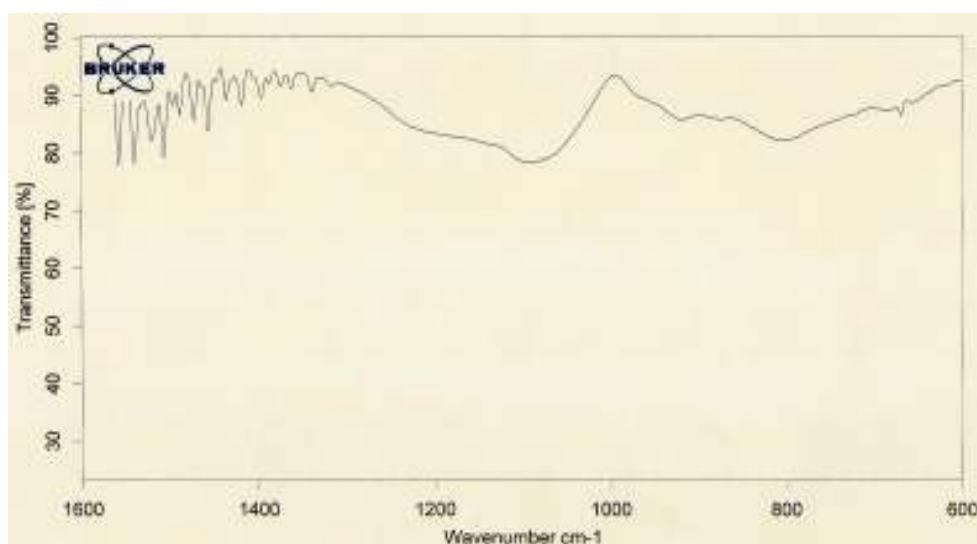


Figure 10.34 The FTIR of STA82(550)

10.6 Characterization of STA92

STA9 series catalysts were prepared following direct hydrothermal synthesis procedure by using TEOS as the silica source. 16.9 g of silicotungstic acid was used to adjust the W/Si ratio of 1.00 in the synthesis solution. The pH of the final synthesis solution was found as 1.2.

Some part of this sample was taken, without applying washing stage and calcined at 550°C and called as STA91(550) .

The remaining part was washed with deionize water and calcined at different temperatures. The calcination temperature was decided considering the results of TGA and DSC result of uncalcined STA92, which are given Figure 10.47 and 10.49, respectively. STA92(350), STA92(475) and STA92(550) are named according to the calcination temperature i.e., 350°C, 475°C and 550°C, respectively.

XRD, EDS, SEM, FTIR characterizations were done and presented in this part.

10.6.1 XRD

In Figure 10.35, the XRD diagram of STA92(550) is plotted. Some of the peaks corresponding to crystal structure of heteropolyacid were observed unlike the peak at 2θ value of 10° . Also, the diffractogram of STA91(550) was plotted on the same graph. The characteristic low angle diffraction peak of MCM41 is more clearly seen and the intensity of peaks associated to crystalline STA becomes higher when the prepared sample is washed before calcination.

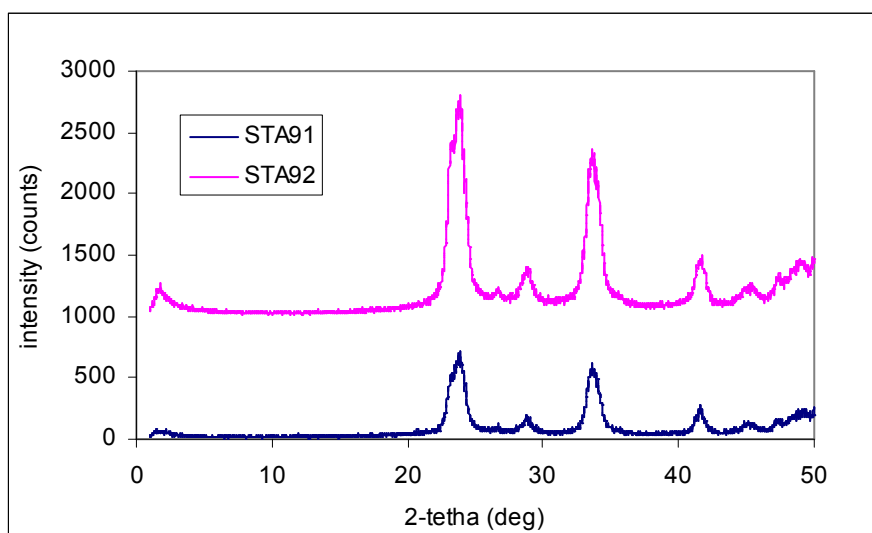


Figure 10.35 XRD patterns of STA91(550) and STA92(550)

The XRD diagram of uncalcined STA92, STA92(475) and STA92(550) are plotted together in Figure 10.36. These broad signals indicated large crystal formation was not occurred.

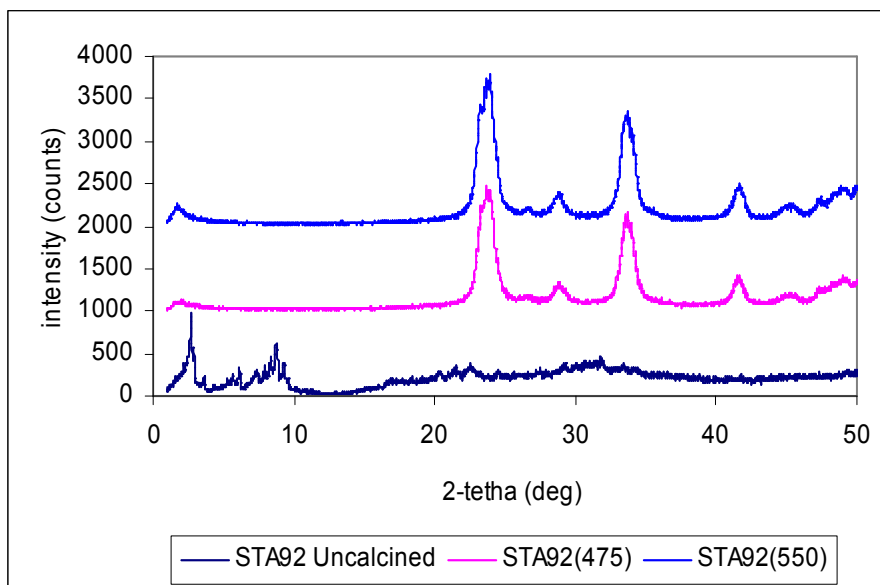


Figure 10.36 XRD patterns of STA92 before and after calcined at different temperatures

10.6.2 EDS

The molar W/Si ratio for these novel silicotungstic acid catalyst obtained from EDS characterization are given in Table 10.7. For all the calcined samples W/Si atomic ratio was found between 0.75-0.85. This is slightly lower than the W/Si ratio in the synthesis solution. One important conclusion is that W/Si ratio did not decrease after washing the solid product, indicating that STA was successfully incorporated into the lattice of novel mesoporous catalyst.

10.6.3 SEM

The SEM photographs of STA92(550) in Figure 10.37 and Figure 10.38. In Figure 10.39, SEM photograph of STA92(475) is seen.

Table **10.7** EDS analysis results of STA9 catalysts

Sample	Element	Weight Conc%	Atom Conc %	W/Si Ratio	
				weight	atomic
STA91(550)	W	83.06	42.83	4.90	0.75
	Si	16.94	57.17		
STA92(uncalcined)	W	88.05	52.96	7.37	1.13
	Si	11.95	47.04		
STA92(475)	W	83.23	43.13	4.96	0.76
	Si	16.77	56.87		
STA92(550)	W	84.76	45.93	5.56	0.85
	Si	15.24	54.07		

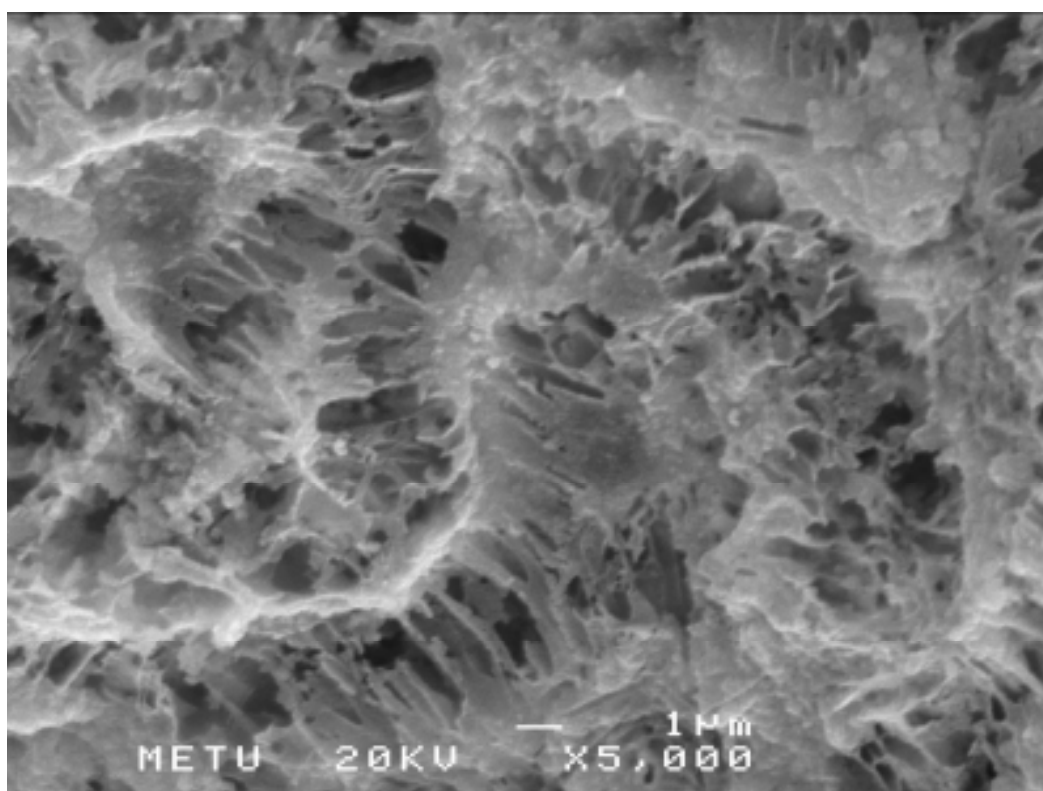


Figure 10.37 SEM images of STA92(550), (Magnification X5,000)

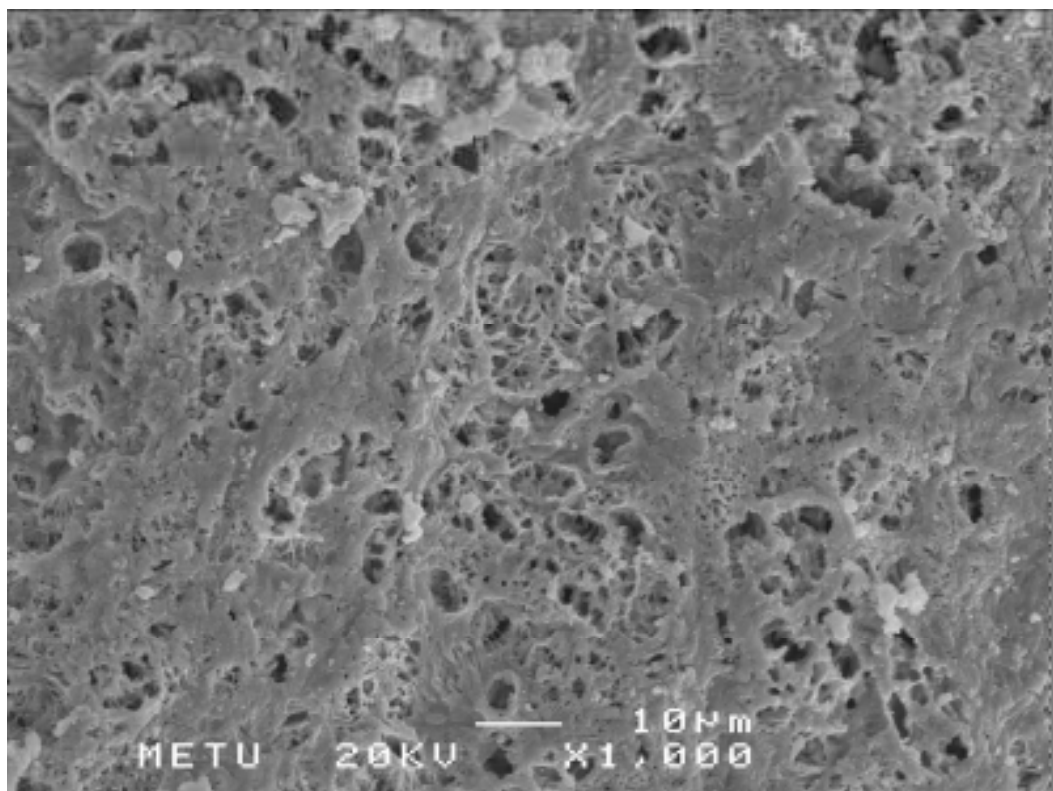


Figure 10.38 SEM images of STA92(550) (Magnification X1,000)

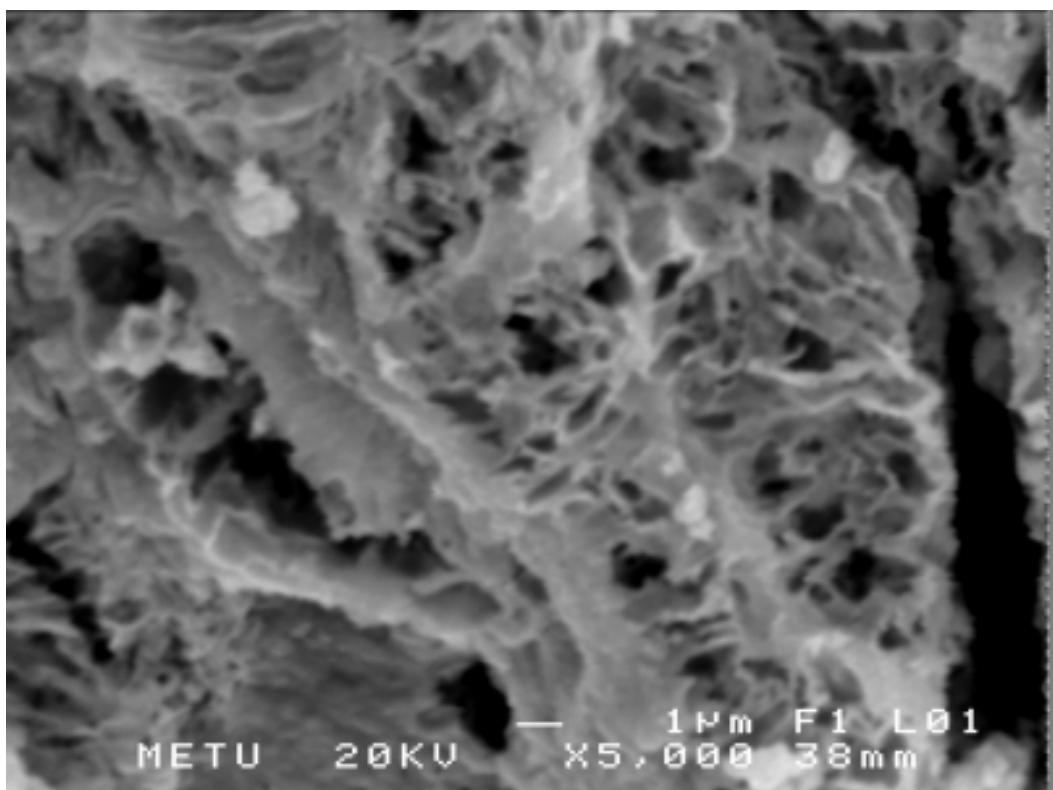


Figure 10.39 SEM images of STA92(475)

10.6.4 Nitrogen Physisorption

STA92(550) has a single point and BET surface area of 94.4 and 97.0 m²/g, respectively. BJH adsorption cumulative surface area of pores are 127.689 m²/g; BJH adsorption cumulative volume of pores are 0.195551 cm³/g and BJH Adsorption average pore width is 61.258 Å. A Type-IV type adsorption-desorption isotherm plot was obtained for STA92(550).

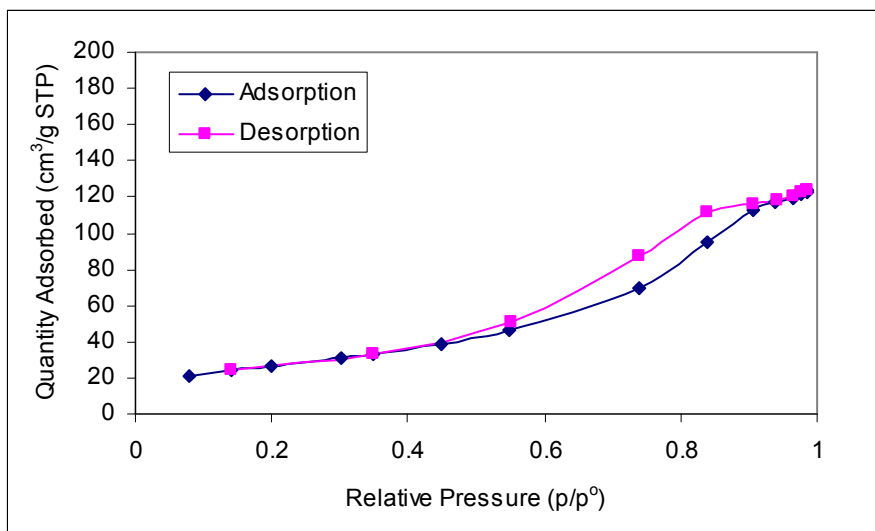


Figure 10.40 Isotherm Linear Plot of STA92(550)

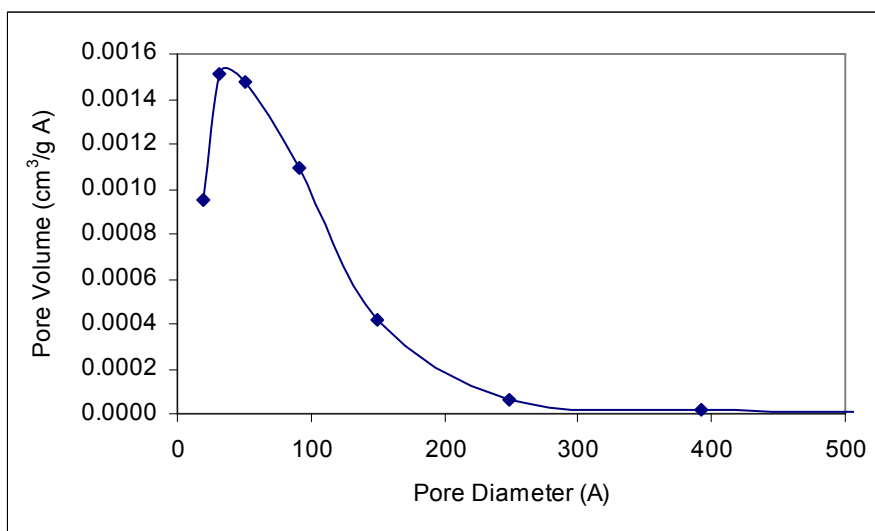


Figure 10.41 The Pore Size Distribution of STA92(550)

10.6.5 FTIR

The main four peaks corresponding to heteropolyacids were observed for uncalcined STA92 (Figure 10.42) whereas after calcined this sample at 475°C and 550°C, only one of them could be seen (Figures 10.43 and 10.44).

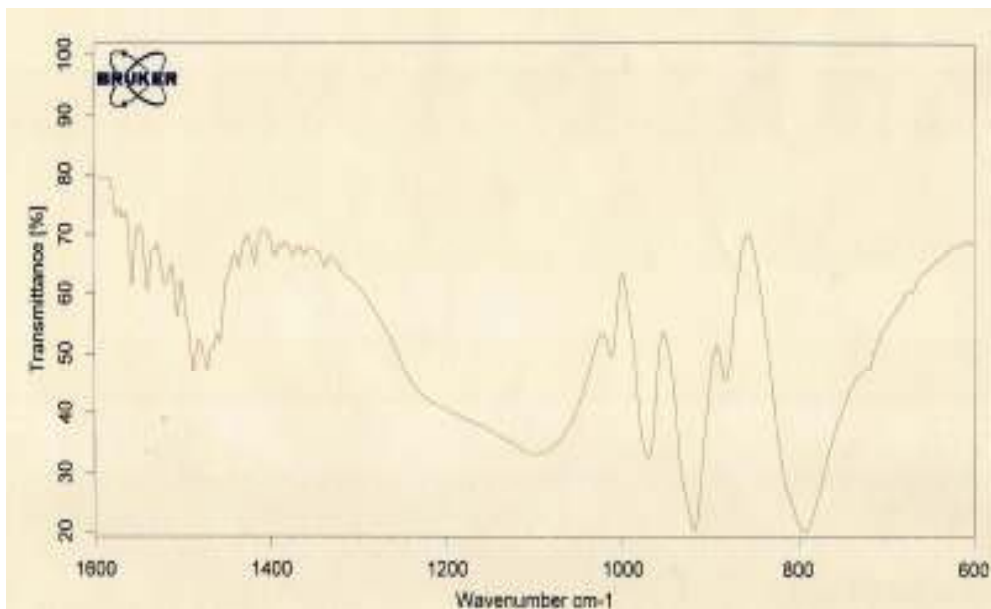


Figure 10.42 FTIR plot of uncalcined STA92

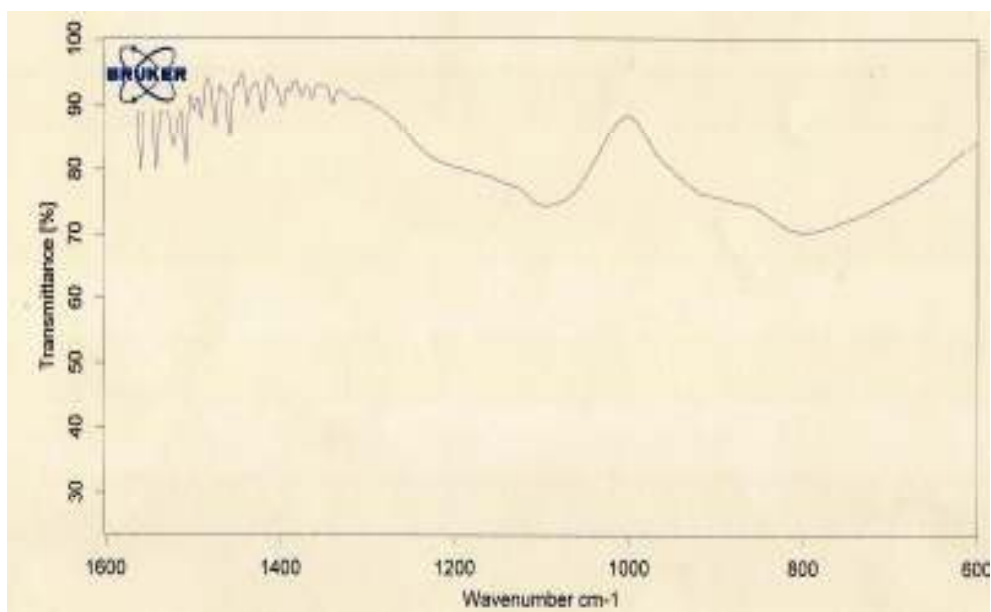


Figure 10.43 FTIR plot of STA92(475)

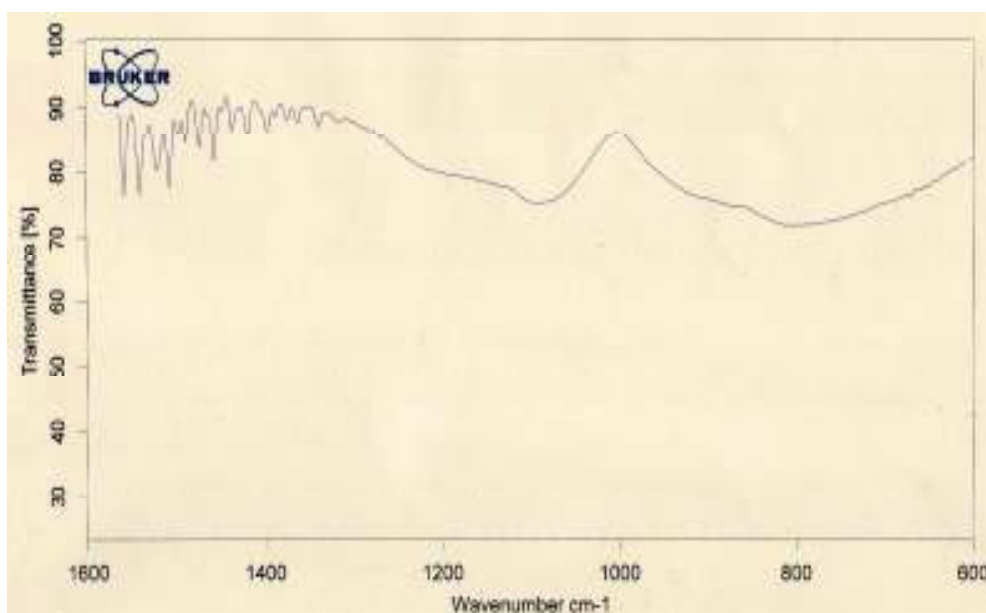


Figure 10.44 FTIR plot of STA92(550)

10.7 Comparison of Catalysts Prepared with Direct Hydrothermal Synthesis

In the following table characterization results of catalysts synthesized by direct hydrothermal methods are summarized.

Table 10.8 Characterization results of catalysts prepared with direct hydrothermal synthesis method

Catalyst	W/Si Molar Ratio	BET Surface Area (m ² /g)	Pore volume (cm ³ /g)	Avg pore diamete (nm)
STA52(550)	trace	687	1.21	4.9
STA62(550)	0.19	326	0.59	4.9
STA72(550)	0.05	360	0.65	6.7
STA82(550)	0.34	155	0.31	5.9
STA92(550)	0.85	97	0.20	6.1
STA62(350)	0.16	393	0.55	5.5
STA82(350)	0.47	178.7	0.45	10

Among the catalysts given in the in this Table STA52 which contains negligible amount of tungsten in its structure has the highest BET surface area, 687m²/g. The surface area of STA62 which has an atomic W/Si ratio of 0.19 is 326 m²/g and that of STA82 which has an atomic ratio of 0.34 is 155m²/g. STA92 which has the highest amount of tungsten atom in its structure, i.e. atomic ratio of 0.85, has the lowest surface area which is 97m²/g. According to these results, it can be summarized that as the amount of tungsten atom entering the structure increases, the surface area of the catalyst decreases. Among the catalysts STA82(350) has a largest average pore diameter

10.7.1 Thermal Analysis of the Synthesized Catalysts

The TGA, DTA characterization results of uncalcined STA62 and uncalcined STA82, uncalcined STA92 are presented in Figures 10.45, 10.46, 10.47, respectively. In all these plots, weight loss of the sample observed in the temperature range of 230-290°C (with a maximum loss at around 260°C) corresponds to the removal of surfactant present in the synthesized material. In this temperature range, weight loss of STA62, STA82 and STA92 were about 50 %, 38 % and 18 %, respectively. The pore volumes of these materials (after calcination) are 0.58 cm³/g, 0.30 cm³/g and 0.19 cm³/g, respectively. Considering that pores were formed by the removal of surfactant from the structure, TGA and pore volume results support each other. The second weight loss peak of these materials was observed between 350°C-430°C (giving maximum in the differential TGA curves at around 410°C). The weight loss of the materials within this temperature range were about 5 %, 10 % and 18 % for STA62, STA82 and STA92, respectively. These numbers follow the same trend of the amount of STA incorporated into the mesoporous material. For these three materials W/Si ratios in the catalysts are 0.19, 0.34 and 0.85, respectively. This second TGA peak observed at about 410°C corresponds to the decomposition of the synthesized material, probably by losing some of its protons, which might cause a decrease in its acidity. The DTA peak observed at around 375°C for STA62 (Figure 10.45) and the DSC peaks observed between 373°C-448°C for STA82 (Figure 10.48) and STA92 (Figure 10.49) also supported the TGA results that within this temperature range some decomposition of the synthesized materials occurred.

In the article of Thomas et al. (2005) it was demonstrated that, ¹H MAS NMR spectra of pure STA gave a sharp peak at about 9 ppm which corresponds

to the protons of anhydrous material. This peak disappeared at a temperature higher than 400°C. Their conclusion was that STA in is protonated from was stable upto 400°C which is higher than tungstophosphoric acid. Our TGA, DTA and DSC results also supported the conclusions of Thomas et al. (2005).

Basing on the TGA, DTA, DSC results and NMR results of Thomas et al. (2005) it is seen that at temperatures higher than 375°C some deterioration of the catalyst and loss of some protons took place. These results indicated that calcination temperature of the synthesized material should be lower than 375°C. Ethanol dehydration reaction results discussed in the following sections also proved the importance of calcination temperature on the catalyst activity. This is the main reason of calcining the catalyst at different temperatures in the 350°C–550°C range. Also, some different washing procedures were applied before the calcination step for the removal of surfactant without destroying the catalyst strcture.

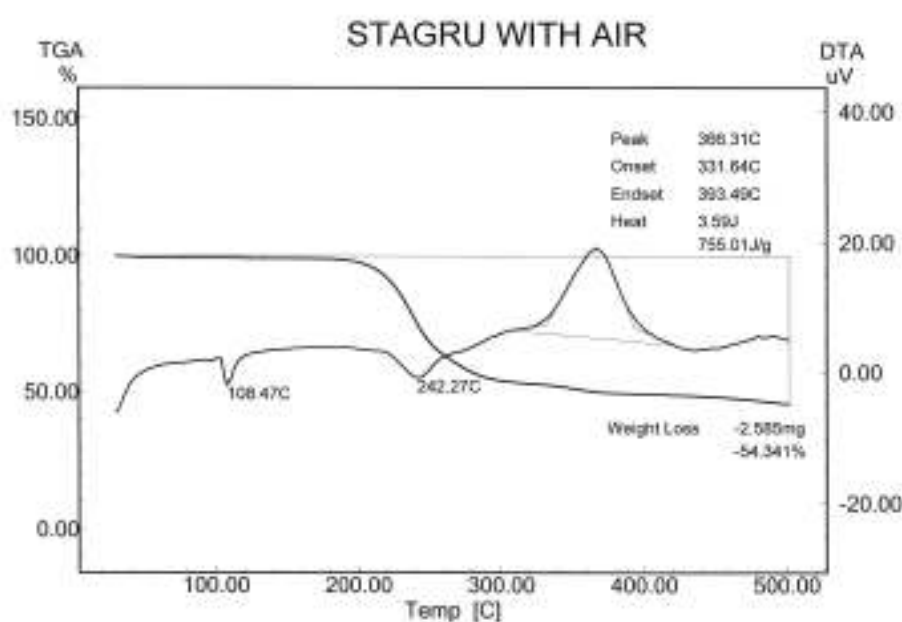


Figure 10.45 TGA Result of uncalcined STA62

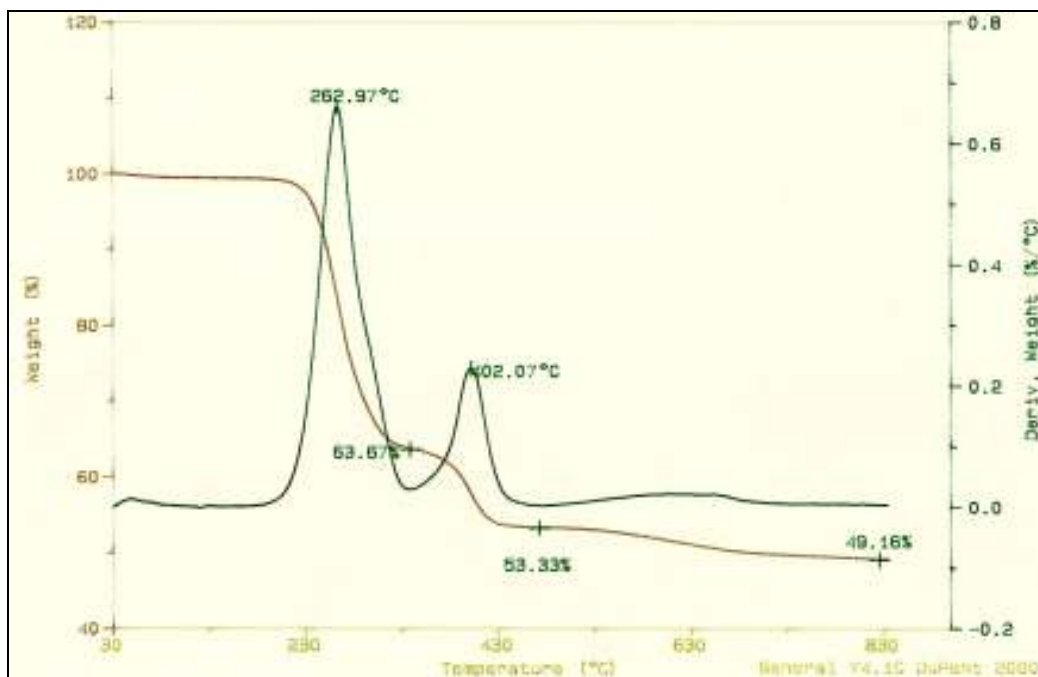


Figure 10.46 TGA of uncalcined STA82

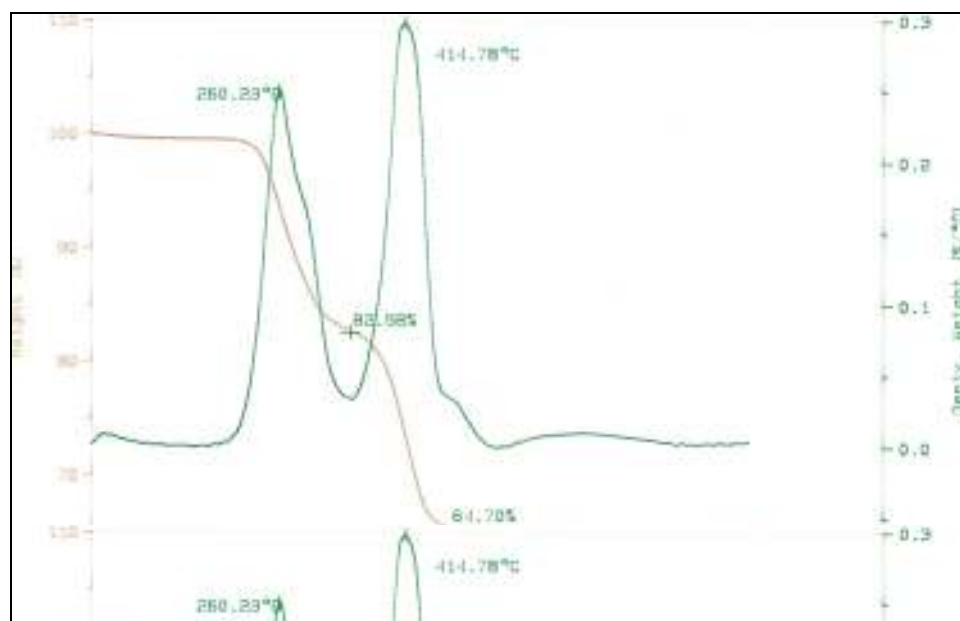


Figure 10.47 TGA of uncalcined STA92

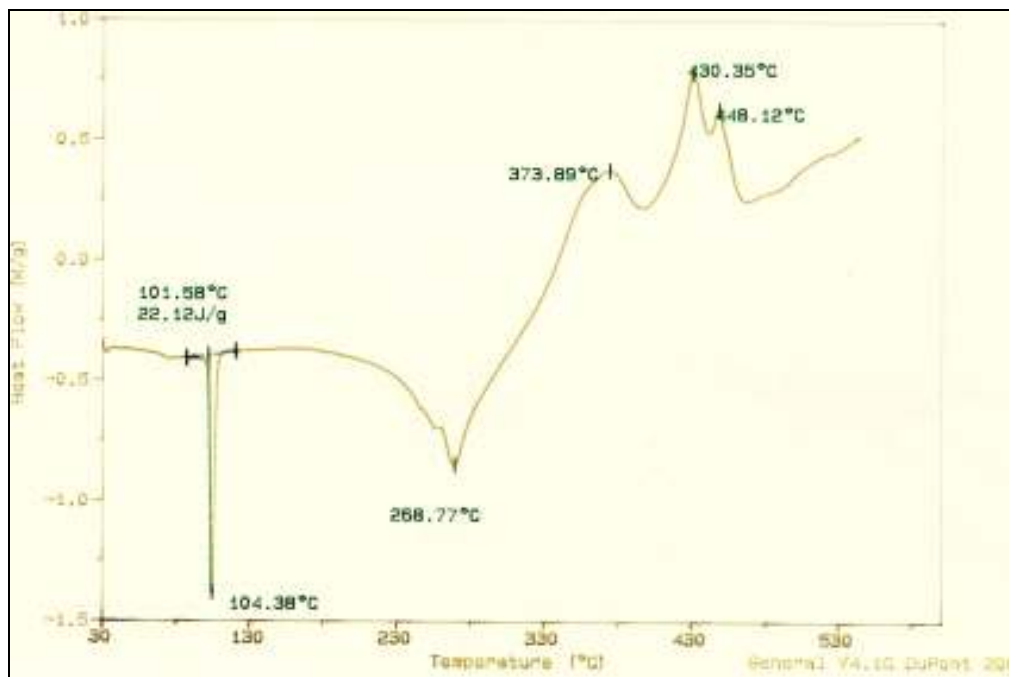


Figure 10.48 DSC of uncalcined STA82

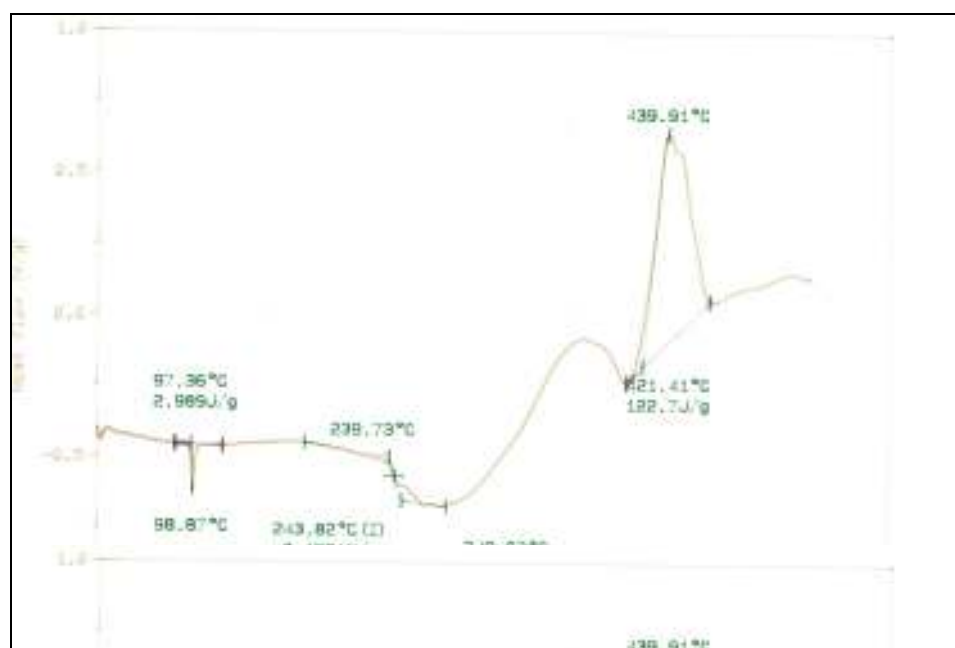


Figure 10.49 DSC of uncalcined STA92

10.8 Characterization of STA impregnated on MCM41 Catalysts

In this part, catalysts which are prepared by the impregnation method are characterized. MCM-41 is used as a support for silicotungstic acid.

Two different samples were prepared, namely STAMCM41U and STAMCM41C. For the former, silicotungstic acid is impregnated on the uncalcined MCM-41 and then it was calcined at 350°C. To prepare the latter one, firstly MCM-41 is prepared and calcined at 550°C and then used as a support for silicotungstic acid. The final product is characterized and used in catalytic activity tests without further calcination.

10.8.1 XRD

The XRD patterns corresponding to STAMCM41U and STAMCM41C are given together in Figure 10.50. XRD peaks in the 2θ range of 20-40° are quite wide, indicating well dispersion of STA on the MCM-41 surfaces. Large crystals were not formed.

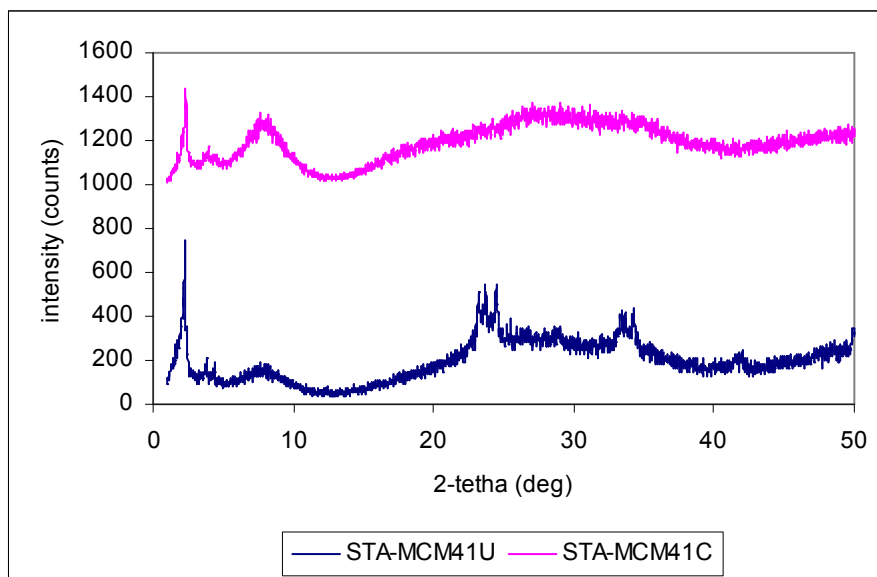


Figure 10.50 XRD patterns of STA imp MCM41 catalysts

10.8.2 EDS

The molar W/Si ratio for pure MCM-41 and two Silicotungstic acid impregnated on MCM-41 catalysts are given in Table 10.9.

Table 10.9 EDS analysis results of samples prepared with impregnation

Sample	Element	Weight Conc%	Atom Conc %	W/Si Ratio	
				weight	atomic
MCM-41	Si	100	100	trace	trace
	W	trace	trace		
STAMCM41(U)	Si	32.66	76.04	2.06	0.32
	W	67.34	23.96		
STAMCM41(C)	Si	38.63	80.47	1.59	0.24
	W	61.37	19.53		

10.8.3 Nitrogen Physisorption

The isotherm of STAMCM41U and STAMCM41C are presented in Figure 10.51 and 10.52, respectively. The pore size distribution for these two sample is compared in Figure 10.53.

A typical Type 4 adsorption isotherm was obtained, especially for STAMCM41C. The pore size distribution of STAMCM41C is also much narrower than STAMCM41U (Figure 10.53). The average pore diameter for STAMCM41U is 4.8 nm and for STAMCM41C it was 4.4 nm. The former one has a total pore volume of 0.33 cm³/g and the latter one has 0.35 cm³/g. These results indicated that impregnation of STA into calcined MCM-41 did not destroy the MCM-41 structure.

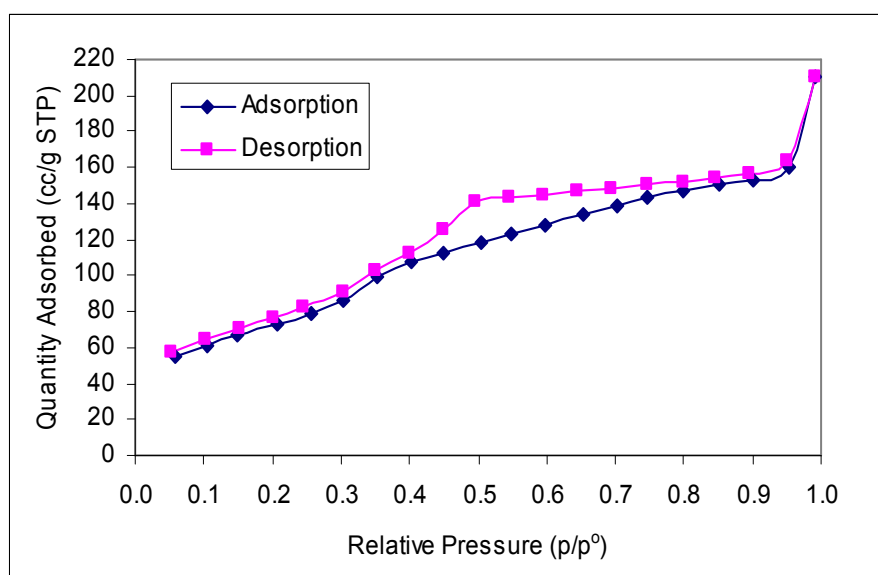


Figure 10.51 The isotherm for STAMCM41U

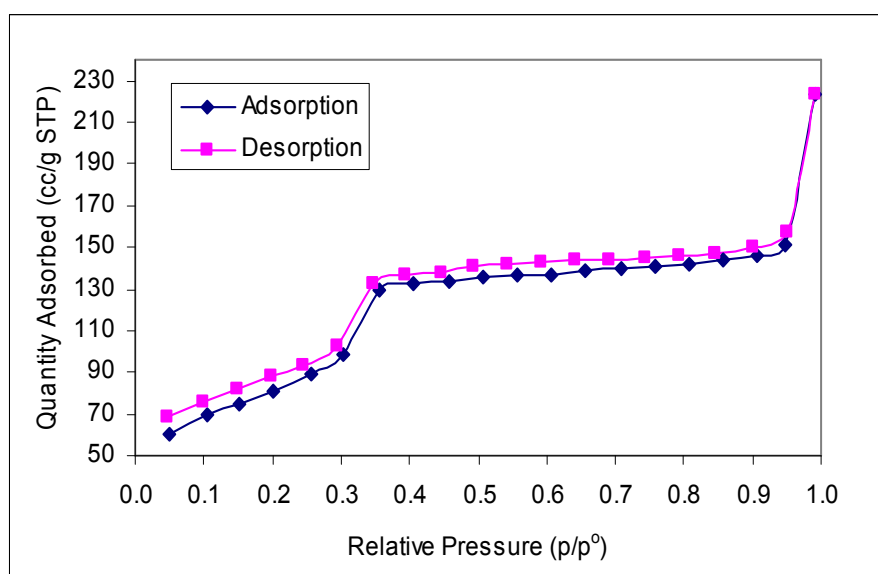


Figure 10.52 The isotherm for STAMCM41C

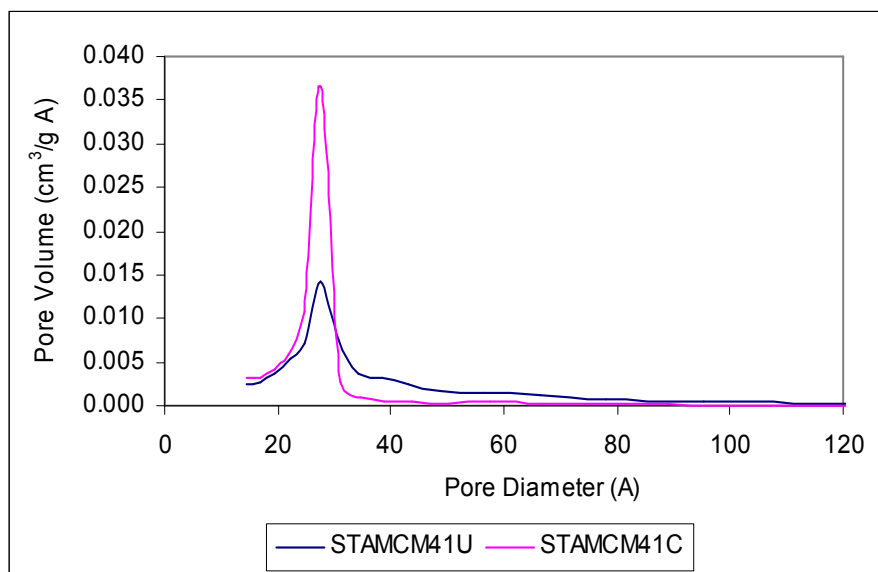


Figure 10.53 The pore size distribution of different STA impregnated on MCM41

10.9 Characterization of STA impregnated on Aluminosilicate

In this part the characterization results of pure mesoporous aluminosilicate and silicotungstic acid impregnated aluminosilicate which is called as STA(MAS) catalysts are presented.

10.9.1 XRD

In Figure 10.54 and 10.55, the XRD patterns corresponding to pure aluminosilicate and STA impregnated aluminosilicate are presented.

For the impregnated material wide XRD bands were observed at 2θ values of about 8° and between $20-40^\circ$. These results also indicated that large STA crystals were not formed within the pores of mesoporous aluminosilicate. STA is well dispersed on the pore walls.

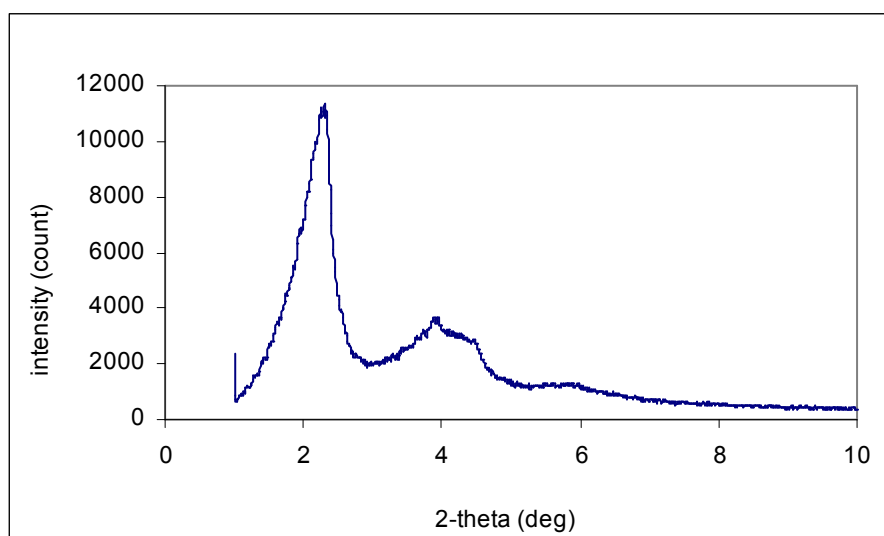


Figure 10.54 XRD patterns of Pure aluminosilicate

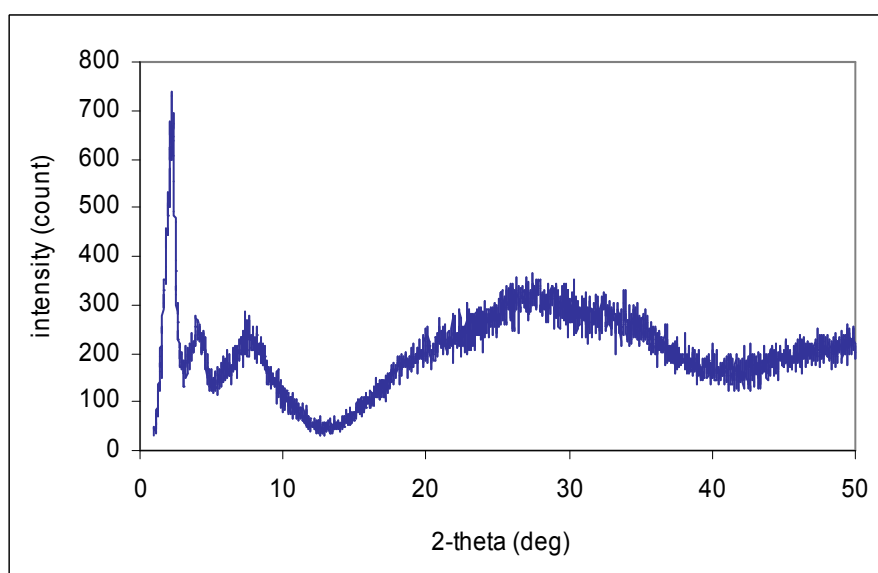


Figure 10.55 XRD patterns of STA impregnated aluminosilicate

10.9.2 Nitrogen Adsorption

The isotherm of pure aluminosilicate and silicotungstic acid impregnated on aluminosilicate is presented in Figure 10.56 and 10.57 respectively. The Type IV isotherm was not changed with impregnation. The pore size distribution of STA(MAS) is given in Figure 10.58. In this catalyst the pores lie between 2.5-3.5 nm.

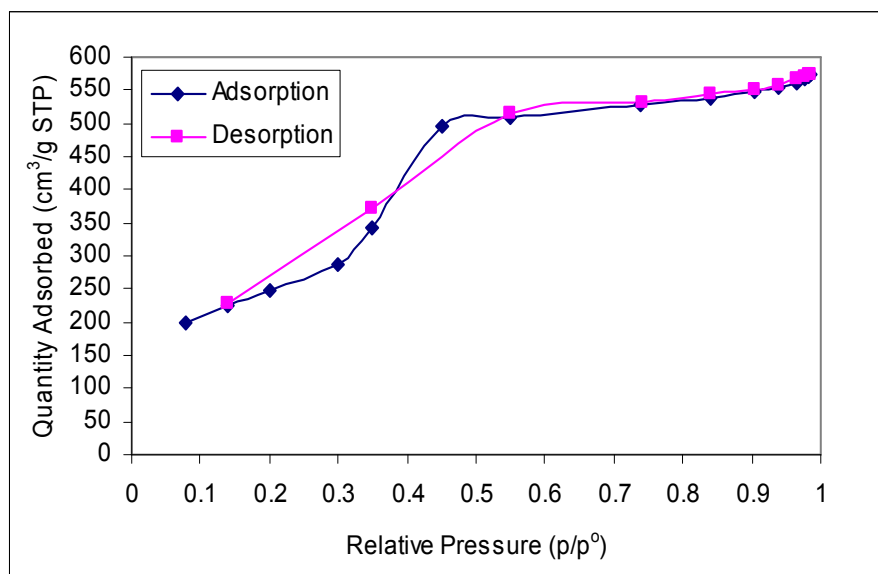


Figure 10.56 Isotherm of pure aluminosilicate

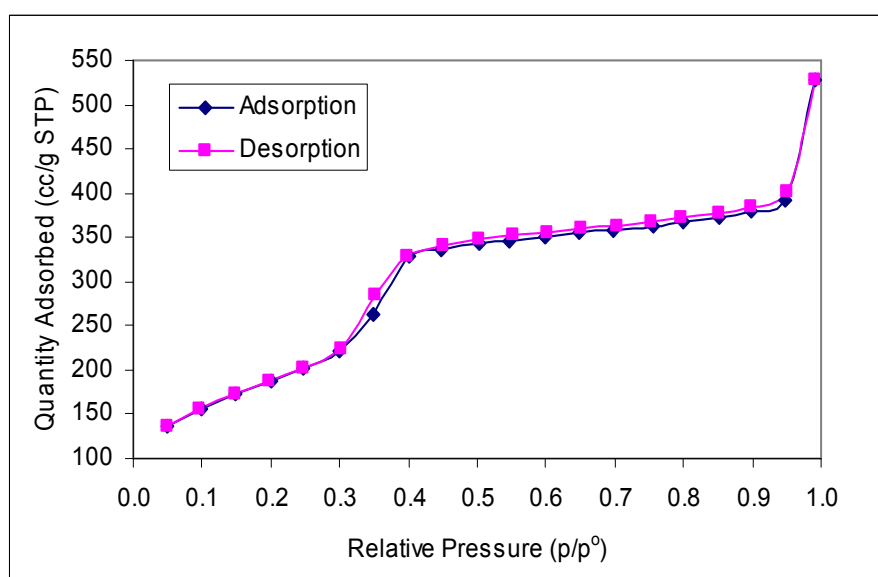


Figure 10.57 Isotherm of STA impregnated aluminosilicate

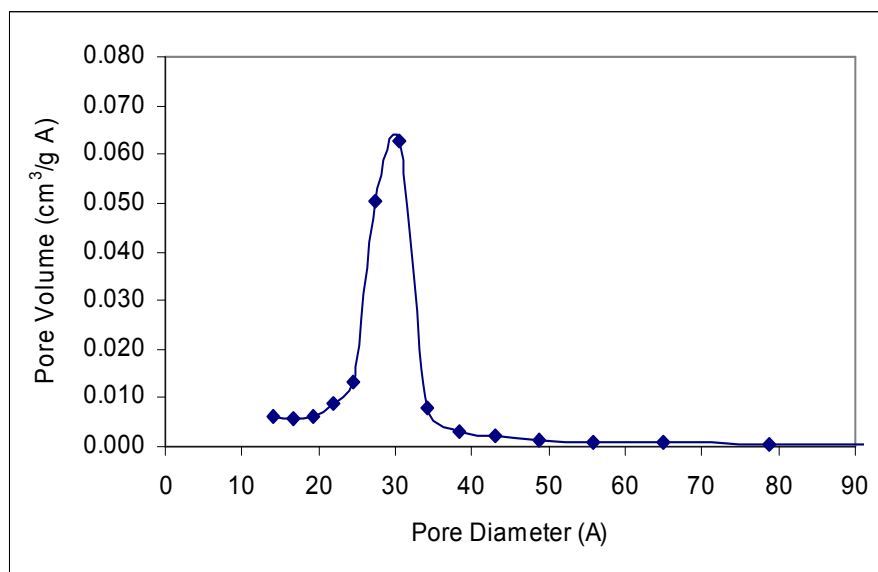


Figure 10.58 Pore size distribution for STA impregnated aluminosilicate

CHAPTER 11

RESULTS OF ETHANOL DEHYDRATION OVER NOVEL SILICOTUNGSTIC ACID CATALYSTS SYNTHESIZED IN THIS WORK

In this chapter, results of ethanol dehydration reactions over novel silicotungstic acid catalysts are presented.

Novel silicotungstic acid catalysts are synthesized by either direct hydrothermal or impregnation method, as given in Chapter 8. Activities of these catalysts were investigated in a temperature range of 180°C-400°C.

11.1 Results obtained with STA52

STA52, which was prepared by direct hydrothermal synthesis procedure, has a BET surface area of 687 m²/g. It has BJH adsorption pore volume and pore diameter of 1.21 cm³/g and 49.75 Å, respectively. The atomic ratio of tungsten to silica decreased from 0.08 to negligible amount after washing the sample with deionize water which indicated most of the tungsten atoms were not chemically bonded to the structure.

The catalytic activity of STA52 was investigated in ethanol dehydration reaction in the experimental set up, whose properties were given in Chapter 7. Feed stream was prepared with pure ethanol and helium. The total flowrate of feed stream was adjusted to 44.24 ml/min at room temperature by keeping the molar ratio of ethanol in the mixture was at 48%. 0.1 gram of STA 52 was

placed in a differential tubular reactor and the reaction temperature was altered from 180°C to 400°C.

Experiments which were carried out in these conditions showed that very low ethanol conversion values, around 2 % was obtained with STA52 at a temperature range of 180-400°C (Figure 11.1). This result is not surprising since this catalyst is composed of mainly silica which is not appropriate for ethanol dehydration reaction due to its low acidity.

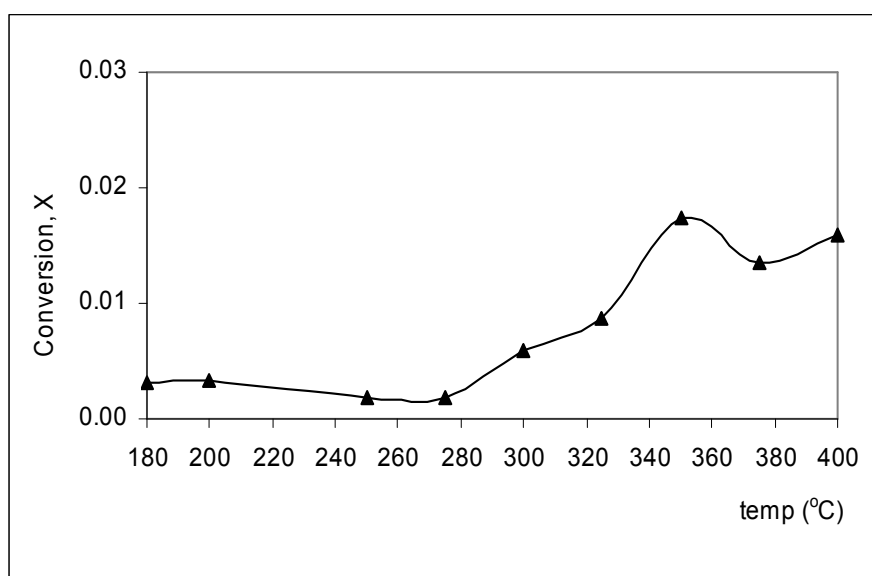


Figure 11.1 The variation in ethanol conversion with 0.1 g of STA52, EtOH/(EtOH&He):0.48

When the product distribution was investigated, mainly ethylene and acetaldehyde formation was observed while DEE, which is one of the main products of ethanol dehydration reaction, was not produced in these experiments (Figure 11.2). Especially at low reaction temperatures acetaldehyde formation is more favorable, after 300°C the conversion value started to increase (Figure 11.1) due to formation of ethylene.

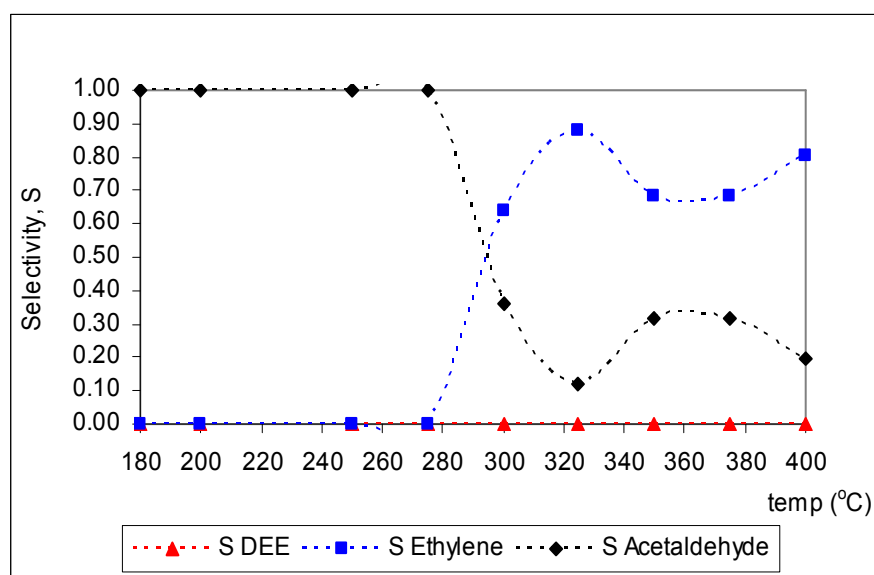


Figure 11.2 The variation of selectivities of products with 0.1 g of STA52, EtOH/(EtOH&He):0.48

11.2 Results obtained with STA62

STA62 which is a novel silicotungstic acid catalyst is prepared with direct hydrothermal synthesis method. The details of the preparation procedure is given in Chapter 8. The sample called as STA62(550) was calcined at 550°C and the sample called as STA62(350) was calcined at 350°C

For STA62(550), the atomic ratio of tungsten to silica was found as 0.19 from EDS analysis (Table 10.8). Nitrogen physisorption analysis gave that, its surface area was 326 m²/g; its BJH adsorption pore volume and pore diameter were 0.59 cm³/g and 49.05 Å, respectively.

The catalytic activities of STA62(350) and STA62(550) were investigated with ethanol dehydration reaction in the experimental set up that is presented in Chapter 7. In all experiments, a mixture of ethanol and helium was used as a feed stream with a total flow rate value of 44.24 ml /min. The ratio of ethanol to mixture was adjusted at 48% at room temperature. The reaction temperature was altered in the range of 180-400°C.

Firstly, experiments were done by using 0.2 gram of STA62(550) with given feed composition and the effect of reaction temperature on the ethanol

conversion was investigated. Then, the amount of catalyst was reduced to 0.1 g to see the effect of space time at the same feed flowrate and feed composition.

Ethanol dehydration reaction was also carried out over STA62(350) with a feed stream of 44.24 ml/min. The ethanol molar ratio in the mixture was kept as 0.48 and 0.2 gram of catalyst was used and reaction temperature was investigated in the temperature range of 180-350°C.

11.2.1 Effect of Reaction Temperature

Results of experiments with 0.2 g of STA62(550) showed that catalytic activity of this catalyst was very low at a reaction temperature lower than 275°C. Indeed, only 2% of ethanol is converted to the products up to this temperature. A rapid increase is seen in the conversion of ethanol after 275°C; further increase in reaction temperature positively affects the catalytic activity of STA62(550). The conversion value which is 0.30 at 300°C becomes 0.63 at 400°C (Figure 11.3).

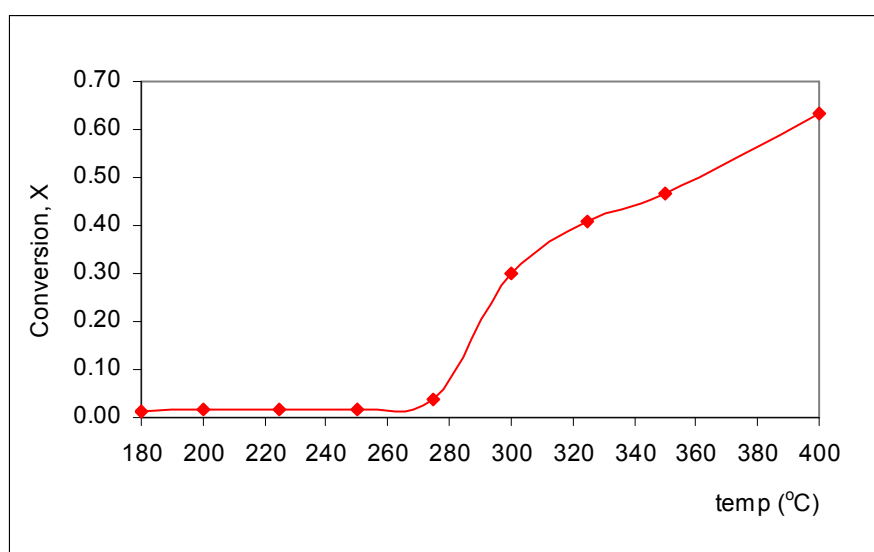


Figure 11.3 The variation in ethanol conversion with 0.2 g STA62(550), EtOH/(EtOH&He):0.48

Ethanol dehydration reactions mainly take place over acidic catalysts. For our novel catalysts, the acidity is coming from the silicotungstic acid. The difference in conversion profiles of STA52(550) and STA62(550) is a very good indication of the importance of heteropolyanions in the catalytic activity. The

tungsten atom which is found in the heteropolyanion, is rarely observed in STA52(550) and very low ethanol conversion, at around 0.02, is obtained (Figure 11.1). In the case of STA62(550), the atomic ratio of W/Si is 0.19 and the ethanol conversion value of 0.63 is obtained (Figure 11.3).

Pure ethanol is mainly converted to DEE, ethylene, acetaldehyde and water over STA62(550) at the given experimental conditions. The selectivities of DEE, ethylene and acetaldehyde are calculated at different reaction temperatures and compared in Figure 11.4.

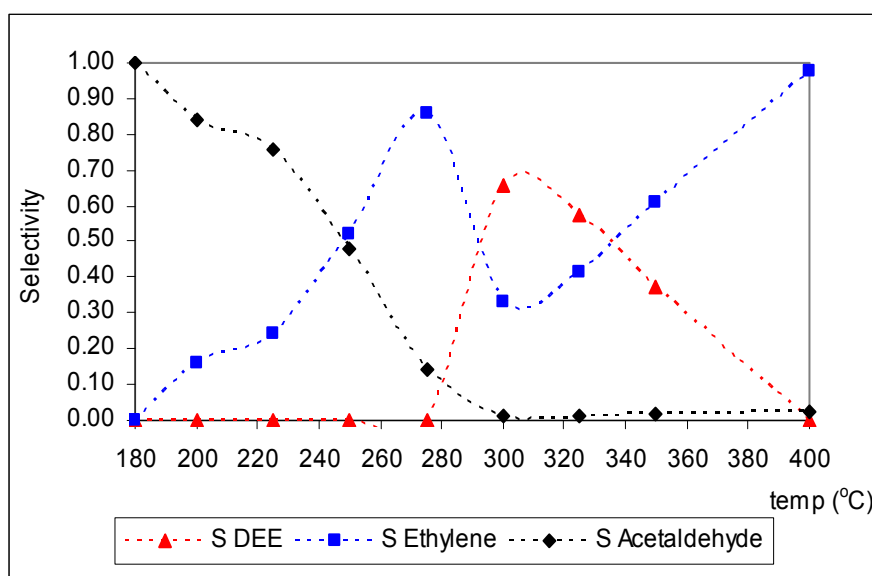


Figure 11.4 The variation in product selectivities with 0.2 g of STA62(550) EtOH/(EtOH&He):0.48

Upto 275°C, acetaldehyde and ethylene formation is observed but their yields are very low, approximately 0.03 (Figure 11.5). The selectivity of ethylene increases with temperature until 275°C at which DEE is observed in the product stream at first. When the reaction temperature is further increased from 275 to 300°C, the selectivity of ethylene decreases from 0.86 to 0.33. As shown in Figure 11.4, upto 300°C the selectivity of acetaldehyde decreases continuously and it reaches to a negligible amount. At 300°C the maximum selectivity for DEE (0.66) is obtained and then a decrease in selectivity of this product is observed.

In order to explain the different behavior of products more clearly, a reaction mechanism should have been derived. For this aim, a DRIFT Reflectance

FT-IR study is carried out and presented in Chapter 12. The experimental results deduced from ethanol dehydration reaction over novel silicotungstic acid catalyst may be very useful in the derivation of the reaction mechanism. As shown in Figure 11.4 the disappearance of acetaldehyde is followed by an increase in DEE selectivity, this may be a result of a series reaction between acetaldehyde and DEE. Firstly some acetaldehyde may be produced on the catalyst surface then it may give another reaction to produce DEE. Simultaneous production of DEE and Ethylene takes place after 300°C at the same figure, this can be an indicator of parallel reaction of ethanol to produce these two valuable products. At high temperatures further decomposition of DEE to ethylene may be the reason of observing a maximum in the DEE yield at about 320°C.

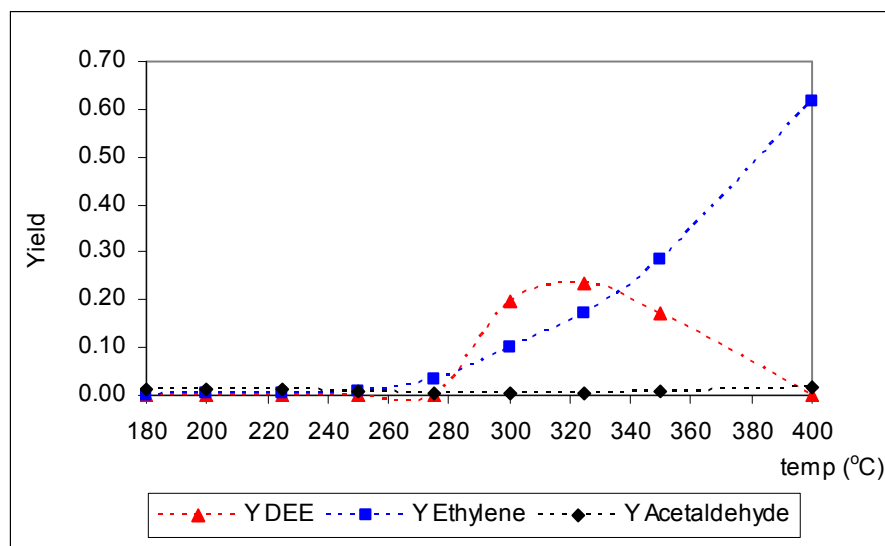


Figure 11.5 The variation in product yields with 0.2 g of STA62(550)
EtOH/(EtOH&He):0.48

11.2.2 Effect of Space Time

In order to investigate the effect of space time on the total conversion of ethanol, the amount of STA62(550) was reduced to 0.1 g. As in the previous case, the total flow rate of feed stream was set to 44.24 ml/min by adjusting the ethanol flow rate at 21 ml/min and helium flowrate at 23 ml/min. The reaction temperature was changed from 180 to 400°C.

The conversion of ethanol obtained by using 0.1 gram of STA62(550) was plotted together with the results obtained for 0.2 gram of STA62(550), in Figure

11.6, in order to show the effect of space time. As mentioned in the previous section, STA62(550) shows low activity for dehydration reaction, at temperatures lower than 275°C; further increase in reaction temperature give rise to higher conversion of ethanol. Comparison related to the operating conditions can be done more clearly at temperatures higher than 275°C. Space time has an enhancing effect on the total conversion of ethanol, i.e. increasing the amount of catalyst packed into reactor caused an increase in conversion of ethanol. For example, at 300°C the ethanol conversion value was increased from 0.12 to 0.30 by doubling the amount of catalyst from 0.1 g to 0.2 g (Figure 11.6). With the given feed conditions, maximum conversion value that could be obtained with 0.1g of STA62(550) was 0.40 which was at a temperature of 375°C. It is expected that increasing space time shifts the maximum conversion value to higher numbers.

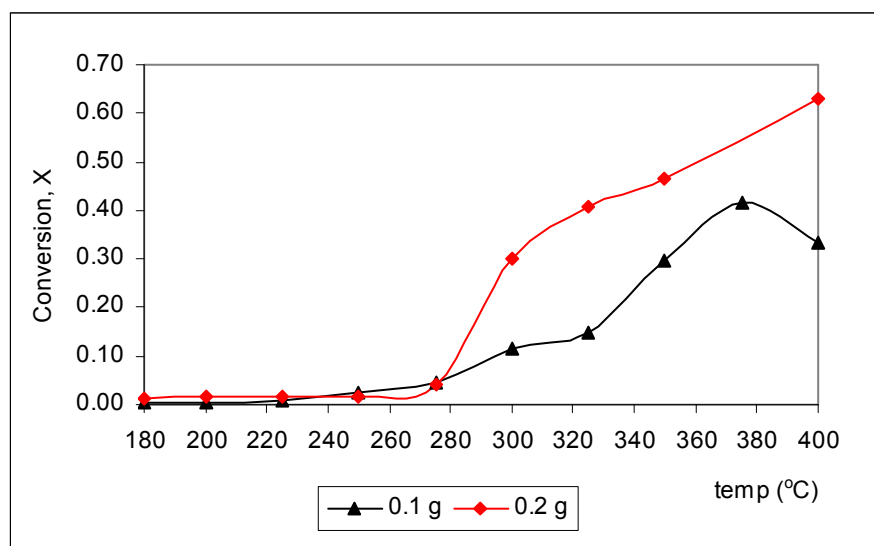


Figure 11.6 The variation in ethanol conversion with the amount of STA62(550), EtOH/(EtOH&He):0.48

The effects of space time on product selectivities were also investigated. When 0.1 g of STA62(550) was used in the reaction medium, ethanol was converted into ethylene, water and acetaldehyde. On the other hand, DEE was so low and could not be quantitatively determined (Figure 11.7).

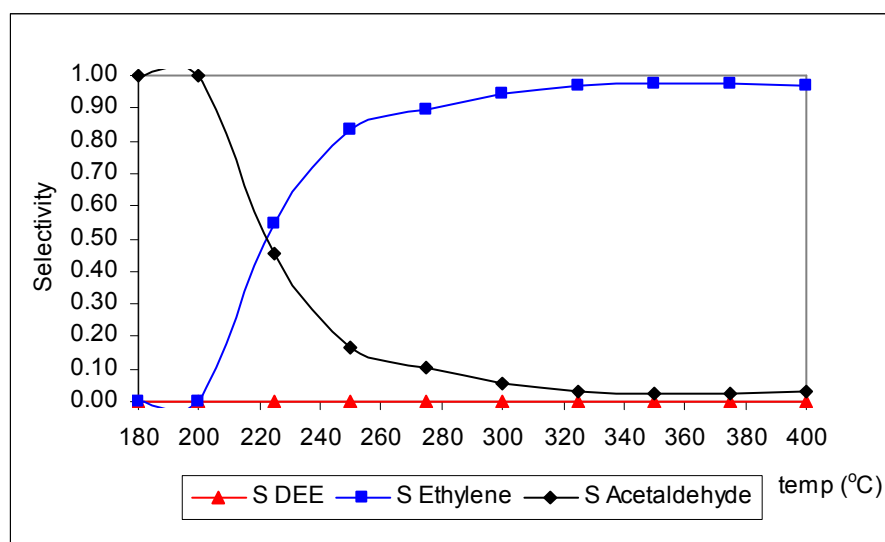


Figure 11.7 The selectivity profiles with 0.1 g of STA62(550), EtOH/(EtOH&He):0.48

As presented in Figure 11.8, the greatest effect of space time occurs on DEE formation. When 0.2 g of STA62(550) was used in the reaction, the selectivity of DEE reached to 0.65 at 300°C. In addition a maximum yield value of 0.24 was obtained at 325°C for this product (Figure 11.9). However, DEE formation could not be observed with 0.1 g of STA62(550) (Figure 11.8). The required contact time may not be sufficient for the latter case to produce DEE in the reaction medium.

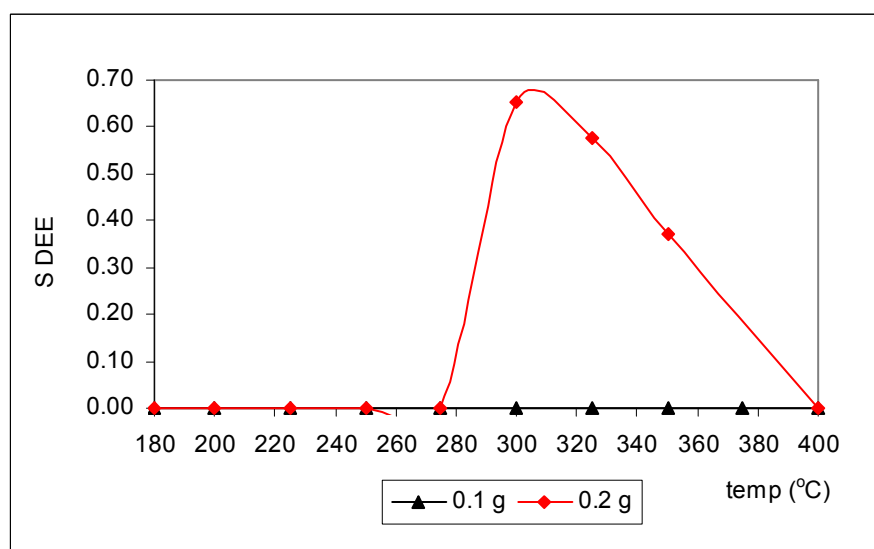


Figure 11.8 The variation in DEE selectivity with amount of STA62(550), EtOH/(EtOH&He):0.48

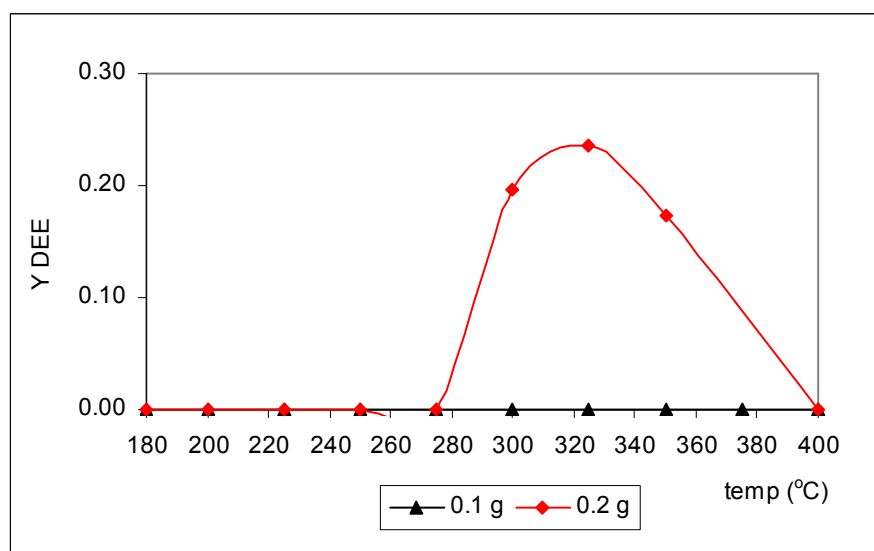


Figure 11.9 The variation in DEE selectivity with amount of STA62(550), EtOH/(EtOH&He):0.48

As shown in Figure 11.7, ethylene is the main product of ethanol dehydration reaction carried out over 0.1 g of STA62(550). There is a continuous increase in selectivity of this product with reaction temperature upto 325°C, such as, the selectivity values at 255°C and 275°C are 0.55 and 0.90, respectively. It reaches to 0.97 at 325°C and becomes constant after that temperature.

When 0.2 g of catalyst is used, a peak, having a value of 0.86, is observed in selectivity profile of ethylene at 275°C at which DEE formation has just started. At 300°C, the selectivity of ethylene drops to 0.33 where the selectivity of DEE reaches to its maximum value of 0.66. These type of behaviour can not be observed for lower space time. Ethylene and acetaldehyde formation steps are much more favorable at low space times. However at temperatures higher than 320°C, decomposition of DEE to ethylene contributes to the ethylene formation.

11.2.3 The Effect of Calcination Temperature

Due to lower calcination temperature, the catalytic activity of catalyst is expected to arise. As discussed in the previous section calcination temperature is very important as for the structure of the catalyst. NMR, DTA, DSC results indicated that over 375°C structure of the catalyst was changed by losing some of the protons of the catalyst. Calcination at higher temperatures causes some

deformation of the catalyst structure and a decrease in acidity of the catalyst. Decrease of acidity of pure STA was also reported by Thomas et al. (2005) using NMR results.

While the conversion of ethanol is around 0.02 at a temperature range of 180-275°C for STA62(550), it takes a value between 0.50-0.55 at the same temperature interval for STA62(350) (Figure 11.10). So ethanol dehydration reaction can be carried out at low temperatures like 180°C with a 50% conversion by using STA62(350).

Moreover with this catalyst, higher conversion values can be obtained with further increase in temperature, such as 0.64 at 350°C and 0.81 at 375°C (Figure 11.10). The corresponding values for STA62(550) at these temperatures are 0.47 and 0.55, respectively.

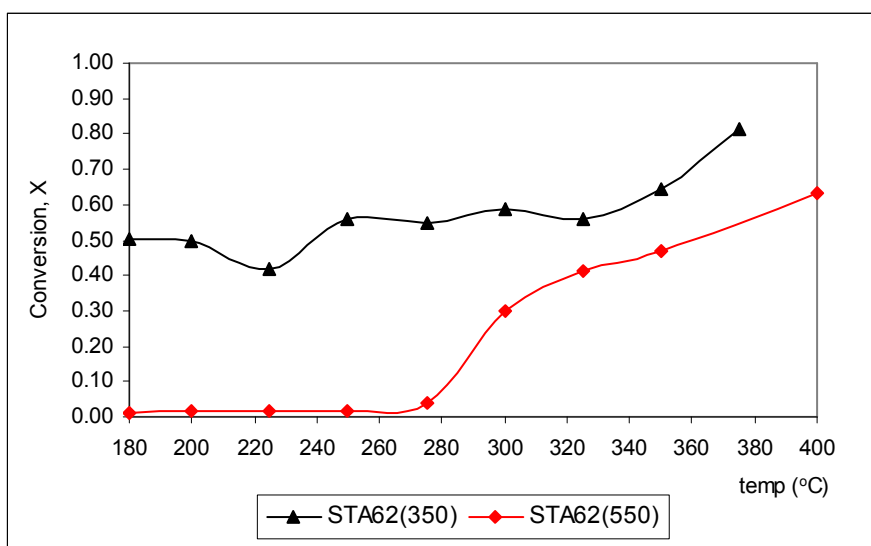


Figure 11.10 The effect of calcination temperature on activity of STA62 catalysts, EtOH/(EtOH&He):0.48, catalyst amount:0.2 g

As a result of ethanol dehydration reaction over STA62(350), ethanol is converted to ethylene, DEE, acetaldehyde and water. The DEE formation starts after 225°C and continues upto 325°C. Outside the indicated range, it can not be analyzed due to its low amount (Figure 11.11). Ethylene formation takes place with an increasing trend from 180 to 375°C, continuously. The amount of acetaldehyde produced by using STA62(350) attracts the attention. It is produced throughout the reaction period with a decreasing amount.

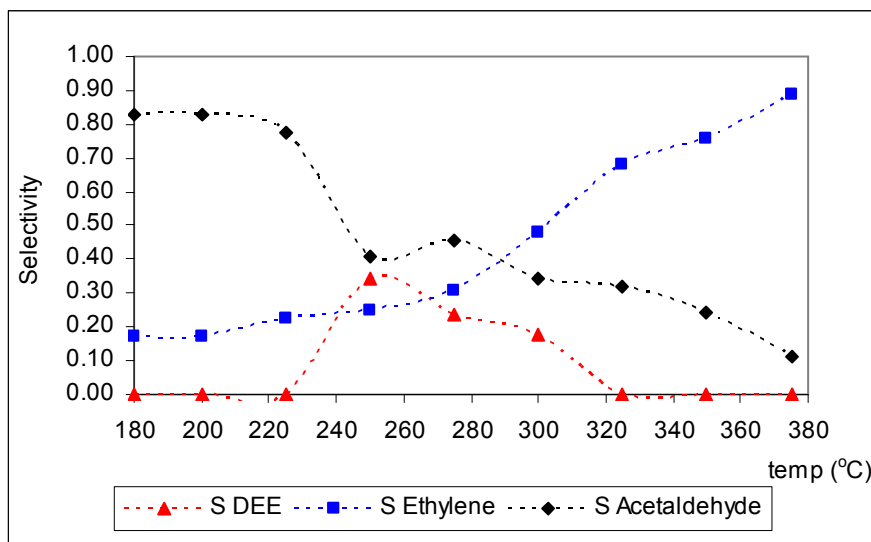


Figure 11.11 The variation in selectivities of products with 0.2 g of STA62(350) EtOH/(EtOH&He):0.48

Although the selectivity profile shifts to lower temperature by using STA62(350), the maximum DEE selectivity value that could be obtained with this catalyst decreases (Figure 11.12). Numerically, 0.66 is the maximum DEE selectivity which is observed at 300°C for STA62(550) whereas 0.35 is the maximum value which is observed at 250°C for STA62(350).

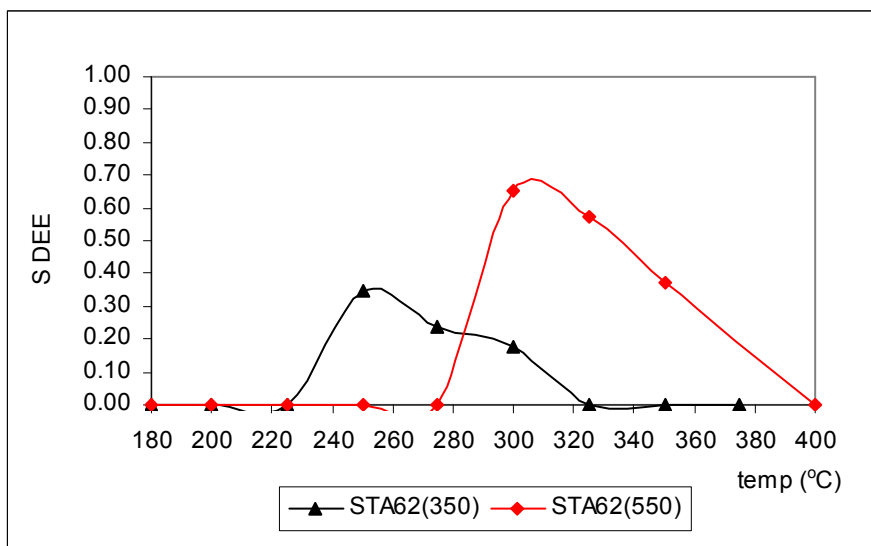


Figure 11.12 The effect of calcination temperature of STA62 on selectivity of DEE, EtOH/(EtOH&He):0.48, catalyst amount: 0.2 g

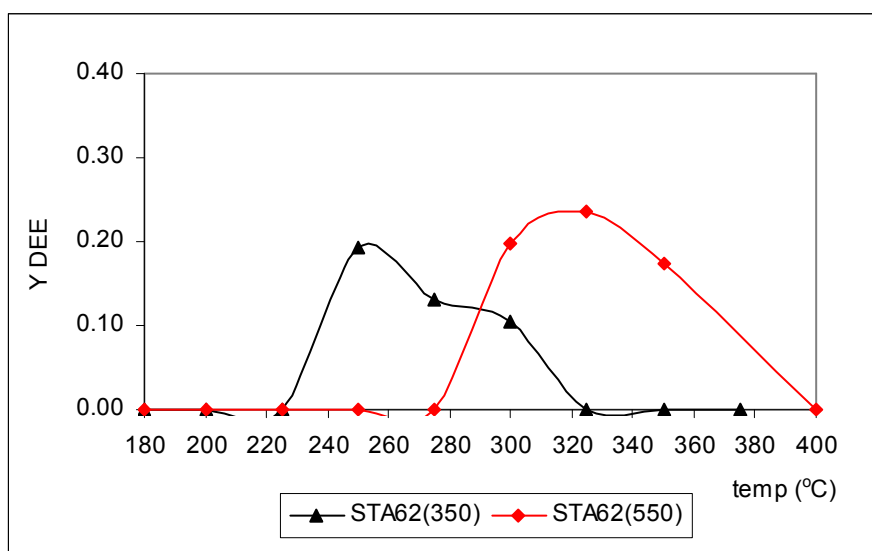


Figure 11.13 The effect of calcination temperature of STA62 on yield of DEE, EtOH/(EtOH&He):0.48, catalyst amount: 0.2 g

The highest DEE yield value did not change so much, indeed it was 0.19 for STA62(350) and 0.24 for STA62(550) (Figure 11.13).

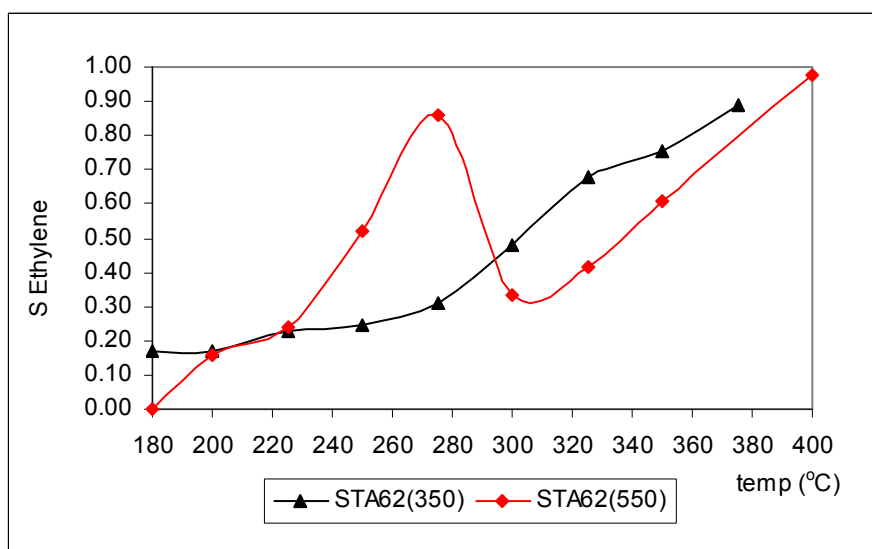


Figure 11.14 The effect of calcination temperature of STA62 on selectivity of Ethylene, EtOH/(EtOH&He):0.48, catalyst amount: 0.2 g

The cavity which is observed in ethylene selectivity profile for STA62(550) is not observed for STA62(350) (Figure 11.14). The selectivity of ethylene increases from 0.17 to 0.89 with an increase in reaction temperature from 180

to 375°C. Decreasing the calcination temperature applied during the synthesis procedure has an improving effect on the production of ethylene. Obtaining an ethylene yield of 0.72 (Figure 11.15) at 375°C with STA62(550) is a promising result for this novel catalyst, in industrial point of view.

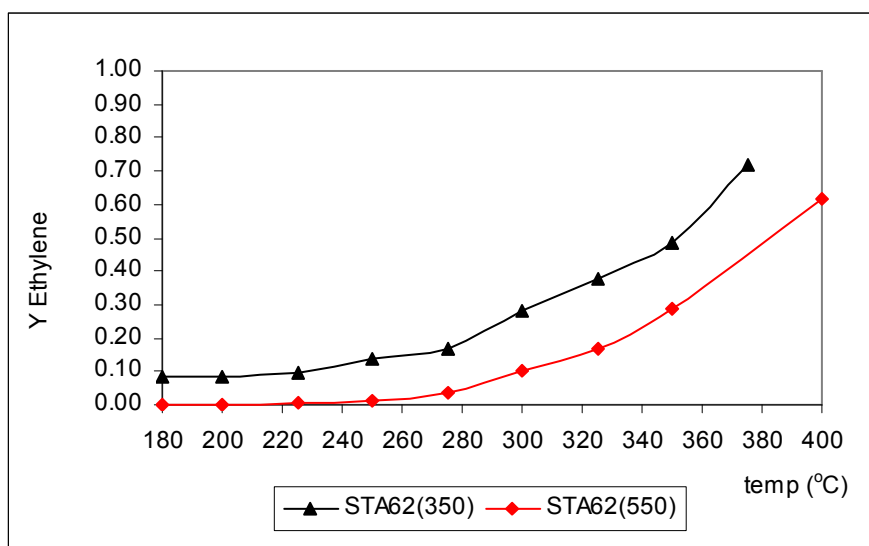


Figure 11.15 The effect of calcination temperature of STA62 on yield of Ethylene, EtOH/(EtOH&He):0.48, catalyst amount 0.2 g

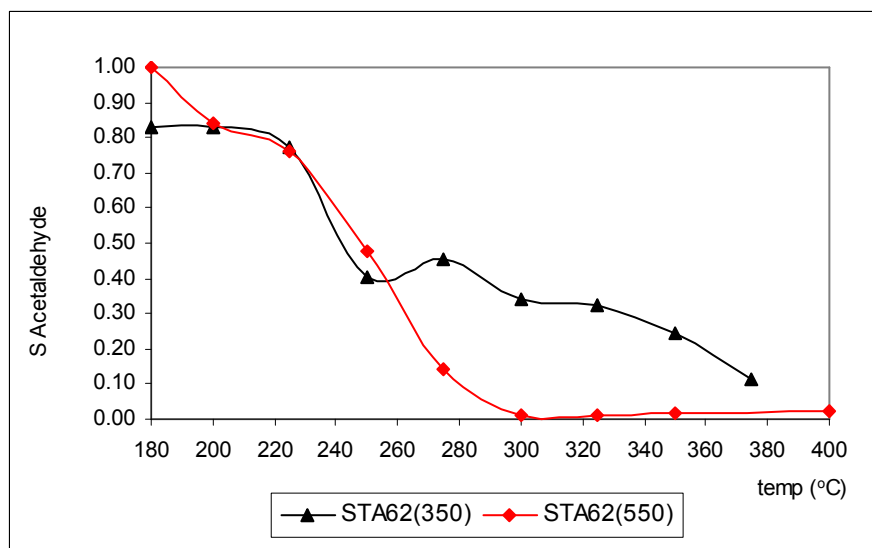


Figure 11.16 The effect of calcinations temperature of STA62 on selectivity of Acetaldehyde, EtOH/(EtOH&He):0.48

Acetaldehyde is observed at low temperatures for both catalyst at the same reaction conditions (Figure 11.16). Since the catalytic activity is so low for STA62(550) at temperatures lower than 275°C, the obtained yield for acetaldehyde is very low. On the contrary, due to higher activity of STA62(350) even at low temperature, like 180°C, high acetaldehyde yields are obtained such as it is 0.40 at 180°C. Moreover, the selectivity of acetaldehyde drops to negligible amount at 300°C when STA62(550) is used in the reaction medium. On the other hand STA62(350) provides the formation of acetaldehyde with a yield value of 0.20 and 0.09 at 300 and 375°C, respectively (Figure 11.17).

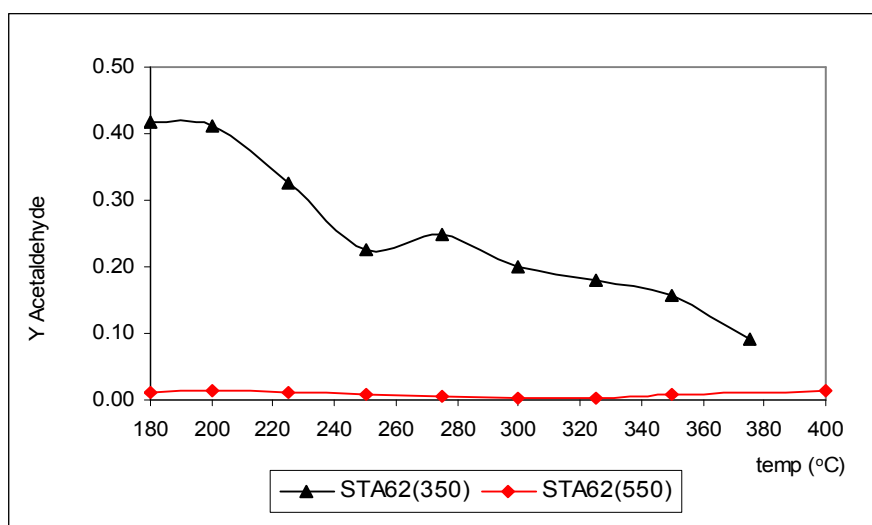


Figure 11.17 The effect of calcinations temperature of STA62 on yield of Acetaldehyde, EtOH/(EtOH&He):0.48

11.3 Results obtained with STA72

In order to carry out ethanol dehydration reaction over STA72(550), a feed mixture of ethanol and helium was prepared with a total flow rate of 44.24 ml/min keeping the molar ratio of ethanol in the feed at 0.48. The reaction temperature was changed from 180 to 350°C and 0.1 of STA72(550) was seen.

Results showed that very low conversion of ethanol was obtained with this catalyst (Figure 11.18). Note that this catalyst was prepared following a basic route using sodium silicate as the Si source. This synthesis route did not produce active catalysts with high acidity for ethanol dehydration reaction.

Figure 11.19 indicated that some ethylene and acetaldehyde were formed but DEE did not form using this catalyst.

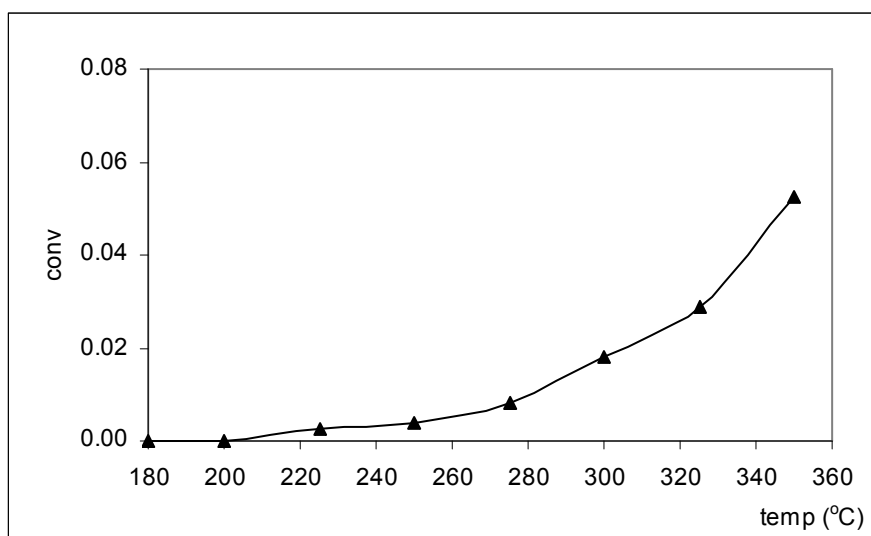


Figure 11.18 The conversion profile of ethanol over 0.1 g of STA72(550) EtOH/(EtOH&He):0.48

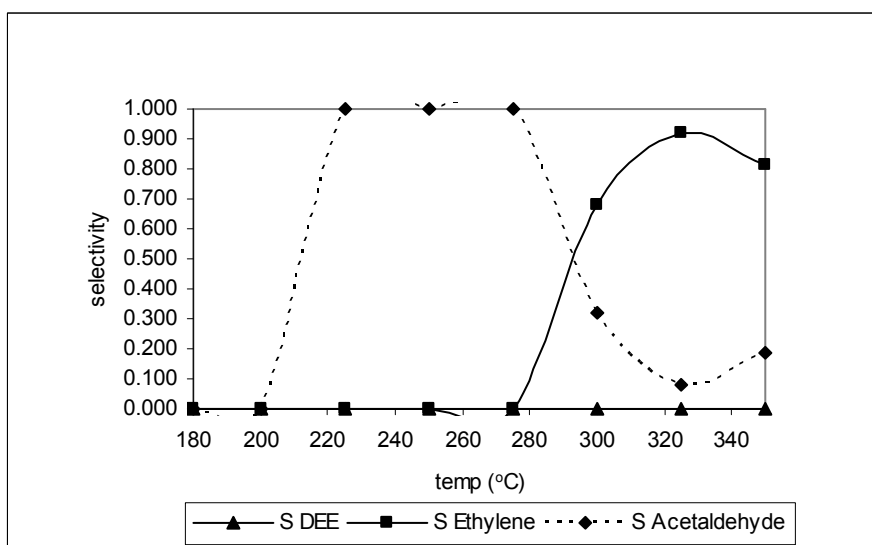


Figure 11.19 The selectivity profile of products over 0.1 g of STA72(550) EtOH/(EtOH&He):0.48

11.4 Results obtained with STA82

Another novel silicotungstic acid catalyst prepared by direct hydrothermal synthesis is STA82. While preparing this catalyst, parameters, such as washing step and calcination temperature are changed.

STA82(550) is prepared following the procedure given in Chapter 8. As indicated in the notation, the calcination temperature was first set to 550°C. This novel catalyst has a BET surface area of 156 m²/g. BJH adsorption cumulative surface area of pores, volume of pore are found as 209 m²/g and 0.307 m³/g, respectively. BJH adsorption average pore diameter is 58.53 Å. In order to carry out ethanol dehydration reaction over STA82(550), a feed mixture of ethanol and helium was prepared in a total flow rate of 44.24 ml/min keeping the molar ratio of ethanol in the feed at 0.48. The reaction temperature was changed from 180 to 375°C to see the effects of reaction temperature. Experiments were repeated with 0.1 and 0.2 g of STA82(550) to see the effect of space time.

11.4.1 The effect of Reaction Temperature

As in the case of STA62(550), very low conversion values, i.e. 0.03, was obtained with 0.2 g of STA82(550) upto a reaction temperature of 275°C. Further increase in reaction temperature caused an increase in conversion of ethanol reaching to 0.63 at 375°C (Figure 11.20).

When the product stream is analyzed, it is seen that ethanol is converted to DEE, ethylene, acetaldehyde and water over STA82(550) at the give reaction conditions (Figure 11.21). DEE formation takes place in a temperature range of 275-350°C with a highest yield of 0.17 (Figure 11.22). Acetaldehyde is produced in the reaction medium at temperatures lower than 300°C but its yield is in the magnitude of 0.01 (Figure 11.22). Ethylene formation is observed between 180 and 375°C. When the reaction temperature is 350°C the yield of ethylene reaches to 0.50, and it becomes 0.63 at 375°C.

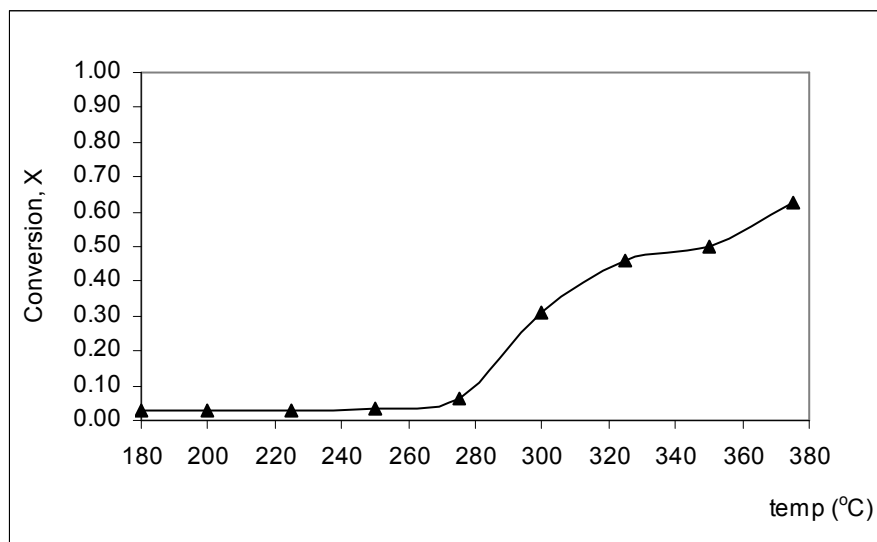


Figure 11.20 The variation of conversion over 0.2 g STA82(550) EtOH/(EtOH&He):0.48

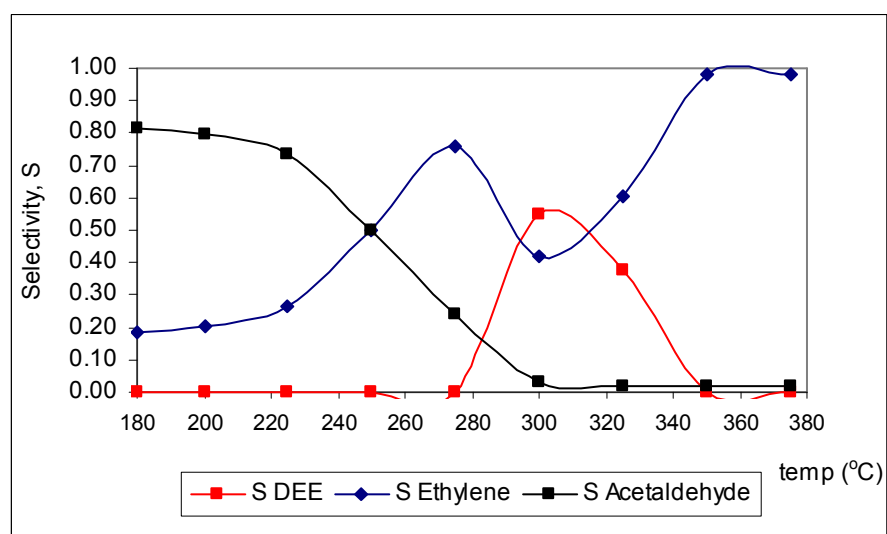


Figure 11.21 The variation in selectivities of products over 0.2 g STA82(550) EtOH/(EtOH&He):0.48

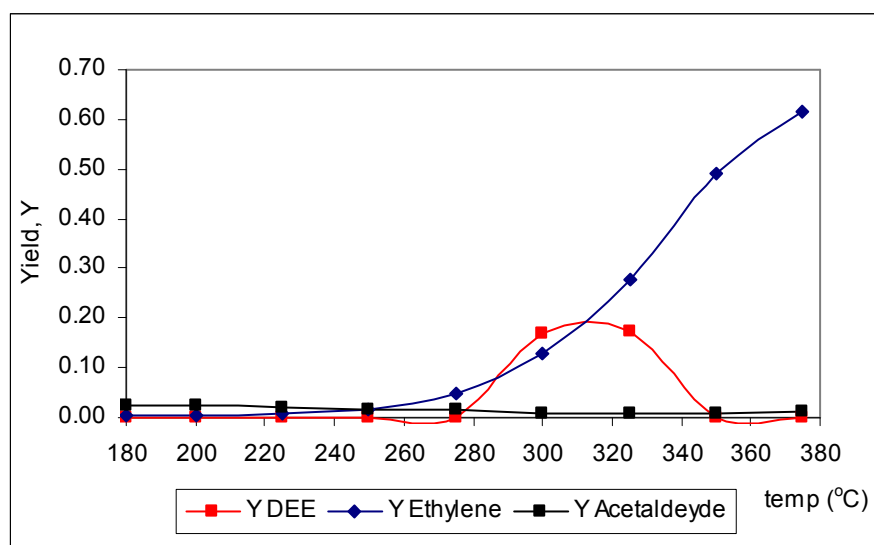


Figure 11.22 The variation in yields of products over 0.2 g STA82(550) EtOH/(EtOH&He):0.48

The selectivity and yield profiles for STA82(550) resembles that of STA62(550). The idea proposed for the reaction mechanism investigating the experimental results of 0.2 g of STA62(550) is supported by the experimental results of 0.2 g of STA82(550). In that proposal it is said that a possible series reaction between acetaldehyde and DEE may occur, formation of DEE and ethylene from ethanol may occur in parallel paths, especially at lower temperatures. However, over 300°C decomposition of DEE to ethylene may cause the maximum in DEE selectivity.

11.4.2 The effect of Calcination Temperature

Calcination step of the direct hydrothermal synthesis procedure is important step to remove the template from the structure. However, it is important to prevent the structure of the molecule during the calcination. For this reason, decision of calcination temperature is important and should be done considering the TGA and DSC results of uncalcined sample.

In Figure 11.23, the variation in catalytic activity of STA82 due to difference in calcination temperature is clearly seen. For a feed containing ethanol in molar ratio of 0.48, the conversion of ethanol is 0.93 at 375°C with 0.2 gram of STA 82, using a catalyst calcined at 350°C. However this value decreases to 0.63 when calcination temperature of STA82 is 550°C. A maximum

in DEE selectivity is observed at 200°C at the same experimental conditions for STA82 calcined at 350°C, this maxima shifts to higher temperature, namely 300°C, when the calcination temperature of the sample is increased to 550°C (Figure 11.24).

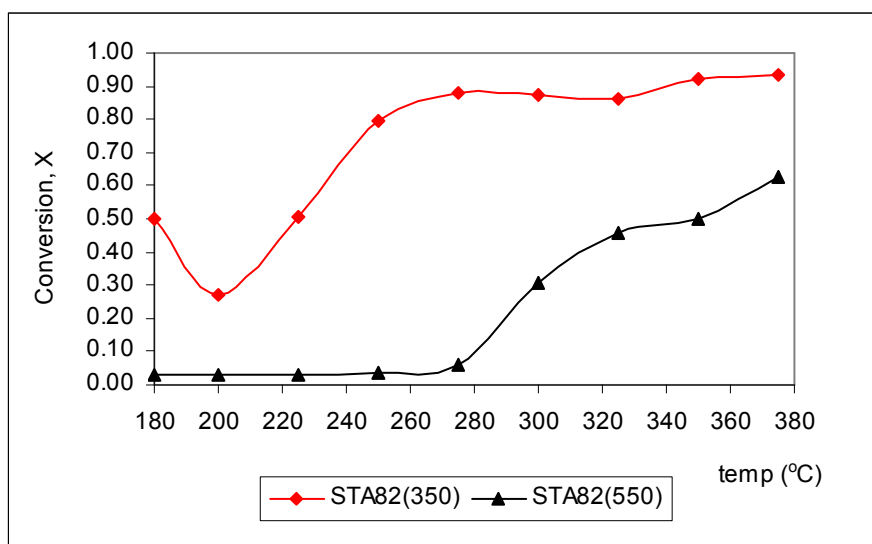


Figure 11.23 The effect of calcination temperature on ethanol conversion, 0.2g of STA82 calcined at 350 & 550°C

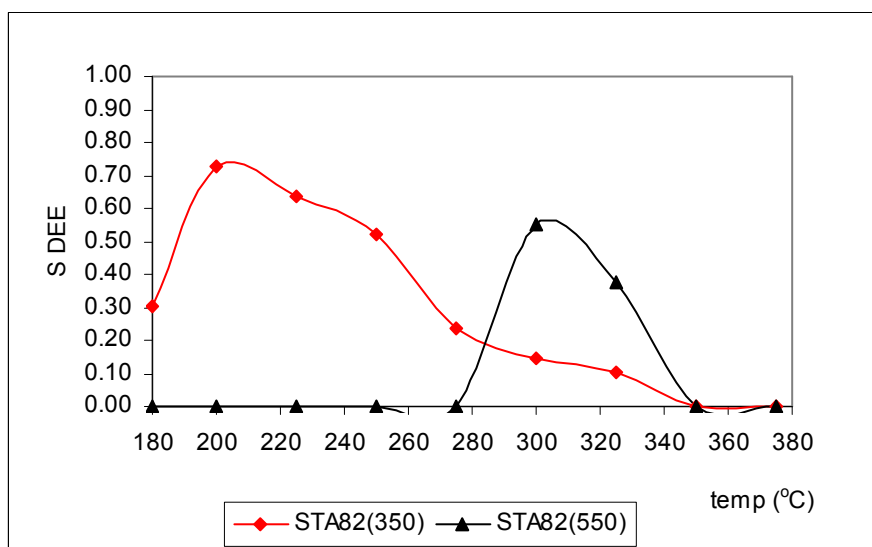


Figure 11.24 The effect of calcinations temperature on DEE selectivity, 0.2g of STA82, calcined at 350 & 550°C

When the calcination temperature is 550°C, DEE formation takes place in a temperature range from 275 to 350°C. This interval becomes larger and extended from 180 to 350°C due to decrease in calcination temperature (Figure 11.24). All these results also indicate decomposition of DEE to ethylene at higher temperatures.

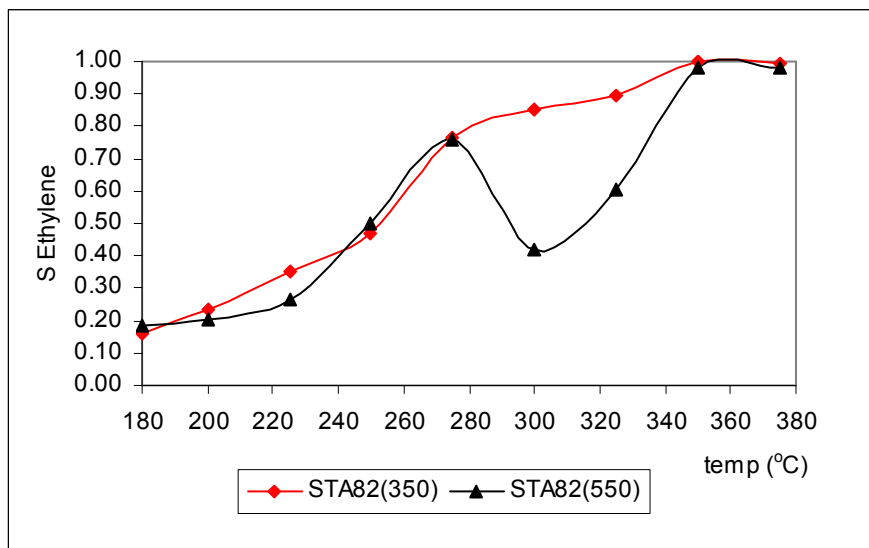


Figure 11.25 The effect of calcination temperature on Ethylene selectivity, 0.2g of STA82, calcined at 350 & 550°C

As seen in Figure 11.25, the same trend is observed in ethylene selectivity up to 275°C for STA calcined at 350 and 550°C. After that temperature value, ethylene formation continues to increase with an increase in temperature for STA82 calcined at 350°C. In the case of STA calcined at 550°C, due to formation of DEE during the reaction (Figure 11.24), ethylene selectivity shows a minimum at 300°C and then starts to increase again. Finally, for both samples, 99 % ethylene selectivity is obtained at 350°C, which is very high and promising to produce petrochemicals from bio-ethanol. As shown in Figure 11.28, an ethylene yield value approaching 0.9 was obtained over 350°C.

The acetaldehyde formation is much observable for STA82(550) than STA82(350) (Figure 11.26) however its yield is very low (Figure 11.29).

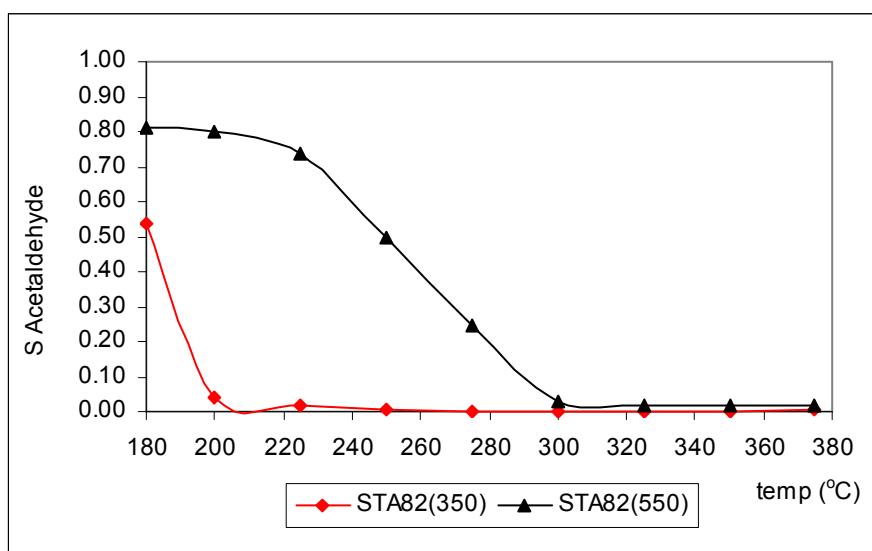


Figure 11.26 The effect of calcination temperature on acetaldehyde selectivity, 0.2g of STA82, calcined at 350 & 550°C

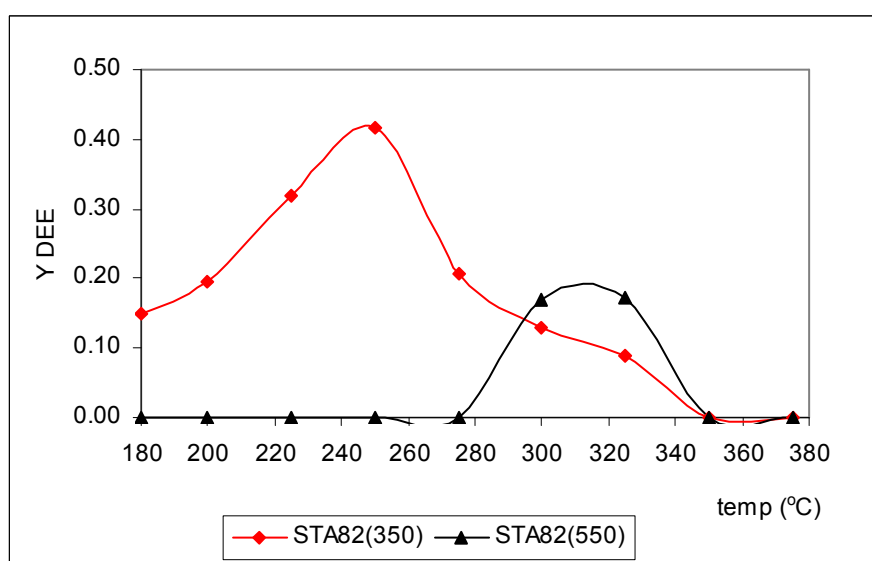


Figure 11.27 The effect of calcination temperature on DEE yield, 0.2g of STA82, calcined at 350 & 550°C

The maximum DEE yield obtained with STA 82 calcined at 550°C is around 0.20, this value is increased to 0.40 by decreasing the calcination temperature of STA82 (Figure 11.27) to 350°C.

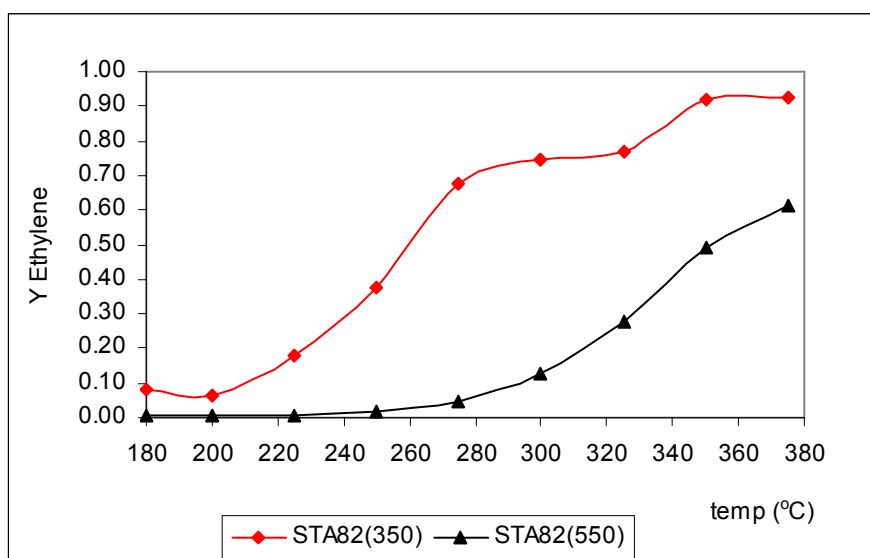


Figure 11.28 The effect of calcination temperature on Ethylene yield, 0.2g of STA82, calcined at 350 & 550°C

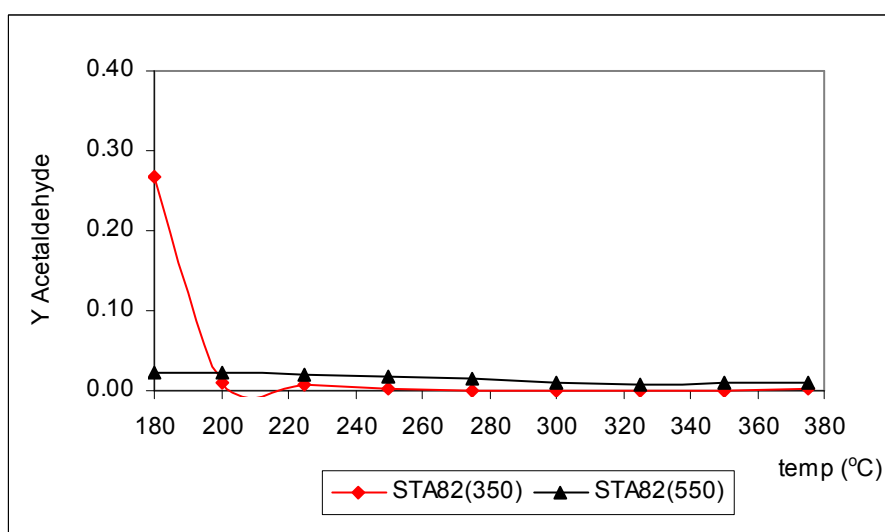


Figure 11.29 The effect of calcination temperature on Ethylene yield, 0.2g of STA82, calcined at 350 & 550°C

Calcination temperature is an important parameter for catalyst preparation. As given in Figure 11.28 very high ethylene yield which is 0.75 at 275°C, 0.92 at 350°C, is obtained for STA82 calcined at 350°C.

11.4.3 The effect of Washing Step of Catalyst Synthesis using Different Solvents

In the washing step of the synthesis procedure, generally dionize water is used for removal of template. For sample STA81, besides dionize water, HCl-EtOH mixture and H_3PO_4 solution were also used as solvent in the washing procedure. Also, instead of washing, part of the sample is treated with supercritical CO_2 in an extraction unit. After the calcination at 350°C in a tubular furnace, 0.2 gram of each catalyst is used in ethanol dehydration reaction with an ethanol-helium stream containing 48% ethanol.

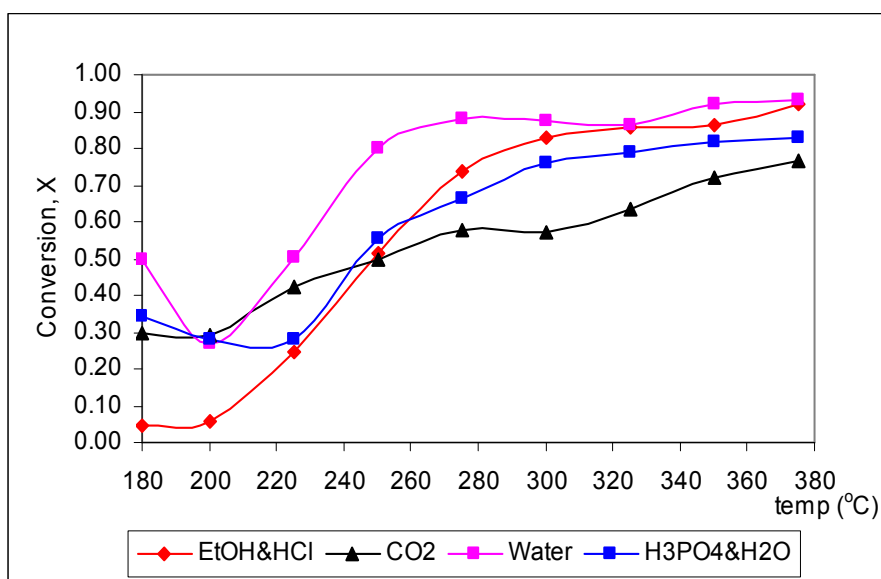


Figure 11.30 The effect of washing step on ethanol conversion with 0.2g of STA81 treated

In Figure 11.30, the variation in ethanol conversion with STA81 treated with different solvents are presented. As shown in this figure, the general trend of temperature dependence of conversion using the catalyst treated with different solvents is similar. However, the sample washed with water showed the highest activity.

In Figure 11.31 and 11.32, temperature dependence of DEE and ethylene selectivities are presented for the catalysts treated with different solvents. Ethylene selectivity values are quite close to each other for each treatment procedure. Some differences were observed in DEE selectivities. The catalyst

washed with water showed highest DEE selectivity at low temperatures (Figure **11.31**). In the case of acetaldehyde selectivities, H₃PO₄ treated sample showed the highest selectivity at temperatures lower than 220°C (Figure **11.33**).

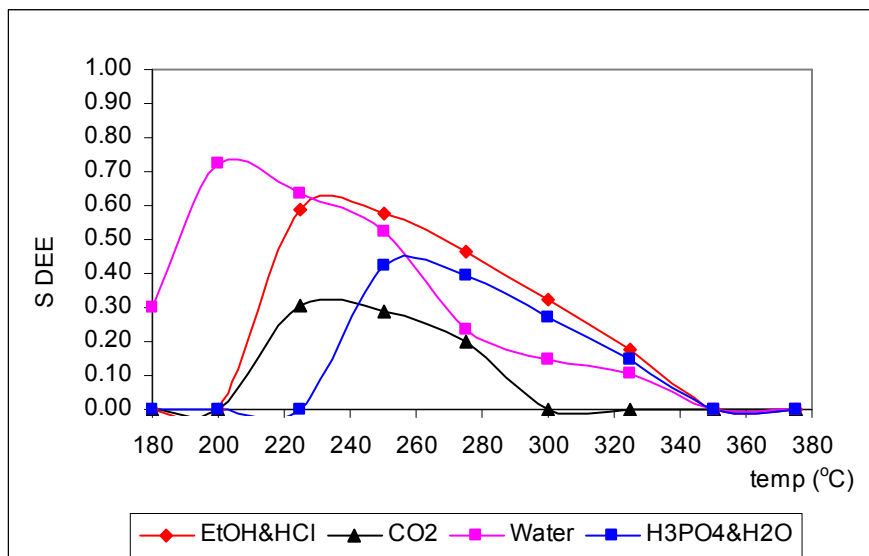


Figure **11.31** The effect of washing step on DEE selectivity with 0.2g of STA81 treated

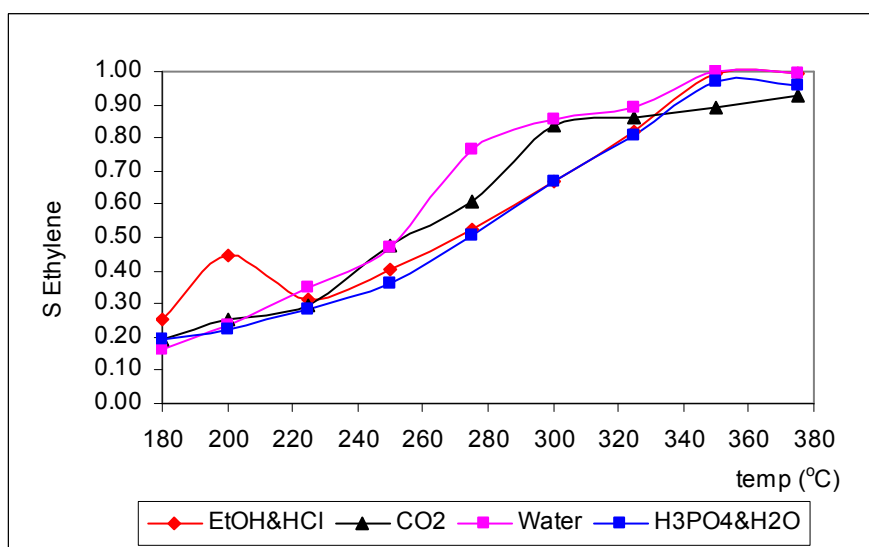


Figure **11.32** The effect of washing step on Ethylene selectivity with 0.2g of STA81 treated

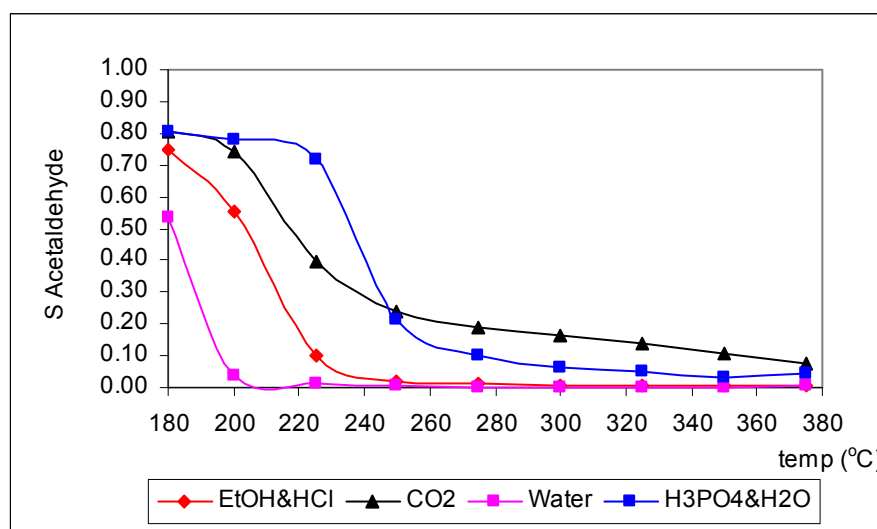


Figure 11.33 The effect of washing step on Acetaldehyde selectivity with 0.2g of STA81 treated

The maxima observed in DEE yield occurs at a lower temperature for the catalyst prepared by using water in the washing step (Figure 11.34).

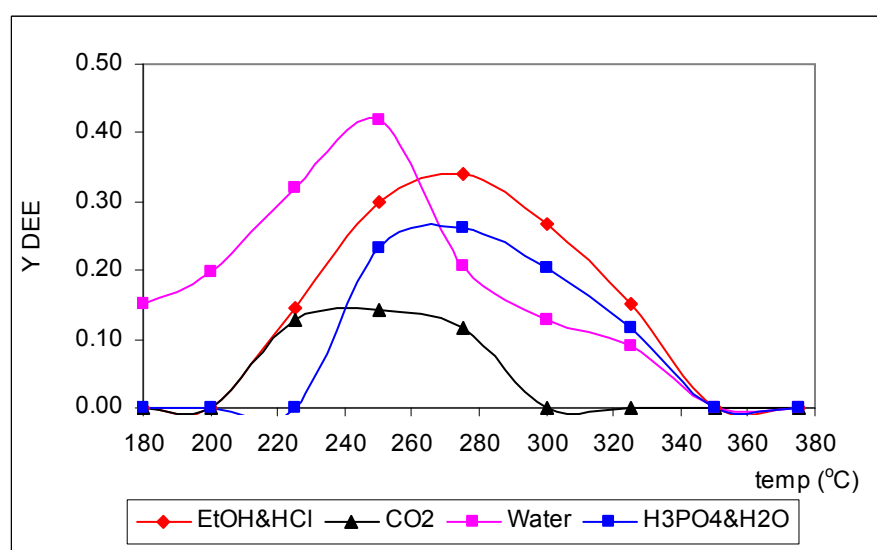


Figure 11.34 The effect of washing step on DEE yield with 0.2g of STA81 treated

Higher ethylene and DEE yields are obtained with STA81 catalysts washed with water (Figures 11.34 and Figure 11.35). Acetaldehyde yields are quite low for catalysts washed by HCl and H_3PO_4 . It was concluded that washing with

deionized water gave the best results among the other washing steps as far as overall conversion, DEE and ethylene yields were concerned.

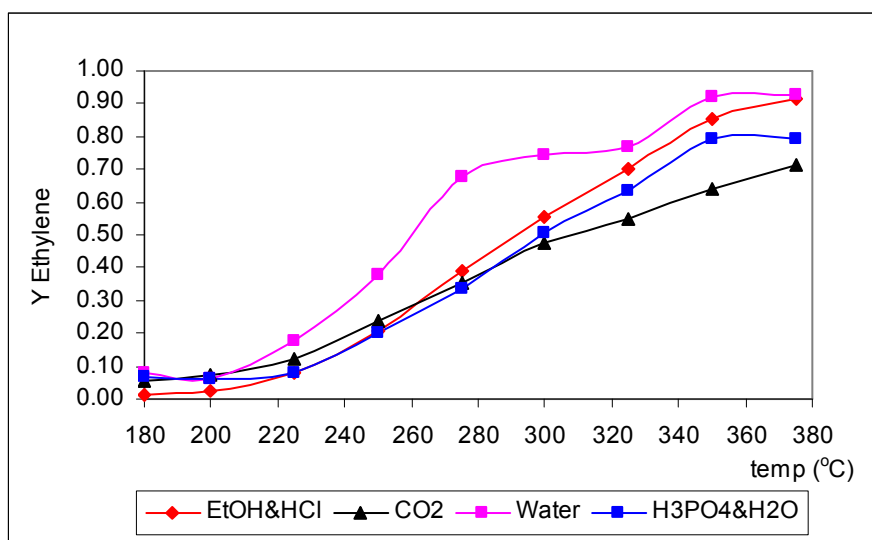


Figure 11.35 The effect of washing step on Ethylene yield with 0.2g of STA81 treated

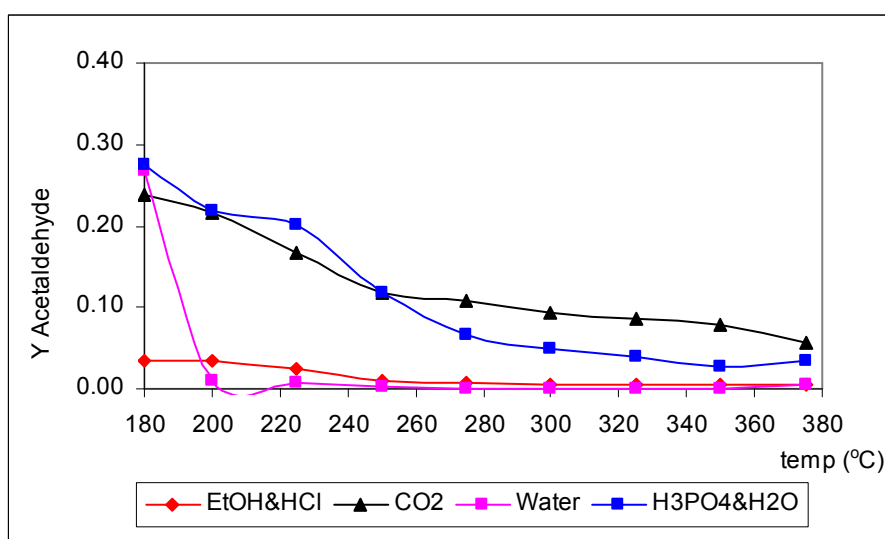


Figure 11.36 The effect of washing step on Acetaldehyde yield with 0.2g of STA81 treated

In this part, finally the result obtained for the novel catalyst that was treated both washing and supercritical extracted. 0.1 g of this catalyst was used and conversion values reaching to 0.90 was achieved (Figure 11.37). Also

ethylene yields reached to very high values, around 0.90 was obtained (Figure 11.38). These results proved the potential of using supercritical extraction to obtain catalysts with very high activities and ethylene yields, especially at temperatures over 300°C. Within the scope of this work only two samples were prepared by supercritical extraction. As a recommendation for future work supercritical extraction experiments can be carried out at different conditions (pressure, temperature, flow rate, extraction time, etc.) and also using some other supercritical fluids such as ethanol-CO₂, water-CO₂ mixtures etc.

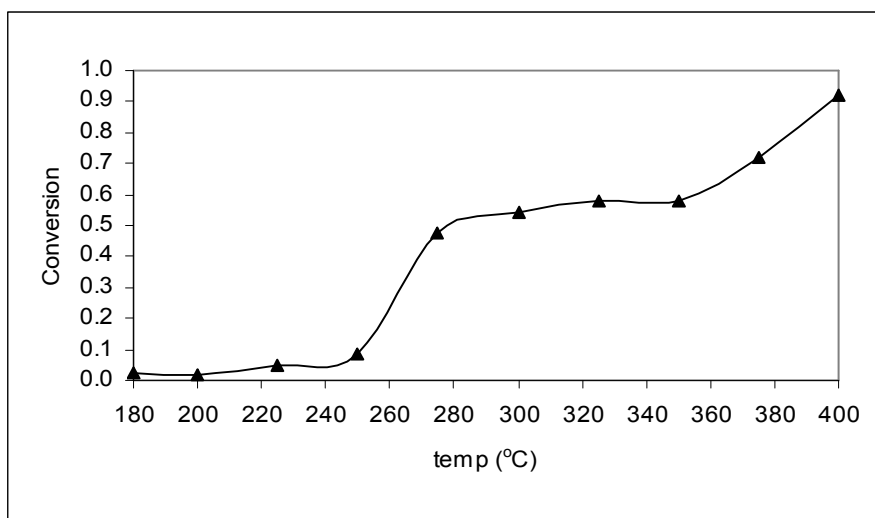


Figure 11.37 The conversion profile for catalyst both washed and extracted with CO₂, 0.1 g of catalyst

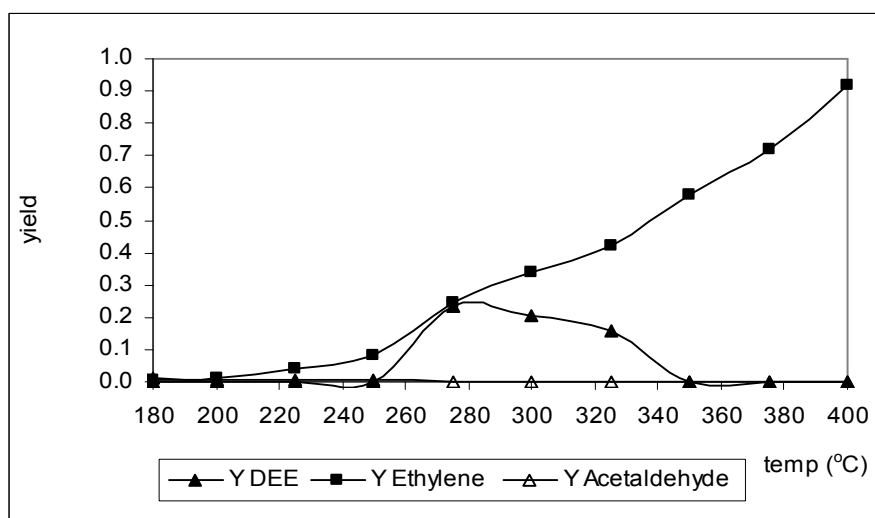


Figure 11.38 The yield of proucts for catalyst both washed and extracted with CO₂, 0.1 g of catalyst

11.5 Results obtained with STA92

STA92 is also a novel silicotungstic acid catalyst which is prepared by direct hydrothermal synthesis method. Its W/Si ratio is higher than STA62, STA72 and STA82. The detail of the preparation procedure is given in Chapter 8. While preparing STA92 catalyst, the temperature applied in the calcination stage was varied according to the result of TGA and DSC characterization tests. Different calcination temperatures were selected as 350°C, 400°C, 475°C and 550°C and the samples calcined at these temperatures were called as STA92(350), STA92(400), STA92(475) and STA92(550), respectively.

In order to investigate the catalytic activities of these catalysts for ethanol dehydration reaction, different experimental sets were prepared. In all sets of experiments, a mixture of ethanol and helium is used as a feed stream with a total flow rate value of 44.24 ml/min. The ratio of ethanol to mixture is adjusted at 48% at room temperature.

Firstly, experiments were carried out to see the effect of reaction zone temperature on the catalytic activity of the catalyst. Reaction was carried out using 0.2 gram of STA92(550) with the given feed conditions, by changing the reaction temperature in the range of 180-400°C. Then, in order to see the effect of space time on reaction results, the amount of STA92(550) is reduced to 0.1 g by keeping other parameters unchanged.

Afterwards, experiments were repeated using 0.2 gram of STA92(350), STA92(400) and STA92(475) with the same feed flow rate, ethanol composition and reaction temperature as in the case of STA92(550). The obtained experimental results provide a comparison of calcination temperature on the properties of catalyst.

11.5.1 The effect of Reaction Temperature

As in the experimental results obtained from STA62(550) and STA82(550) catalysts, ethanol conversion is very low in temperature range of 180-275°C (Figure 11.39).

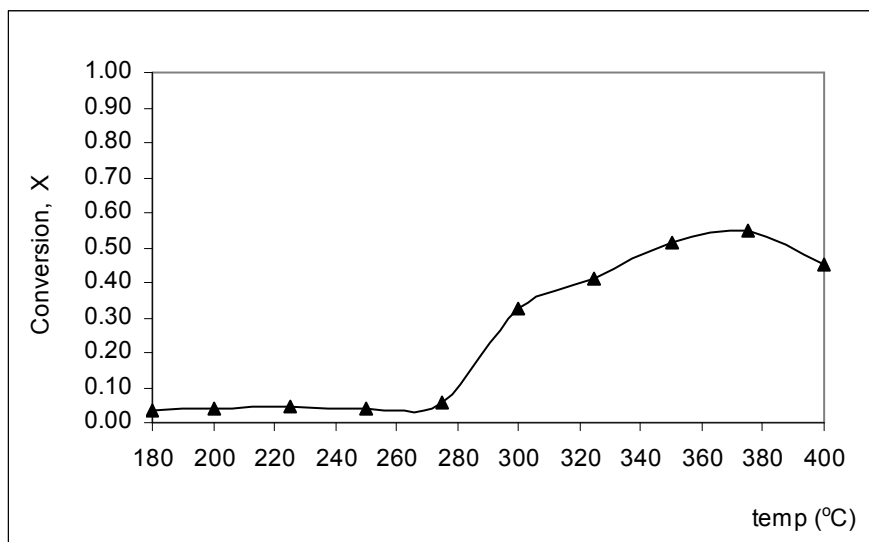


Figure 11.39 The variation in ethanol conversion with 0.2 g of STA92(550), EtOH/(EtOH&He):0.48

Pure ethanol is mainly converted to DEE, ethylene, acetaldehyde and water over STA92(550) at the given experimental conditions, based on the product distribution data obtained by the online analysis of product effluent stream. The selectivities of DEE, ethylene and acetaldehyde are calculated at different reaction temperatures and compared with each other in Figure 11.40.

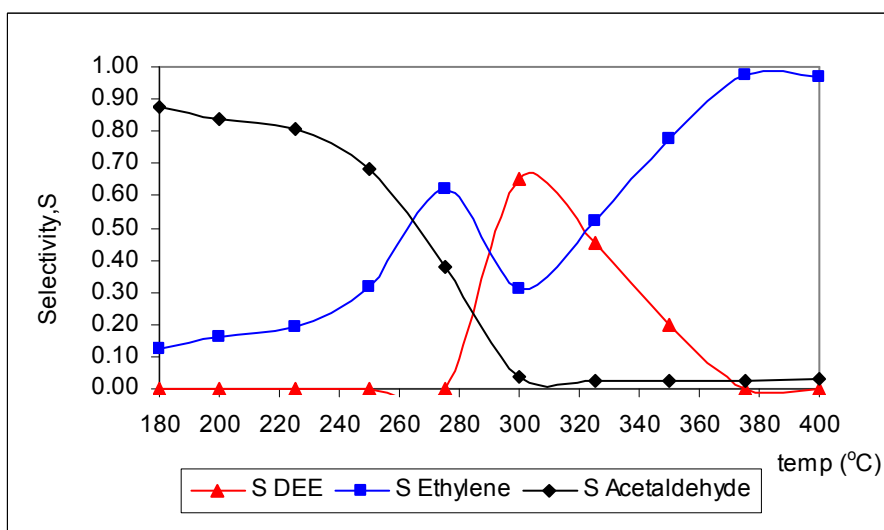


Figure 11.40 The variation in product selectivities with 0.2 g of STA92(550), EtOH/(EtOH&He):0.48

Acetaldehyde shows high selectivity at low temperatures (Figure 11.40). However, due to low conversion of ethanol at these temperatures, the obtained yield of acetaldehyde is quite low, just around 0.03 (Figure 11.41).

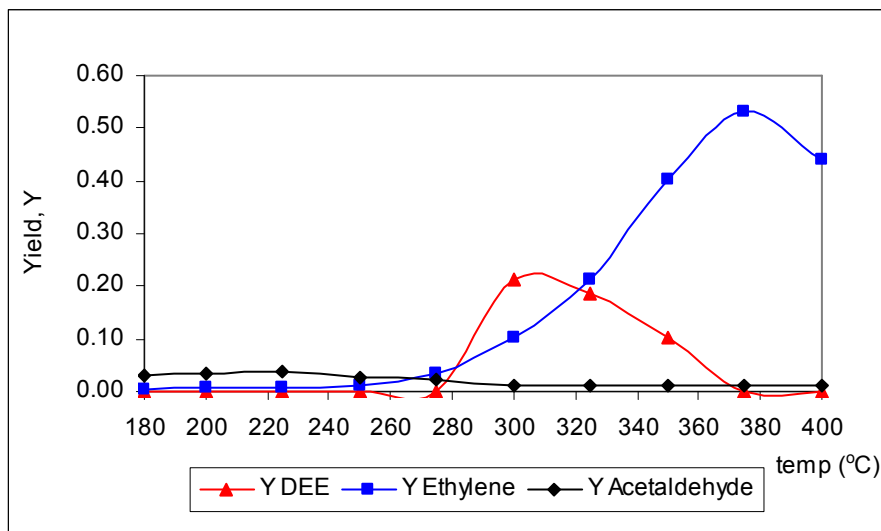


Figure 11.41 The variation in product yield with 0.2 g of STA92(550), EtOH/(EtOH&He):0.48

DEE formation was observed in the temperature interval of 275-375°C, having a maximum point corresponding to 0.65 in the selectivity profile at 300°C (Figure 11.40). 0.21 is the maximum DEE yield which is observed at 300°C in this set of experiment (Figure 11.41).

As seen in Figure 11.41, ethylene is obtained throughout the experiment and its value is increased from 0.04 to 0.53 by increasing the reaction temperature from 275 to 375°C. At this temperature, it becomes the main product of ethanol dehydration reaction over 0.2 g of STA92(550). The decrease of ethylene yield over 380°C may be due to catalyst deactivation by coke formation.

11.5.2 The effect of Space Time

In order to see the effect of space time on ethanol conversion and product selectivities, experiments are repeated with 0.1 and 0.2 gram of STA92(550) for a feed containing 48 % ethanol in ethanol-helium mixture. The reaction temperature changes from 180 to 400°C in this set of experiments.

As mentioned earlier, this catalyst shows low catalytic activity up to the reaction temperature of 275°C (Figure 11.42). After this temperature ethanol conversion value increases with an increase in temperature. Increasing the catalyst amount have favored the conversion of ethanol into products. As an example, 27 % of ethanol is converted to products at 375°C with 0.1 g STA92. When the catalyst amount is increased to 0.2 g, conversion value is reached to 55% at the same temperature.

The effect of space time on the formation DEE is very remarkable. DEE selectivity is increased from 0.10 to 0.84, which is calculated at 300°C, by increasing the amount of STA92(550) from 0.1 to 0.2 g (Figure 11.43). In the other words, DEE yield is increased from zero level to 0.20 with increasing space time (Figure 11.46).

Ethylene selectivity profile shows a different pattern (Figure 11.44). When higher amount of catalyst is used, ethylene formation is observed at low temperatures (< 225°C). But, after this temperature higher selectivities obtained at low space space time. However, when the yield of ethylene is considered, the space time should be higher (Figure 11.47).

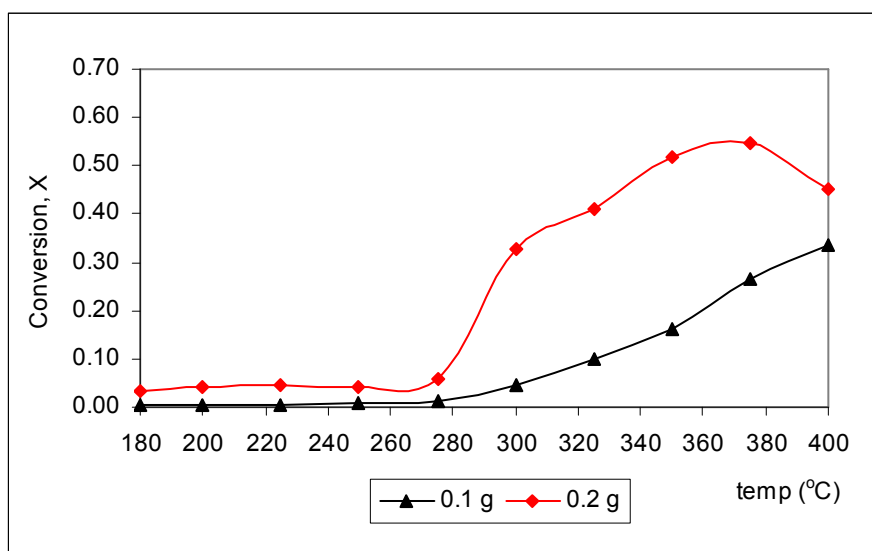


Figure 11.42 The variation in ethanol conversion with amount of STA92(550), EtOH/(EtOH&He):0.48

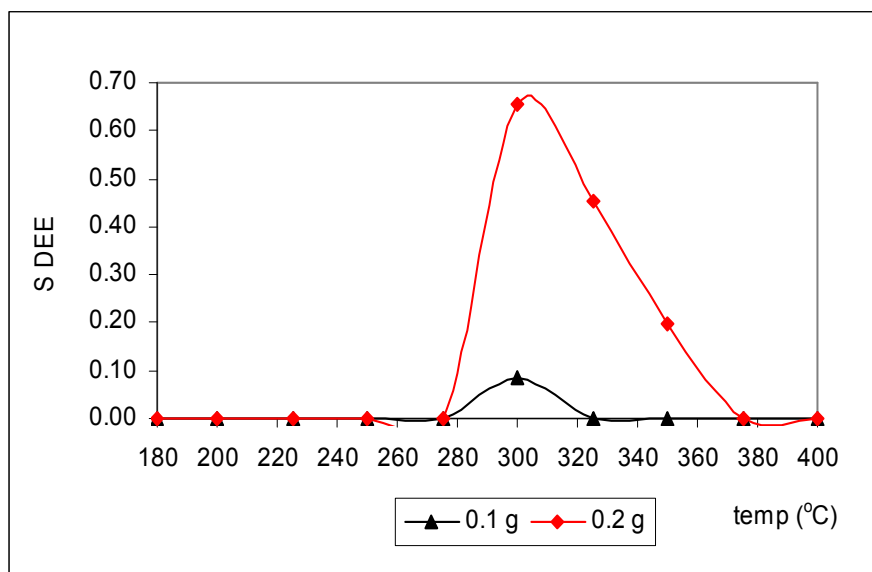


Figure 11.43 The variation in DEE selectivity with amount of STA92(550), EtOH/(EtOH&He):0.48

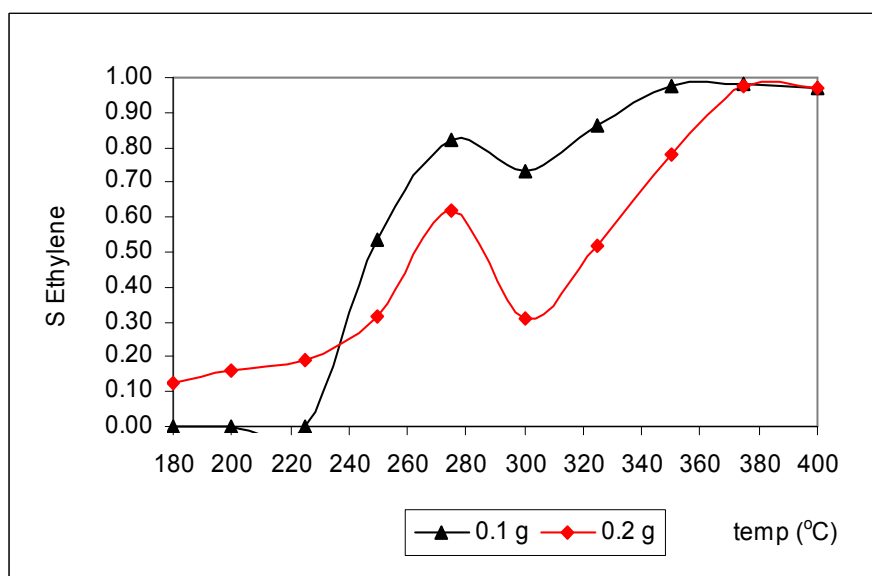


Figure 11.44 The variation in Ethylene selectivity with amount of STA92(550), EtOH/(EtOH&He):0.48

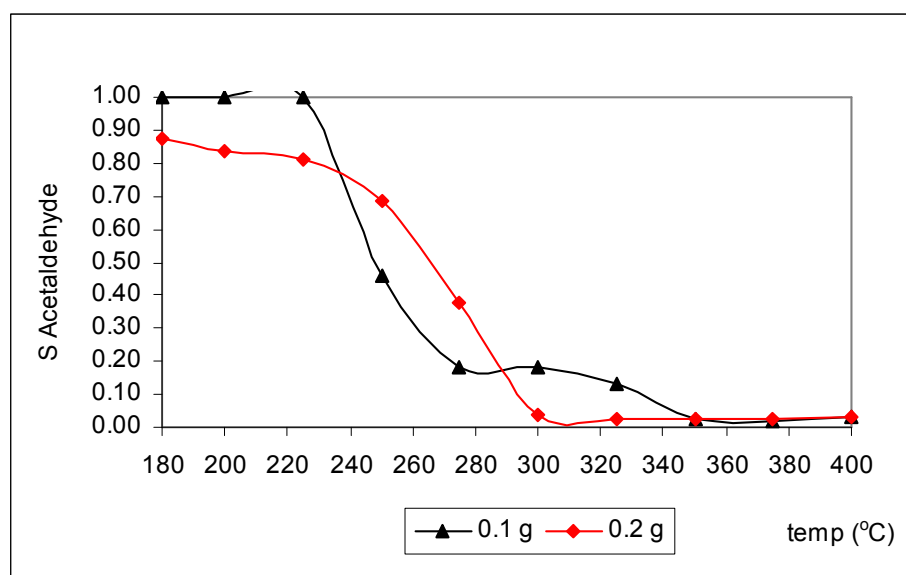


Figure 11.45 The variation in Acetaldehyde selectivity with amount of STA92(550), EtOH/(EtOH&He):0.48

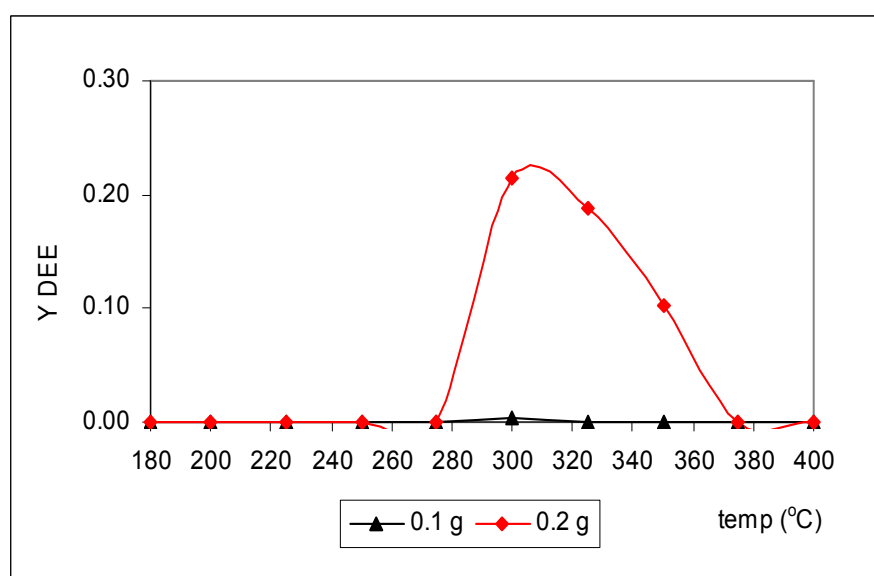


Figure 11.46 The variation in DEE yield with amount of STA92, EtOH/(EtOH&He):0.48

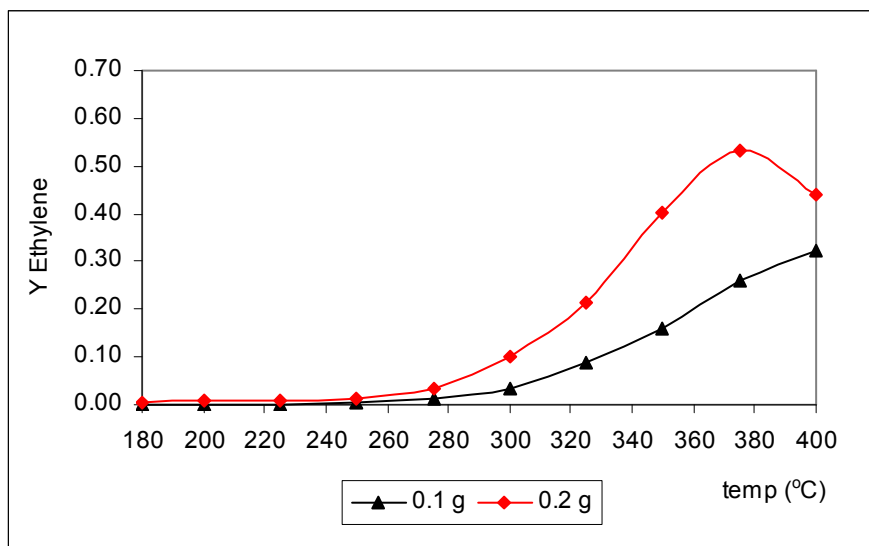


Figure 11.47 The variation in Ethylene yield with amount of STA92, EtOH/(EtOH&He):0.48

11.5.3 The effect of Calcination Temperature

During the calcinations stage applied to STA92, temperature is selected as 350°C, 400°C, 475°C and 550°C considering the TGA and DSC results.

Results obtained with STA92 whose degradation temperature is 414°C is a very good example of this situation. In these experiments, uncalcined STA92 samples are treated in tubular furnace at 475 and 550°C with dry air and ethanol conversion values are followed (Figure 11.48). As shown in this figure the catalysts calcined at 350°C and 400°C have much higher activities than the catalysts calcined at higher temperatures. TGA, DSC, DTA and NMR results discussed in previous section had already indicated that at higher temperatures the catalyst decomposed losing some of its protons.

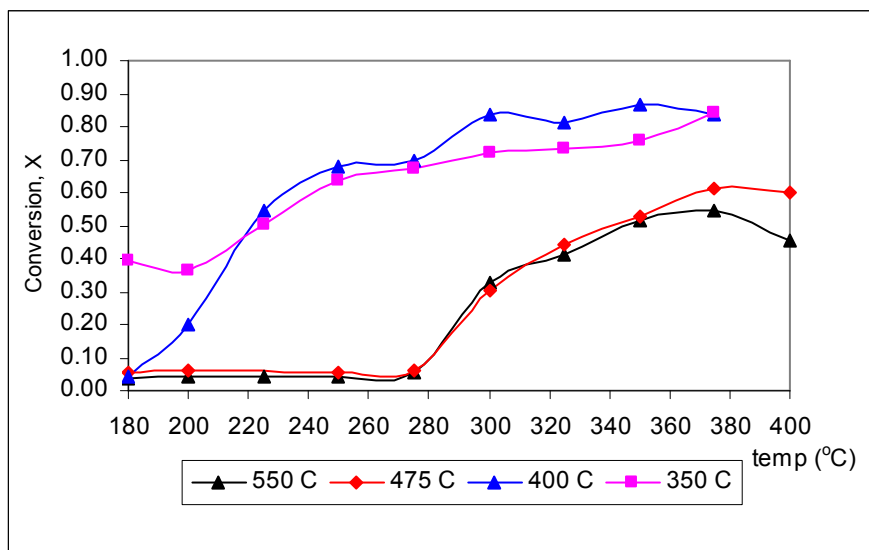


Figure 11.48 The variation in ethanol conversion with 0.2g of STA92, calcined at different temperatures

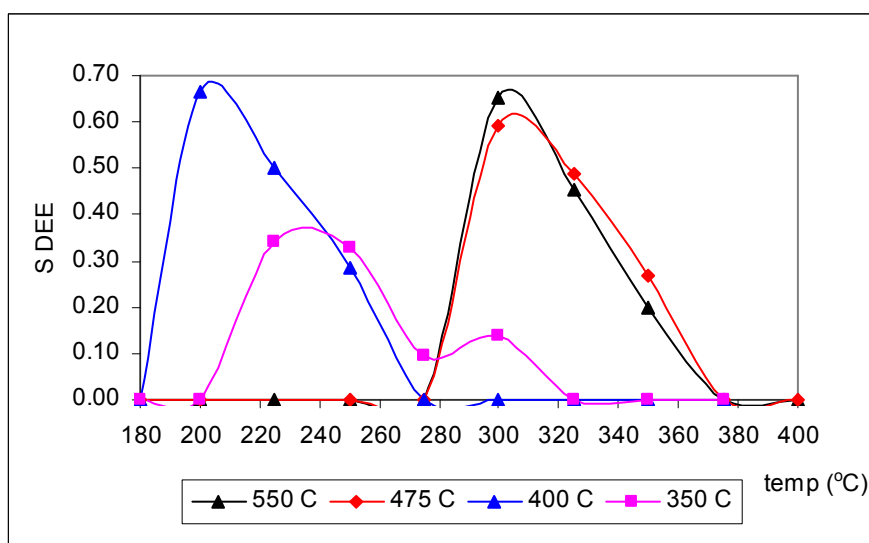


Figure 11.49 The effect of calcination temperature on DEE selectivity with 0.2g of STA92, calcined at different temperatures

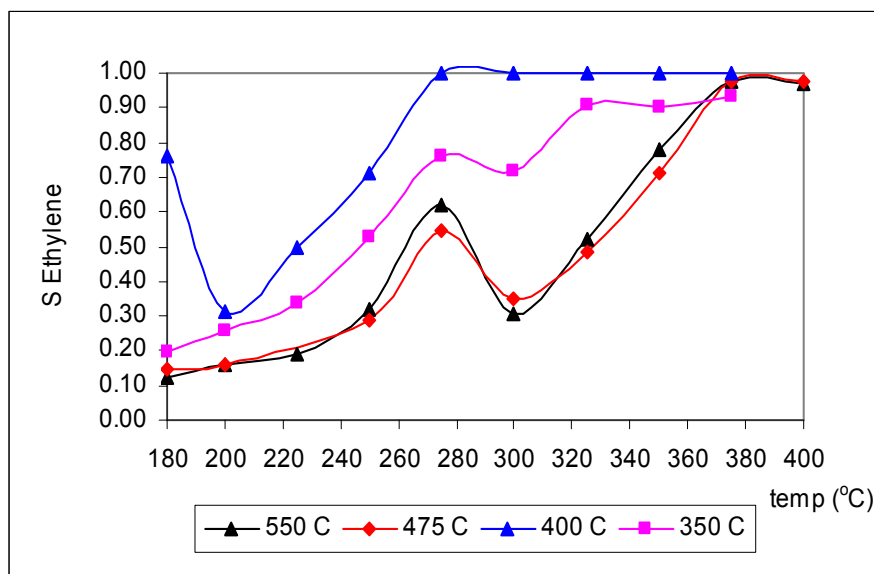


Figure 11.50 The effect of calcination temperature on Ethylene selectivity with 0.2g of STA92, calcined at different temperatures

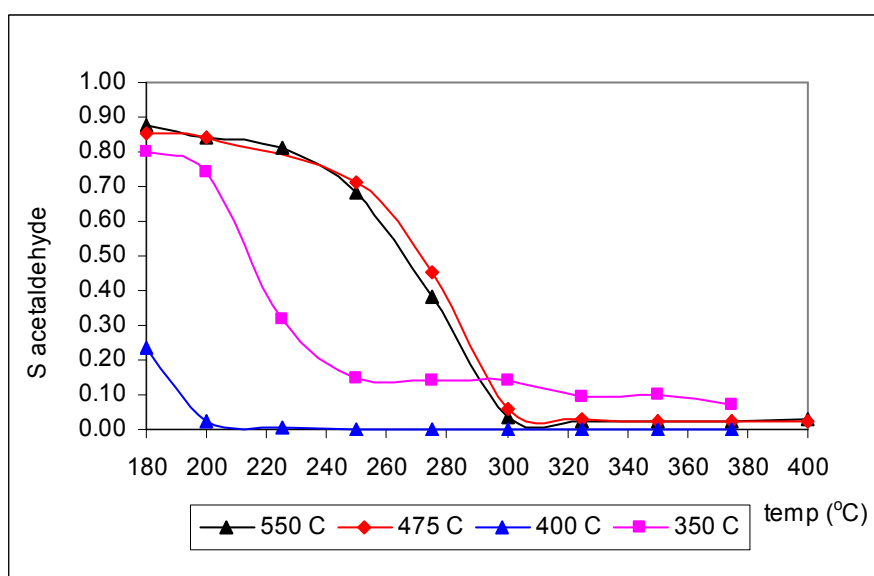


Figure 11.51 The effect of calcination temperature on acetaldehyde selectivity with 0.2g of STA92, calcined at different temperatures

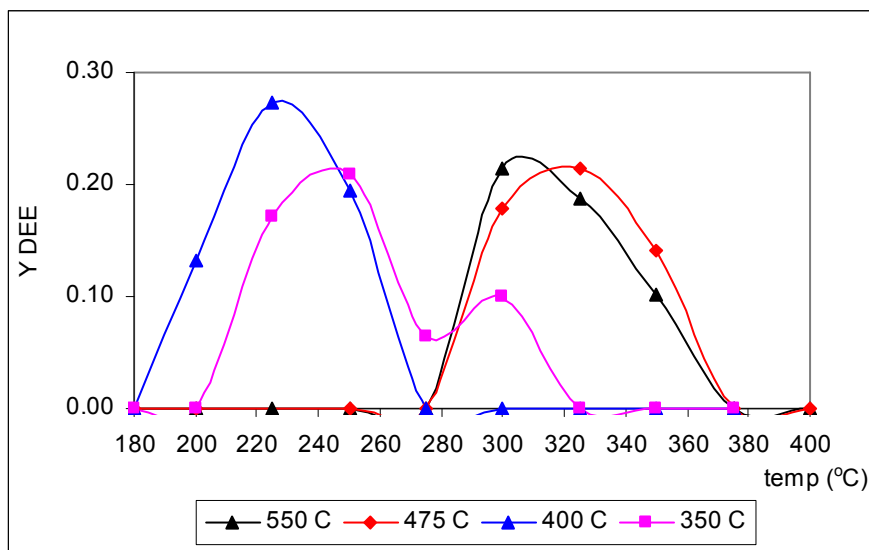


Figure 11.52 The effect of calcination temperature on DEE yield with 0.2g of STA92, calcined at different temperatures

Selectivity value of DEE and Ethylene obtained with STA92 calcined at 350°C, 400°C, 475°C and 550°C are presented in Figure 11.49 and 11.50. The catalysts calcined at lower temperatures gave maximum in DEE selectivities at lower temperatures. This result also showed that calcination at temperatures lower than 400°C gave catalysts having higher acidity and activity.

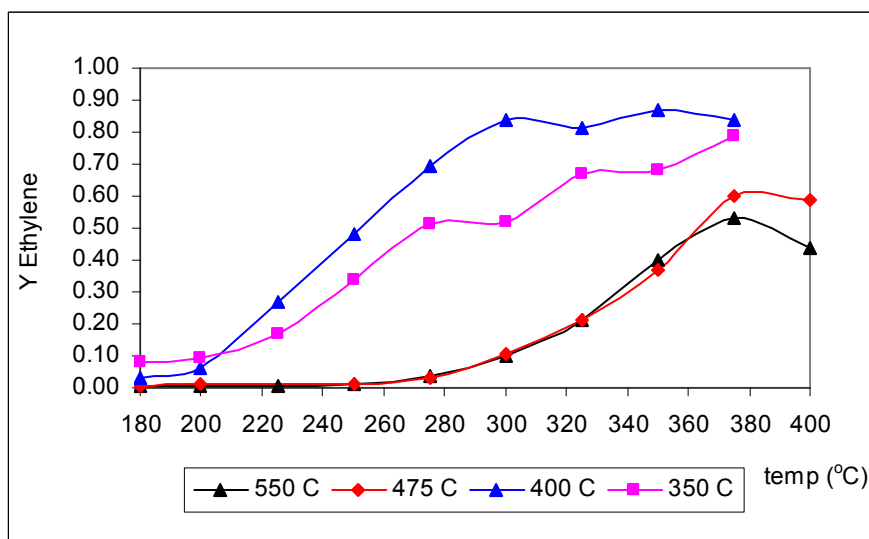


Figure 11.53 The effect of calcination temperature on Ethylene yield with 0.2g of STA92, calcined at different temperatures

In Figures 11.52 and 11.53, the variation in yield of DEE and Ethylene, respectively, is given.

The selectivity and yield change of acetaldehyde at different calcination temperature was discussed in In Figures 11.51 and 11.54. Acetaldehyde is much more produced when the catalyst that are calcined at higher temperatures 475 and 550°C as compared to the one calcined at 350°C. However the catalyst calcined at 350°C gives the highest acetaldehyde yield.

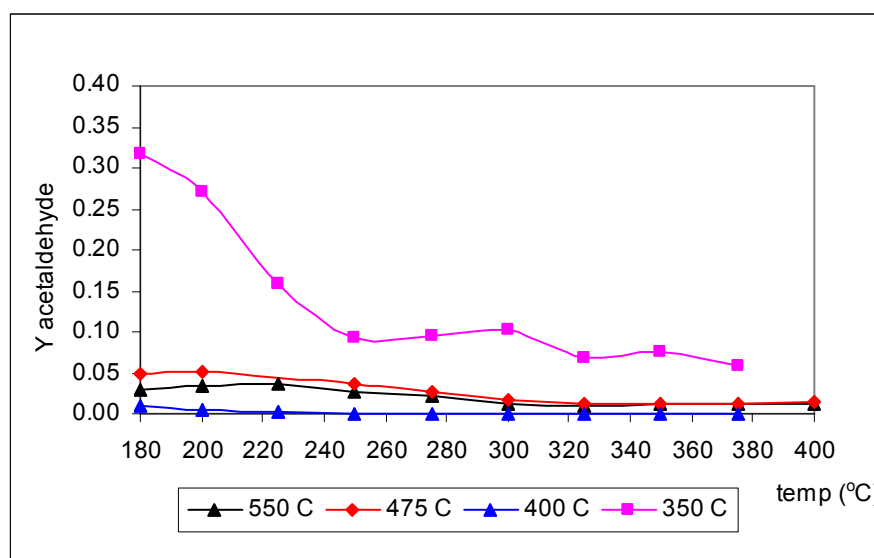


Figure 11.54 The effect of calcination temperature on Ethylene yield with 0.2g of STA92, calcined at different temperatures

11.6 Comparison of these catalysts

Ethanol conversion (Figure 11.55), DEE selectivity (Figure 11.57) and ethylene selectivity (Figure 11.59) and acetaldehyde selectivity (Figure 11.61) results obtained with STA62(550), STA82(550) and STA92(550) were found to be quite close to each other. These results indicated that the amount of STA incorporated into the lattice of the synthesized mesoporous catalysts did not change the activity of these catalysts significantly. DEE yield values of about 0.2 were observed at about 320°C using the catalysts calcined at 550°C (Figure 11.63). However, ethylene yield values reaching to 0.6 (Figure 11.65) were

obtained at about 380°C. Acetaldehyde yield values were quite low (Figure 11.67).

For the catalysts calcined at 350°C conversion values are higher at lower temperatures as compared to the catalysts calcined at 550°C. In this case the highest activity was observed with STA82(550) (Figure 11.56). Also highest DEE selectivity at relatively low temperatures (Figure 11.58) were observed with this catalyst. Ethylene selectivity (Figure 11.60), DEE yield (Figure 11.64) and ethylene yield (Figure 11.66) values are also higher for this catalyst than the values obtained with the other catalysts.

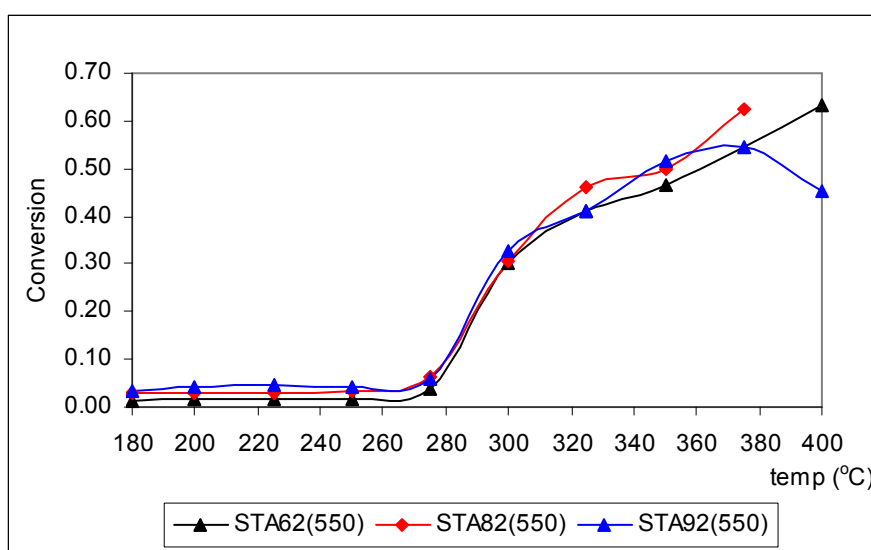


Figure 11.55 Comparison of ethanol conversion by using 0.2g of different novel catalysts calcined at 550°C, EtOH/(EtOH&He): 0.48

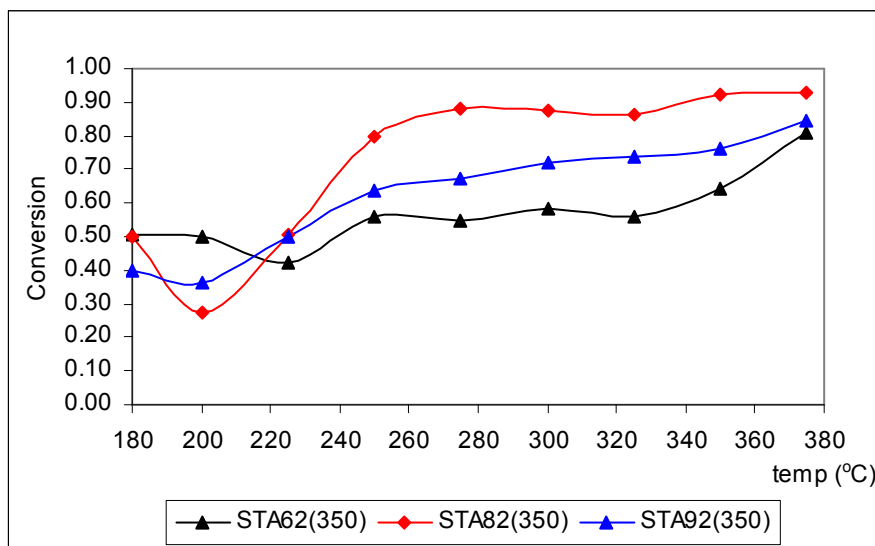


Figure 11.56 Comparison of ethanol conversion by using 0.2g of different novel catalysts calcined at 350°C, EtOH/(EtOH&He): 0.48

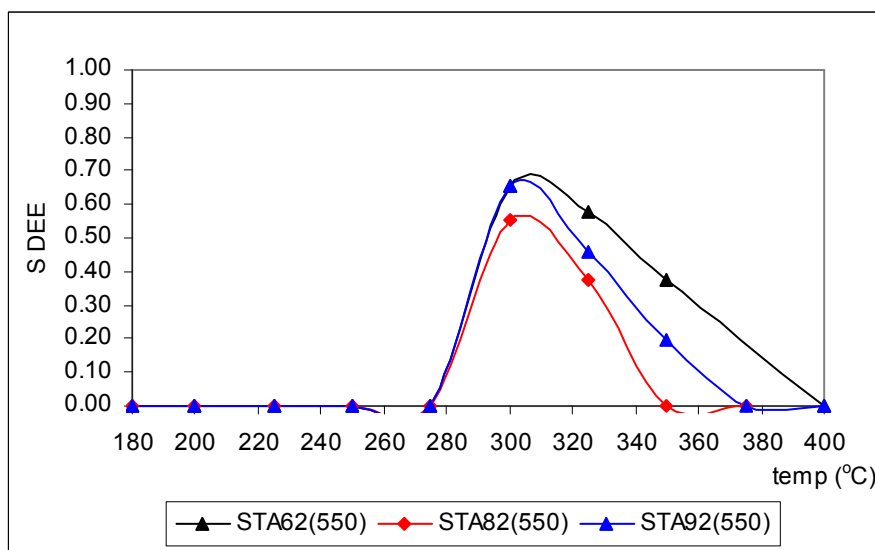


Figure 11.57 Comparison of DEE selectivity by using 0.2g of different novel catalysts calcined at 550°C, EtOH/(EtOH&He): 0.48

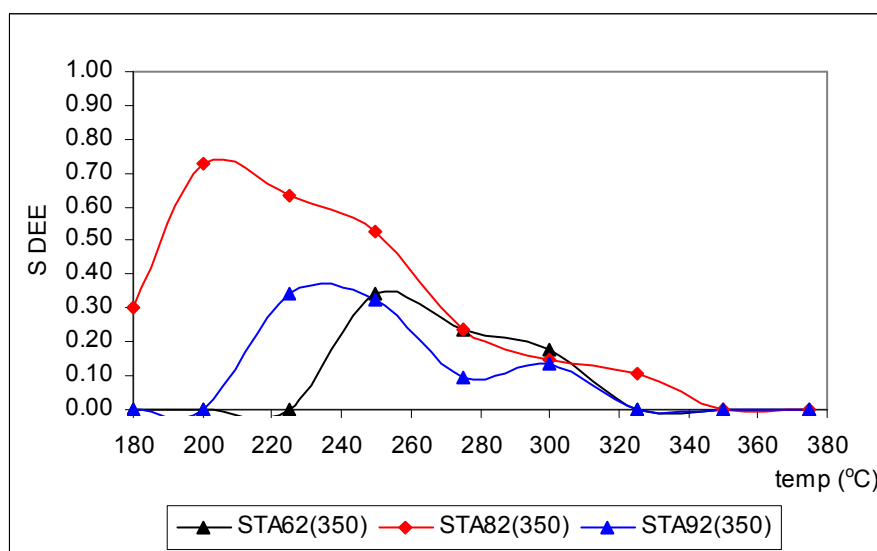


Figure 11.58 Comparison of DEE selectivity by using 0.2g of different novel catalysts calcined at 350°C, EtOH/(EtOH&He): 0.48

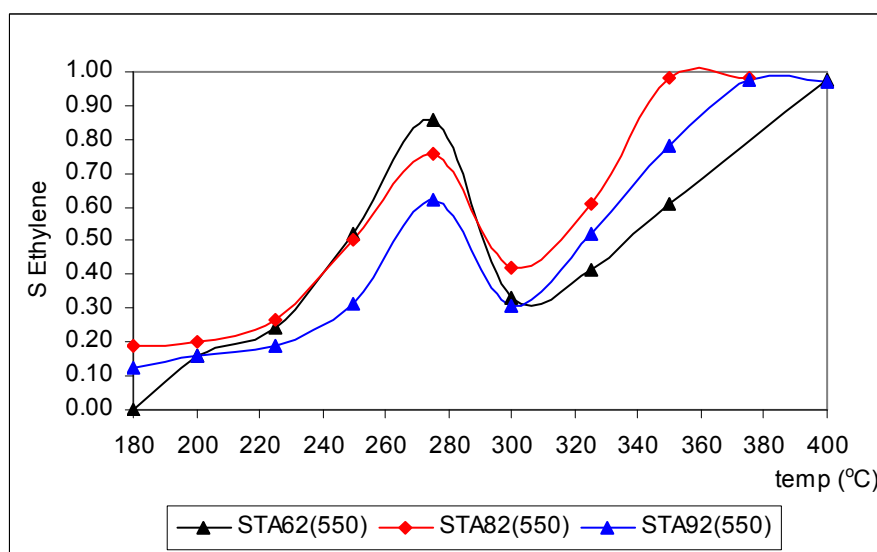


Figure 11.59 Comparison of Ethylene selectivity by using 0.2g of different novel catalysts calcined at 550°C, EtOH/(EtOH&He): 0.48

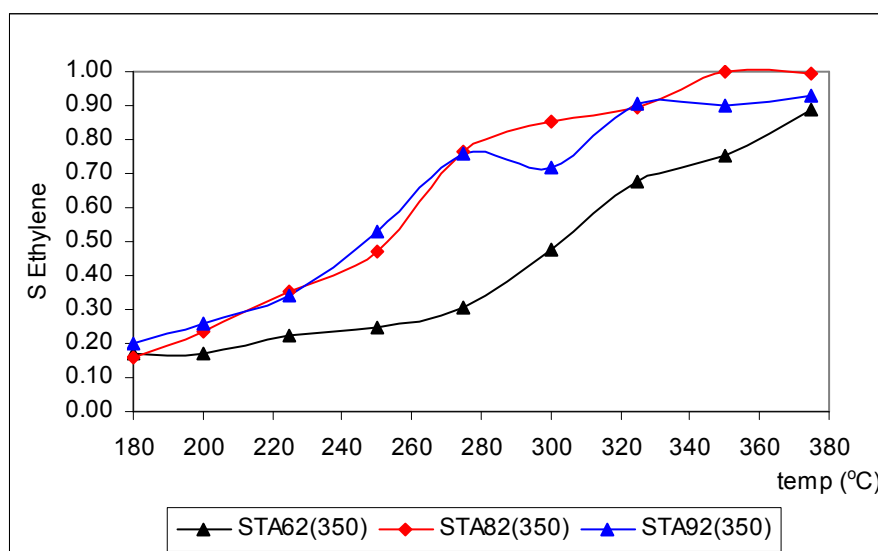


Figure 11.60 Comparison of Ethylene selectivity by using 0.2g of different novel catalysts calcined at 350°C, EtOH/(EtOH&He): 0.48

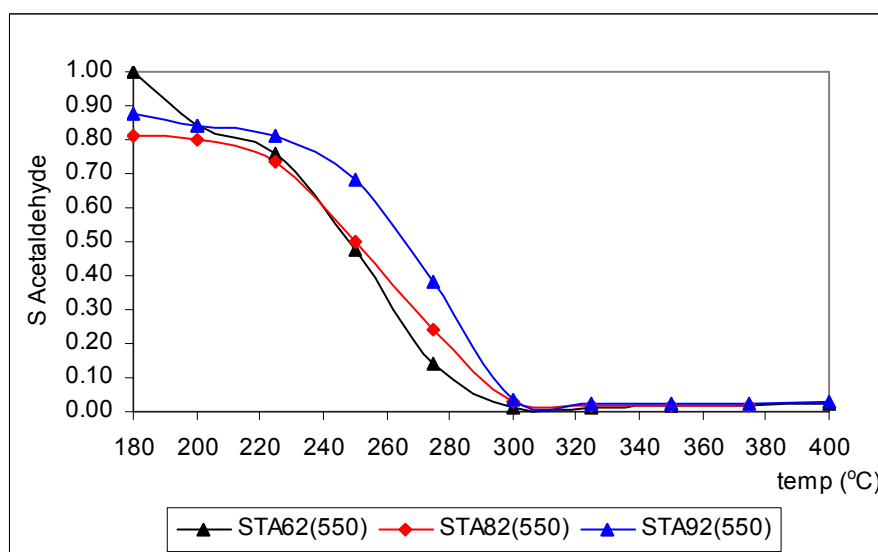


Figure 11.61 Comparison of Acetaldehyde selectivity by using 0.2g of different novel catalysts calcined at 550°C, EtOH/(EtOH&He): 0.48

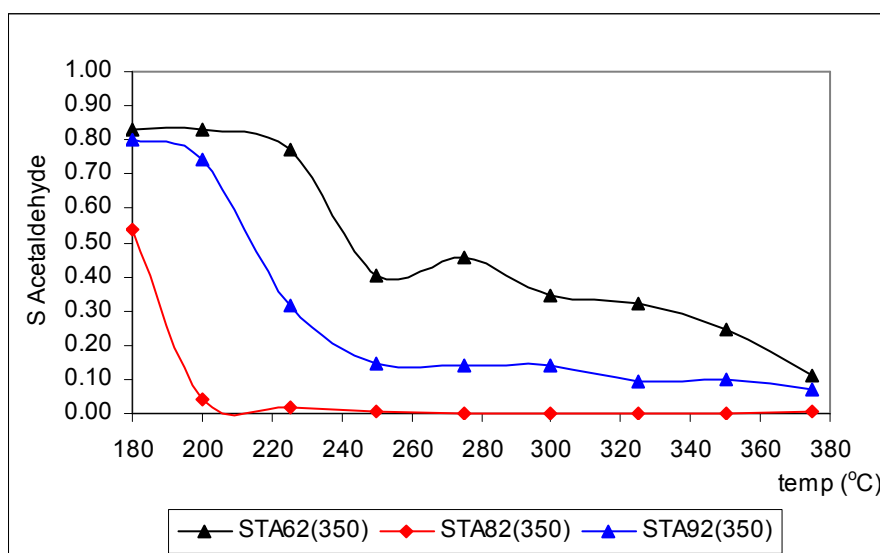


Figure 11.62 Comparison of Acetaldehyde selectivity by using 0.2g of different novel catalysts calcined at 350°C, EtOH/(EtOH&He): 0.48

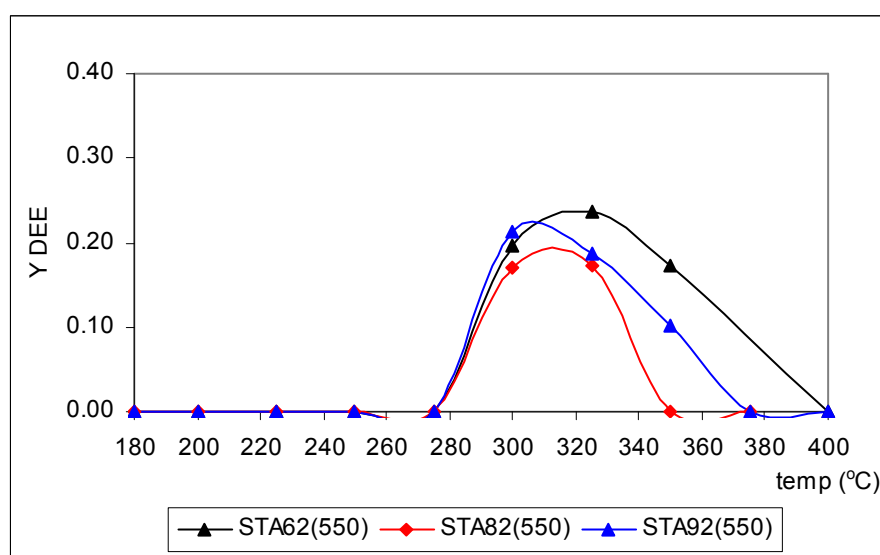


Figure 11.63 Comparison of DEE yield by using 0.2g of different novel catalysts calcined at 550°C, EtOH/(EtOH&He): 0.48

Acetaldehyde selectivity (Figure 11.62) and yield values (Figure 11.68) are lowest with the STA82(350) catalyst. STA82(350) contains higher amount of STA than STA62(350). Increase of STA in the catalyst structure caused a decrease in its surface area. STA92(350) has higher amount of STA but its surface area is quite low. Among the catalysts synthesized in this study STA82(350) showed the highest activity for producing both DEE and ethylene.

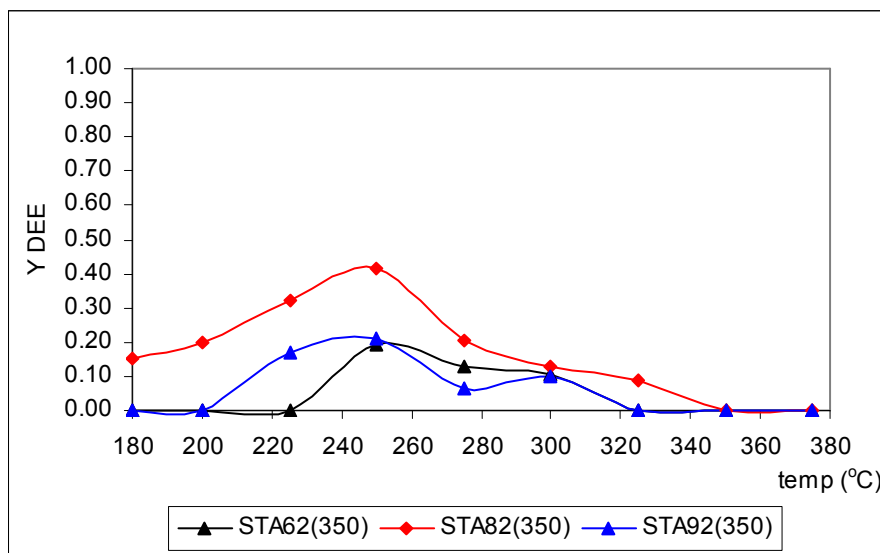


Figure 11.64 Comparison of DEE yield by using 0.2g of different novel catalysts calcined at 350°C, EtOH/(EtOH&He): 0.48

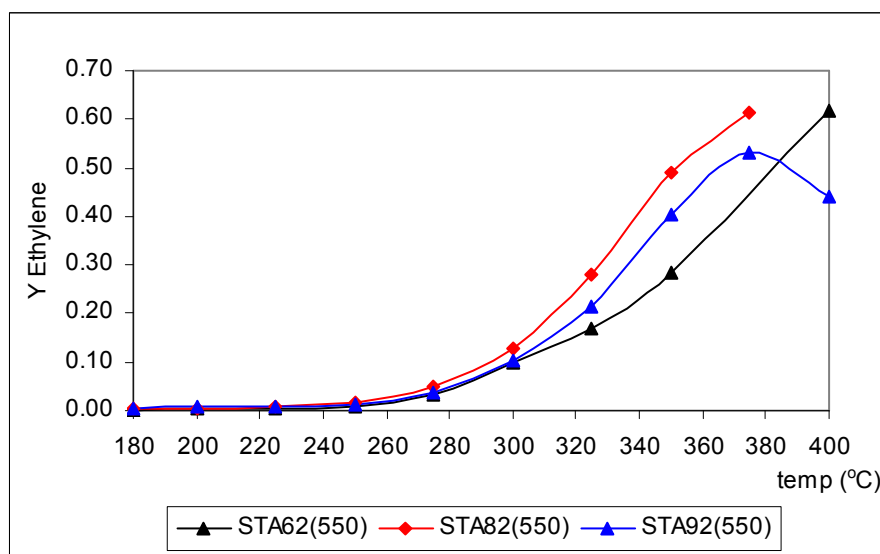


Figure 11.65 Comparison of Ethylene yield by using 0.2g of different novel catalysts calcined at 550°C, EtOH/(EtOH&He): 0.48

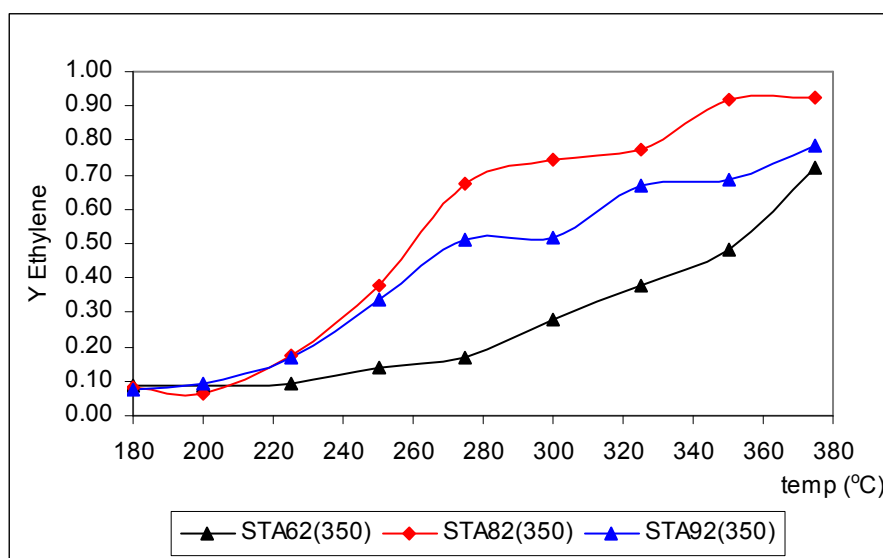


Figure 11.66 Comparison of Ethylene yield by using 0.2g of different novel catalysts calcined at 350°C, EtOH/(EtOH&He): 0.48

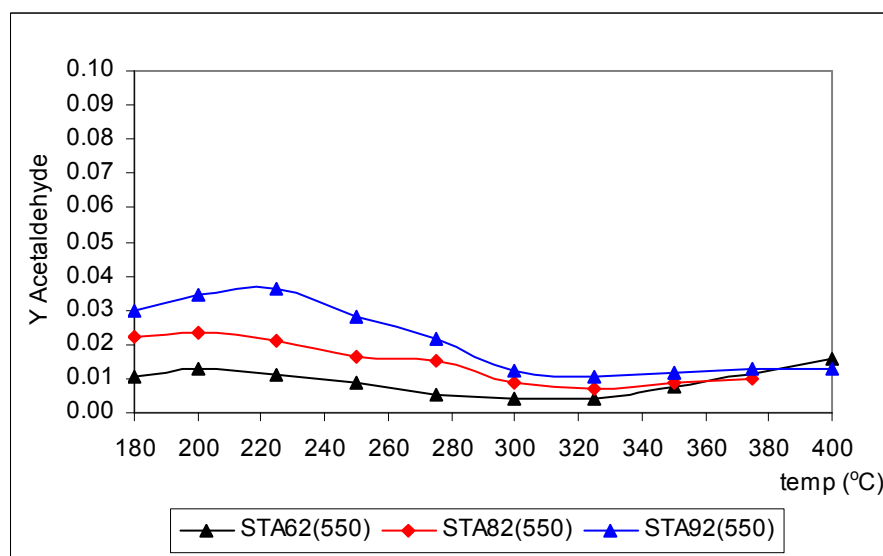


Figure 11.67 Comparison of Acetaldehyde yield by using 0.2g of different novel catalysts calcined at 550°C, EtOH/(EtOH&He): 0.48

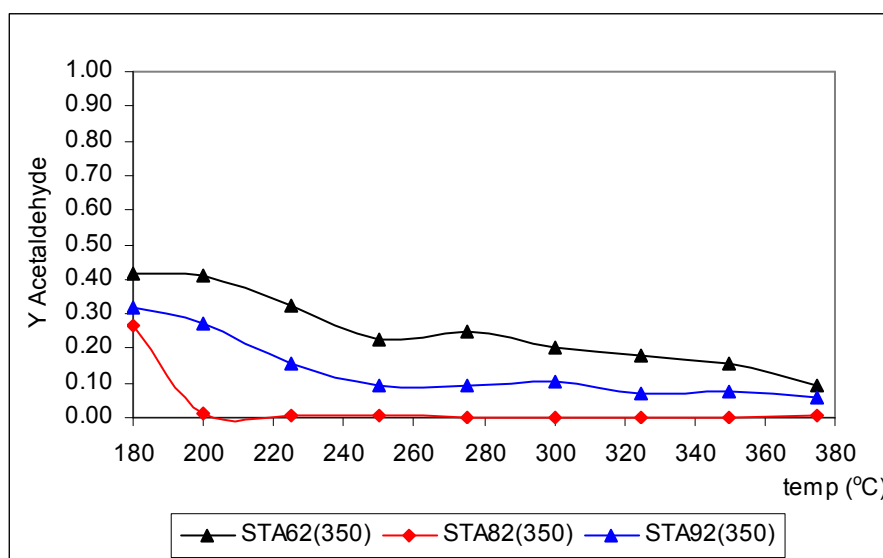


Figure 11.68 Comparison of Acetaldehyde yield by using 0.2g of different novel catalysts calcined at 350°C, EtOH/(EtOH&He): 0.48

11.7 Results obtained with STA impregnated MCM41

In order to prepare novel silicotungstic acid catalysts either direct hydrothermal synthesis or impregnation methods can be used. Briefly, in direct hydrothermal synthesis method, silicotungstic acid is added to synthesis solution and these catalyst were called as STA52, STA62, STA72, STA82 and STA92. The properties and catalytic activities of them have been discussed up to now. Catalysts prepared by direct synthesis are quite stable and STA do not wash out after washing with water and/or alcohol.

In this part, results obtained with the catalyst prepared with the other procedure, namely by impregnation, are reported. Firstly, MCM-41 was prepared following the procedure given in Chapter 8 until the calcination step. Before applying calcination step, some part of the sample was separated and used as a support for silicotungstic acid. This catalyst is called as STAMCM41U.

The remaining part was calcined at 550°C with dry air and then used as a support for heteropolyacid and the resulting catalyst is called as STAMCM41C. All the details for preparation of these catalyst are presented in Chapter 8.

In order to investigate the catalytic activities of STAMCM41U and STAMCM41C, a tubular reactor was packed with 0.2 gram catalyst and a feed

stream containing 48% pure ethanol in ethanol helium mixture was used. The total feed flow rate was set to 44.24 ml/min at room temperature. Reaction temperature was changed from 180 to 350°C and the total conversion of ethanol and product distributions were scanned in this interval.

As shown in Figure 11.69, STAMCM41C has much higher activity than STAMCM41U in ethanol dehydration reaction. Close to 100 % conversion of ethanol was observed at temperatures higher than 250°C by using STAMCM41C catalyst.

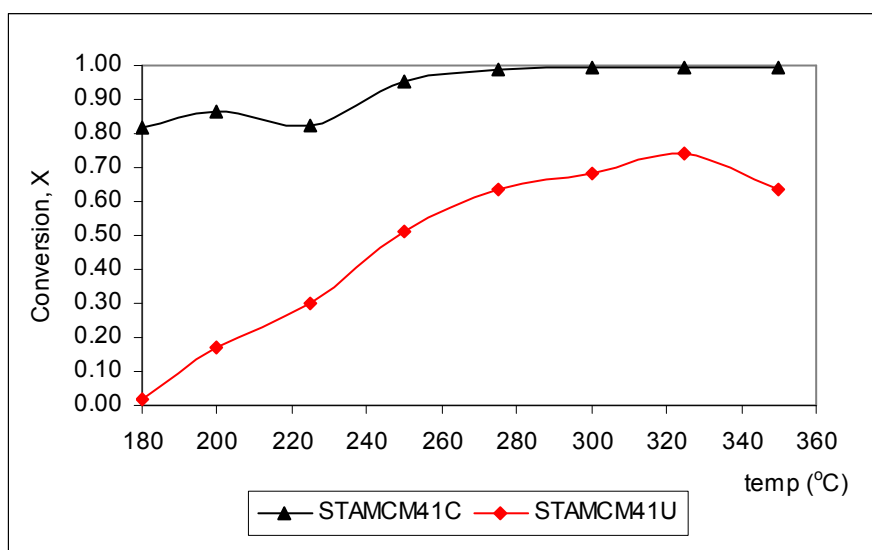


Figure 11.69 The variation in ethanol conversion at different temperatures using 0.2 g of STA impregnated on MCM-41

DEE selectivity profile had a maximum at around 200°C for STAMCM41U. Unlike STAMCM41U, DEE formation started at much lower temperatures with STAMCM41C (Figure 11.70) such as 180°C with an approximately 0.90 selectivity value.

For reaction temperatures higher than 200°C, ethylene selectivity values obtained with STAMCM41C catalyst was higher than that of STAMCM41U. STAMCM41C showed very high ethylene selectivities reaching to 100% (Figure 11.71).

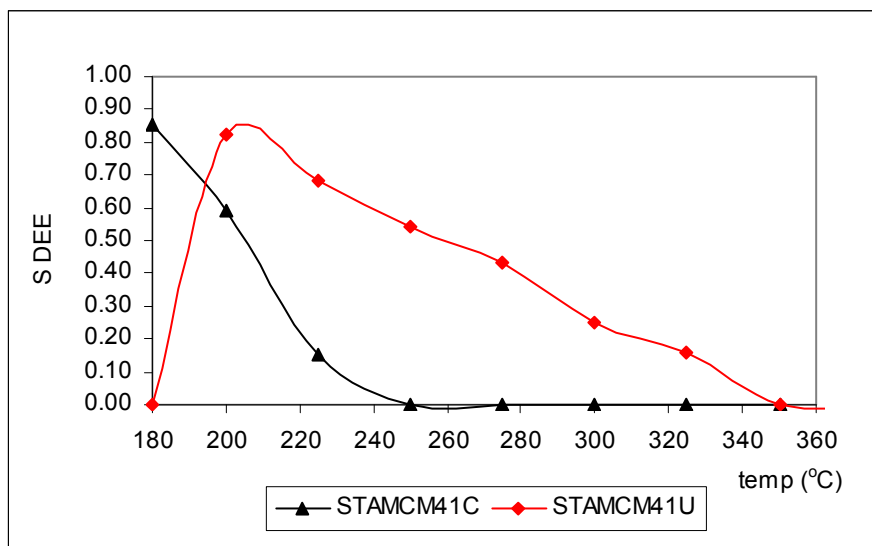


Figure 11.70 The selectivity of DEE at different temperatures using 0.2 g of STA impregnated on MCM41

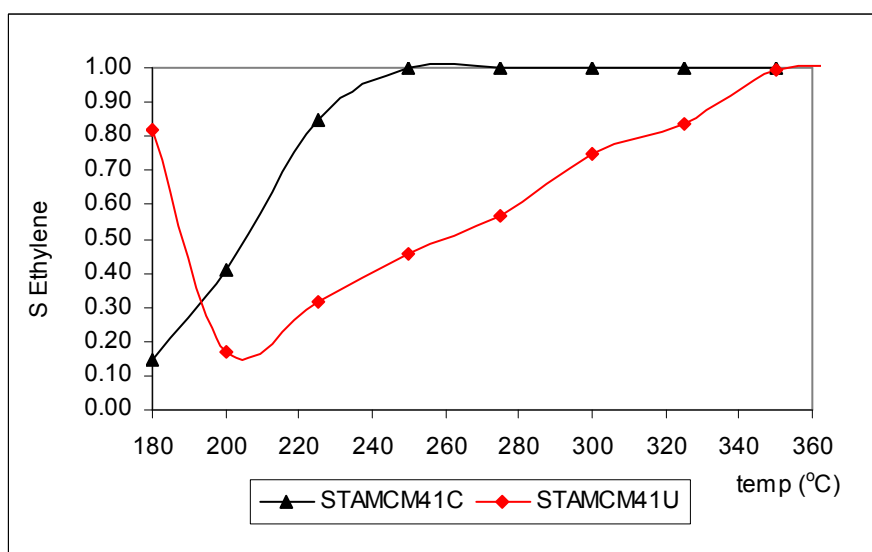


Figure 11.71 The selectivity of ethylene at different temperatures using 0.2 g of STA impregnated on MCM41

Variation in DEE and ethylene yields using STAMCM41C and STAMCM41U are given in Figure 11.72 and Figure 11.73, respectively. The highest DEE ethylene yield value obtained with STAMCM41C was 0.7 and it was observed at 180°C. For temperature values higher than 250°C, DEE yield became negligible for this catalyst. When STAMCM41U was used in experiments, DEE yield reached only 0.30 whereas its formation was observed at the temperature range of 180-

350°C (Figure 11.72). The increase in ethylene yield was observed for both catalysts. However, STAMCM41C gave higher ethylene yields than STAMCM41U. After 250°C, ethylene yield value reached to 100 % when STAMCM41C was used. In the case of STAMCM41U approximately 70 % ethylene yield was obtained at 360°C (Figure 11.73).

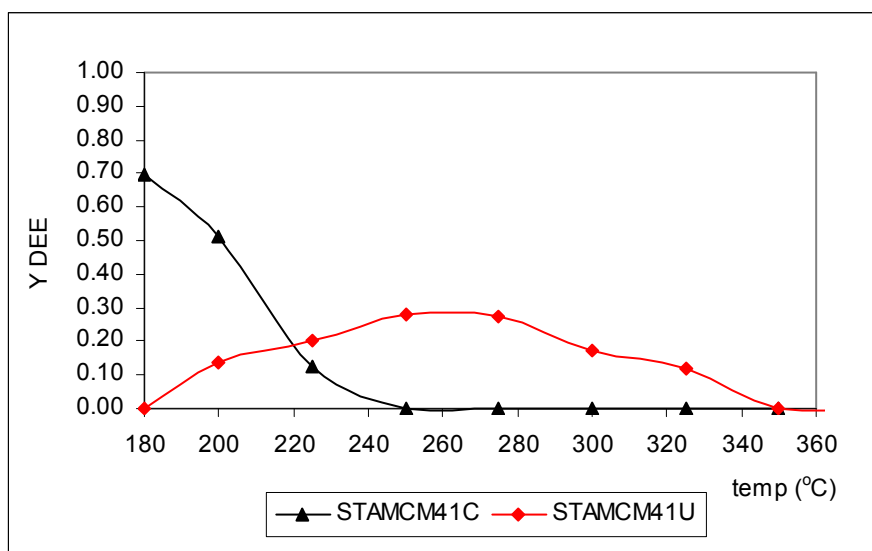


Figure 11.72 The yield of DEE at different temperatures using 0.2 g of STA impregnated on MCM41

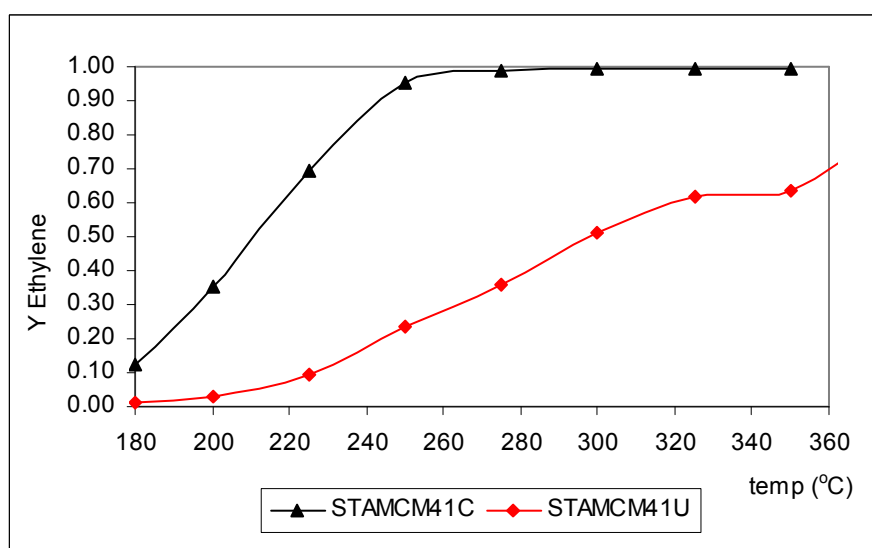


Figure 11.73 The yield of ethylene at different temperatures using 0.2 g of STA impregnated on MCM41

11.8 Results obtained with STA impregnated on Aluminosilicate

The catalytic activity of silicotungstic acid impregnated on Aluminosilicate (STAMAS) was tested in ethanol dehydration reaction for a feed which has a flowrate of 44.24 ml/min and containing 48% ethanol in helium. 0.2 g of this new catalyst was used and the reaction temperature was changed from 180°C to 325°C.

Very high conversion values were obtained with this catalyst (Figure 11.74). At 250°C, total ethanol conversion was calculated as 0.86. By increasing temperature to 320°C, complete conversion of ethanol was observed.

In ethanol dehydration reaction over silicotungstic acid impregnated on aluminosilicate, ethylene and DEE were obtained as main products. Acetaldehyde was not produced with this catalyst. This catalyst showed high activity at temperatures over 220°C (Figure 11.74).

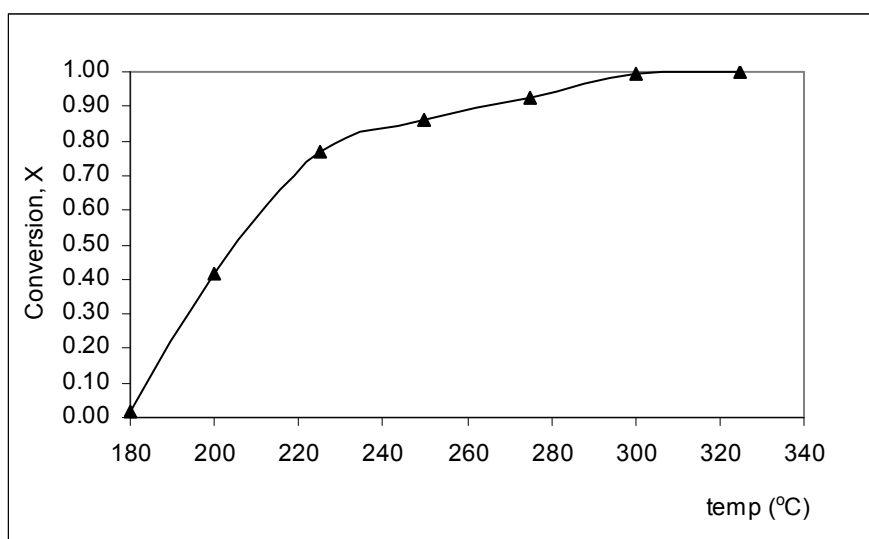


Figure 11.74 The ethanol conversion at different temperatures using 0.2 g of STA impregnated on Aluminosilicate

In Figure 11.75, the selectivity of DEE and Ethylene at different reaction temperatures are presented. DEE selectivity showed a maxima at around 210°C. At temperatures higher than 275°C, the selectivity of DEE became zero and the selectivity of ethylene reached to 1 after that temperature.

By using silicotungstic acid impregnated on aluminosilicate (STAMAS), a yield value of 0.55 was obtained for DEE at 225°C and a yield value of 0.99 was obtained at 300°C for ethylene (Figure 11.76).

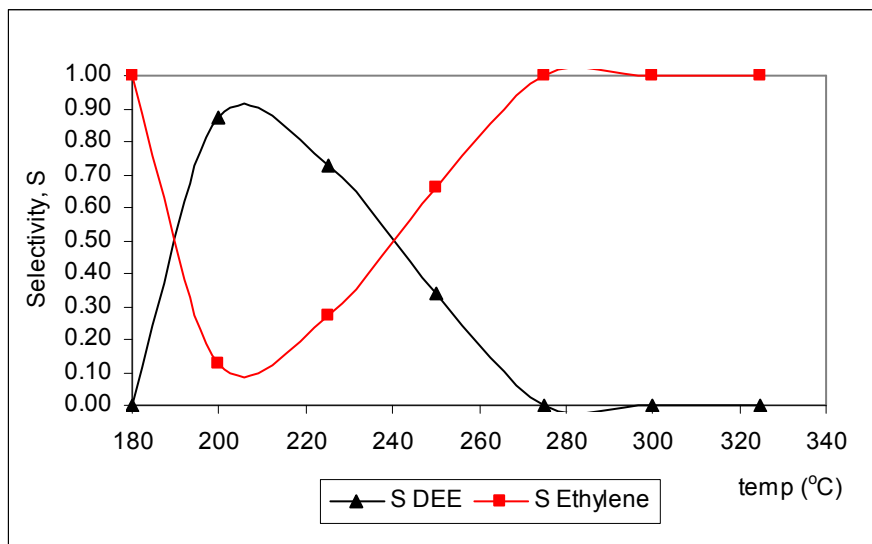


Figure 11.75 The selectivities of products at different temperatures using 0.2 g of STA impregnated on Aluminosilicate

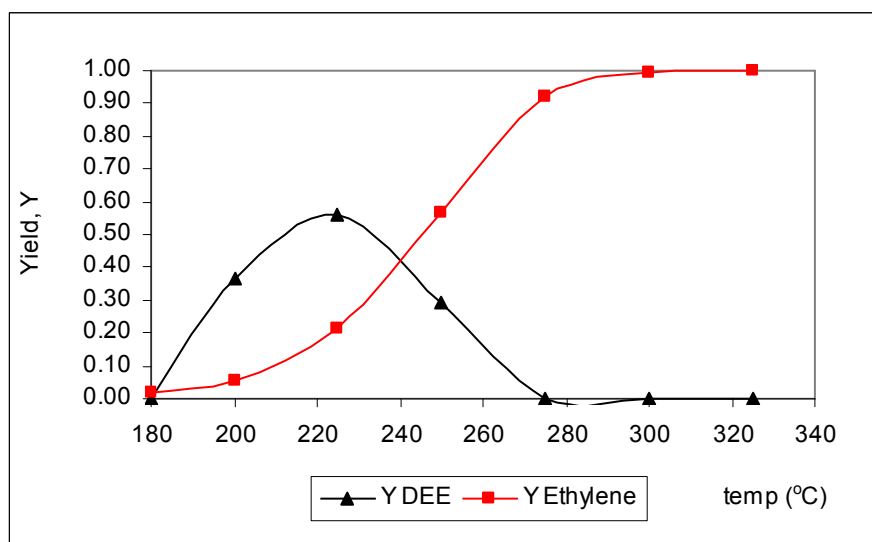


Figure 11.76 The yield of products at different temperatures using 0.2 g of STA impregnated on Aluminosilicate

Although the impregnated catalysts show very high activities, they tend to loose impregnated STA if they are washed with polar solvents. So they can

not be used in liquid phase reactions. These catalysts are much less stable than the catalysts synthesized following the direct hydrothermal synthesis route (STA62, STA82, STA92).

CHAPTER 12

RESULTS OF REACTION MECHANISM

In order to get information about the reaction mechanism and about the adsorbed species involved in the reaction steps, Diffuse Reflectance FT-IR (DRIFTS) experiments were carried out in the system described in Chapter 8. These experiments were carried out using 0.2 g TPA catalyst placed into the heated pan of the reaction chamber of the DRIFTS instrument. During these experiments a gas stream containing 48% ethanol in Helium flowed over the catalyst layer in the reaction chamber of the DRIFTS cell. The total flow rate of the gas stream was 44.24 ml/min and DRIFTS experiments were carried out in the temperature range of 180-350°C. DRIFT spectra of the adsorbed species were obtained by taking the differences of the spectra obtained with ethanol and helium mixture and pure helium flowing over the catalyst surface. By this way FT-IR peaks corresponding to the catalyst surface were eliminated.

Typical DRIFT spectra obtained at 180°C and 350°C are shown in Figure 12.1. As shown in this figure, the spectra obtained for these two temperatures are quite similar, indicating similar adsorbed species on the surface. The broad band observed between 3100 cm^{-1} – 3400 cm^{-1} corresponds to the OH stretches of the hydrogen bonded network of adsorbed alcohol molecules. This result indicated that some of the alcohol molecules are adsorbed on the acid sites (Type 2 sites) in molecular form and also among themselves forming hydrogen bonds. Similar results were reported by Dogu et al. (2001) for adsorption of alcohols on acidic resin catalyst. A small peak observed at around 3751 cm^{-1} corresponds to the hydroxysilanol groups (Si-OH) on the catalyst surface (Resini et al., 2005).

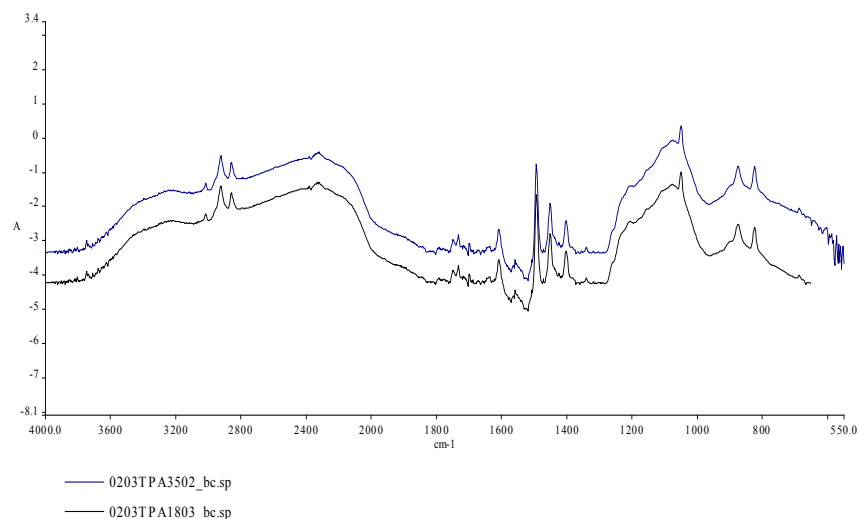


Figure 12.1 DRIFT spectra obtained at 180 and 350°C

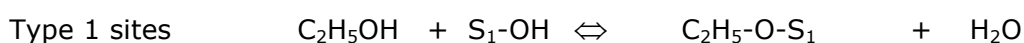
Typical IR bands observed at 1051 cm^{-1} (C-O stretch), 1340 cm^{-1} (CH_2 wag), 876 cm^{-1} (C-C stretch) and the small band at about 1265 cm^{-1} (CH_2 scissors) indicate the presence of ethoxy ($\text{CH}_3\text{CH}_2\text{O}-$) species on the catalyst surface. A small band observed at 687 cm^{-1} may also be due to ethoxy species (NIST). Presence of ethoxy species on acidic surfaces were also reported by Karamullaoglu and Dogu (2003) for ethanol adsorption on Amberlyst-15.

The IR bands observed between 1733 cm^{-1} – 1751 cm^{-1} indicated the presence of CO stretching on adsorbed molecule. As reported by Golay et al. (1998) O-C-O vibration of acetate like species are expected to give bands between 1480 cm^{-1} – 1560 cm^{-1} . The bands observed in our case at 1494 cm^{-1} and 1559 cm^{-1} and also the bands observed between 1733 cm^{-1} – 1751 cm^{-1} indicated the presence of acetate like adsorbed species on the surface. Desorption of these species give acetaldehyde in the product stream.

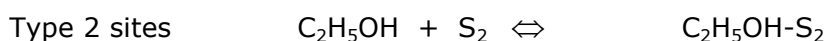
The band observed at about 1610 cm^{-1} corresponds to C=C stretching. This indicated the possible presence of ethyl like species on the catalyst surface ($\text{CH}_2=\text{CH}-\text{O}$). The bands observed at 2860 cm^{-1} , 2925 cm^{-1} and 3018 cm^{-1} correspond to the CH stretching (of CH_3) of adsorbed species (Dogu et al., 2001;

Resini et al., 2005). Also the bands observed at 1403 cm^{-1} and 1451 cm^{-1} correspond to the CH_3 and CH_2 deformation bands of adsorbed species. CH band of acetaldehyde like molecules are also expected to give an IR band at 1403 cm^{-1} (NIST). The band at 824 cm^{-1} correspond to CH_3 rocking band of adsorbed species.

All these DRIFTS results indicated the presence of adsorbed ethoxy, acetate, ethyl like species in addition to adsorbed ethanol molecules. These results indicated that ethanol is adsorbed on the surface in molecular form (on Type 2 sites) and also in ethoxy form by dissociation of one hydrogen atom (on Type 1 sites).

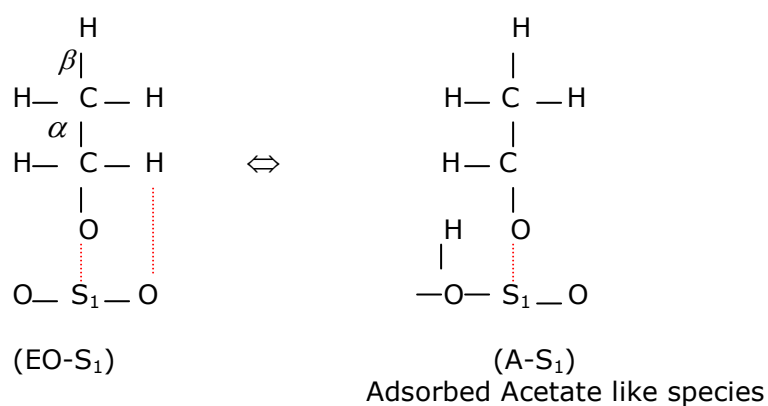


Adsorbed ethoxy (EO-S1)

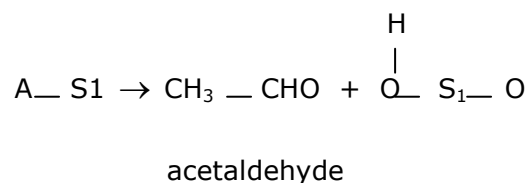


Adsorbed ethanol (EtOH-S2)

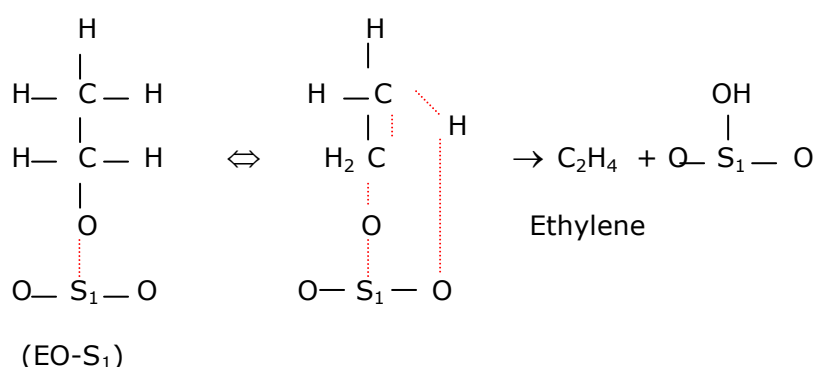
Adsorption of alcohol on two different types of sites was also proposed by Golay et al. (1998) for DEE production on γ -alumina catalyst. Their proposal involved adsorbed ethanol and ethene molecules on different sites. Our results indicated the presence of acetate like molecules on the catalyst surface. Formation of these species might be due to dissociation of a hydrogen from the α -carbon of adsorbed ethoxy species.



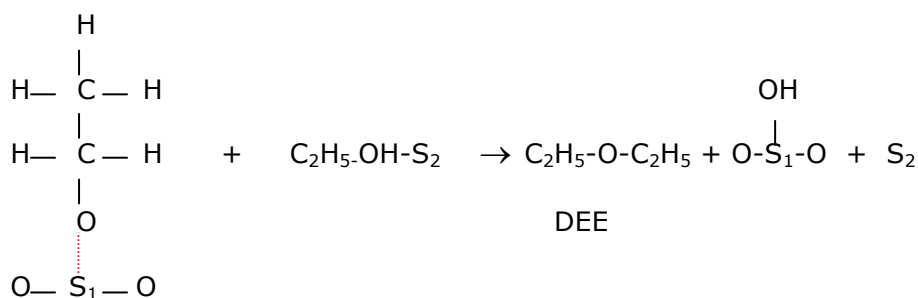
Desorption of A-S₁ gives acetaldehyde



The observation indicating the presence of ethyl like species on the surface indicating removal of hydrogen from β -carbon of ethoxy species by forming a bridge structure between C, H and surface oxygen. A possible mechanism of formation of ethylene might be as follows;



Formation of diethyl ether (DEE) is proposed to be due to the reaction of adsorbed ethoxy and adsorbed ethanol species on the catalyst surface.



A small peak observed at 1076 cm⁻¹ band in the DRIFT spectra corresponds to C-O-C bond of ethers which might be due to adsorbed DEE.

Saito and Niiyama (1987) also proposed the presence of chemisorbed and physisorbed ethanol on heteropolyacid catalyst. They also proposed formation of

DEE by the reaction of chemisorbed and physisorbed ethanol and formation of ethylene from the chemisorbed ethanol. Our results showed that DEE and ethylene were most probably took place through parallel reactions at lower temperatures, DEE formation is due to the reaction between adsorbed ethoxy and ethanol species. At high temperatures decomposition of DEE might also contribute to the production of ethylene. These DRIFTS results and reaction results reported in the previous sections supported these conclusions.

CHAPTER 13

CONCLUSION

Heteropolyacid catalysts have very high acidity and they are excellent catalysts for dehydration reactions of alcohols. As a result of experiments carried out with silicotungstic acid (STA), tungstophosphoric acid (TPA), molybdophosphoric acid (MPA) and with other solid acid catalysts such as Nafion and mesoporous aluminosilicate, we concluded that silicotungstic acid was the best catalyst giving highest activity at temperatures as low as 180-250°C.

Two main reaction products of dehydration reactions are diethyl ether (DEE) and ethylene. With an increase in temperature, an increase in ethylene selectivity with a corresponding decrease in DEE selectivity was observed using pure heteropolyacid catalyst. Using tungstophosphoric acid catalyst increase of space time in the reactor (increase in catalyst amount charged to reactor) caused an increase in overall conversion but ethylene and DEE selectivities were not influenced much. These results indicated formation of ethylene and DEE through two parallel routes over pure TPA at temperatures lower than 250°C. This conclusion was also justified by the DRIFTS results obtained in these temperature ranges.

Very high ethylene yield values (over 0.70) were observed at temperatures higher than 250°C. Our results also showed that presence of water in the feed stream caused some reduction in the activity of catalyst. However, DEE selectivities were increased in experiments carried out at temperatures lower than 230°C.

In the case of dimethyl ether (DME) production by methanol dehydration reaction STA showed higher activity than TPA at temperatures higher than 225°C. Very high DME selectivities approaching to 1 were obtained. Formaldehyde formation at temperatures lower than 225°C indicated the occurrence of methanol dehydrogenation reaction in parallel to dehydration reaction. For DME production mesoporous aluminosilicate gave the best result, no coke formation was observed upto 450°C. At this temperature DME yield values of about 0.7 were observed.

Considering that heteropoly acid catalyst have very low surface area (in the order of magnitude of 10), and also they dissolve in polar solvents, we synthesized novel mesoporous catalysts with much higher stability and much higher surface area.

Novel mesoporous silicotungstic acid catalysts were prepared by direct hydrothermal synthesis method (STA62, STA82, STA92) and impregnation method (STAMCM41C, STAMCM41U and STAMAS). In direct hydrothermal synthesis procedure TEOS and sodium silicate were used as a silica source. From our characterization results of STA62, STA82 and STA92 we concluded that TEOS was a better silica source and pH should be acidic in the synthesis of these mesoporous catalysts for the incorporation of STA into the mesoporous structure of the catalyst.

Among these catalysts hydrothermally synthesized ones were highly stable and they did not dissolve in polar solvents. STA62(550), STA82(550) and STA92(550) have wide pore size distribution in the range of 2-20 nm which are in the mesoporous range. The adsorption isotherms of these mesoporous novel catalysts are Type 4 indicating capillary condensation at a relative pressure higher than 0.6. The surface areas of the catalysts are inversely proportional to the molar ratio of the STA incorporated into the synthesized catalysts. As the amount of STA incorporated into the mesoporous material, the pore volume of the materials also decreased. The molar ratio of STA62(550), STA82(550) and STA92(550) are 0.19, 0.34 and 0.85 respectively; the corresponding pore volumes are 0.53 cm³/g, 0.30 cm³/g and 0.19 cm³/g and corresponding surface areas are 326 m²/g, 156 m²/g and 97 m²/g, respectively.

Basing on our TGA, DSC, DTA studies and also NMR results reported in the literature we concluded that calcination of the catalyst over 375°C caused

some loss of protons and some degradation in structure. In fact reaction activity test results for ethanol dehydration showed that the catalyst calcined at 350°C showed much high activity than the one calcined at 550°C.

The catalyst calcined at 550°C showed activity in ethanol dehydration at temperatures higher than 280°C. DEE selectivities increased upto a temperature of 300°C and then decreased however ethylene selectivity increased over 300°C. This result indicated decomposition of some of DEE to ethylene at higher temperatures. However, we had already concluded that at lower temperatures DEE and ethylene were formed in parallel routes. For the catalysts calcined at 350°C very high DEE selectivities (0.7) were observed at much lower temperatures (about 200°C). Ethylene yield values approaching to 0.90 were observed at around 360°C. These results may open a new pathway to produce ethylene from a nonpetroleum feedstock, namely Bioethanol.

In the case of STA impregnated catalysts (on MCM-41) very high activities were observed with these catalysts, DEE yield values of about 0.7 were obtained at 180°C while ethylene yield values approaching to 1 at 250°C. However stability of the impregnated catalysts are not expected as high as direct hydrothermally synthesized catalysts due to easy wash out of STA from the catalyst structure.

From the DRIFTS results it was concluded that ethanol was observed on the catalyst surface in two parallel routes, namely by the formation of ethoxy species and also by physically adsorbed in molecular form. DRIFTS results also proved the presence of acetate like and ethyl like adsorbed species on the catalyst surface. From these results we concluded that DEE was formed by the reaction of adsorbed ethoxy species and physisorbed ethanol molecule.

REFERENCES

- Ar, F., 2006. Şeker Sanayii ve Biyoethanol Üretimi. Biyoyakıt Dünyası. Eylül, p.44-48
- Beck, J.S., Vartuli, J.C., Roth, W.J., Leonowicz, M.E., Kresge, C.T., Schmitt, K.D., Chu, C.T.-W., Olson, D.H., Sheppard, E.W., McCullen, S.B., Higgins, J.B., Schlenker, J.L., 1992. A new family of mesoporous molecular sieves prepared with liquid crystal templates. *Journal of the American Chemical Society*, 114, 10834-10843.
- Blasco, T., Corma, A., Martinez, A. and Martinez-Escolano, P., 1998. Supported Heteropolyacid (HPW) Catalysts for the Continuous Alkylation of Isobutane with 2-Butene: The Benefit of Using MCM-41 with Large Pore Diameters. *Journal of Catalysis* 177, pp.306-313.
- Bollon, F., 2007. DME and LPG. AEGPL Conference Nice 6-8 June 2007.
- Caliman, E., Dias, J.A., Dias, S.C.L., Prado, A.G.S., 2005. Solvent effect on the preparation of $H_3PW_{12}O_{40}$ supported on alumina. *Catalysis Today*, 107-108, pp. 816-825.
- Ciesla, U., Schüth, F., 1999. Review Ordered Mesoporous Materials. *Microporous and Mesoporous Materials* 27, pp.131-149.
- Corma, A. 1995. Inorganic Solid Acids and Their Use in Acid-Catalyzed Hydrocarbon Reactions. *Chem. Rev.* 95, pp.559-614.
- Corma, A., 1997. From Microporous to Mesoporous Molecular Sieve Materials and Their Use in Catalysis. *Chemical Reviews*, 97 (6), pp.2373-2420.
- Damyanova, S., Cubeiro, M.L. and Fierro, J.L.G., 1999. Acid-redox properties of titania-supported 12-molybdophosphates for methanol oxidation. *Journal of Molecular Catalysis A: Chemical*, 142, pp. 85-100.
- Damyanova, S., Dimitrov, L., Mariscal, R., Fierro, J.L.G., Petrov, L., Sobrados, 2003. Immobilization of 12-molybdophosphoric and 12-tungstophosphoric

- acids on metal-substituted hexagonal mesoporous silica. *Applied Catalysis A:General* 256, 183-197.
- Devassy, B.M., Halligudi, S.B., 2005. Zirconia-supported heteropolyacids: Characterization and catalytic behavior in liquid-phase veratrole benzylation. *Journal of Catalysis*, 236, pp. 313-323.
- Di Cosimo, J.I., Diez, V.K., Xu, M., Iglesia, E. and Apesteguía, C. R., 1998. Structure and Surface and Catalytic Properties of Mg-Al Basic Oxides. *Journal of Catalysis*, 178, pp. 499-510.
- Dogu, T., Boz, N., Aydin, E., Oktar, N., Murtezaoglu, K., Dogu, G., 2001. DRIFT Studies for the Reaction and Adsorption of Alcohols and Isobutylene on Acidic Resin Catalysts and the Mechanism of ETBE and MTBE Synthesis. *Industrial & Engineering Chemistry Research*, 40, pp. 5044-5051.
- Doğu, T., Varışlı, D., 2007. Alcohols as Alternates to Petroleum for Environmentally Clean Fuels and Petrochemicals. *Turkish Journal of Chemistry*, in press.
- Doheim, M. M., Hanafy, S. A. and El-Shobaky, G. A., 2002. Catalytic conversion of ethanol and isopropanol over the $\text{Mn}_2\text{O}_3/\text{Al}_2\text{O}_3$ system doped with Na_2O . *Material Letters*, 5, pp.304-311.
- Eberhardt, J.J., 1997. Future Fuels for Heavy-Duty Trucks. *Alternative Fuels in Trucking*, Volume6, Number 2.
- El-Sharkawy, E. A. , El-Hakam, S. A. and Samra, S. E. 2000. Effect of thermal treatment on the various properties of iron(III)-aluminum(III) coprecipitated hydroxide system. *Materials Letters*, 42, pp.331-338.
- Gao, X., Wachs, I., 1999. Titania-silica as catalysts: molecular structural characteristics and physico-chemical properties. *Catalysis Today*, 51, pp.233-254.
- Gayubo, A.G., Aguayo, A.T., Alonso, A., and Bilbao, J., 2007. Kinetic Modelling of the Methanol-to-Olefins Process on Silicoaluminophosphate (SAPO-18) Catalyst by Considering Deactivation and the Formation of Individual Olefins. *Industrial & Engineering Chemistry Research*, 46, pp. 1981-1989.
- Gayubo, A.G., Aguayo, A.T., Alonso, A., Atutxa, A., Bilbao, J., 2005. Reaction scheme and kinetic modelling for the MTO process over a SAPO-18 catalyst. *Catalysis Today* 106, pp. 112-117.

- Golay, S., Doepper, R., Renken, A., 1998. In-situ characterisation of the surface intermediates for the ethanol dehydration reaction over γ -alumina under dynamic conditions. *Applied Catalysis A: General* 172, pp. 97-106.
- Golay, S., Kiwi-Minsker, L., Doepper, R. and Renken, A., 1999. Influence of the catalyst acid/base properties on the catalytic ethanol dehydration under steady state and dynamic conditions. In situ surface and gas-phase analysis. *Chemical Engineering Science*, 54, pp. 3593-3598.
- Gucbilmez, Y., 2005. Vanadium and Molybdenum Incorporated MCM-41 Catalysts for Selective Oxidation of Ethanol. PhD Thesis, June 2005, METU.
- Gucbilmez, Y., Dogu, T., Balci, S., 2006. Ethylene and Acetaldehyde Production by Selective Oxidation of Ethanol Using Mesoporous V-MCM-41 Catalysts. *Industrial & Engineering Chemistry Research*, 45, pp. 3496-3502.
- Haber, J., Pamin, K., Matachowski, L., Mucha, D., 2003. Catalytic performance of the dodecatungstophosphoric acid on different supports. *Applied Catalysis A: General* 256, pp. 141-152.
- Haber, J., Pamin, K., Matachowski, L., Napruszewska, B., Poltowicz, J., 2002. Potassium and Silver Salts of Tungstophosphoric Acid as Catalysts in Dehydration of Ethanol and Hydration of Ethylene. *Journal of Catalysis* 207, pp.296-306.
- Harmer, M.A., Farneth, W.E. and Sun, Q., 1996. High Surface Area Nafion Resin/Silica Nanocomposites: A New Class of Solid Acid Catalyst. *Journal of the American Chemical Society*, 118, pp. 7708-7715.
- Inui, T., Yamamoto, T., Inoue, M., Hara, H., Takeguchi, T. and Kim, J.B., 1999. Highly effective synthesis of ethanol by CO₂-hydrogenation on well balanced multi-functional FT-type composite catalysts. *Applied Catalysis A: General*, 186, pp. 395-406.
- Izumi, Y., Hasebe, R. and Urabe, K., 1983. Catalysis by Heterogeneous Supported Heteropoly Acid. *Journal of Catalysis* 84, 402-409.
- Izumi, Y., Kurakata, H. and Aika, K., 1998. Ethanol Synthesis from Carbon Dioxide on [Rh₁₀Se]/TiO₂Catalyst Characterized by X-Ray Absorption Fine Structure Spectroscopy. *Journal of Catalysis*, 175, pp. 236-244.
- Jalil, P.A., Tabet, N., Faiz, M., Hamdan, N.M., Hussain, Z., 2004. Surface investigation on thermal stability of tungstophosphoric acid supported on

- MCM-41 using synchrotron radiation. *Applied Catalysis A: General* 257, p.1-6.
- Kannan, S., Sen, T. and Sivasanker, S., 1997. Catalytic Transformation of Ethanol over Microporous Vanadium Silicate Molecular Sieves with MEL Structure (VS-2). *Journal of Catalysis* 170, pp. 304-310.
- Karamullaoglu, G., Dogu, T., 2003. Oxidative Dehydrogenation of Ethane Over A Monolith Coated by Molybdenum-Vanadium-Niobium Mixed-Oxide Catalyst. *Chemical Engineering Communications*, 190, pp.1427-1438.
- Kawi, S., Lai, M.W., 1998. Supercritical fluid extraction of surfactant template from MCM-41. *Chem. Commun.* pp. 1407-1408.
- Kim, H., Jung, J.C., Kim, P., Yeom, S.H., Lee, K.-Y., Song, I.K., 2006. Preparation of H₃PMo₁₂O₄₀ catalyst immobilized on surface modified mesostructured cellular foam (SM-CF) silica and its application to the ethanol conversion reaction. *Journal of Molecular Catalysis A: Chemical* 259, pp 150-155.
- Kito-Borsa, T., and Cowley, S.W., 2004. Kinetics, Characterization and Mechanism for the Selective Dehydration of Ethanol to Diethyl Ether over Solid Acid Catalysts. *Am. Chem.Soc.Div.Fuel Chem.*, 49 (2), p.856.
- Kozhevnikov, I.V., 1998, "Catalysis by Heteropoly Acids and Multicomponent Polyoxometalates in Liquid-Phase Reactions", *Chem. Rev.* 98, pp.171-198.
- Liu, Q.-Y., Wu, W.-L., Wang, J., Ren, X.-Q., Wang, Y.-R., 2004. Characterization of 12-tungstophosphoric acid impregnated on mesoporous silica SBA-15 and its catalytic performance in isopropylation of naphthalene with isopropanol. *Microporous and Mesoporous Materials* 76, 51-60.
- Mao, D., Yang, W., Xia, J., Zhang, B. and Lu, G., 2006. The direct synthesis of dimethyl ether from syngas over hybrid catalysts with sulfate-modified γ -alumina as methanol dehydration components. *Journal of Molecular Catalysis A: Chemical*, 250, pp. 138-144.
- Marin, F.C., Mueden, A. and Castilla, C.M., 1998. Surface-Treated Activated Carbons as Catalysts for the Dehydration and Dehydrogenation Reactions of Ethanol. *Journal of Physical Chemistry B*, 102, pp. 9239-9244.

- Miller Jothi, N.K., Nagarajan, G., Renganarayanan, S., 2007. Experimental studies on homogeneous charge CI engine fueled with LPG using DEE as an ignition enhancer. *Renewable Energy* 32, 1581-1593.
- Mokoya, R., 2001. Hydrothermally-induced morphological transformation of mesoporous MCM-41 silica. *Microporous and Mesoporous Materials*, 44-45, pp.119-127.
- Molnár, Á., Keresszegi, C., Török, B., 1999. Heteropoly acids immobilized into a silica matrix: characterization and catalytic applications. *Applied Catalysis A: General* 189, pp. 217-224.
- Nandhini, K.U., Arabindoo, B., Palanichamy, M., Murugesan, V., 2006. Al-MCM-41 supported phosphotungstic acid: Application to symmetrical and unsymmetrical ring opening of succinic anhydride. *Journal of Molecular Catalysis A: Chemical* 243, p.183-193.
- Nowińska, K., Fórmaniak, R., Kaleta, W., Wąclaw, A., 2003. Heteropoly compounds incorporated into mesoporous material structure. *Applied Catalysis A: General* 256, pp. 115-123.
- Ogawa, T., Inoue, N., Shikada, T., Ohno, Y., 2003. Direct Dimethyl Ether Synthesis. *Journal of Natural Gas Chemistry* 12, p.219-227.
- Ohno, Y., Omiya, M., 2003. Coal Conversion into Dimethyl Ether as an Innovative Clean Fuel. DME Project JFE Holdings, Inc., 12th ICCS-November
- Olah, G.A., Goeppert, A., Prakash, G.K.S., 2006. *Beyond Oil and Gas: The Methanol Economy*, Wiley-VCH Verlag GmbH & Co.
- Pizzio, L.R., Caceres, C.V., Blanco, M.N., 1998. Acid catalysts prepared by impregnation of tungstophosphoric acid solutions on different supports. *Applied Catalysis A: General* 167, p.283-294.
- Pizzio, L.R., Vazquez, P.G., Caceres, C.V., Blanco, M.N., Alesso, E.N., Torviso, M.R., Lantano, B., Moltrasio, G.Y., Aguirre, J.M., 2005. C-alkylation reactions catalyzed by silica-supported Keggin heteropolyacids. *Applied Catalysis A: General* 287, pp. 1-8.
- Ramos, F.S., Duarte de Farias, A.M., Borges, L.E.P., Monterio, J.L., Fraga, M.A., Sousa-Aguiar, E.F., Appel, L.G., 2005. Role of dehydration catalyst acid properties on one-step DME synthesis over physical mixtures. *Catalysis Today*, 101, p. 39-44.

- Rao, P.M., Wolfson, A., Kababya, S., Vega, S., Landau, M.V., 2005. Immobilization of molecular $\text{H}_3\text{PW}_{12}\text{O}_{40}$ heteropolyacid catalyst in alumina-grafted silica-gel and mesostructured SBA-15 silica matrices. *Journal of Catalysis* 232, pp.210-225.
- Resini, C., Montanari, T., Busca, G., Jehng, J.-M., Wachs, I.E., 2005. Comparison of alcohol and alkene oxidative dehydrogenation reactions over supported vanadium oxide catalysts: in situ infrared, Raman and UV-vis spectroscopic studies of surface alkoxide intermediates and of their surface chemistry. *Catalysis Today*, 99, pp. 105-114.
- Roh, H.S., Jun, K.W., Kim, J.W., Vishwanathan, V., 2004. Superior dehydration of CH_3OH over double layer bed of solid acid catalysts-A novel approach for dimethyl ether (DME) synthesis. *Chemistry Letters*, 33 (5), p.598-599.
- Saito, Y., Niiyama, H., 1987. Reaction Mechanism of Ethanol Dehydration on/in Heteropolyacid Compounds: Analysis of Transient Behavior Based on Pseudo-Liquid Catalysis Model. *Journal of Catalysis*, 100, p. 329-338.
- Sener, C., 2006. Synthesis and Characterization of Pd-MCM-Type Mesoporous Nanocomposite Materials. Ph.D. Thesis, January 2006, METU, Ankara.
- Sloczynski, J., Grabowski, R., Kozłowska, A., Olszewski, P., Stoch, J., Skrzypek, J. and Lachowska, M., 2004. Catalytic activity of the $\text{M}/(3\text{ZnO}\cdot\text{ZrO}_2)$ system ($\text{M} = \text{Cu}, \text{Ag}, \text{Au}$) in the hydrogenation of CO_2 to methanol. *Applied Catalysis A: General*, 278, pp. 11-23.
- Sloczynski, J., Grabowski, R., Olszewski, P., Kozłowska, A., Stoch, J., Lachowska, M. and Skrzypek, J., 2006. Effect of metal oxide additives on the activity and stability of $\text{Cu}/\text{ZnO}/\text{ZrO}_2$ catalysts in the synthesis of methanol from CO_2 and H_2 . *Applied Catalysis A: General*, 310, pp. 127-137.
- Soled, S., Miseo, S., McVicker, G., Gates, W.E., Gutierrez, A., Paes, J., 1997. Preparation of bulk and supported heteropolyacid salts. *Catalysis Today* 36, pp. 441-450.
- Song, C., 2006. Global Challenges and strategies for control, conversion and utilization of CO_2 for sustainable development involving energy, catalysis, adsorption and chemical processing. *Catalysis Today*, 115, pp. 2-32.
- Song, J., Huang, Z., Qiao, X., Wang, W., 2004. Performance of controllable premixed combustion engine fueled with dimethyl ether. *Energy Conversion and Management* 45, p.2223-2232.

- Staiti, P., Freni, S., Hocevar, S., 1999. Synthesis and characterization of proton-conducting materials containing dodecatungstophosphoric and dodecatungstosilic acid supported on silica. *Journal of Power Sources* 79, pp. 250-255.
- Sun, K.P., Lu, W.W., Qiu, F.Y., Liu, S.W., Xu, X.L, 2003. Direct Sythesis of DME over bifunctional catalysts: surface properties and catalytic performance. *Applie Catalysis A-General*, 252 (2), p. 243-249.
- Suppes, G.J., Terry J.G., Burkhart, M.L. and Cupps, M.P., 1998. Compression-Ignition Fuel Properties of Fischer-Tropsch Syncrude. *Industrial & Engineering Chemistry Research* 37, pp. 2029-2038.
- Takahara, I., Saito, M., Inaba, M., Murata, K., 2005. Dehydration of ethanol into ethylene over solid acid catalysts. *Catalysis Letters* Vol. 105, No. 3-4. p. 249-252.
- Tarlani, A., Abedini, M., Nemati, A., Khabaz, M., Amini, M.M., 2006. Immobilization of Keggin and Preyssler tungsten heteropolyacids on various functionalized silica. *Journal of Colloid and Interface Science* 303, 32-38.
- Thomas, A., Dablemont, C., Basset, J.-M., Lefebvre, F., 2005. Comparison of H₃PW₁₂O₄₀ and H₄SiW₁₂O₄₀ heteropolyacids supported on silica by H MAS NMR. *C.R.Chimie* 8, 1969-1974.
- Udayakumar, S., Ajaikumar, S., Pandurangan, A., 2007. Electrophilic substitution reaction of phnols with aldehydes: Enhance the yield of bisphenols by HPA and supported HPA. *Catalysis Communications* 8, pp. 366-374.
- Varisli, D., Dogu,T., Dogu, G., 2007. Ethylene and diethyl-ether production by dehydration reaction of ethanol over different heteropolyacid catalysts. *Chemical Engineering Science*, 62, pp. 5349-5352.
- Vázquez, P., Pizzio, L., Cáceres, C., Blanco, M., Thomas, H., Alesso, E., Finkielstein, L., Lantano, B., Moltrasio, G., Aguirre, J., 2000. Silica-supported heteropolyacids as catalysts in alcohol dehydration reactions. *Journal of Molecular Catalysis A: Chemical* 161, pp. 223-232.
- Verhoef, M.J., Kooyman, P.J., Peters, J.A., Van Bekkum, H., 1999. A study on the stability of MCM-41-supported heteropolyacids under liquid- and gas-phase esterification conditions. *Microporous and Mesoporous Materials* 27, p. 365-371.

- Vishwanathan, V., Jun, K.-W., Kim, J.-W., Roh, H.-S., 2004. Vapour phase dehydration of crude methanol to dimethyl ether over Na-modified H-ZSM-5 catalysts. *Applied Catalysis A: General*, 276, p.251-255.
- Wang, H.W., Zhou, L.B., 2003. Performance of direct injection diesel engine fuelled with a dimethyl ether/diesel blend *Proceedings of the Institution of Mechanical Engineers Part D-Journal of Automobile Engineering*, 217(D9), p. 819-824.
- Wang, Y., Liu, J., Li, W., 2000. Synthesis of 2-butoxy ethanol with narrow-range distribution catalyzed by supported heteropolyacids. *Journal of Molecular Catalysis A: Chemical* 159, 71-75.
- Shell Chemicals, www.shellchemicals.com, last accessed date June 2007.
- Green Car Congress, www.greencarcongress.com, last accessed date June 2007.
- JFE Holdings, Inc., www.jfe-holdings.co.jp, the last accessed date May 2007.
- Yang, C., Ma, Z., Zhao, N., Wei, W., Hu, T. and Sun, Y., 2006. Methanol synthesis from CO₂-rich syngas over a ZrO₂ doped CuZnO catalyst. *Catalysis Today*, 115, pp.222-227.
- Yang, J.I., Lee, D.W., Lee J.H., Hyun, J.C. and Lee, K.Y., 2000. Selective and high catalytic activity of Cs_nH_{4-n}PMo₁₁VO₄₀ (n≥3) for oxidation of ethanol. *Applied Catalysis A: General*, 194-195, pp. 123-127.
- Yaripour, F., Baghaei, F., Schmidt, I., Perregaard, J., 2005. Catalytic dehydration of methanol to dimethyl ether (DME) over solid-acid catalysts. *Catalysis Communications*, 6, pp. 147-152.
- Zaki, T., 2005. Catalytic dehydration of ethanol using transition metal oxide catalysts. *Journal of Colloid and Interface Science*, 284, p. 606-613.
- Zhang, Y., Du, Z., Min, E., 2004. Effect of acidity and structures of supported tungstophosphoric acid on its catalytic activity and selectivity in the liquid phase synthesis of ethylbenzene. *Catalysis Today* 93-95, pp. 327-332.
- Zhang, Y., Fei, J., Yu, Y. and Zheng, X., 2006. Methanol synthesis from CO₂ hydrogenation over Cu based catalyst supported on zirconia modified γ-Al₂O₃. *Energy Conversion and Management*, 47, pp. 3360-3367.
- Zholobenko, V.L., Plant, D., Evans, A.J., Holmes, S.M., 2001. Acid Sites in Mesoporous Materials: a DRIFTS Study. *Microporous and Mesoporous Materials*, 44-45, pp.793-799.

APPENDIX A

CALIBRATION OF GAS CHROMATOGRAPH

Before starting ethanol dehydration reaction experiments, the calibration factors for DEE, ethylene, water were calculated. In the following part, the calculation methods and the experimental data of calibration experiments are given in the following sections.

A.1 Calibration Factor for DEE

Calibration factor for DEE is calculated using the following relations,

$$y_{DEE} = \frac{A_{DEE} \times \beta_{DEE}}{A_{DEE} \times \beta_{DEE} + A_{C_2H_5OH} \times \beta_{C_2H_5OH}}$$

$$y_{C_2H_5OH} = \frac{A_{C_2H_5OH} \times \beta_{C_2H_5OH}}{A_{DEE} \times \beta_{DEE} + A_{C_2H_5OH} \times \beta_{C_2H_5OH}}$$

DEE –Ethanol mixtures are prepared in two different ratio, 1/3 and ½. The mole fractions for both cases are calculated as follow:

$$\text{For DEE : } 1ml \times \frac{0.71g / ml}{74g / mole} = 0.00959mole$$

$$\text{For Ethanol : } 3ml \times \frac{0.789g / ml}{46.07g / mole} = 0.05138mole$$

$$N_{total} = N_{DEE} + N_{C_2H_5OH} = 0.00959 + 0.05138 = 0.06097$$

$$y_{DEE} = \frac{0.00959}{0.06097} = 0.157$$

$$y_{C_2H_5OH} = \frac{0.05138}{0.06097} = 0.843$$

$$\text{For DEE : } 1ml \times \frac{0.71g / ml}{74g / mole} = 0.00959mole$$

$$\text{For Ethanol : } 2ml \times \frac{0.789g / ml}{46.07g / mole} = 0.03425mole$$

$$N_{total} = N_{DEE} + N_{C_2H_5OH} = 0.00959 + 0.03425 = 0.04384$$

$$y_{DEE} = \frac{0.00959}{0.04384} = 0.219$$

$$y_{C_2H_5OH} = \frac{0.03425}{0.04384} = 0.781$$

A.2 Calibration Factor for Ethylene

In order to find the calibration factor of ethylene,

$$\frac{\beta_{C_2H_4} \times A_{C_2H_4}}{\beta_{C_2H_6} \times A_{C_2H_6}} = 1$$

$$\beta_{C_2H_4} = \beta_{C_2H_6} \times \frac{A_{C_2H_6}}{A_{C_2H_4}}$$

$$\beta_{CO_2} = \beta_{C_2H_6} \times \frac{A_{C_2H_6}}{A_{CO_2}}$$

$$\beta_{CH_4} = \beta_{C_2H_6} \times \frac{A_{C_2H_6}}{A_{CH_4}}$$

$$\beta_{C_2H_2} = \beta_{C_2H_6} \times \frac{A_{C_2H_6}}{A_{C_2H_2}}$$

A.3 Calibration Factor for Water

$$\frac{mole_{H_2O}}{mole_{C_2H_5OH}} = \frac{\beta_{H_2O} \times A_{H_2O}}{\beta_{C_2H_5OH} \times A_{C_2H_5OH}}$$

$$\frac{\rho_{C_2H_5OH, liquid}}{\rho_{C_2H_5OH, vapor}} = \frac{0.789}{1.809 \times 10^{-3}} = 436.15$$

$$\frac{\rho_{H_2O, liquid}}{\rho_{H_2O, vapor}} = \frac{1.0}{7.067 \times 10^{-4}} = 1414.98$$

For Ethanol: $0.0485 cm^3 / min \times 0.8 \times 436.15 = 16.92 cm^3 / min$

For Water: $0.0485 cm^3 / min \times 0.2 \times 1414.98 = 13.73 cm^3 / min$

$$\frac{mole_{H_2O}}{mole_{C_2H_5OH}} = \frac{F_{H_2O}}{F_{C_2H_5OH}} = \frac{13.73 ml / min}{16.92 ml / min} = 0.811$$

Table A.1 Calibration Results

Component	Calibration factor. α
Carbondioxide, CO ₂	1.78
Diethyl Ether, DEE	0.76
Ethane, C ₂ H ₆	1.67
Ethanol, C ₂ H ₅	1.00
Ethylene, C ₂ H ₄	1.61
Methane, CH ₄	2.93
Water	2.53
Acetaldehyde	1.33

APPENDIX B

SAMPLE CALCULATION

B.1 Sample Calculation

Calculation of EtOH flowrate

$$c = \frac{P}{RT} \Rightarrow \rho = \frac{PM}{RT} = \frac{0.96atm \times 46.07}{82.05 \times 298} = 0.0018cm^3 / \text{min (at room temperature)}$$

When 20 cc syringe is used with flow rate of $0.0485cm^3 / \text{min}$ (10) in the syringe pump,

$$\frac{\rho_{liq}}{\rho_{vap}} = \frac{0.789}{0.0018} = 438$$
$$438 \times 0.0485cm^3 / \text{min} = 21.24cm^3 / \text{min} = 21.24ml / \text{min}$$

Calculation of He flowrate

$$\frac{10ml}{26 \text{ sec}} \times 60 \text{ sec} / \text{min} = 23.00ml / \text{min}$$

Total Flowrate

$$F_{EtOH} + F_{He} = 21.24ml / \text{min} + 23.00ml / \text{min} = 44.24ml / \text{min}$$

Ratio

$$\frac{F_{EtOH}}{F_{EtOH} + F_{He}} = \frac{21.24 \text{ ml} / \text{min}}{44.24 \text{ ml} / \text{min}} = 0.48$$

Conversion of EtOH and Selectivities of Products

$$n_{TOTAL} = \beta_{ethylene} \times A_{ethylene} + \beta_{EtOH} \times A_{EtOH} + 2 \times \beta_{DEE} \times A_{DEE}$$

$$X_{EtOH} = \frac{(n_{TOTAL} - n_{EtOH})}{n_{TOTAL}}$$

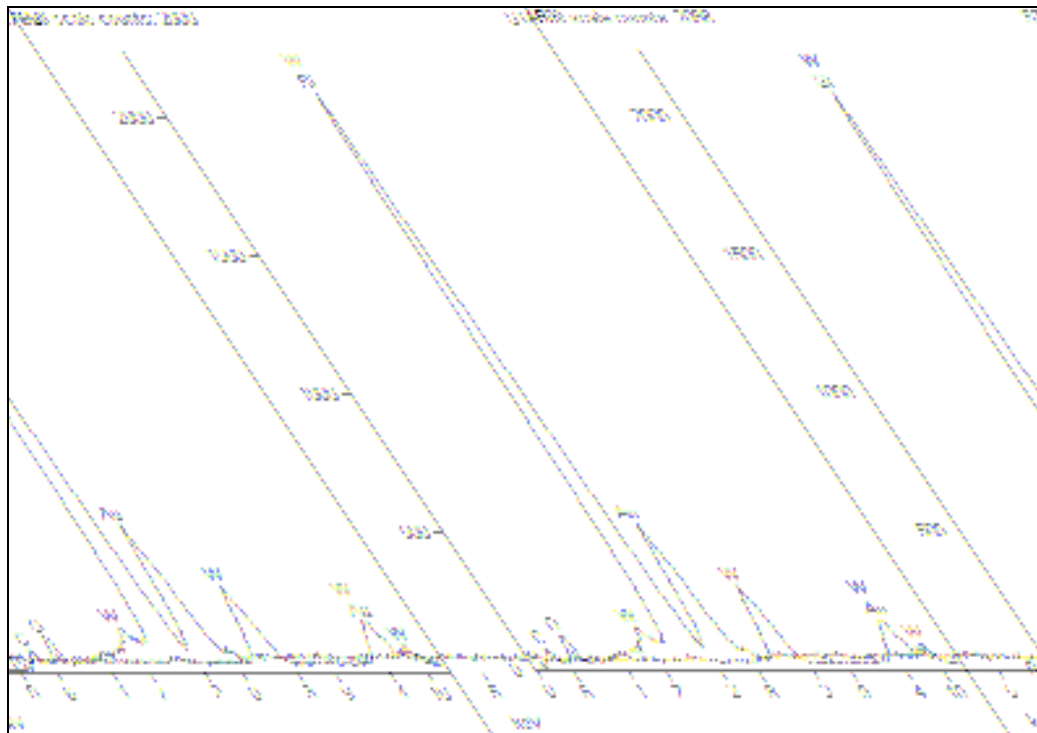
$$S_{DEE} = \frac{2 \times n_{DEE}}{(n_{TOTAL} - n_{EtOH})}, Y_{DEE} = X_{EtOH} \times S_{DEE}$$

$$S_{Ethylene} = \frac{n_{Ethylene}}{(n_{TOTAL} - n_{EtOH})}, Y_{Ethylene} = X_{EtOH} \times S_{Ethylene}$$

APPENDIX C

SAMPLE of EDS CHARACTERIZATION RESULT

C.1 Sample of EDS Result of STA92(550)



Element	Weight Conc %	Atom Conc %
Si	15.24	54.07
W	84.76	45.93

CURRICULUM VITAE

PERSONAL INFORMATION

Surname, Name: Varışlı, Dilek
Nationality: Turkish (TC)
Date and Place of Birth: 19 April 1979 , Ankara
Marital Status: Single
Phone: +90 312 210 43 65
Fax: +90 312 210 26 00
email: dvarisli@metu.edu.tr

EDUCATION

Degree	Institution	Year of Graduation
MS	METU Chemical Engineering	2003
BS	METU Chemical Engineering	2000
High School	Yahya Kemal Beyatlı Lisesi Ankara	1995

WORK EXPERIENCE

Year	Place	Enrollment
2000- Present	METU Department of Chemical Engineering	Research Assistant

FOREIGN LANGUAGES

Advanced English

PUBLICATIONS

Papers

1. Varışlı, D., Dogu, T., Dogu, G., 2007. Ethylene and diethyl-ether production by dehydration reaction of ethanol over different heteropolyacid catalysts, Chem. Eng. Sci., 62, pp. 5349-5352
2. Doğu, T., Varışlı, D. Alcohols as Alternates to Petroleum for Environmentally Clean Fuels and Petrochemicals. Turkish Journal of Chemistry, in pres.

National and International Congress

1. Varışlı, D., Dogu, T., Dogu, G., Novel Mesoporous Si-W Oxide Catalysts For Simultaneous Dehydration And Dehydrogenation Of Ethanol, Abstracts P12-45, Europacat 8, 26-31 August, Turkuabo, Finland 2007

2. Dilek Varışlı, Canan Sener, Ekin Ozdogan, Timur Dogu, Novel Mesoporous Nanocomposite Catalysts For Reforming And Dehydration Reactions, Somer Symposium Series 1,P.82, May 14-15, Metu, Ankara, Turkey
3. Dilek Varışlı, Timur Doğu, Gülşen Doğu, ' Ethanol Deyhdration over Solid Acid Catalysts Silicotungstic Acid, Tungstophosphoric Acid, Molybdophsphoric Acid and Nafion', First National Catalysis Conference, p. 57, 17-20 January 2007, METU Northern Cyprus Campus, Güzelyurt, TRNC
4. Varışlı, D., Doğu, T., Doğu, G., ' Etil Alkolün Dehidrasyon Reaksiyonu', 7.Ulusal Kimya Mühendisliği Kongresi, Bildiri Özetleri Kİtabı sayfa 449, 5-8 Eylül 2006, Eskişehir.
5. Varisli, D., Dogu, T., Dogu,G., ' Ethylene and Diethyl-Ether Production by Dehydration Reaction of Ethanol Over Different Heteropolyacid Catalysts', ISCRE 19, 19th International Symposium on Chemical Reaction Engineering,Book of Abstracts p. 448, September 3-6, 2006, Potsdam/Berlin, GERMANY
6. Dogu, G., Arslan, K., Oktar, N., Murtezaoglu, K., Varisli, D., Dogu, T., ' Dehydration of Ethanol Over Solid Acid Catalysts Such As Amberlyst-15, Nafion and Tungstophosphoric Acid', Abstract Book p.42, 1st European Chemistry Congress 27-31 August Budapest HUNGARY
7. Varışlı, D., Doğu, T., Doğu, G., 'MCM-like Novel Mesoporous Silicotungstic Acid Catalysts', NANOMAT 2006 international workshop on nanostructured materials, proceedings p. 165, Antalya Turkey, June 21-23, 2006,

Research Projects

1. TUBİTAK Grant Number 106M073, 'Etanolden Hidrojen ve Etilen Üretimi için Pd, Ni ve Silikotungstik Asit ile Aktifleştirilmiş MCM-41 Türü Mezogözenekli Nanokompozit Katalizörler Geliştirilmesi'.
2. BAP0304DPT2003(K12092017), 'Geleceğin Yakıtı Olarak Düşünülen Dimetil Eter ve Dietil Eter Üretimi'.